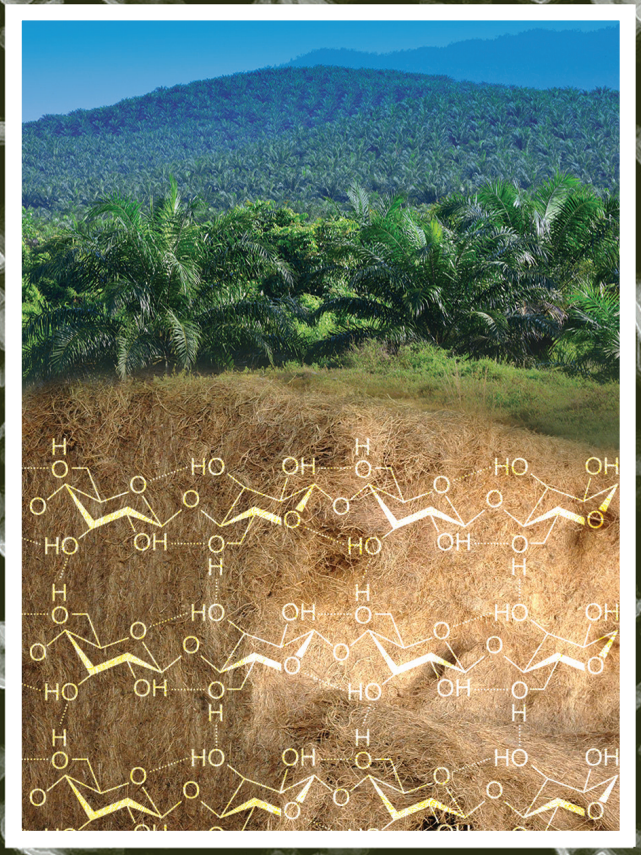
EARLY VIEW
Available online
http://jopr.mpob.gov.my/?myCat=InPress



Journal of Oil Palm Research

Vol. 33 (3) September 2021

REVIEW ARTICLE

Potential of Functionalised Cellulose from Oil Palm Biomass as Nitrogen and Phosphorus-based Nutrient Adsorbent – A Review

ISSN 1511-2780

JOURNAL OF OIL PALM RESEARCH (formerly known as ELAEIS)

RM30 per issue for Malaysians. USD15 per issue for international subscribers. Allow 14 days for delivery after receipt of order.

JOURNAL OF OIL PALM RESEARCH, an international refereed journal, carries full-length original research papers, short communications and scientific review papers on various aspects of oil palm and palm oil and other palms. JOURNAL OF OIL PALM RESEARCH is published four times per year, *i.e.* March, June, September and December.

© Malaysian Palm Oil Board, 2021

All rights reserved. No part of this publication may be reproduced in any form or by any means without the written permission of the Malaysian Palm Oil Board.

Impact Factor:
2.057
data from *2020 Journal Citation Report*® Science Edition
– A Clarivate Analytics product.

For more information on advertisement for the JOURNAL OF OIL PALM RESEARCH, please write to:

Editor-in-Chief
Journal of Oil Palm Research
Malaysian Palm Oil Board
6 Persiaran Institusi, Bandar Baru Bangi
43000 Kajang, Selangor, Malaysia

Tel: *603-8769 4400*
E-mail: *pub@mpob.gov.my*
Website: *jopr.mpob.gov.my*

DISCLAIMER
Views of writers expressed in this publication are not necessarily endorsed by or represent the views of the Malaysian Palm Oil Board.

ADVERTISEMENT RATES

POSITION	RATE	DIMENSION
Full Page (Black and White)	RM600/USD300	Full page : 280 mm × 190 mm
Full Page (Colour)	RM800/USD400	Bleed : 300 mm × 210 mm

ARTWORK

Advertisers are required to submit their colour artwork via email or Cloud Share to pub@mpob.gov.my

CLOSING DATES

March Issue – 1 February
June Issue – 1 May
September Issue – 1 August
December Issue – 1 November

Published by the Malaysian Palm Oil Board

JOURNAL OF OIL PALM RESEARCH

Vol. 33 (3) September 2021

CONTENTS

REVIEW ARTICLE

387 Potential of Functionalised Cellulose from Oil Palm Biomass as Nitrogen and Phosphorus-based Nutrient Adsorbent – A Review
Mei Mei Chong; Lian See Tan; Nurfatehah Wahyuny Che Jusoh; Masafumi Goto and Sumathi Sethupathi

RESEARCH ARTICLES

400 Neural Networks Method in Predicting Oil Palm FFB Yields for the Peninsular States of Malaysia
Yousif Y Hilal; Yahya, A; Ismail, W I W and Asha'ari, Z H

413 Preliminary Study on Efficiency of Different Time and Light Source in Light Traps for Capturing Population of Adult Oil Palm Bunch Moth, *Tirathaba mundella* (Lepidoptera: Pyralidae)
Mohamad Rosman Sulaiman; Saharul Abillah Mohamad; Mohamed Mazmira Mohd Masri; Siti Nurulhidayah Ahmad and Norman Kamarudin

425 Identification and Determination of the Spectral Reflectance Properties of Live and Dead Bagworms, *Metisa plana* Walker (Lepidoptera: Psychidae) using VIS/ NIR Spectroscopy
Mohd Najib Ahmad; Abdul Rashid Mohamed Shariff; Ishak Aris; Izhal Abdul Halin and Ramle Moslim

436 Oil Palm Male Meiosis Profiling: From Field Observation to Cytogenetics Analysis
Nordiana, H M N; Madon, M; Singh, R; Sritharan, K; Muhammad Azwan, Z and Zaki, N M

447 Molecular Cloning of *Elaeis guineensis* Phytoene Synthase (*Egpsy*) and its Expression in Mesocarp Tissues
Wan Nur Syuhada, W S; Rasid, O A and Ghulam Kadir Ahmad Parveez

458 Quality Improvement of Palm Kernel Cake as Broiler Feed using Pre-Cleaning System
Rohaya Mohamed Halim; Ridzuan Ramli; Che Rahmat Che Mat; Nu'man Abdul Hadi; Mohd Firdaus Othman and Astimar Abd Aziz

473 Production of Furfural from Oil Palm Fibres
Nur Eliyanti Ali Othman; Astimar Abd Aziz; Wan Hasamudin Wan Hassan; Nor Faizah Jailani; Fazliana Abd Hamid and Noorshamsiana Abdul Wahab

482 Drying of Oil Palm Lumber by Combining Forced-air Drying and Modified Super-Fast Drying Methods
Muhammad Nadzim, M N; Edi, S B; Mojtaba, S; Zaidon, A and Lee, S H

493 Quality of Commercial Palm-based Cooking Oil Packed in Plastic Pouch and Polyethylene Terephthalate (PET) Bottle
Norazura Aila Mohd Hassim; Nur Haqim Ismail; Sivaruby Kanagaratnam; Wan Rosnani Awg Isa and Noor Lida Habi Mat Dian

514 Prediction of Acid, Peroxide and TBA Values of Heat-Treated Palm Oil using a Partial Least Squares-Ordinary Least Squares Model Based on Fourier Transform Infrared Spectroscopy
Kusnandar, F; Lioe, H N; Faridah, D N; Anggraeni, R and Pricilia

524 Development of Palm-based Vanaspati (Vegetable Ghee): Effects of Crystallisation Procedures on the Product Texture
Rafidah Abd Hamid; Sivaruby Kanagaratnam; Norazura Aila Mohd Hassim; Nur Haqim Ismail; Wan Rosnani Awg Isa and Noor Lida Habi Mat Dian

532 Is Palm Mid Fraction a Healthier Choice as a Cocoa Butter Equivalent?
Voon, P T; Toh, S W H; Ng, T K W; Lee, V K M; Yong, X S; Ng, Y T and Nesaretnam, K

542 Rheological Properties of Palm-based Carboxymethyl Cellulose Solutions
Nor Zuliana Yusof; Zafarizal Aldrin Azizul Hasan; Nur Eliyanti Ali Othman and Yusrabbil Amiyati Yusof

SHORT COMMUNICATION

555 Principal Component Analysis (PCA) Evaluation of Liquid Chromatography-mass Spectrometry (LC-MS) Datasets of *Ganoderma boninense* Intracellular Metabolites
Zain Nurazah; Abrizah Othman and Umi Salamah Ramli

Cover picture: Potential cellulosic products from oil palm biomass.

EDITORIAL BOARD

(1 January 2021 – 31 December 2021)

Dr. Ahmad Parveez Ghulam Kadir
Malaysia (Editor-in-Chief)

Dr. Gee Ping Tou
Malaysia

Dr. Trevor Anthony Jackson
New Zealand

Dr. Carl Traeholt
Malaysia

Prof. Dr. Tom Sanders
United Kingdom

Prof. Dr. Matthias Finkbenier
Germany

Mr. Roch Desmier de Chenon
Australia

Prof. Dr. Stanislav Miertus
Slovakia

Dr. Julie Flood
United Kingdom

Prof. Douglas G Hayes
USA

Prof. Dr. Dahlan Ismail
Malaysia

Prof. Dr. Zarinah Hamid
Malaysia

Prof. Dr. Dirk Prufer
Germany

PUBLICATION COMMITTEE

CHAIRPERSON
Dr. Ahmad Parveez Ghulam Kadir

SECRETARY
Anita Taib

COMMITTEE MEMBERS
Dr. Zainab Idris
Dr. Ramle Moslim
Rosidah Radzian
Dr. Astimar Abdul Aziz
Dr. Mohamad Arif Abd Manaf
Dr. Idris Abu Seman
Dr. Yeong Shoot Kian
Dr. Aki @ Zaki Aman
Ruba'ah Masri
Fauziah Arshad
Mohd Saufi Awang
Iptisam Abdul Wahab

REVIEW ARTICLE

Journal of Oil Palm Research Vol. 33 (3) September 2021 p. 387-399
DOI: https://doi.org/10.21894/jopr.2020.0088

POTENTIAL OF FUNCTIONALISED CELLULOSE FROM OIL PALM BIOMASS AS NITROGEN AND PHOSPHORUS-BASED NUTRIENT ADSORBENT - A REVIEW

MEI MEI CHONG[1]; LIAN SEE TAN[1]*; NURFATEHAH WAHYUNY CHE JUSOH[1]; MASAFUMI GOTO[1] and SUMATHI SETHUPATHI[2]

ABSTRACT

By the year 2020, oil palm biomass in Malaysia is projected to reach between 85 to 110 million tonnes per year. Instead of disposing off such a massive amount of biomass as waste, the oil palm biomass could be converted into value-added products. Since lignocellulosic materials could be a suitable adsorbent for nitrogen and phosphorus-based nutrients from aquaculture effluent based on studies conducted by other countries, it would be an excellent opportunity to monetise oil palm biomass for a similar purpose as well. There are many well-established extraction methods introduced by researchers. However, only a handful of the extraction method involved the use of green chemicals. This article provides a review of the extraction and modification for oil palm biomass towards becoming a potential adsorbent for nitrogen and phosphorus-based nutrients.

Keywords: adsorption, cellulose, nitrate, oil palm biomass, phosphate.

Received: 11 November 2019**; Accepted:** 8 July 2020**; Published online:** 14 October 2020.

INTRODUCTION

Malaysia is the second-largest palm oil producer globally, following behind Indonesia (Abdullah and Sulaiman, 2013; Kushairi *et al.*, 2019). Oil palm was introduced to Malaya in the year 1871 and the first commercial oil palm plantation started in the year 1917 at Tennamarran Estate in Selangor, Malaya (Awalludin *et al.*, 2015; Onoja *et al.*, 2019). Since then, oil palm has been planted extensively in Malaysia until present as Malaysia's tropical weather suits the required condition to plant the oil palm trees (Kamil and Omar, 2016). Subsequently, the amount of biomass from oil palm also inadvertently increases with the extensive planting of oil palm. By the year 2020, oil palm biomass in Malaysia is projected to reach between 85 to 110 million tonnes per year (Malaysian-German Chamber of Commerce and Industry, 2017). Generally, oil palm generates six types of biomass, namely oil palm fronds (OPF), oil palm trunk (OPT), oil palm empty fruit bunch (OPEFB), fresh-pressed fibre, oil palm shell, and palm oil mill effluent (POME) (Abdullah and Gerhauser, 2008; Shuit *et al.*, 2009; Umar *et al.*, 2013; Zakaria *et al.*, 2014; Lamaming *et al.*, 2017; Mohd Rasli *et al.*, 2017; Mohtar *et al.*, 2017). According to Onoja *et al.* (2019), 75% of the oil palm biomass is from OPF and OPT while the other biomass covers the remaining 25%. Comparing OPF and OPT, OPF has higher cellulose content with 60% of the cellulose is in the basal portion, and 40% in the leaf (Malaysia Innovation Agency, 2013). However, currently, usage of OPF is limited to a few industries such

[1] Department of Chemical and Environmental Engineering, Malaysia - Japan International Institute of Technology, Universiti Teknologi Malaysia, Jalan Sultan Yahya Petra, 54100 Kuala Lumpur, Malaysia.

[2] Department of Environmental Engineering, Faculty of Engineering and Green Technology, Universiti Tunku Abdul Rahman, Jalan Universiti, Bandar Barat, 31900 Kampar, Perak, Malaysia.

* *Corresponding author e-mail: tan.liansee@utm.my*

as for steam production, bio-sugar production and fertiliser (Malaysia Innovation Agency, 2013). Rather than treating it as a common agricultural waste, the high cellulose content can be extracted and isolated for modification into a useful adsorbent.

On the other hand, other than oil palm production, Malaysia covers 1% of the world's seafood supply (Mohamed Omar, 2017b). Here is where the aquaculture industry plays a role where numerous aquaculture industrial zones were reserved for farmed fishes for the purpose of satisfying the global seafood demand (FAO, 2016). Aquaculture in Malaysia is categorised into marine and freshwater, whereby freshwater fishes are highly in demand and provide the most job opportunities compared to marine aquaculture (Mohamed Omar, 2017a). However, the downside of freshwater aquaculture is that the water used to farm fishes has to be replaced once every several months due to excessive nutrients content. Nutrients such as nitrate and phosphate are the main source of eutrophication condition (Cripps and Bergheim, 2000; Wang *et al.*, 2010; Castine *et al.*, 2013; Hokkanen *et al.*, 2016; Kim *et al.*, 2016; Yin *et al.*, 2018; Pan *et al.*, 2018; Wu *et al.*, 2019; Karthikeyan *et al.*, 2019; Lee *et al.*, 2019). It can disrupt the fishes' respiratory system and decrease the dissolved oxygen in the water (Kioussis *et al.*, 2000; Anirudhan *et al.*, 2006; Ng *et al.*, 2018). Other than aquaculture effluent, the sources of nitrate and phosphate nutrients in running water are livestock manure (Yin *et al.*, 2017) and excessive use of fertiliser in industries (Keränen *et al.*, 2013). These would eventually cause the nitrate and phosphate nutrients to leach into receiving water bodies and contaminating it. Overdose of phosphate nutrients can also cause disorder in the growth of seaweed and aquatic plants (Kioussis *et al.*, 2000; Anirudhan *et al.*, 2012; Turcios and Papenbrock, 2014). Over the concentration threshold of nitrate anion nutrients can result in methemoglobinaemia 'baby blue' syndrome in infants, formation of carcinogenic nitrosamines, and nitrosamides upon human consumption (Hamoudi and Belkacemi, 2013). Hence, proper effluent treatment is required to reduce the concentration of both nitrate and phosphate nutrients in the aquaculture effluent before it can be released to receiving water bodies or reused back into aquaculture.

Various treatments based on biological (Lin *et al.*, 2002; Akinbile and Yusoff, 2012) and physicochemical (Kioussis *et al.*, 2000; Orlando *et al.*, 2002; Wang *et al.*, 2007; Anirudhan and Senan, 2011; Keränen *et al.*, 2013; Sehaqui *et al.*, 2016; Fan and Zhang, 2018; Qiao *et al.*, 2019; Stjepanović *et al.*, 2019; Shojaipour *et al.*, 2020) methods have been studied for the adsorption of nutrients from wastewater. However, the adsorption method using biomass must be brought to attention as agriculture waste is relatively cheap, and it serves great flexibility in the aquaculture industry. Typically, activated carbon was used as an adsorbent but due to the increasing cost, many ventured into cheaper alternative solutions to adsorb the nutrients (Stjepanović *et al.*, 2019; Yu *et al.*, 2019).

Therefore, this article aims to review the current trend of adsorption of the nitrate and phosphate nutrients and delve into the potential of functionalised cellulose from oil palm biomass as nitrate and phosphate nutrients adsorbent.

ADSORPTION OF NITRATE AND PHOSPHATE

The adsorption of nitrate and phosphate nutrients from aquaculture effluent has been studied using different lignocellulosic materials and water treatments. *Table 1* shows a summary of the study on the adsorption of nitrate and phosphate anion nutrients previously conducted by other researchers. Based on the studies, the adsorption of the nutrients can generally be conducted at ambient conditions. Biological methods would require a longer duration (between weeks to months) to obtain significant results. Meanwhile, adsorption of the nutrients via adsorption method can be accomplished within hours. These studies accentuate the efficiency of the adsorption method for adsorption of the nitrogen and phosphorus-based nutrients.

The modification of polymer hydrogel was created to have positive charge ends to attract the negatively charged nitrate and phosphate by Kioussis *et al.* (2000). A hydrogel is a three-dimensional polymer with hydrophilic property. Polymer hydrogel can be made of different polymer composition depending on the desirable properties. Based on Kioussis *et al.* (2000), poly(ally amine) hydrochloride was used to make the polymer hydrogel. It is a water-soluble cationic polymer and can be highly water-swollen hydrogel with chemical crosslinking. The poly(ally amine) hydrochloride polymer hydrogel has pendant primary amino groups where it will selectively attract anion nutrients via electrostatic force and trap the nutrients in the gel network. The equilibrium adsorption of nitrate and phosphate anion nutrients was obtained in 3 hr with a neutral pH of the wastewater. In addition, the hydrogels could potentially be reusable for up to five cycles to achieve maximum adsorption. Shojaipour *et al.* (2020) conducted a study on the efficiency of nitrate adsorption on modified hydrogel with quaternary ammonium salt. The gum tragacanth biopolymer hydrogel was functionalised with N-(trimethylsilyl) imidazole and (3-chloropropyl) trimethoxysilane to adsorb nitrate anion nutrient via ion exchange. The highest adsorption of nitrate anion nutrient obtained was at a neutral pH (pH 7.0) in 20 min. This would allow the hydrogels to be conveniently used without using pH adjuster in wastewater.

TABLE 1. COMPILATION OF MULTIPLE TREATMENT TYPE FOR NITRATE AND PHOSPHATE ANION NUTRIENTS

Type of treatment	Parameter			Recovery/ removal performance	Reference
	Temperature (°C)	pH	Time		
Amine cross-linked tea waste via adsorption	25.0	3.0-10.0	60 min	Nitrate: 136.43 mg g^{-1} Phosphate: 98.73 mg g^{-1}	Qiao *et al.* (2019)
Brewer's spent grain via adsorption	25.0	4.0-10.0	60 min	Nitrate: 22.65 mg g^{-1}	Stjepanović *et al.* (2019)
Constructed wetlands system	24.3-29.6	-	1-7 months	Nitrate: 86.0%-98.0% Phosphate: 32.0%-71.0%	Lin *et al.* (2002)
Corn stalks cellulose via adsorption	25.0	6.80	6 hr	Nitrate: 13.6054 mg g^{-1} Phosphate: 22.8833 mg g^{-1}	Fan and Zhang (2018)
Gum tragacanth carbohydrate produce hydrogel via adsorption	25.0	Neutral	20 min	Nitrate: 98.26%	Shojaipour *et al.* 2020)
Nanofibres from waste pulp residues via adsorption	25.0	5.0-7.0	24 hr	Nitrate: 39.0% Phosphate: 61.0%	Sehaqui *et al.* (2016)
Novel cellulose-based via adsorption	30.0	6.0	6 hr	Phosphate: 99.1%	Anirudhan and Senan (2011)
Pine sawdust, pine bark, spruce bark, birch bark, birch pear via adsorption	25.0	3.0-10.0	5-10 min	Nitrate: 70.0%-86.0%	Keränen *et al.* (2013)
Polymer hydrogels via adsorption	25.0	7.7	3 hr	Nitrate: 50.0% Phosphate: 98.0%	Kioussis *et al.* (2000)
Sugarcane bagasse via adsorption	30.0	6.5	24 hr	Nitrate: 9.0 mg $litre^{-1}$ Phosphate: 4.0 mg $litre^{-1}$	Orlando *et al.* (2002)
Water hyacinth and lettuce via biological method	25.0-35.0	6.72	1-4 weeks	Nitrate: 90.92%, 39.78% Phosphate: 83.59%, 55.90%	Akinbile and Yusoff (2012)
Wheat straw via adsorption	24.0	6.8	150 min	Nitrate: 80%	Wang *et al.* (2007)

Besides hydrogel, lignocellulosic materials such as corn stalks, waste pulp residues, sugarcane bagasse, and wheat straws were studied as an adsorbent for nitrate and phosphate nutrients as well. These lignocellulosic materials were pre-treated to extract and isolate cellulose compound, and it was further modified via cationisation to form a positively charged ends (Orlando *et al.*, 2002; Wang *et al.*, 2007; Keränen *et al.*, 2013; Sehaqui *et al.*, 2016; Fan and Zhang, 2018; Qiao *et al.*, 2019; Stjepanović *et al.*, 2019). These positively charged ends will attract the negatively charged nitrate and phosphate ions present in the aquaculture effluent via electrostatic attraction (Keränen *et al.*, 2013; Qiao *et al.*, 2019; Stjepanović *et al.*, 2019). Electrostatic attraction force creates a strong bond between the positively and negatively charged particles and provides easy desorption by adding used adsorbent into sodium chloride (NaCl) solution (Keränen *et al.*, 2013).

Cationisation of cellulose performed to functionalise for the adsorption of nitrate and phosphate nutrients is commonly achieved via quaternary ammonium salts. This allows ammonium positive ends to be grafted onto the cellulose, which promotes the adsorption of nitrate and phosphate anion nutrients. The adsorption will then be carried out via electrostatic force and ion exchange (with the presence of chlorine anions from the chemical used for quaternary ammonium salts) (Shojaipour *et al.*, 2020).

During the adsorption of nitrate and phosphate anion nutrients, the surrounding parameters play a significant role. The varying parameters such as pH of adsorbate solution, the temperature of adsorbate solution, and contact time between the adsorbent and adsorbate should be monitored to obtain high adsorption capacities of nitrate and phosphate anion nutrients. Studies have shown that pH of aquaculture effluent within the range of 3.0-10.0 would be an optimal range for the adsorption of nitrate and phosphate (Kioussis *et al.*, 2000; Orlando *et al.*, 2002; Wang *et al.*, 2007; Keränen *et al.*, 2013; Sehaqui *et al.*, 2016; Fan and Zhang, 2018; Yin *et al.*, 2018; Karthikeyan *et al.*, 2019; Qiao *et al.*, 2019; Stjepanović *et al.*, 2019; Wu *et al.*, 2019). However, the highest adsorption capacities of the nitrate and phosphate anion nutrients were usually achieved within a pH of 5.0-6.5 (Keränen *et al.*, 2013; Qiao *et al.*, 2019; Stjepanović *et al.*, 2019). This could be because of the dominant presence of chloride (Cl^-) ions on

the surface of active sites of the adsorbent when the pH is lower than 3.0, thus, reducing the electrostatic force between nitrate and phosphate anions and the active sites of the adsorbent (Stjepanović *et al.*, 2019). When the pH is higher than 10.0, the competition between OH^- ions and both nitrate and phosphate anions will occur, leading to electrostatic repulsion and lower available active sites on the surface of the adsorbent (Qiao *et al.*, 2019).

The temperature of the solution plays a vital role in the adsorption of nitrate and phosphate anion nutrients as well. As reported by Shojaipour *et al.* (2020), increasing the temperature from 25°C-45°C, the adsorption capacity of nitrate anion nutrients had decreased. The decrease in adsorption capacity is due to the exothermic reaction exerted during the adsorption process (Shojaipour *et al.*, 2020). Thus, with higher temperatures, the electrostatic bond between the nitrate anion and cationic end of adsorbent might be weakened.

The effect of contact time between the adsorbent and the nitrate and phosphate anion nutrients serve as a function to provide sufficient time for nitrate and phosphate anion nutrients to fill up all vacant pores on the surface of the adsorbent. Hence, reaching an equilibrium concentration before the used adsorbent undergoes desorption for reusability purposes. As shown in *Table 1*, constructed wetlands systems (Lin *et al.*, 2002) and biological method of adsorption via water hyacinth and lettuce (Akinbile and Yusoff, 2012) required a longer time to achieve better adsorption capacity of nitrate and phosphate anion nutrients. Although the biological method is an alternatively cheap method, it reacts relatively slow when the effluent contains a high load of nitrate and phosphate anion and low temperature (Stjepanović *et al.*, 2019). The same concept applies to constructed wetland systems where it is dependent on the microbial's reactivity to treat the nitrate and phosphate anion loaded effluent (Lin *et al.*, 2002).

OIL PALM BIOMASS

Since lignocellulosic material is currently in focus to act as an adsorbent, oil palm biomass could be a good representation of lignocellulosic material. In *Figure 1*, the detailed composition of oil palm biomass consists of cellulose, hemicellulose, and lignin. Each type of biomass has its unique characteristic which differs from one another.

Lignin is the aromatic polymer in the lignocellulose components. It has a random substitution arrangement of phenylpropane monomeric units which consist of syringly and guaiacyl *p*-hydroxylphenyl units (Klemm *et al.*, 2005). On the other hand, hemicellulose has different monosaccharide units which are pentose sugar dominant. It can exist in the forms of either homo-polymer or hetero-polymer, and it is alkali-soluble (Malaysia Innovation Agency, 2013; Kumneadklang *et al.*, 2019) Hence, it is the main component in the production of bio-sugar due to its high sugar composition and easy hydrolysis process (Malaysia Innovation Agency, 2013). Meanwhile, cellulose is a linear homopolymer formed from the repeating D-anhydroglucosepyranose (AGU) monomers which are connected by β-(1,4)-glycosidic linkages (Klemm *et al.*, 2005). Each monomer is rotated 180° with respect to one another in the arrangement of the polymer, giving it the crystalline structure. Hence, this structure makes cellulose resistant to acid and enzymatic hydrolysis.

Since oil palm biomass is a major representation of lignocellulosic material in Malaysia with an abundance amount, the cellulose content can be extracted and functionalised to adsorb nitrate and phosphate nutrient ions. This study aids in reducing the amount of oil palm biomass by expanding its product value as well as providing an alternative method in wastewater treatment.

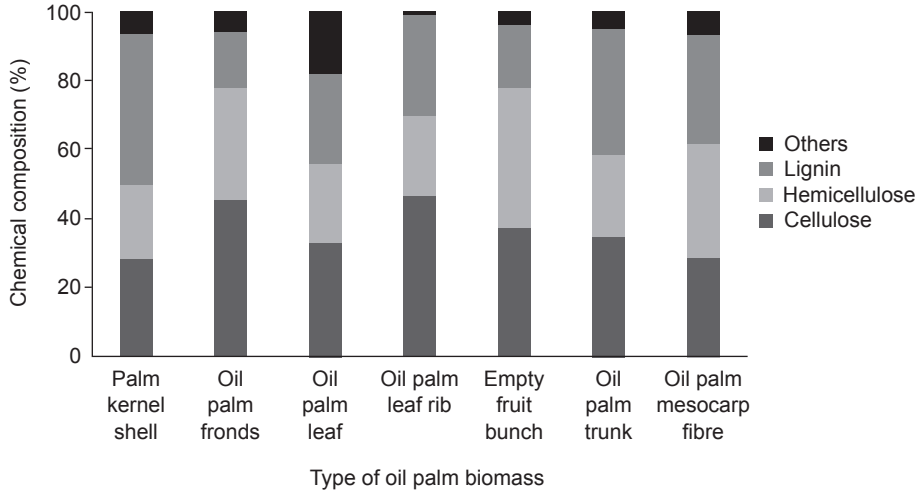


Figure 1. Chemical composition of different types of oil palm biomass (% dry weight).

GENERAL USE OF OIL PALM BIOMASS IN ADSORPTION

For the past years, oil palm biomass was studied to expand its product value (Abdullah and Gerhauser, 2008; Sumathi *et al.*, 2008; Abnisa *et al.*, 2011; Tan and Lee, 2012; Nazir *et al.*, 2013; Zakaria *et al.*, 2014; Awalludin *et al.*, 2015; Lefatshe *et al.*, 2017; Ooi *et al.*, 2017). The expansion of oil palm biomass as an adsorbent was one of the studies which are still ongoing in the current research field. Researchers had been utilising the lignocellulosic material into adsorbing pollutants, especially dyes and heavy metals, in various forms of the adsorbent. *Table 2* shows a summary of the usage of different types of oil palm biomass in adsorption of dye and heavy metal studies through the years.

Oil palm biomass had been mainly used in the study of adsorption on dyes and heavy metals. The oil palm biomass was either used in its isolated cellulose form (Hasnain *et al.*, 2007; Saman *et al.*, 2018), or it was further processed into microcrystalline cellulose (Hussin *et al.*, 2016), activated carbon (Ooi *et al.*, 2017), or biochar (Daneshfozoun *et al.*, 2017). This showed the flexibility of using lignocellulose material, such as oil palm biomass itself, to be an excellent adsorbent for charged ions with or without pre-treatment.

The introduction of oil palm biomass into adsorption started with using oil palm ash. Oil palm ash is the leftover after oil palm biomass was used in burners to produce steam. Essentially, Hasnain *et al.* (2007) discovered that this oil palm ash contains carbonaceous compounds with the presence of pores on them. Therefore, the ash was used to adsorb dyes such as disperse blue and disperse red which are commonly found in textile related industrial wastewater due to colouring of products (Hasnain *et al.*, 2007). Methylene blue was another common adsorbate for study on the adsorption towards oil palm biomass (Hussin *et al.*, 2016; Shanmugarajah *et al.*, 2019). The adsorption of dyes towards oil palm biomass was proven to be feasible under certain parameters. However, the modification of pH was often needed for high adsorption efficiency.

Another form of adsorbate used to study the adsorption capability of oil palm biomass was heavy metals. Iron (III), lead (VI), lead (II), hexavalent chromium (VI), copper (II), zinc (II), nickel (II), and manganese (II) are examples of heavy metals used by previous researchers in their field of study on adsorption of heavy metals on oil palm biomass (Hasnain *et al.*, 2008; Khosravihaftkhany *et al.*, 2013; Daneshfozoun *et al.*, 2017; Saman *et al.*, 2018). The studies indicated good adsorption performance under alkaline pH and with quick equilibrium adsorption contact time. Hence, it is safe to say that the study of adsorption on oil palm biomass with dyes and heavy metals are well established. In addition, as shown in *Table 2*, the tested methylene blue dye favoured adsorption in acidic solution while heavy metals favoured adsorption in alkaline solution. This condition would require an additive to adjust the pH of wastewater prior to the adsorption process, and it could incur additional cost and a more complex operational handling. The concentration of the dye and heavy metals in the wastewater plays a vital role as well, due to the limitation of adsorption capacity of the adsorbent. Thus, usually, the higher the concentration, the lower the percentage removal of the dye and heavy metals. The highest removal percentage (~100%) was mostly achieved in the lowest concentration level (Hasnain *et al.*, 2008). However, none of the studies conducted on the usage of oil palm biomass as adsorbent tested its feasibility for the adsorption of nitrogen and phosphorus based nutrients. Hence, the subsequent sections of this article focus on reviewing methods for the aforementioned purpose.

GREEN EXTRACTION OF CELLULOSE FROM OIL PALM BIOMASS

The extraction of cellulose from oil palm biomass has been well established over the years. Cellulose may come in many forms such as alpha-cellulose, microcrystalline cellulose, and nanocrystalline cellulose. Alpha-cellulose is the main focus in this article as it is quicker to extract from oil palm biomass as compared to the extraction of microcrystalline and nanocrystalline cellulose and separate from adsorbate solution once it is used as an adsorbent. The green method has recently been the highlight amongst researchers due to its environmental friendly advantages such as the usage of environmental friendly chemicals (*i.e.* formic acid and acetic acid) (Nazir *et al.*, 2013). This could eliminate the use of sodium chlorite as a bleaching agent due to its ability to release chlorine ions during the extraction of cellulose from oil palm biomass.

The green method can further be categorised into eco-friendly reagent, ionic liquid, ozonolysis, and hydrothermal pre-treatment (Noorshamsiana *et al.*, 2017). However, ozonolysis and hydrothermal pre-treatment methods are not suitable for the extraction of cellulose from palm oil biomass. This is because ozonolysis generally only removes the high content of lignin neglecting the removal of hemicellulose from the lignocellulosic composition (Noorshamsiana *et al.*, 2017). Meanwhile, hydrothermal pretreatment is mainly used in the extraction of glucose for bio-sugar production and bioethanol production (Malaysia Innovation Agency, 2013). In lieu, only eco-friendly reagent and ionic liquid shall be discussed in this section.

TABLE 2. COMPILATION ON THE STUDY OF OIL PALM BIOMASS AS AN ADSORBENT FOR WATER TREATMENT

Oil palm biomass	Pre-treatment	Pollutant	Type of pollutant	Parameters			Findings	Reference
				pH	Concentration	Time		
Oil palm ash	-	Disperse blue and disperse red	Dye	2.0-5.0	50-250 mg litre^{-1}	1-90 min	99% of adsorption was obtained a pH 2.0. Adsorption obeyed Langmuir isotherm and pseudo-second order kinetic.	Hasnain Isa *et al.* (2007)
Oil palm frond	20% active alkaline and 30% sulfidity was used to conduct Kraft Pulping process.Acetic acid, hydrochloric acid and sodium hydrochlorite was used in the extraction of microcrystalline cellulose and alpha-cellulose	Methylene blue	Dye	-	100 mg litre^{-1}	-	The microcrystalline cellulose showed significantly higher adsorption capacity compared to the alpha-cellulose.	Hussin *et al.* (2016)
Oil palm empty fruit bunch	NaOH and sodium chlorite were used for bleaching. The bleached sample were further hydrolised using sulphuric acid	Methylene blue	Dye	2.0-11.0	50-300 mg litre^{-1}	0-200 min	The highest removal efficiency (~90%) was obtained between pH of 8.0 to 10.0. Adsorption obeyed Langmuir isotherm and pseudo-second order kinetics.	Shanmugarajah *et al.* (2019)
Oil palm fibre	Sulphuric acid with heat	Hexavalent chromium (VI)	Heavy metal	1.5-5.0	20-200 mg litre^{-1}	0-6.0 hr	100% of removal efficiency was obtained at pH 1.5. Adsorption obeyed Freundlich and pseudo-second order kinetics.	Hasnain Isa *et al.* (2008)

TABLE 2. COMPILATION ON THE STUDY OF OIL PALM BIOMASS AS AN ADSORBENT FOR WATER TREATMENT (continued)

Oil palm biomass	Pre-treatment	Pollutant	Type of pollutant	Parameters			Findings	Reference
				pH	Concentration	Time		
Oil palm bark, oil palm frond, oil palm leaves	Wash, dry, and sieved at 200-1 400 µm	Iron (III) and Lead (VI) heavy metal ions	Heavy metal	1.5-6.0	500 mg litre^{-1}	0-80 min	The highest removal efficiency was obtained between pH 5.0-6.0, with OPB removing 78%, of iron (III) and lead (VI) respectively. Adsorption obeyed Langmuir and pseudo-second order kinetics.	Khosravihaftkhany *et al.* (2013)
Oil palm empty fruit bunch	Sonicated together with iron (II) oxide	Lead (II), Copper (II), Zinc (II), Nickel (II), Manganese (II)	Heavy metal	3.0-10.0	100-1 000 mg litre^{-1}	0-100 min	The highest removal (~90%) for each heavy metal ions was obtained between pH of 5.0-7.0.	Daneshfozoun *et al.* (2017)
Oil palm trunk	Dewaxed with toluene/ethanol (2/1, v/v), and bleached using sodium hydroxide + hydrogen peroxide	Aurum (III)	Precious metal	3.0-7.0	10-205 mg litre^{-1}	0-1440 min	100% removal was obtained in an acidic condition for low concentration of 10 mg litre^{-1}. However increasing concentration led to lower percentage removal due to the limitation of active site. Adsorption obeyed Langmuir isotherm and pseudo-second kinetics.	Saman *et al.* (2018)
Palm kernel shell	Washed with nitric acid, carbonised and treated with sulphuric acid	Urea	Uremic toxins	-	38 500 µmol	0-120 min	Adsorption of urea increase with increasing temperature of 400°C-600°C due to increasing pore sizes.	Ooi *et al.* (2017)

TABLE 3. COMPILATION ON METHODS OF CELLULOSE EXTRACTION FROM OIL PALM BIOMASS

Type of Biomass	Solvent	Parameter			Findings	Reference
		Temperature (°C)	pH	Time		
Oil palm empty fruit bunch	Fungal and phosphoric acid	-	-	-	Cellulose: 53.81%	Isroi *et al.* (2012)
Oil palm empty fruit bunch	Formic acid, sodium hydroxide, hydrogen peroxide, ethanol	85.0-121.0	7.0-11.0	90 min	Alpha-cellulose: 93.7%	Nazir *et al.* (2013)
Oil palm fronds	Soda-AQ, magnesium sulphate, hydrogen peroxide, acetic acid	70.0-160.0	4.0-5.0	30 min-1 hr	Alpha-cellulose: 96.50%	Dungani *et al.* (2017)
Oil palm frond	Sodium hydroxide, sodium chlorite	80.0	-	2-4 hr	Cellulose: 40.0%	Mohd Rasli *et al.* (2017)
Oil palm mesocarp fibre	Sodium hydroxide, acetic acid, hydrogen peroxide, sulphuric acid	70.0-160.0	-	1-24 hr	Cellulose: 88.8%	Megashah *et al.* (2018)
Oil palm empty fruit bunch					Cellulose: 93.0%	
Oil palm frond					Cellulose: 94.6%	
Oil palm trunk	Ethanol, toluene, sodium chlorite, potassium hydroxide, sulphuric acid	20.0-70.0	4.0-5.0	1-24 hr	Alpha-cellulose: 51.75%	Lamaming *et al.* (2015)
Oil palm trunk and oil palm frond	Sodium hydroxide, sulphuric acid, acetic acid, ethanol, toluene, sodium chlorite	80.0	Neutral	60 min	Alpha-cellulose: 41.55%-64.42%	Lai and Idris (2013)

Table 3 summarises the methods of cellulose extraction from oil palm biomass. Thus far, cellulose extraction from oil palm biomass could be achieved at a minimum yield of 40% using conventional solvents as a bleaching agent. According to Nazir *et al.* (2013), the replacement of sodium chlorite as a bleaching agent by a mixture solution of formic acid with hydrogen peroxide gives a great advantage in reducing the amount of hazardous ions (chloride ions) released. Coupled with steam explosion, this method can soften the lignin and gives better penetration of the bleaching agent to remove lignin and hemicellulose easily. An estimation of 93.7% of alpha-cellulose with 70% crystallinity was obtained using the method. This proves the efficiency of formic acid with hydrogen peroxide when it is coupled with steam explosion method.

Ionic liquid is another effective method in removing lignin and hemicellulose from the lignocellulosic material that originated from oil palm biomass (Noorshamsiana *et al.*, 2017). Ionic liquid is also known as a designers' solvent due to its strong dissolution properties which are made suitable to breakdown complex macromolecules and polymeric materials in the recalcitrant cellulose (Tan and Lee, 2012). According to Mohtar *et al.* (2017), ionic liquid's superior solvency properties came from its capability to disrupt strong linkages between cellulose and lignin via hydrogen bond and dipole bond formation. An added advantage of ionic liquid's method of extraction is the ability to recycle the solvent used for extraction purposes, this method also provides an alternative to replace the usage of harmful organic solvents (Mohtar *et al.*, 2017). However, the solvent used to perform ionic liquid's method is indeed costly. It is also of high viscosity and is usually less effective in removing hemicellulose compared to acid hydrolysis (Jana and Ulla, 2011). Hence, there was a need for further alkaline treatment in the process to improve the yield of cellulose (Mohtar *et al.*, 2017).

MODIFICATION OF CELLULOSE

After most of the alpha-cellulose is extracted, it can be modified chemically to enhance the electrostatic attraction between the adsorbent and adsorbate. Since nitrate and phosphate are negatively charged naturally, it would be of advantage if the adsorbent is positively charged. A modification method proposed by Orlando *et al.* (2002) using epichlorohydrin, dimethylformamide, pyridine, and dimethylamine has inspired many researchers to continue the method of modification and altered to suit different conditions. This method was tested and repeated on a few other lignocellulosic materials such as *Moringa oleifera* hull, lauan sawdust, coconut husk, rice hull, persimmon tealeaf, pine bark

sugarcane bagasse (Orlando *et al.*, 2002), banana stem (Anirudhan *et al.*, 2006), wheat straw (Wang *et al.*, 2007), and corn stalk (Fan and Zhang, 2018). The findings obtained from the studies showed encouraging results with the adsorption of 80%-50% for nitrate and up to 90% for phosphate depending on the individual or selective adsorption (Orlando *et al.*, 2002; Anirudhan *et al.*, 2006; Wang *et al.*, 2007; Fan and Zhang, 2018). However, in those studies, there was no proper pre-treatment done to extract the cellulose from the lignocellulosic material. This might eventually affect the attachment of the cations towards the lignocellulosic material. Neither were most of the articles studying the selectivity of nitrate and phosphate nutrient adsorption. In lieu, it was more towards the individual adsorption of nitrate or phosphate nutrient onto the functionalised cellulose of lignocellulosic material.

Aside from the typical cationisation, there were a few studies on creating a neutral charge modification towards commercial cellulose (Anirudhan and Senan, 2011; Anirudhan *et al.*, 2012). Anirudhan and Senan (2011) modified commercial cellulose by grafting it with iron(III) and amino-functionalised poly(glycidylmethacrylate). The modified commercial cellulose showed good adsorption towards phosphate at a pH of 6.0, with a constant agitation of 200 rpm for 2.0 hr of contact time under room temperature of 20°C. These parameters assisted in the adsorption of phosphate, achieving the removal of 99.1%. Although the parameters and result outcome were promising, the modification was conducted onto commercial cellulose and would impose a higher costing price as compared to sourcing it from biomass. Another study conducted by Anirudhan *et al.* (2012) grafted commercial cellulose with epichlorohydrin, and polyethyleneimine with N,N'-methylene bisacrylamide as a crosslinking agent and azetobis isobutyro nitrile as initiator. This method also showed favourable phosphate adsorption with the removal of 99.6% at pH 4.5 for 180 min of contact time. As the desired pH is lower, it is worth noting that the phosphate ions which were predominant in the study were dihydrogen phosphate ($H_2PO_4^-$) ions instead of the typical phosphate (PO_4^{3-}) ions. This is due to the point of zero charge pH of the functionalised cellulose which is pH 4.8. Hence, any pH more than pH 4.8 will cause the surface of the adsorbent to have a negative charge instead of a positive (Anirudhan *et al.*, 2012). They were causing the cationic ends attached to the adsorbent to repel the adsorbate.

CHALLENGES AND FUTURE DIRECTION

The main challenge in the study of adsorption of nitrate and phosphate anion nutrients is the tendency of adsorbent to perform selective adsorption towards both desired nutrients. Thus far, many studies had been conducted to adsorb nitrate and phosphate anion nutrients with a variety of adsorbent material. However, most studies are conducted with either anion nutrient present in the sample solution instead of having both the existences of anion nutrient simultaneously in the sample solution (Keränen *et al.*, 2013; Qiao *et al.*, 2019; Stjepanović *et al.*, 2019). These studies would only provide an ideal situation instead of a real-life application due to other co-existing anion nutrients present which might lower the adsorption capacity of nitrate and phosphate anion nutrients in real-life application.

As for the number of researchers who had studied on the selectivity of anion nutrients in the effluent, the outcome showed that the selectivity adsorption is favourable towards sulphate anion (Orlando *et al.*, 2002; Sehaqui *et al.*, 2016). Meanwhile, in the presence of only nitrate and phosphate anion nutrients in the effluent the outcome contradicts amongst the researchers as in some situation, the nitrate anion is much favourable due to single negative electron needed to be filled (Orlando *et al.*, 2002). Others found that with the requirement of three negative electrons, phosphate anion, it is stronger to attract the cationic ends of the adsorbent (Sehaqui *et al.*, 2016). Therefore, the need of creating an adsorbent which is able to balance the selectivity of adsorption towards nitrate and phosphate anion nutrients in the presence of other anion nutrients would be another challenge in the field.

Another challenging part of this area of study is to functionalise the extracted cellulose to obtain the positively charged ends that fulfil the criteria of green chemistry. This positively charged end enables the cellulose to act as an adsorbent in adsorbing the nitrate and phosphate, which is negatively charged, via electrostatic attraction. Although there are numerous methods introduced to functionalise the extracted cellulose, these functionalisation methods kept focusing on only targeting the hydroxyl group on sixth carbon (C6). Since C6 hydroxyl group is the primary group, it is easier to functionalise it as it is more reactive (Börjesson and Westman, 2015). However, if the functionalisation method can focus even on C2 and C3 hydroxyl groups, it would increase the number of active sites in the adsorbent for nitrate and phosphate anion nutrients.

As for the parameters of adsorption, the pH of effluent is expected to remain in the neutral range, at ambient temperature and the concentration is of the pollutant could vary significantly. Therefore, to enable the application of the modified adsorbent directly by the aquaculture industry, the adsorbent should be robust and able to perform effectively without pH adjustor, water heater/cooler and concentration level indicator.

CONCLUSION

Oil palm biomass is an excellent representation of lignocellulosic material in Malaysia due to its abundant amount produced every year. Therefore, it would be a significant step forward in using the oil palm biomass as an added feature of nitrate and phosphate anion nutrients adsorbent in order to expand its product value. With proper practice of extraction and modification of cellulose using green chemicals into effective adsorbent, it can contribute towards the safety of receiving water bodies from excessive nitrate and phosphate nutrients.

ACKNOWLEDGEMENT

The authors are grateful for the financial support given from Long Term Research Grant Scheme (LRGS) 1/2018 (UTAR-4411/S01) (UTM PY/2020/03532), Ministry of Higher Education.

REFERENCES

Abdullah, N and Gerhauser, H (2008). Bio-oil derived from empty fruit bunches. *Fuel*, *87(12)*: 2606-2613.

Abdullah, N and Sulaiman, F (2013). The oil palm wastes in Malaysia. *Biomass Now - Sustainable Growth and Use* (Matovic, M D ed.). IntechOpen. DOI: 10.5772/55302.

Abnisa, F; Daud, W M A W; Husin, W N W and Sahu, J N (2011). Utilization possibilities of palm shell as a source of biomass energy in Malaysia by producing bio-oil in pyrolysis process. *Biomass Bioenerg., 35(5)*: 1863-1872.

Akinbile, C O and Yusoff, M S (2012). Assessing water hyacinth (*Eichhornia crassopes*) and lettuce (*Pistia stratiotes*) effectiveness in aquaculture wastewater treatment. *Int. J. Phytoremediation, 14(3)*: 201-211.

Anirudhan, T S; Noeline, B F and Manohar, D M (2006). Phosphate removal from wastewaters using a weak anion exchanger prepared from a lignocellulosic residue. *Environ. Sci. Technol., 40(8)*: 2740-2745.

Anirudhan, T S; Rauf, T A and Rejeena, S R (2012). Removal and recovery of phosphate ions from aqueous solutions by amine functionalized epichlorohydrin-grafted cellulose. *Desalination, 285*: 277-284.

Anirudhan, T S and Senan, P (2011). Adsorption of phosphate ions from water using a novel cellulose-based adsorbent. *Chem. Ecol., 27(2):* 147-164.

Awalludin, M F; Sulaiman, O; Hashim, R and Nadhari, W N A W (2015). An overview of the oil palm industry in Malaysia and its waste utilization through thermochemical conversion, specifically via liquefaction. *Renew. Sustain. Energy Revi., 50*: 1469-1484.

Börjesson, M and Westman, G (2015). Crystalline Nanocellulose - Preparation, modification, and properties. *Cellulose - Fundamental Aspects and Current Trends.* p. 159-191.

Castine, S A; McKinnon, A D; Paul, N A; Trott, L A and de Nys, R (2013). Wastewater treatment for land-based aquaculture: Improvements and value-adding alternatives in model systems from Australia. *Aquac. Environ. Interact., 4(3)*: 285-300.

Cripps, S J and Bergheim, A (2000). Solids management and removal for intensive land-based aquaculture production systems. *Aquac. Eng., 22(1-2)*: 33-56.

Daneshfozoun, S; Abdullah, M A and Abdullah, B (2017). Preparation and characterization of magnetic biosorbent based on oil palm empty fruit bunch fibers, cellulose and *Ceiba pentandra* for heavy metal ions removal. *Ind. Crops Prod., 105*: 93-103.

Dungani, R; Owolabi, A F; Saurabh, C K; Abdul Khalil, H P S; Tahir, P M; Hawzan, C I C M; Ajijolakewu, K A; Masri, M M; Rosamah, E and Aditiawati, P (2017). Preparation and fundamental characterization of cellulose nanocrystal from oil palm fronds biomass. *J. Polym. Environ., 25(3)*: 692-700.

Fan, C and Zhang, Y (2018). Adsorption isotherms, kinetics and thermodynamics of nitrate and phosphate in binary systems on a novel adsorbent derived from corn stalks. *J. Geochem. Explor., 188*: 95-100.

FAO (2016). Fisheries and aquaculture - National aquaculture sector overview – Malaysia. *Food and Agriculture Organization of the United Nation*. http://www.fao.org/fishery/countrysector/naso_malaysia/en, accessed on 19 April 2020.

Hamoudi, S and Belkacemi, K (2013). Adsorption of nitrate and phosphate ions from aqueous solutions using organically-functionalized silica materials: Kinetic modelling. *Fuel: The Science and Technology of Fuel and Energy, 110*: 107-113.

Hasnain, I M; Ibrahim, N; Aziz, H A; Adlan, M N; Sabiani, N H M; Zinatizadeh, A A L and Kutty, S R M (2008). Removal of chromium (VI) from aqueous solution using treated oil palm fibre. *J. Hazard. Mater., 152(2)*: 662-668.

Hasnain, I M; Siew, L L; Asaari, F A H; Aziz, H A; Azam, R N and Dhas, J P A (2007). Low cost removal of disperse dyes from aqueous solution using palm ash. *Dyes Pigments, 74(2)*: 446-453.

Hokkanen, S; Bhatnagar, A and Sillanpää, M (2016). A review on modification methods to cellulose-based adsorbents to improve adsorption capacity. *Water Res., 91*: 156-173.

Hussin, M H; Pohan, N A; Garba, Z N; Kassim, M J; Rahim, A A; Brosse, N; Yemloul, M; Fazita, M R N and Haafiz, M K M (2016). Physicochemical of microcrystalline cellulose from oil palm fronds as potential methylene blue adsorbents. *Int. J. Biol. Macromol., 92*: 11-19.

Isroi; Ishola, M M; Millati, R; Syamsiah, S; Cahyanto, M N; Niklasson, C and Taherzadeh, M J (2012). Structural changes of oil palm empty fruit bunch (OPEFB) after fungal and phosphoric acid pretreatment. *Molecules, 17(12)*: 14995-15002.

Jana, H and Ulla, L (2011) Ionic liquids in the performance of lignocellulosic biomass. *Ionic Liquids: Applications and Perspectives*. IntechOpen. p. 545-560.

Kamil, N N and Omar, S F (2016). Climate variability and its impact on the palm oil industry. *Oil Palm Industry Economic J., 16*: 18-30.

Karthikeyan, P; Banu, H A T and Meenakshi, S (2019). Removal of phosphate and nitrate ions from aqueous solution using La 3+ incorporated chitosan biopolymeric matrix membrane. *Int. J. Biol. Macromol., 124*: 492-504.

Keränen, A; Leiviskä, T; Gao, B Y; Hormi, O and Tanskanen, J (2013). Preparation of novel anion exchangers from pine sawdust and bark, spruce bark, birch bark and peat for the removal of nitrate. *Chem. Eng. Sci., 98*: 59-68.

Khosravihaftkhany, S; Morad, N; Teng, T T; Abdullah, A Z and Norli, I (2013). Biosorption of Pb(II) and Fe(III) from aqueous solutions using oil palm biomasses as adsorbents. *Water, Air Soil Pollut., 224*: 1455.

Kim, J; Hwang, M J; Lee, S J; Noh, W; Kwon, J M; Choi, J S and Kang, C M (2016). Efficient recovery of nitrate and phosphate from wastewater by an amine-grafted adsorbent for cyanobacterial biomass production. *Bioresour. Technol., 205*: 269-273.

Kioussis, D R; Wheaton, F W and Kofinas, P (2000). Reactive nitrogen and phosphorus removal from aquaculture wastewater effluents using polymer hydrogels. *Aquac. Eng., 23(4)*: 315-332.

Klemm, D; Heublein, B; Fink, H P and Bohn, A (2005). Cellulose: Fascinating biopolymer and sustainable raw material. *Angew. Chem. Int. Ed., 44(22)*: 3358-3393.

Kumneadklang, S; O-Thong, S and Larpkiattaworn, S (2019). Characterization of cellulose fiber isolated from oil palm frond biomass. *Mater. Today: Proc., 17*: 1995-2001.

Kushairi, A; Ong-Abdullah, M; Nambiappan, B; Hishamuddin, E; Bidin, M N I Z; Ghazali, R; Subramaniam, V; Sundram, S and Parveez, G K A (2019). Oil palm economic performance in Malaysia and R&D progress in 2018. *J. Oil Palm Res., 31(2)*: 165-194.

Lamaming, J; Hashim, R; Sulaiman, O; Leh, C P; Sugimoto, T and Nordin, N A (2015). Cellulose nanocrystals isolated from oil palm trunk. *Carbohydr. Polym. Elsevier Ltd., 127*: 202-208.

Lamaming, J; Chew, S C; Hashim, R; Sulaiman, O and Sugimoto, T (2017). Extraction of microcrystalline cellulose from oil palm trunk. *J. Jpn. Inst. Energy, 96(11)*: 513-518.

Lee, S Y; Choi, J W; Song, K G; Choi, K; Lee, Y J and Jung, K W (2019). Adsorption and mechanistic study for phosphate removal by rice husk-derived biochar functionalized with Mg/Al-calcined layered double hydroxides via co-pyrolysis. *Comp. B Eng., 176*: 107209.

Lefatshe, K; Muiva, C M and Kebaabetswe, L P (2017). Extraction of nanocellulose and *in-situ* casting of ZnO/cellulose nanocomposite with enhanced photocatalytic and antibacterial activity. *Carbohydr. Polym., 164*: 301-308.

Lin, Y; Jing, S; Lee, D and Wang, T (2002). Nutrient removal from aquaculture wastewater using a constructed wetlands system. *Aquac., 209*: 169-184.

Lai, L W and Idris, A (2013). Disruption of oil palm trunks and fronds by microwave-alkali pretreatment. *BioResources, 8(2)*: 2792-2804.

Malaysian-German Chamber of Commerce and Industry (2017). Oil palm biomass and biogas in Malaysia. *EU-Malaysia Chamber of Commerce and Industry (EUMCCI)*, 15. https://businessmalaysia.eu/admin/js/fileman/Uploads/BiomassBiogas2018_Final_20180508.pdf, accessed on 20 April 2020.

Malaysia Innovation Agency (2013). National Biomass Strategy 2020: New wealth creation

for Malaysia's palm oil industry. https://www.cmtevents.com/MediaLibrary/BStgy2013RptAIM.pdf, accessed on 3 January 2019.

Megashah, L N; Ariffin, H; Zakaria, M R and Hassan, M A (2018). Properties of cellulose extract from different types of oil palm biomass. *IOP Conf. Ser.: Mater. Sci. Eng., 368(1)*: 012049.

Mohamed Omar, A F (2017a). Fisheries country profile: Malaysia. http://www.seafdec.org/fisheries-country-profile-malaysia/, accessed on 3 January 2019.

Mohamed Omar, A F (2017b). Fisheries country profile: Malaysia – SEAFDEC. http://www.seafdec.org/fisheries-country-profile-malaysia/, accessed on 3 January 2019.

Mohd Rasli, S R A; Ahmad, I; Mat, L A and Hamzah, A (2017). Extraction and characterization of cellulose from agricultural residue - Oil palm fronds. *Malays. J. Anal. Sci., 21(5)*: 1065-1073.

Mohtar, S S; Tengku Malim Busu, T N Z; Md Noor, A M; Shaari, N and Mat, H (2017). An ionic liquid treatment and fractionation of cellulose, hemicellulose and lignin from oil palm empty fruit bunch. *Carbohydr. Polym., 166*: 291-299.

Nazir, M S; Wahjoedi, B A; Yussof, A W and Abdullah, M A (2013). Eco-friendly extraction and characterization of cellulose from oil palm empty fruit bunches. *BioRes., 8(2)*: 2161-2172.

Ng, L Y; Ng, C Y; Ong, C B and Mohammad, A W (2018). A review of the management of inflow water, wastewater and water reuse by membrane technology for a sustainable production in shrimp farming. *J. Water Process Eng., 23*: 27-44.

Noorshamsiana, A W; Nur Eliyanti, A O; Fatiha, I and Astimar, A A (2017). A review on extraction processes of lignocellulosic chemicals from oil palm biomass. *J. Oil Palm Res., 29(4)*: 512-527.

Onoja, E; Chandren, S; Abdul Razak, F I; Mahat, N A and Wahab, R A (2019). Oil palm (*Elaeis guineensis*) biomass in Malaysia: The present and future prospects. *Waste Biomass Valori., 10(8)*: 2009-2117.

Ooi, C H; Sim, Y L and Yeoh, F Y (2017). Urea adsorption by activated carbon prepared from palm kernel shell. *AIP Conf. Proc., 1865*: 1-6.

Orlando, U S; Baes, A U; Nishijima, W and Okada, M (2002). Preparation of agricultural residue anion exchangers and its nitrate maximum adsorption capacity. *Chemosphere, 48(10)*: 1041-1046.

Pan, J; Gao, B; Song, W; Xu, X; Jin, B and Yue, Q (2018). Column adsorption and regeneration study of magnetic biopolymer resin for perchlorate removal in presence of nitrate and phosphate. *J. Clean. Prod., 213*: 762-775.

Qiao, H; Mei, L; Chen, G; Liu, H; Peng, C; Ke, F; Hou, R; Wan, X and Cai, H (2019). Adsorption of nitrate and phosphate from aqueous solution using amine cross-linked tea wastes. *Appl. Surf. Sci., 483*: 114-122.

Saman, N; Tan, J W; Mohtar, S S; Kong, H; Lye, J W P; Johari, K; Hassan, H and Mat, H (2018). Selective biosorption of aurum (III) from aqueous solution using oil palm trunk (OPT) biosorbents: Equilibrium, kinetic and mechanism analyses. *Biochem. Eng. J., 136*: 78-87.

Sehaqui, H; Mautner, A; Perez de Larraya, U; Pfenninger, N; Tingaut, P and Zimmermann, T (2016). Cationic cellulose nanofibers from waste pulp residues and their nitrate, fluoride, sulphate and phosphate adsorption properties. *Carbohydr. Polym., 135*: 334-340.

Shanmugarajah, B; Chew, I M L; Mubarak, N M; Choong, T S Y; Yoo, C K and Tan, K W (2019). Valorization of palm oil agro-waste into cellulose biosorbents for highly effective textile effluent remediation. *J. Clean. Prod., 210*: 697-709.

Shojaipour, M; Ghaemy, M and Amininasab, S M (2020). Removal of NO_3^- ions from water using bioadsorbent based on gum tragacanth carbohydrate biopolymer. *Carbohydr. Polym., 227(3)*: 115367.

Shuit, S H; Tan, K T; Lee, K T and Kamaruddin, A H (2009). Oil palm biomass as a sustainable energy source: A Malaysian case study. *Energy, 34(9)*: 1225-1235.

Stjepanović, M; Velić, N; Lončarić, A; Gašo-Sokač, D; Bušić, V and Habuda-Stanić, M (2019). Adsorptive removal of nitrate from wastewater using modified lignocellulosic waste material. *J. Mol. Liq., 285*: 535-544.

Sumathi, S; Chai, S P and Mohamed, A R (2008). Utilization of oil palm as a source of renewable energy in Malaysia. *Renew. Sustain. Energy Rev., 12(9)*: 2404-2421.

Tan, H T and Lee, K T (2012). Understanding the impact of ionic liquid pretreatment on biomass and enzymatic hydrolysis. *Chem. Eng. J., 183*: 448-458.

Turcios, A E and Papenbrock, J (2014). Sustainable treatment of aquaculture effluents - What can we learn from the past for the future? *Sustainability, 6*: 836-856.

Umar, M S; Jennings, P and Urmee, T (2013). Strengthening the palm oil biomass renewable energy industry in Malaysia. *Renew. Energy, 60*: 107-115.

Wang, W Y; Yue, Q Y; Xu, X; Gao, B Y; Zhang, J; Li, Q and Xu, J T (2010). Optimized conditions in preparation of giant reed quaternary amino anion exchanger for phosphate removal. *Chem. Eng. J., 157(1)*: 161-167.

Wang, Y; Gao, B Y; Yue, W W and Yue, Q Y (2007). Preparation and utilization of wheat straw anionic sorbent for the removal of nitrate from aqueous solution. *J. Environ. Sci., 19(11)*: 1305-1310.

Wu, K; Li, Y; Liu, T; Huang, Q; Yang, S; Wang, W and Jin, P (2019). The simultaneous adsorption of nitrate and phosphate by an organic-modified aluminum-manganese bimetal oxide: Adsorption properties and mechanisms. *Appl. Surf. Sci., 478(13)*: 539-551.

Yin, Q; Zhang, B; Wang, R and Zhao, Z (2017). Biochar as an adsorbent for inorganic nitrogen and phosphorus removal from water: A review. *Environ. Sci. Pollut. Res., 24(34)*: 26297-26309.

Yin, Q; Ren, H; Wang, R and Zhao, Z (2018). Evaluation of nitrate and phosphate adsorption on Al-modified biochar: Influence of Al content. *Sci. Total Environ., 631-632*: 895-903.

Yu, L J; Rengasamy, K; Lim, K Y; Tan, L S; Tarawneh, M; Zulkoffli, Z B and Se Yong, E N (2019). Comparison of activated carbon and zeolites' filtering efficiency in freshwater. *J. Environ. Chem. Eng., 7(4)*: 103223.

Zakaria, M R; Hirata, S and Hassan, M A (2014). Combined pretreatment using alkaline hydrothermal and ball milling to enhance enzymatic hydrolysis of oil palm mesocarp fiber. *Bioresour. Technol., 169*: 236-243.

Journal of Oil Palm Research Vol. 33 (3) September 2021 p. 400-412
DOI: https://doi.org/10.21894/jopr.2020.0105

NEURAL NETWORKS METHOD IN PREDICTING OIL PALM FFB YIELDS FOR THE PENINSULAR STATES OF MALAYSIA

YOUSIF Y HILAL[1]*; YAHYA, A[2]; ISMAIL, W I W[2] and ASHA'ARI, Z H[3]

ABSTRACT

Reliable and accurate predictions in oil palm production can provide the basis for management decisions of budgeting, storage, distribution and marketing. Artificial Neural Network (ANN) and Non-linear Autoregressive Exogenous Neural Network (NARX) models were developed based on 19 440 data set of 15 inputs variables, namely, percentage of mature area and percentage of immature area, rainfall, rainy days, humidity, radiation, temperature, surface wind speed, evaporation and cloud cover, ozone (O_3), carbon monoxide (CO), nitrogen dioxide (NO_2), sulphur dioxide (SO_2), and particulate matter of less than 10 microns in size (PM_{10}) for predicting oil palm fresh fruit bunch (FFB). The results were validated with an independent validation dataset. Results showed that NARX models performed more accurately with multiple coefficients of determination (R^2) reached 97% and mean square errors (MSE) between 0.0104%-0.0665%, besides being an easy-to-use tool. Generally, NARX models proved to give more accurate predictions than the predictions of common ANN and Multi Linear Regression (MLR) models. Finally, 15-10-4-1 is chosen as the architecture of NARX for the states of Kedah, Kelantan, Perak, Pahang, Selangor and Terengganu. The 15-7-4-1 is the best architecture of NARX for the state of Melaka and Pulau Pinang, while 15-13-4-1 architecture is for the state of Johor. This study showed that all of these architectures gave high accuracy with acceptable MSE values.

Keywords: climate factors, forecasting, linear regression, NARX, oil palm yield predictions.

Received: 22 May 2020; **Accepted:** 8 September 2020; **Published online:** 25 November 2020.

INTRODUCTION

Environmental change is widely believed to bring the world into a scarcity of food. It is one of the significant factors affecting development and oil palm production. Climate change has some effects on oil palm growth and yield. The dominant factors for climate parameters are rainfall, temperature, sunshine periods per day, water deficit and many others (Corley and Tinker, 2016; Saadon *et al*., 2014). In other words, environmental factors can significantly influence oil palm growth and geographic distribution.

Vegetation has been affected by the amount of rainfall and period (number of rainy days) which are the most vital factors in agriculture. Rainfall in the period of pollinator's mating or several hours after pollination may cause pollination process failure (Oettli *et al*., 2018; Corley and Tinker, 2016). Fresh fruit bunch (FFB) yield reductions are critically influenced by water deficit. For example, there is an exponential decline down to <10 t of fruit bunches per hectare per year at water deficits of >500 mm (Paterson

[1] Department of Agricultural Machines and Equipment, College of Agriculture and Forestry, University of Mosul, Iraq.

[2] Department of Biological and Agricultural Engineering, Faculty of Engineering, Universiti Putra Malaysia, 43400 UPM Serdang, Selangor, Malaysia.

[3] Department of Environmental Sciences, Faculty of Environmental Studies, Universiti Putra Malaysia, 43400 UPM Serdang, Selangor, Malaysia.

* *Corresponding author e-mail: yousifyakoub@yahoo.com*

et al., 2017). Temperature or intensity of heat energy plays an active role in agricultural processes and air temperatures which govern chemical processes and physical states within the palm. Diffusion rates of liquids, the solubility of different substances, and gases in oil palm are dependent on temperature. Corley and Tinker (2016) found a 30% decrease in oil palm yields for every 2°C increase in temperature above the optimal range of growing oil palm. Humidity influences the water requirement of plants. Mean minimum relative humidity for oil palm lies above 45%, with the best relative humidity lying between 70% and 95% (Do Amaral Teles *et al*., 2016).

The objective of modelling applications is to create a high-resolution predictive model, based on the readily available response variables in the database. The number of available predictions has significant effects on the model formulation (Kapadia *et al*., 2017; Gaber *et al*., 2020).

Many of the studies to understand crop production potential under climate change in Malaysia have focused in using statistical approaches. Studies were often based on single climate scenarios, without relating to differences and overlapping variables. Several analyses have also been conducted to study climate change impacts at regional levels in Malaysia, using statistical models. For example, models by Soon and Hong (2001); Foster (2003); Verdooren (2003); Ahmad Tarmizi *et al*. (2004) and Shanmuganathan and Narayanan (2012) had indicated the effects of weather on oil palm yield and prediction results showed a lower value of R^2 that ranged from 0.15-0.36.

Multi Linear Regression (MLR) is very commonly used in the oil palm industry (Rahman and Robson, 2016; Antle *et al*., 2017). MLR models in oil palm production, such as models by Keong and Keng (2012), have shown a much reliable performance, the previous developed with a much better value of R^2 of 0.68. Traditional methods are unable to capture the full variability of the sub-seasonal weather and are limited in their ability to project changes in the future. Furthermore, conventional statistical models have limited illustrative capacity, and do not apply to the development of adaptation measures to climate change.

To date, an appropriate framework for modelling an integrated system in palm oil production has not yet been developed. However, the components to create such a system are currently available. Operations Simulator (OPSIM) and Agricultural Production Systems Simulator (APSIM) oil palm model have been developed and tested in the main production regions (Huth *et al*., 2014; Garrett *et al*., 2016). Fan *et al*. (2015) concluded that most models have not yet aimed at the full picture of water, air pollution, and energy exchanges between land and atmosphere and remain to be coupled with a limited number of climatic elements.

The challenge in modeling oil palm yield is that it does not follow a linear behaviour. The crop growth and yield production normally have a non-linear and sigmoidal type of relationship (Hilal *et al*., 2018). In modeling a non-linear curve, the problem becomes more complex with their numerous independent variables. The major hindrance in modeling the behaviour of yield is the challenge of extracting the constants of the mathematical models (Quaranta *et al*., 2020).

Non-linear methods can be used to address many issues as powerful predictive tools. Neural Networks (NN) are one method of modeling non-linear (accommodating multivariate) and non-parametric data with a model-free estimation (Harahap and Lubis, 2018; Waheeb and Ghazali, 2019). Exploratory research on artificial intelligence has revealed that little has been done on oil palm yield (Khamis *et al*., 2006; Zuhaimy and Azme, 2011). NN are a diverse set of techniques concocted to meet the diverse needs of forecast modeling. Unlike traditional regression-based methods, NN can reliably model non-linear relationships (Majumdar *et al*., 2016; Da Silva *et al*., 2017). The concept of the NN is based on the human brain, which comprises billions of interconnected neurons through their synapses. NN have three significant advantages: parallelism, the ability to learn, and the ability to generalise. The parallelism is ideal for complicated tasks such as pattern recognition, which would be much more challenging to accomplish serially. Another significant advantage of NN is their ability to learn by training. Training consists of supplying the NN with many training samples, each of which includes a set of inputs and the desired sets of outputs (Asta, 2015). Due to their efficient capacity to learn and generalise (Khairunniza-Bejo *et al*., 2014), NN have garnered widespread attention among researchers in various fields, to generate and analyse experimental data. NN are a significant modeling instrument that has terrific potential in many areas of studies, especially in the area of oil palm production where modeling is very useful. Therefore, the main objectives of the research are to develop and propose the preferred Artificial Neural Network (ANN) and Non-linear Autoregressive Exogenous Neural Network (NARX) architectures for predicting oil palm FFB yield within multiple areas in Peninsular Malaysia. It also develops MLR models to predict FFB, and compares with the final NN models.

MATERIAL AND METHODS

Description of the Study Area

Peninsular Malaysia is one of the major oil palm production regions in Malaysia. Its area is

130 598 km^2 and extends from latitude 1° 20′ N to 6° 40′ N and from longitude 99° 35′ E to 104° 20′ E. The latitude and longitude for Peninsular Malaysia include the nine states, as described in *Table 1.*

Input and output data for FFB models. The models were developed to predict FFB oil palm yield based on prior values of the environment (climatic change and air pollution) and types of oil palm areas (mature and immature). Monthly data were collected using 15 variables as inputs and one variable for the output. Data were obtained from the Malaysian Palm Oil Board (MPOB), Meteorological Department, and Department of Statistics, Prime Minister's Department, Malaysia as described in *Table 2.*

The whole data for nine states were 19 440 numbers. The total data for each state was 2160 numbers. The data were partitioned into two data sets consisting of the development set and the simulation set. The simulation set was not used during model development that was held back in the evaluation of the final model. The available data, from January 2005 to December 2015 were used in the development set, while the data, from January to March 2020 were applied in the simulation set.

Development of ANN Models for FFB Yield

The best ANN model simulations that use hypothetical data were conducted to forecast the FFB yield by the effect of input data that affects the productivity of oil palm plantations. The ANN is programmed by MATLAB's Neural Network Toolbox. The architecture of ANN consists of three layers; the input layer, a hidden layer, and an output layer. There are three kinds of neurons, input, hidden and output neurons. Each of the following needs to be examined to understand how a neuron produces an output from its arbitrary inputs.

TABLE 1. DESCRIPTIONS OF THE STUDY SITES

Fresh fruit bunch area			
District	**State**	**Location**	**Oil palm planted areas (ha)**
Kubang Pasu	Kedah	6.3726° N, 100.4370° E	2 373
Kota Bahru	Kelantan	6° 09′ 49″ N,102° 18′ 02″ E	24
Kota Tinggi	Johor	1.7294° N, 103.8992° E	149 684
Melaka Tengah	Melaka	2° 16′ N, 102° 15′ E	1 997
Seberang Prai Selatan	Pulau Pinang	5.1958° N, 100.4921° E	6 895
Hilir Perak	Perak	4.0209° N, 101.0230° E	107 630
Kuantan	Pahang	3.7634° N, 103.2202° E	81 592
Kuala Langat	Selangor	2.8038° N, 101.4951° E	33 114
Kuala Terengganu	Terengganu	5° 23′ N,103° 6′ E	3 679

TABLE 2. INPUT AND OUTPUT VARIABLES

Input data	Source
Types of the oil palm area Percentage of mature (%) Percentage of immature (%)	Malaysian Palm Oil Board (MPOB)
Climate Rainfall (mm) Rain day Humidity (%) Radiation (Mjm^{-2}) Temperature (^{o}C) Surface wind speed (m s^{-1}) Evaporation (mm) Cloud cover (oktas)	Malaysian Meteorological Department Department of Statistics, Prime Minister's Department, Malaysia
Air pollution (ppm) Ozone (O_3) Carbon monoxide (CO) Nitrogen dioxide (NO_2) Sulphur dioxide (SO_2) Particulate matter of less than 10 microns in size (PM_{10})	Department of Statistics, Prime Minister's Department, Malaysia Department of Environment, Ministry of Natural Resources and Environment, Malaysia
Output FFB yield t ha^{-1}	MPOB

Input neurons. The neuron can have an arbitrary number of inputs. Typically, a neuron has more than one input. In this study, we have used variables, 15 input variables to predict FFB yield. In general, ANN randomly selects a sample of 70% for training, a sample of 15% for cross-validation and 15% used for a test (Harahap and Lubis, 2018).

Hidden neurons and output neurons. The hidden neurons do an intermediate computation before directing the input to output neurons. The treatments in the hidden neurons vary according to the NN structure. The number of neurons in the hidden layer is determined through experimentation and the discretion of the network designer. It usually has been decided by trial and error. Actually, 5, 7, 10 and 13 hidden neurons (nodes) are suggested for this network topology. There are output neurons that are connected to input fields. Each output neuron computes one dependent variable.

Training function. The training process was employed to find optimal weight matrices and bias vectors that minimise a predetermined error function. The proposed ANN model used in this study is the supervised learning, and Levenberg-Marquardt backpropagation (LM algorithm), which is the most widely-utilised optimisation algorithm. It is commonly used because it outperforms simple gradient descent and other conjugate gradient methods.

Transfer function. This study used the continuous non-linear function which publishes values by entering them in accordance with the scale of schedule in the emerging amount. The non-linear, curved S-shape function is called the sigmoid function, which is the most popular transfer function for a non-linear relationship. It is mathematically well behaved, differentiable and strictly increasing function. It publishes values by entering them by the scale of schedule in the emerging amount (Kyurkchiev and Markov, 2015).

Development of NARX Models for FFB Yield

The NARX is a recurrent dynamic network, with feedback connections including many layers of the net. The series-parallel NARX dynamic network will be used as a basis for the models in this study with a structure as shown in *Figure 1*. The NARX model is commonly used in time-series modelling. The NARX consists of the following parts:

Part 1. Layers and neurons of the NARX. The structure of a neuron in NARX is similar to ANN. Therefore, the architecture of the NARX consists of three layers which are: input, hidden and output layers, with some variations that include, Tapped Delay Line (TDL), of which the delay line is applied to feed the network with the past values of inputs. In this study, the delay values are four for each NARX model architecture (Guzman *et al*., 2017). The number of neurons in the input layer will be equal to the number of inputs provided to the networks. Using additional layers makes the model more complicated and increases the time required for training and simulation. The default number of hidden neurons at a hidden layer is set to 10; in this work 5, 7, 10 and 13 hidden neurons are suggested for NARX topology. Each output neuron computes an architecture of NARX for FFB yield models.

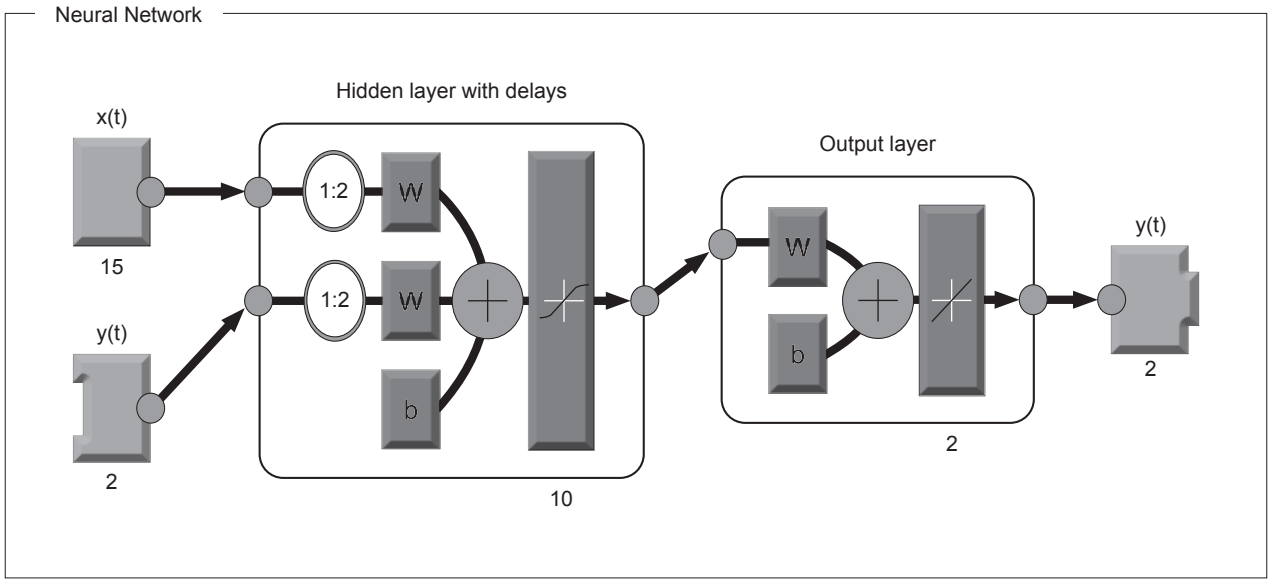


Figure 1. Snapshot of series-parallel Non-linear Autoregressive with Exogenous Neural Network (NARX) dynamic network.

Part 2. Training and transfer functions. Training is mapping the objectives within the neuron range and training the network using an algorithm that is suited for such an implementation. The MATLAB® Neural Network Toolbox provides a detailed survey of algorithms suitable for different applications. LM is the best algorithm for NARX networks approximation and actual output (default by MATLAB®). This study will use the sigmoid neurons (default by MATLAB®), which have been extensively used in most of the NN applications. The datasets were distributed into three partitions as training, validation and testing partitions. The constructions of 70%:15%:15% were set up for implementation (Harahap and Lubis, 2018).

Development of MLR for FFB Yield

The data was analysed using the Design-Expert Version 9.0.1 software (Stat-Ease Inc., Minneapolis, USA). The objective is to build MLR models to predict the oil palm FFB yield. Briefly, steps to build a multiple regression model are as follows:

- Step 1. Define parameters and read the data in the linear models. This step is designed for importing data that already exists. Fifteen input variables and one output variable were selected for the most significant variables in FFB models.
- Step 2. Transformation of the response. Design-Expert provides extensive diagnostic capabilities to check if the statistical assumptions underlying the data analysis are met.
- Step 3. Model selection. The most appropriate mathematical models were chosen for predicting the interactive effects of input parameters on oil palm production. Evaluate a model after it has been run; there are three choices; the p-value, Adjusted R-Squared and the analysis of variance (ANOVA). The MSE results from performing a linear method in the ANOVA. In this work, the following performance measurement functions in Equation (1) and (2) were employed:

$$\text{R-Squared} = 1 - [SS_{\text{Pure Error}} / (SS_{\text{Model}} + SS_{\text{Pure Error}})] \quad (1)$$

$$\text{Adj.R-Squared} = 1 - (SS_{\text{Pure Error}} / DF_{\text{Pure Error}}) / [(SS_{\text{Model}} + SS_{\text{Pure Error}}) / (DF_{\text{Model}} + DF_{\text{Pure Error}})] \quad (2)$$

where:
$SS_{\text{Pure Error}}$ - pure error sum of squares.
SS_{Model} - the model sum of squares.
$DF_{\text{Pure Error}}$ - pure error degrees of freedom.
DF_{Model} - model degrees of freedom.

Forecasting Simulation Models

Simulation modeling is necessary to measure the robustness and efficiency of any developed forecasting algorithm. It allows verifying the robustness of the different algorithms, to consider the component combination on the model to obtain the test scenario. The performance of the model can be evaluated by the validity of its estimation, its ability to reproduce the actual yield in simulation and its stability. Hence, the estimated model in this study will be validated and evaluated on the basis of its forecasting power by using MSE. We want to regularly forecast monthly in 2020 ahead and produce a new forecast each month.

The simulation and prediction functions were developed and compiled into an application with a functional user interface in the MATLAB network programmer. The following performance measure functions in Equation (3) were employed (Ranjit and Sinha, 2016):

1-Mean square error (MSE) for evaluating the accuracy of the proposed ANN, NARX and linear models.

$$\text{MSE} = \frac{1}{N} \Sigma^{N} (Ti - Yi)^2 \quad (3)$$

where:
Ti - the actual yield.
Yi - the forecasted yield.
N - the number of data points for i= 1, 2…. N.

RESULTS AND DISCUSSION

Development of Oil Palm FFB Yield Models

For the best training, the initial connectivity weights of neurons and biases are selected as following the connection weights and biases between the input layer, the hidden layer and the output layer are selected randomly as small numbers.

Tables 3 and *4* present the performance of the ANN, NARX and MLR models at nine states. The outcome of the ANN and NARX models contains 15 inputs and one output (FFB). It is seen from *Table 3* the values of R^2 are very high for ANN and NARX models, almost all of the R^2 values were between 0.842%-0.974% during the network training. On the other hand, the R^2 values of MLR models significantly decrease in most states. Moreover, the best performance of the network model is shown by its sensitivities to the difference of the number of hidden neurons.

Table 4 shows that the effect of a different number of hidden neurons on MSE in nine states. MSE is the lowest that provided the best model performances. It can be seen the values of MSE are

very low for most ANN and NARX models, where most MSE values were between 0.0104%-0.0665%. There was a significant increase in MSE values for MLR models in most states. For example, MSE values calculated for the MLR models for Pahang, Selangor and Terengganu, was 0.7410%, 0.1272% and 0.4182%, respectively.

Based on the evaluations, there are a critical number of hidden units existing for minimising the error rate for each state. If there are too many hidden units, a network can simply memorise the correct response to each pattern in its training set instead of learning a general solution. The number of hidden neurons to be used in a layer is rather arbitrary and it has usually been decided through trial and error. In this study, the variation of R^2 and MSE for all phases against several iterations for a different number of hidden neurons were 5, 7, 10 and 13. On the other hand, utilising more than 13 neurons in the network makes the computation process more complicated and expensive. Currently, there is no reliable method exists despite several efforts to arrive at an approximate formula. It also takes a long time to train the network. Therefore, trial and error are still employed to derive some empirical rules to find the optimal network sizes (Gaurang *et al*., 2011).

With several trials and errors, the variation of the learning rate and the best performance of the model is obtained with seven hidden neurons in Kedah, Johor and Perak. There were 10 hidden neurons in Kelantan, Melaka, Pulau Pinang, Selangor and Terengganu, while 13 hidden neurons for Pahang for the best ANN architecture in nine states. The best number of hidden neurons for NARX models is seven hidden neurons of Melaka and Pulau Pinang, and 10 hidden neurons in Kedah, Kelantan, Perak, Pahang, Selangor, and Terengganu. The best number of hidden neurons for Johor is 13 neurons as shown in *Table 5*.

TABLE 3. EFFECT OF HIDDEN NEURON NUMBERS ON COEFFICIENT OF DETERMINATION (R^2) OF MODELS IN NINE STATES

Models	ANN R^2				NARX R^2				MLR R^2
No. of hidden neurons	5	7	10	13	5	7	10	13	-
Kedah	0.897	0.946	0.895	0.888	0.884	0.896	0.953	0.903	0.249
Kelantan	0.908	0.909	0.960	0.902	0.893	0.911	0.960	0.914	0.407
Johor	0.868	0.960	0.869	0.889	0.903	0.895	0.915	0.974	0.352
Melaka	0.887	0.893	0.954	0.875	0.910	0.962	0.891	0.910	0.191
Pulau Pinang	0.909	0.906	0.950	0.902	0.892	0.958	0.891	0.890	0.540
Perak	0.902	0.962	0.886	0.906	0.904	0.906	0.968	0.908	0.327
Pahang	0.891	0.906	0.905	0.961	0.917	0.914	0.964	0.918	0.336
Selangor	0.883	0.905	0.962	0.888	0.883	0.888	0.969	0.895	0.310
Terengganu	0.878	0.876	0.942	0.842	0.876	0.877	0.949	0.871	0.434

Note: ANN - Artificial Neural Network; NARX - Non-linear Autoregressive Network with exogenous inputs; MLR - Multi Linear Regression.

TABLE 4. EFFECT OF HIDDEN NEURON NUMBERS ON MSE OF MODELS IN NINE STATES

Models	ANN MSE				NARX MSE				MLR MSE
No. of hidden neurons	5	7	10	13	5	7	10	13	-
Kedah	0.050	0.036	0.051	0.047	0.036	0.059	0.027	0.066	0.090
Kelantan	0.015	0.011	0.011	0.017	0.014	0.015	0.010	0.012	0.055
Johor	0.023	0.017	0.019	0.020	0.021	0.022	0.018	0.014	0.149
Melaka	0.041	0.047	0.031	0.037	0.033	0.020	0.033	0.026	0.088
Pulau Pinang	0.020	0.016	0.020	0.019	0.029	0.015	0.029	0.021	0.083
Perak	0.016	0.014	0.012	0.013	0.019	0.016	0.012	0.016	0.045
Pahang	0.020	0.018	0.018	0.016	0.018	0.021	0.018	0.019	0.741
Selangor	0.022	0.020	0.014	0.019	0.018	0.013	0.011	0.017	0.127
Terengganu	0.025	0.023	0.022	0.026	0.018	0.025	0.011	0.022	0.418

Note: ANN - Artificial Neural Network; NARX - Non-linear Autoregressive Network with exogenous inputs; MLR - Multi Linear Regression; MSE - mean square error.

TABLE 5. ARCHITECTURE OF BEST NEURAL NETWORKS MODELS

States	Architecture of best ANN models	Architecture of best NARX models
Kedah	15-7-1	15-10-4-1
Kelantan	15-10-1	15-10-4-1
Johor	15-7-1	15-13-4-1
Melaka	15-10-1	15-7-4-1
Pulau Pinang	15-10-1	15-7-4-1
Perak	15-7-1	15-10-4-1
Pahang	15-13-1	15-10-4-1
Selangor	15-10-1	15-10-4-1
Terengganu	15-10-1	15-10-4-1

Note: ANN - Artificial Neural Network; NARX - Non-linear Autoregressive Network with exogenous inputs.

The total results demonstrated that the forecasting ability of ANN and NARX NN is sensitive to the number of hidden neurons. These results concurred with Arbain and Wibowo (2012). Due to results which contradict with Taskaya-Temizel and Casey (2005), they then concluded that the forecasting ability of NN is not sensitive to the number of hidden nodes.

Scatter plots of predicted output oil palm FFB yield against actual values are shown in *Figures 2* and *3* for the testing data sets. It can be seen that actual and predicted FFB are visual representation which simply suggests deviation in the direction of a line between the actual and predicted for all training with an entire data set for the NARX model. Almost a linear trend can be observed between the actual and predicted FFB, which justifies the efficacy of the model, except for a clear deviation in Pahang as presented. For the ANN model, visual representation strongly suggests deviation in the direction of a line between the actual and predicted FFB for the entire data set because the MSE values varied between models, and the NARX models outperformed ANN models in nine states.

Simulation and Selecting Model

The accuracy of the developed models should always be evaluated with a set of data, not used in the training process (Kline, 2000). During the last section of the FFB model evaluation, the model's response is compared by testing the data. The model verification focused on checking the residuals of the model to determine if any systematic pattern could be removed to improve the chosen model. As shown in *Tables 6* and *7*, a comparison between the MLR with ANN and NARX forecasts, with the actual values based on the MSE within the studied states. The predicted values were very close to the measured values for NARX models. The outputs of the network were found to be closer to the actual values of the FFB yield amount than the linear model. Moreover, the average accuracy for the forecasts by the linear model was very low and largely differed with the actual values.

The finding indicated that the average MSE values were between 15%-75% for the FFB models, which indicated the good performance of the multivariate forecasting model based on the statistical results. This result is in agreement with the theorem, which states that a neural network with a single hidden layer and a sufficiently large number of neurons can well predict any arbitrary continuous function (Khamis *et al*., 2006; Zuhaimy and Azme, 2011).

The best models were used for forecasting the NARX models are superior to that of the other models. The average of MSE values for the forecasts by NARX models had a record lowest value of between 0.0019% and 0.006%. The NARX model achieved high accuracy in the overall forecast during 2020. It indicated that the results fit the available data sufficiently to satisfy the forecasting. Consequently, the NARX model was proven to be an appropriate model for forecasting the data being studied. NARX model can be used as an alternative model to predict the FFB yield of oil palm.

Test the Significance of Independent Variables

The capacity of the oil palm production was explored from the perspective of the NARX models. The analysis was conducted by changing independent variable indicators for different possible changes in various regions. Results showed that the predictive power of the analysis of changes in some of the factors. The independent variable power can be determined with the distinction between the highest and lowest values for each scenario.

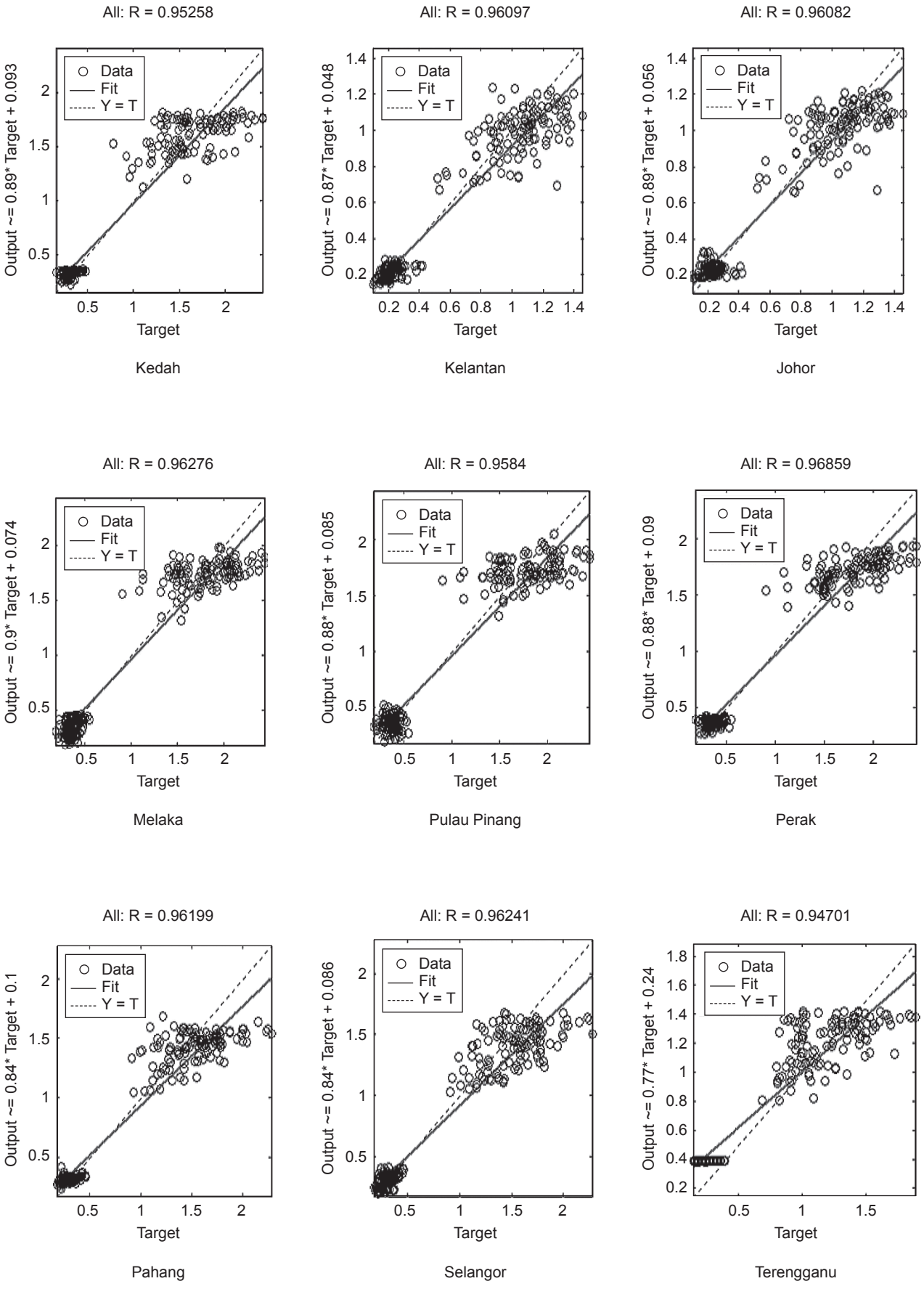


Figure 2. The scatter plots of Artificial Neural Network (ANN) models predicted vs. *actual values.*

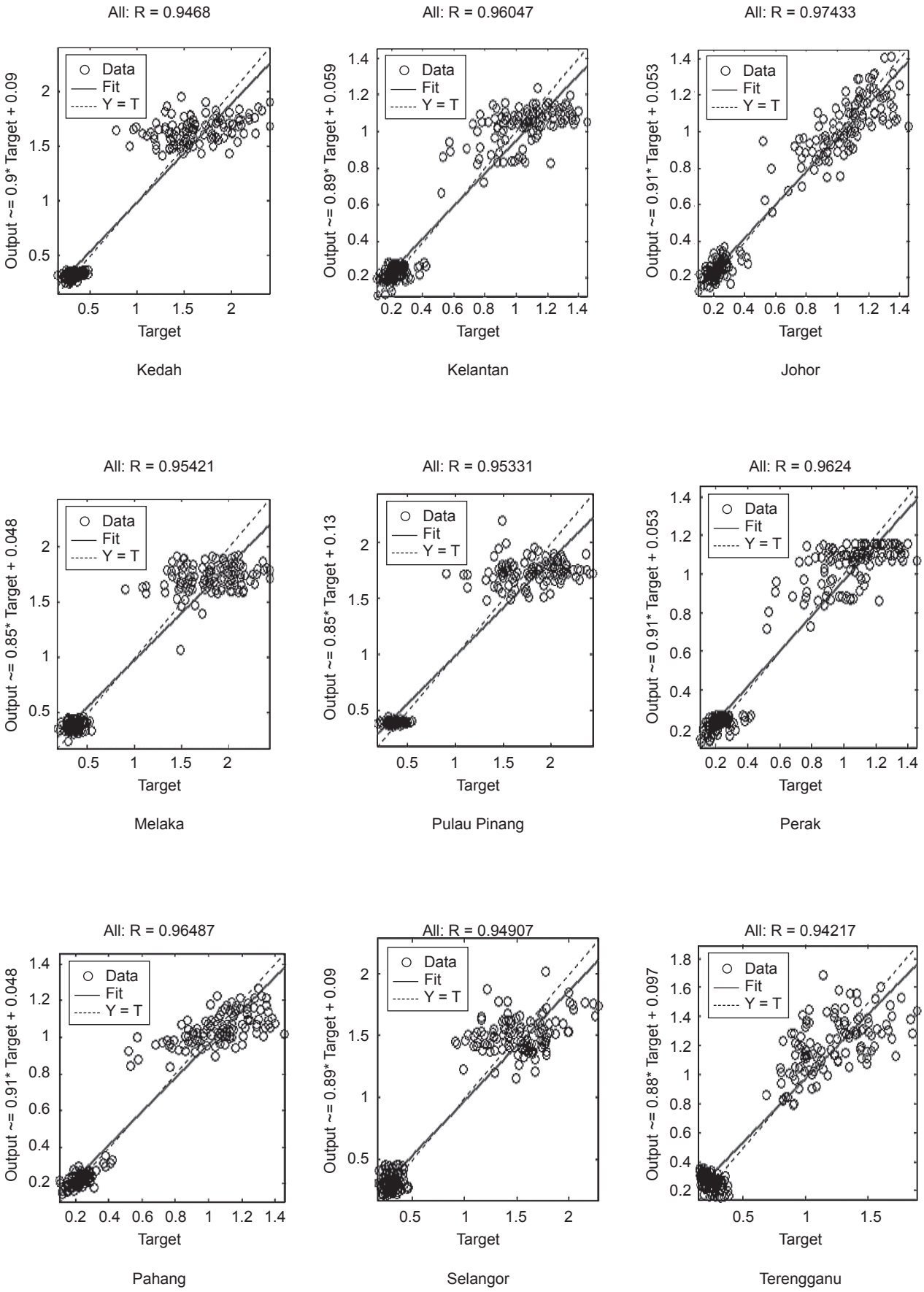


Figure 3. The scatter plots of Non-linear Autoregressive Exogenous Neural Network (NARX) models predicted vs. *actual values.*

TABLE 6. FORECAST MODELS WITH THE ACTUAL YIELD IN 2020 FOR THE EAST COAST OF PENINSULAR MALAYSIA

States	Forecasting by	Date of 2020			Forecast performance
		t			
		January	February	March	MSE
Kelantan	FFB yield	0.49	0.55	0.79	-
	ANN	0.46	0.49	0.74	0.0023
	NARX	0.47	0.52	0.75	0.0011
	MLR	0.12	0.13	0.19	0.2244
Terengganu	FFB yield	0.80	0.82	0.97	-
	ANN	0.74	0.76	0.90	0.0040
	NARX	0.76	0.78	0.92	0.0019
	MLR	0.39	0.40	0.47	0.1980
Pahang	FFB yield	0.79	0.92	1.16	-
	ANN	0.7426	0.8648	1.0904	0.0033
	NARX	0.7505	0.8740	1.1020	0.0023
	MLR	0.1975	0.230	0.290	0.5280

Note: ANN - Artificial Neural Network; NARX - Non-linear Autoregressive Network with exogenous inputs; MLR - Multi Linear Regression; MSE - mean square error; FFB - fresh fruit bunch.

TABLE 7. FORECAST MODELS WITH THE ACTUAL YIELD IN 2020 FOR THE WEST COAST OF PENINSULAR MALAYSIA

States	Forecasting by	Date of 2020			Forecast performance
		t			
		January	February	March	MSE
Kedah	FFB yield	1.07	1.55	1.63	-
	ANN	1.0058	1.457	1.5322	0.0074
	NARX	1.0165	1.4725	1.5485	0.0024
	MLR	0.675	0.875	0.475	0.6485
Johor	FFB yield	1.18	1.36	1.42	-
	ANN	1.1092	1.2784	1.3348	0.0063
	NARX	1.121	1.292	1.349	0.0043
	MLR	0.595	0.4	0.55	0.6735
Melaka	FFB yield	0.89	1.33	1.50	-
	ANN	0.8366	1.2502	1.41	0.0057
	NARX	0.8455	1.2635	1.425	0.0040
	MLR	0.522	0.533	0.437	0.6335
Pulau Pinang	FFB yield	0.62	1.20	1.34	-
	ANN	0.5828	1.128	1.2596	0.0043
	NARX	0.589	1.14	1.273	0.0030
	MLR	0.155	0.43	0.5335	0.4865
Perak	FFB yield	1.35	1.61	1.68	-
	ANN	1.269	1.5134	1.5792	0.0086
	NARX	1.2825	1.5295	1.596	0.0060
	MLR	0.5375	0.7025	0.842	0.7286
Selangor	FFB yield	1.17	1.52	1.72	-
	ANN	1.0998	1.4288	1.6168	0.0079
	NARX	1.1115	1.444	1.634	0.0055
	MLR	0.5925	0.638	0.643	0.7571

Note: ANN - Artificial Neural Network; NARX - Non-linear Autoregressive Network with exogenous inputs; MLR - Multi Linear Regression; MSE - mean square error; FFB - fresh fruit bunch.

TABLE 8. EFFECT OF INDEPENDENT VARIABLES IMPORTANCE IN FRESH FRUIT BUNCH (FFB) YIELD FOR THE PENINSULAR STATES OF MALAYSIA

Experiment variables	Peninsular states of Malaysia								
	Kedah	Kelantan	Johor	Melaka	Pulau Pinang	Perak	Pahang	Selangor	Terengganu
% of mature	0.019	0.080	0.08	0.044	0.031	0.056	0.02	0.033	0.039
% of immature	0.071	0.032	0.06	0.057	0.086	0.081	0.047	0.029	0.035
Rainfall	0.063	0.078	0.05	0.038	0.038	0.027	0.037	0.131	0.051
Rain day	0.178	0.065	0.03	0.080	0.047	0.041	0.116	0.048	0.043
Humidity	0.020	0.077	0.04	0.051	0.090	0.053	0.034	0.073	0.098
Radiation	0.066	0.051	0.09	0.122	0.080	0.083	0.096	0.092	0.079
Temperature	0.062	0.057	0.06	0.082	0.059	0.084	0.085	0.085	0.064
Wind speed	0.042	0.127	0.04	0.039	0.139	0.114	0.051	0.078	0.177
Evaporation	0.040	0.043	0.03	0.036	0.066	0.071	0.079	0.055	0.030
Cloud cover	0.031	0.070	0.14	0.094	0.07	0.124	0.155	0.044	0.074
Ozone (O_3)	0.127	0.105	0.07	0.048	0.063	0.014	0.122	0.035	0.048
Carbon monoxide (CO)	0.039	0.034	0.10	0.088	0.069	0.036	0.04	0.044	0.090
Sulphur dioxide (SO_2)	0.084	0.093	0.06	0.029	0.055	0.061	0.041	0.095	0.040
Nitrogen dioxide (NO_2)	0.137	0.033	0.03	0.136	0.054	0.115	0.045	0.030	0.064
Particulate matter of less than 10 microns in size (PM_{10})	0.021	0.054	0.120	0.055	0.053	0.039	0.032	0.127	0.067

As shown in *Table 8*, the findings of this research, using 11 years of climate change and air pollution, have significantly affected the oil palm production. Surface wind speed was recorded at an impact ratio of up to 12.7%, 13.9% and 17.7%, which highly correlates to the productivity of oil palm plantations in Kelantan, Pulau Pinang and Terengganu, respectively. Additionally, the cloud cover is considered as the most essential variable recorded with an impact ratio of up to 14%, 12.4% and 15.5% on FFB yields in Johor, Perak and Pahang while the rainy days, total rainfall and average NO_2 in the air recorded the most significant impact up to 17.8%, 13.1% and 13.6% of FFB yields in Kedah, Selangor and Melaka, respectively. The effect of corresponding variables on production and the possible oil palm productivity which benefitted from direct sunshine was suggested as most of South-east Asia has low incidence of cloud cover, which probably caused higher oil palm yields compared with those of West Africa (Hilal *et al*., 2018). According to the data collected, wind speed, cloud cover, rainfall, and the number of rainy days correlated positively with the productivity of oil palm plantations in the Peninsular states of Malaysia. Corley and Tinker (2016) concluded that the pattern of rainfall and number of rainy days were markedly visible, between July and October. August was recorded as the month with the highest days of rainfall, with an average of 25.6 days. However, the month with the highest total rainfall was in September, which recorded 500 mm. The number of rainy days was most influential during the harvest season.

Air pollution in Peninsular Malaysia can be highly variable from year to year due to biomass burning. The meteorological data for each station in 2006, 2009, 2013, 2014 and 2015, showed monthly averages of ozone (O_3), carbon monoxide (CO), nitrogen dioxide (NO_2), sulphur dioxide (SO_2) and particulate matter of less 10 microns in size (PM_{10}) values higher than normal. Higher values appeared to occur in June to October, which roughly correspond to the drier season and an increase in biomass burning.

CONCLUSION

The current study developed and applied a NN model to predict oil palm FFB yield. The power of a NN was used to produce a fast and efficient solution promptly. The results of this study indicated that the NARX models can be successfully used to predict the variables based on large variables and allowing a much more comprehensive search of the solution. Through the model analysis of the variables, one sees the effect of climate change, air pollution and quality of land for oil palm areas on several elements simultaneously on land productivity. NARX models are easy to apply on a wide range to obtain optimisation prediction models with high precision oil palm yield models.

The results of this study are only based on nine states in Malaysia. Future works will focus in expanding the data, increasing inputs and samples to further explore other areas through similar studies.

REFERENCES

Ahmad Tarmizi, M; Zin, Z; Mohd, T and Ariffin, D (2004). Oil palm fertilizer program: A proposal for higher yield. Presented in MPOB and RISDA Action Plan Meetings, Prime City, Kluang. August 2004.

Antle, J M; Jones, J W and Rosenzweig, C E (2017). Next generation agricultural system data, models and knowledge products: Introduction. *Agric. Syst.*, *155(7)*: 186-190.

Arbain, S H and Wibowo, A (2012). Neural networks based nonlinear time series regression for water level forecasting of Dungun River. *J. Comput. Sci.*, *8(9)*: 1506-1513.

Asta, S (2015). *Machine Learning for Improving Heuristic Optimization*. Doctoral dissertation. University of Nottingham, United Kingdom. 173 pp.

Corley, R H V and Tinker, P B (2016). Reference list and index of citations. *The Oil Palm*. Fifth edition. Wiley. p. 537-626.

Da Silva, I N; Spatti, D H; Flauzino, R A; Liboni, L H B and Dos Reis Alves, S F (2017). *Artificial Neural Networks*. Cham: Springer International Publishing. 305 pp.

Do Amaral Teles, D A; Braga, M F; Antoniassi, R; Junqueira, N T V; Peixoto, J R and Malaquias, J V (2016). Yield analysis of oil palm cultivated under irrigation in the Brazilian Savanna. *J. Am. Oil Chem. Soc.*, *93(2)*: 193-199.

Fan, Y; Roupsard, O; Bernoux, M; Le Maire, G; Panferov, O; Kotowska, M M and Knohl, A (2015). A sub-canopy structure for simulating oil palm in the Community Land Model (CLM-Palm): Phenology, allocation and yield. *Geosci. Model Dev.*, *8(11)*: 3785-3800.

Foster, H L (2003). Assessment of oil palm fertilizer requirements. *Oil Palm: Management for Large and Sustainable Yields* (Fairhurst, T and Hardter, R eds.). Potash and Phosphate Institute (PPI), Potash and Phosphate Institute Canada (PPIC) and Int. Potash Inst. (IPI), Singapore. p. 231-257.

Gaber, J (2020). *Qualitative Analysis for Planning and Policy: Beyond the Numbers*. Routledge, Taylor and Francis. 165 pp.

Garrett, R D; Carlson, K M; Rueda, X and Noojipady, P (2016). Assessing the potential additionally of certification by the round table on responsible soybeans and the roundtable on sustainable palm oil. *Environ. Res. Lett.*, *11(4)*: 045003.

Gaurang, P; Amit, G; Kosta, Y and Devyani, P (2011). Behaviour analysis of multilayer perceptrons with multiple hidden neurons and hidden layers. *Int. J. Comput. Theory Eng.*, *3(2)*: 332-337.

Guzman, S M; Paz, J O and Tagert, M L M (2017). The use of Narx neural networks to forecast daily groundwater levels. *Water Resour. Manage.*, *31(5)*: 1591-1603.

Harahap, I and Lubis, M (2018) Application of an artificial neural network (ANN) model for predicting oil palm fresh fruit bunch (FFB) yield based on rainfall and the yield previously. *Jurnal Penelitian Kelapa Sawit*, *26(2)*: 59-70.

Hilal, Y Y; Ishak, W; Yahya, A and Asha'ari, Z H (2018). Development of genetic algorithm for optimization of yield models in oil palm production. *Chil. J. Agric. Res.*, *78(2)*: 228-237.

Huth, N I; Banabas, M; Nelson, P N and Webb, M (2014). Development of an oil palm cropping systems model: Lessons learned and future directions. *Environ. Modell. Softw.*, *62*: 411-419.

Ismail, Z and Khamis, A (2011). Neural network in modeling Malaysian oil palm yield. *Am. J. Appl.Sci.*, *8(8)*: 796-803.

Kapadia, A S; Chan, W and Moyé, L A (2017). *Mathematical Statistics with Applications*. CRC Press, USA. 896 pp.

Keong, Y K and Keng, W M (2012). Statistical modelling of weather-based yield forecasting for young mature oil palm. *APCBEE Procedia*, *4*: 58-65.

Khairunniza-Bejo, S; Mustaffha, S and Ismail, W I W (2014). Application of artificial neural network in predicting crop yield: a review. *J. Food Sci. Eng.*, *4(1)*: 1-9.

Khamis, A; Ismail, Z; Haron, K and Mohammed, A T (2006). Neural network model for oil palm yield modelling. *J. Appl. Sci.*, *6(2)*: 391-399.

Kline, P (2000). *The Handbook of Psychological Testing*. Psychology Press. 744 pp.

Kyurkchiev, N and Markov, S (2015). *Sigmoid functions: Some approximation and modelling aspects - Some moduli in programming environment mathematica.* LAP Lambert Acad. Publ., Saarbrucken. 110 pp.

Majumdar, J; Mal, A and Gupta, S (2016). Heuristic model to improve feature selection based on machine learning in data mining. *Sixth International Conference on Cloud System and Big Data Engineering (Confluence)*. p. 73-77.

Oettli, P; Behera, S K and Yamagata, T (2018). Climate based predictability of oil palm tree yield in Malaysia. *Sci. Rep.*, *8(1)*: 2271.

Panchal, G; Ganatra, A; Kosta, Y and Panchal, D (2011). Behaviour analysis of multilayer perceptrons with multiple hidden neurons and hidden layers. *Int. J. Comput. Theory Eng.*, *3(2)*: 332-337.

Paterson, R R M; Kumar, L; Shabani, F and Lima, N (2017). World climate suitability projections to 2050 and 2100 for growing oil palm. *The J. Agric. Sci.*, *155(5)*: 689-702.

Quaranta, G; Lacarbonara, W and Masri, S F (2020). A review on computational intelligence for identification of nonlinear dynamical systems. *Nonlinear Dynamics*. p. 1-53.

Rahman, M M and Robson, A J (2016). A novel approach for sugar cane yield prediction using Landsat time series imagery: A case study on Bundaberg region. *Adv. Remote Sens.*, *5(2)*: 93-102.

Ranjit, K P and Sinha, K (2016). Forecasting crop yield: A comparative assessment of ARIMAX and NARX model. *RASHI*, *1(2)*: 72-87.

Saadon, S; Uemura, Y and Mansor, N (2014). Torrefaction in the presence of oxygen and carbon dioxide: The effect on yield of oil palm kernel shell. *Procedia Chem.*, *9*: 194-201.

Shanmuganathan, S and Narayanan, A (2012). Modelling the climate change effects on Malaysia's oil palm yield. 2012 IEEE Symposium on E-Learning, E-Management and E-Services (IS3e). 21-24 October 2012. Kuala Lumpur, Malaysia. 6 pp.

Soon, B B F and Hong, H W (2001). Oil palm responses to N, P, K and Mg fertilizers on two major soil types in Sabah. *Proc. of the Int. Palm Oil Congress - Agriculture*. p. 318-334.

Taskaya-Temizel, T and Casey, M C (2005). A comparative study of autoregressive neural network hybrids. *Neural Networks*, *18(5)*: 781-789.

Verdooren, R (2003). Design and analysis fertilizer experiments. *Oil Palm: Management for Large and Sustainable Yields* (Fairhurst, T and Hardter, R eds.). Singapore: Potash & Phosphate Institute/ Potash & Phosphate Institute of Canada (PPI/ PPIC) and International Potash Institute (IPI). 382 pp.

Waheeb, W and Ghazali, R (2019). A novel error-output recurrent neural network model for time series forecasting. *Neural Comput. & Applic*. p. 1-27.

Zuhaimy, I and Azme, K (2011). Neural network in modeling Malaysian oil palm yield. *Am. J. Appl. Sci.*, *8(8)*: 796-803.

Journal of Oil Palm Research Vol. 33 (3) September 2021 p. 413-424
DOI: https://doi.org/10.21894/jopr.2020.0095

PRELIMINARY STUDY ON EFFICIENCY OF DIFFERENT TIME AND LIGHT SOURCE IN LIGHT TRAPS FOR CAPTURING POPULATION OF ADULT OIL PALM BUNCH MOTH, *Tirathaba mundella* (Lepidoptera: Pyralidae)

MOHAMAD ROSMAN SULAIMAN[1]*; SAHARUL ABILLAH MOHAMAD[1]; MOHAMED MAZMIRA MOHD MASRI[1]; SITI NURULHIDAYAH AHMAD[1] and NORMAN KAMARUDIN[1]

ABSTRACT

The oil palm bunch moth, Tirathaba mundella *(Lepidoptera: Pyralidae) is a pest of oil palm especially those planted on peat soil. The pest has a short life cycle, approximately 30 days (eggs four days, larvae 16 days and pupae 10 days) and therefore, its population build up rapidly and causing severe damage to the oil palm when proper control is not in place. A research was conducted to determine the efficiency of different design of the light traps in capturing the adult bunch moths and also, aimed to observe the moths' behaviour in terms of the night flight pattern in the areas with high level of infestation. The study was carried out in two oil palm estates in Sarawak; Location A, Daro and Location B, Sri Aman, from 17-19 July 2018 and 23-25 January 2019, respectively. Six light traps (Location A) and three light traps (Location B) were tested. Night flight activities were recorded for three different intervals; Interval 1 (1925-2125), Interval 2 (2130-2330) and Interval 3 (2335-0135). The result showed that, light Trap 6 was found to be the most attractive in Location A, capturing significantly higher number of moths (mean=38.6667, $p<0.05$). Whereas, in Location B, Trap 2 recorded the highest number of total individual moths captured but, not significantly different from other designs (mean=18, $p>0.05$). In terms of the moths' behaviour, the third interval showed significantly greater number of individual female moths captured compared to the other two intervals in Location A (mean=16, $p<0.05$). However, in Location B, it was found that the amount of captured female moths in the earlier time intervals (Intervals 1 and 2) was significantly greater (mean=8 and 9.6667 individuals, $p<0.05$) than final time interval (two individuals), which was opposite to the observations made in Location A. The cause of such behaviour is still unknown and thorough study is needed. Thus, in future study, the data as such additional climatic parameters need to be incorporated (*e.g. *ambient temperature, humidity, moon phase and wind speed) for further understanding of the behaviours and preferences of the pest. Furthermore, the study also indicates potential application of light trapping as one of the alternatives to the oil palm pest management.*

Keywords: light trapping, oil palm, *Tirathaba mundella*.

Received: 10 June 2020**; Accepted:** 14 September 2020. **Published online**: 27 October 2020.

INTRODUCTION

The oil palm industry in Malaysia is vital to the national economy. Data in 2019 showed more than 5.90 million hectares of land have been utilised for oil palm planting comprising of more than 60% of the total agricultural area in Malaysia (MPOB, 2020a). In 2017, palm oil and palm kernel oil production recorded close to one-third (75.17 million tonnes) of world total oils and fats production from a planted area of 19.04 million hectares, mainly from Indonesia and Malaysia (Norman *et al.*, 2019). It was reported

[1] Malaysian Palm Oil Board,
6 Persiaran Institusi, Bandar Baru Bangi,
43000 Kajang, Selangor, Malaysia.

* *Corresponding author e-mail: mohamad.rosman@mpob.gov.my*

by Parveez *et al*. (2020), Malaysian oil palm export revenue is contributing more than RM67.12 billion in 2018. In 2019, the number decline to RM64.84 billion as a result of weaker demand and lower export prices. Throughout 2019, the exports of more than 27 million tonnes of oil palm products have generated a value of more than RM63 billion (MPOB, 2020b).

A total of 666 038 ha of peatlands in Malaysia have been developed for oil palm cultivation and this includes 437 174 ha in Sarawak; 207 458 ha in Peninsular Malaysia and 21 406 ha in Sabah (Omar *et al*., 2010). Conversion of such a large area from heterogeneous climatic vegetation into a monospecies crop of oil palm had indirectly distraught the natural biological interaction between the host, pests and natural enemies. Therefore, oil palm cultivation in peat is facing the threats of pest as such termites, nettle caterpillars, bagworms, bunch moth, rhinoceros beetles and rats. Among these common pests, *Tirathaba mundella,* commonly known as the oil palm bunch moth is becoming a very significant bunch feeding pest on oil palm planted on peat soils.

Oil palm bunch moth, *T. mundella* (Lepidoptera: Pyralidae), is a pest that can cause serious damage to oil palms planted in peat soil (Lim, 2012; Zulkefli *et al.,* 2012). The life cycle from eggs to pupae is completed within 30 days (Lim, 2012). According to Yaakop and Shafariza (2015), the development stages of this pest consist of five larval stages, each differentiated by different sizes. The longevity of adult bunch moth is around 8-10 days. Khoo *et al*. (1991) described that the adult female moths lay eggs singly or in batches (4-20 eggs) in the fibrous spathe surrounding the base of the flower spike and adults' moth can survive for 9-12 days (Wood and Ng, 1974). The moth is active mostly in the late afternoon and early evening (Sudharto, 2004). The bunch moth infestation is easily characterised by the presence of long tubes of silk and frass constructed by the larvae (Wood and Ng, 1974; Lim, 2012; Mohamad *et al*., 2017). Generally, it infests the young mature palms (Basri *et al*., 1991). Damages are mostly caused by the larvae as they feed, scrap and later bore holes on immature fruitlets, causing severe damages to the fruitlet (Darus and Basri, 2000). Zulkefli *et al*. (2015) reported serious bunch moth infestation in various oil palm plantations on peats in Sarawak *viz*; Mukah, Sibu and Miri with prematurely abortive fruit bunches. Consequently, the fresh fruit bunches (FFB) yield of the infested areas was affected.

Currently, controlling of the *T. mundella* larvae relies heavily on insecticides. In findings reported by Lim (2012), cypermethrin is the most widely used by oil palm plantation to control the pest populations. The use of non-selective insecticide such as fipronil over a long period negatively impacted the population and activity of beneficial insects such as *Elaeidobius kamerunicus*, which is the primary pollinating insects in oil palm plantations. Furthermore, degradation rate of the compound is slow on peat (Prasetyo *et al*., 2013; Prasetyo and Susanto, 2012; Ismail *et al*., 2012). Other methods in controlling the pest population was elaborated by Basri *et al*. (1991), combining the application of insecticides and the cultural practices, such as field ablation for the control measures. Ming *et al.* (2016) conducted a similar study by comparing the ablation block to non-ablation block to suppress the larvae density in an infested area. Nevertheless, studies mentioned above are all focusing on controlling the larval stages of the pest population and thus the idea to examine the safer and environmental-friendly control methods such as the application of light trapping needs to be explored. It can provide the estate as one of the alternatives and less reliance on chemical insecticides.

Light traps are used to monitor the presence of insects and to determine the seasonal pattern of pest density, which provides useful information on the timing of relative abundance and species composition of the targeted pest. Therefore, it can be the most effective and environmentally safe tool used for the Integrated Pest Management (IPM) purpose as it records large number of species during a relatively short period (Kammar *et al*., 2020). By using light trapping less chemicals are used and the problems of insecticides resistance are avoidable. Studies by various researchers (Kim *et al*., 2018a; 2018b; Brehm, 2017; Infusino *et al*., 2017; Keszthelyi *et al*., 2016; Cheng *et al*., 2016; Wölfling *et al*., 2016; Spalding and Parsons, 2004) have reported light trapping efficiency in attracting lepidopteran. However, studies pertaining to the application of light trapping for monitoring and population control of *T. mundella* have yet to be conducted and there is lack of published information supporting the method. Hence, the main aim of this preliminary trial was to evaluate the efficiency of different light sources in the light traps in capturing and observing the behaviour such as night flight activities of the adult *T. mundella* for better management of the adult bunch moth.

MATERIALS AND METHODS

Experimental Site

The study was conducted in two oil palm estates, namely Location A, Daro and Location B, Sri Aman, both situated in Sarawak, Malaysia. The light traps deployed in both sites were different (*Tables 1* and *2; Figures 1-5*). The deployment of the light traps in Location A was carried out for two consecutive nights from 17-19 July 2018 with three different time intervals. The trapping activity was conducted for the duration of six hours, from 1925 hr (17 July 2018) to 0135 hr (18 July 2018). Meanwhile, trapping

activity for Location B in Sri Aman, Sarawak was conducted from 23-25 January 2019 following similar methods as at Location A, Daro.

Sampling Method and Design

The light traps were installed and deployed along the main road of every trial site. The trap location was selected as its placement in open area can optimise the illumination from the light traps. Traps placed in the harvesting path were presumably to be less attractive, as the light illumination is limited and distrupted by the palms' canopy. In order to test this theory, light trap design 1 (Location A, Daro) and light trap design 2 (Location B, Sri Aman) were installed along the harvesting road, approximately 20 m from the planting row. Plastic sheets (74 cm x 90 cm) were used to capture the flying moths attracted to the light source. The plastic sheets were sprayed with aerosol glue (Anti Pest Sticky Spray; Chemi-Bond) on steel poles around the plastic container and tripod. Additionally, the plastic sheets served to amplify the brightness of the light source, hence increasing its attractiveness. The list of traps deployed for each sampling session are listed in *Tables 1* and 2.

Data Collection

The number of individuals captured in each trap were recorded every 2 hr and the plastic sheets were cleaned before the start of the recording. This data collection represents the efficiency of the different light source in the light trap. The interval for each trapping sessions in Location A and B were divided into three session with Interval 1 (1925-2125); Interval 2 (2130-2330) and Interval 3 (2335-0135). The sexes of the individuals captured were also recorded until the end of trapping session. The data recording on individuals captured were then used to reflect with behaviour of the night flight activity of the moths (Altaf *et al.,* 2016). The sexes of the moth were identified according to the methods described by Mohamad *et al.* (2017); Moore (2001); Basri and Norman (2000) and Khoo *et al*. (1991). It was acknowledged that the study was only preliminary and with that, data related to moon phase was not recorded and the night flight behaviour of the moths' observation only focused on the interval intended. Thus, the light trap trials served as short term monitoring for preliminary information basis with regards to the *T. mundella* population density and its night flight behaviours.

TABLE 1. LIGHT TRAPPING DESIGN USED IN LOCATION A, DARO, SARAWAK

No.	Traps type	Watt	Description
1	Birdhouse design	25	A portable trap design with 1 m long stainless-steel rod as stand equipped with 0.2 m normal fluorescent light.
2	Tripod angel bulb with water basin	8	A joint of three stainless steel rods, slanted at 45°; equipped with normal standard bulb light, hanging 50 cm from the ground, and powered by diesel generator. Three plastic sheets (74 cm x 90 cm) was applied with aerosol glue sprayed (Anti Pest Sticky Spray; Chemi-Bond), and placed adjacently in triangular form to facilitate the moth trapping.
3	Spotlight with water-filled oil drum (3 m)	400	A spotlight hanging 3 m from the ground with a semi-rectangular wooden structure as the pillar; equipped with 50 litre oil drums, and powered by diesel generator.
4	Spotlight with water-filled oil drum (2 m)	400	A spotlight hanging 2 m from the ground with a semi-rectangular wooden structure as the pillar; equipped with 50 litre oil drums, and powered by diesel generator.
5	Fabricate plastic container with funnel	25	Fabricated-household plastic container and funnel; equipped with normal bulb light hanging 50 cm facing the funnel and powered by diesel generator. Three plastic sheets (74 cm x 90 cm) was applied with aerosol glue (Anti Pest Sticky Spray; Chemi-Bond) and placed adjacently in triangular form to facilitate the moth trapping.
6	Fluorescent tube light	8	Standard fluorescent white light tied (1 m) tied vertically, 2 m from the ground with a wooden pole stand; equipped with tarpaulin polyethylene (PE) Sheet (2.74 m x 3.65 m), and powered by diesel generator.

TABLE 2. LIGHT TRAPPING DESIGN USED IN LOCATION B, SRI AMAN, SARAWAK

No.	Traps type	Watt	Description
1	Fluorescent tube light	8	Standard fluorescent white light tied horizontally, 50 cm from the ground, on stainless steel rod slanted at 45°, with water basin for catching moth.
2	LED light	50	LED light with housing, vertically hanging 50 cm from the ground and powered by 220V car battery.
3	Spotlight with water basin	150	A spotlight vertically hanging 1 m from the ground, tied with 45° modified stand, and powered by diesel generator.

TABLE 3. TOTAL CAPTURES AND SEXED-CAPTURES IN LOCATION A ACCORDING TO TRAP TYPES

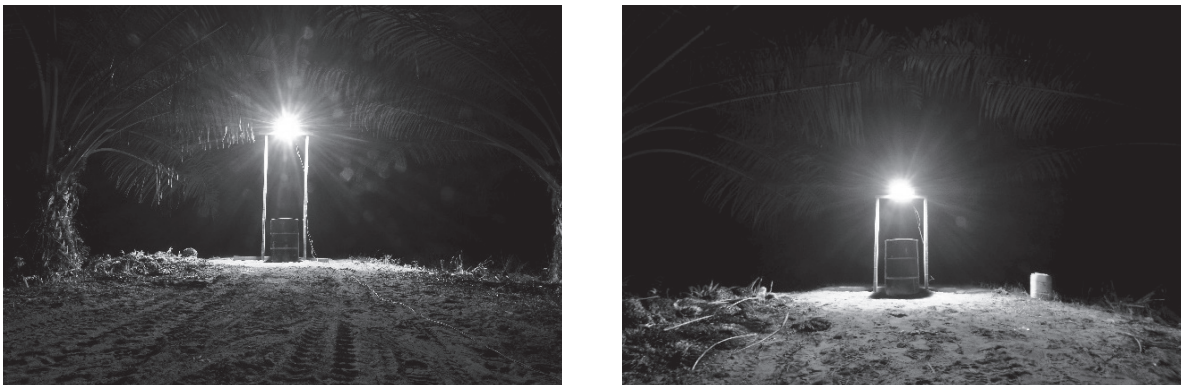
Types of trap	N	Mean total captures		Mean male captures		Mean female captures	
		Mean	P-value	Mean	P-value	Mean	P-value
1	3	1.3333b	0.035	1.3333a	0.291	0.0000b	0.023
2	3	14.3333ab		11.0000a		3.3333b	
3	3	16.0000ab		14.0000a		6.6667ab	
4	3	18.3333ab		3.6667a		12.3333ab	
5	3	20.6667ab		11.3333a		7.0000ab	
6	3	38.6667a		14.0000a		24.6667a	

Note: The same letter after numbers in the same column did not indicate a significantly different by Tukey's test at significant level 95%.



(a) (b)

Figure 1. Light trapping deployed in Location A. (a) Trap 1 was placed on the harvesting path, approximately 20 m from the main collection road. (b) Trap 2 in the middle of the collection road.



(a) (b)

Figure 2. Light trapping deployed in Location A. (a) Trap 3 and (b) Trap 4 both were placed on the collection road.



(a) (b)

Figure 3. Light trapping installed in Location A. (a) Trap 5 and (b) Trap 6 both were placed on the collection road.



(a) (b)

Figure 4. Light trapping installed in Location B. (a) Trap 1 located in the middle of the collection road. (b) Trap 2 located on the harvesting path inside the trial block.



Figure 5. Light trapping installed in Location B. Trap 3 was also located in the middle of the collection road.

Statistical Analyses

Interaction between the types of trap and the time intervals was analysed using two-way analysis of variance (ANOVA). When no interactions were found between the variables, the relationship both factors were then compared using General Linear Model (GLM) (Minitab version 19.0). Comparisons among means were conducted using pairwise multiple comparison procedures (Tukey's method) of significance test at 95%.

RESULTS AND DISCUSSION

The total captures of the adult *Tirathaba* moths were categorised according to the number of individuals captured in each type of traps (*Table 3*). Additionally, the sex of the moths was identified, and the individuals captured were quantified. In Location A, out of the six traps tested, it was found that Trap 6 had captured a significantly higher number of individuals (38.6667 individuals) compared to the other types of light trap ($P<0.05$). In contrast, it was observed that Trap 1 yielded a significantly lower number of captures (1.3333 individuals). No significant differences were observed in the number of males captured between the different types of trap design. However, Trap 6 captured a significantly higher number of female individuals (24.6667 individuals) compared to Trap 2 and Trap 1, which only managed to attract a mean of 3.3333 and 0 females, respectively. Traps 1, 2, 3 and 5 all had higher mean in males captured compared to females.

The high number of moths captured was likely due to the intensity of the light source and the colour of the campsite, which provided greater reflection, hence increasing their attractiveness. As reported by Bowden (1982), the effectiveness of the light trap is very much influenced by trap illumination, hence, the traps that provide better illumination attract more insects. However, although Trap 3 and Trap 4 were using the same types of light source, Trap 4, which was placed lower than Trap 3, was observed to be able to attract more moths. As such, the light source position and height also observed to be influencing its attractiveness. Traps 4, 5, and 6 were all positioned at 1.5 m or less, which made them more accessible to the moths. Previous studies reported that the number of captures could be influenced by trap placement, depending on insect preferences (Mulder *et al*., 2007; Cross *et al*., 2006; Prokopy *et al*., 2001; 2000). Insects such as *Anthonomus eugenii* and *Anthonomus rubi* were reported to be more attracted to traps placed at certain heights compared to others (Fountain *et al*., 2017; Riley and Schuster, 1994). No reports on *Tirathaba* moths light trapping were available prior to this study, so, based on the observation conducted, it can be assumed that the *Tirathaba* moths were more attracted to light traps that were placed under 1.5 m of height. Pyralidae group of moths, in which the *Tirathaba* moths are classed into, are known to be flying lower than other lepidopterans, such as Noctuidae and Sphingidae (Taylor and Brown, 1972), explaining the higher number of catches in lower-placed light traps.

Trap 1 had significantly lower number of captures compared to others. It was possible that the trap illumination was limited since the trap was placed in the harvesting path with frond overlapping making it looked dense compared to other light traps which were placed in the open areas on the main collection road within the oil palm estate. Furthermore, the blue-coloured birdhouse design with roof enclosing the light source was limiting the light emittance from the bulb, making it less attractive to insects. Observation by McGavin (2007), in dense habitats like forests, the range of illumination may be very small. Difference in the light trap design can affect the number of lepidopteran catches (Taylor and French, 1974). The blue-colour trap was unattractive to insects as it has the lowest reflectance compared to other colours (Taha *et al.*, 2012). Study by Sridhar and Senthil Kumaran (2018), mentioned that a yellow bulb with 60 watts was found most efficient in attracting both sexes of Tuta moths, a pest of tomatoes under polyhouse conditions. Therefore, it was assumed that the low amount of the light emittance plus the unsuitable design led to low number of captures.

Only Trap 4 and Trap 6 captured more females than males. Trap 6 captured significantly more females compared to other traps. Interestingly, even when using similar type of light source, Trap 3 and Trap 4 yielded opposite results. The differences were again, as discussed in earlier part of this paper, was the height of the trap. Lower-placed traps (*i.e*. Trap 4 and Trap 6) attracted more females *T. mundella.* Yet, similarly low-placed traps (*i.e*. Traps 2, 3 and 5) attracted more males than females. This indicated that the preference of each gender of *T. mundella* was not conclusive, as various factors are influencing the attractiveness of a light trap. Kim *et al*. (2018b) reported that the phototactic response of another lepidopteran, *Mythimna separata* was significantly influenced by various factors, and sexuality of the moths is one of them. In their report, it was found that significant difference in the phototactic response between both sexes of moth, unmated and mated. This perhaps explains the difference in the number of males and females captured in different types of trap design and light source. Insect phototactic response varies even among similar species, depending on several abiotic and abiotic factors (Park and Lee, 2017; Cheng *et al*., 2011). As such, unless the objective of the trapping was to capture a single gender of *T. mundella*, maybe there was not much significant information that can be obtained from this observation.

In both field trials, the trapping was divided into three-time intervals. In Location A, comparison between the mean of the total individuals and males captured yielded no significant differences among the designated time intervals. However, it was found that for females, a significantly greater number of individuals were captured in the final time interval (16 individuals) compared to earlier periods (Time Interval 2: 8.5 individuals; Time Interval 1: 2.5 individuals). Based on these data, it was observed

that the significantly more females preferred to appear later than the males. As the ambient temperature dropped, the female individuals became more active and easily attracted to light source. These individuals were waiting for suitable ambient temperature to move closer to the light source as weather might influence the effectiveness of light trap (Bowden, 1982; Banerjee, 1967). No information on the diel flight pattern of *T. mundella* were reported previously, and similarly, no literature on the influence of trap design on the number of males and females' catches were available. Several studies reported that various factors influence the flight behaviours of moths according to sexes. For example, in other moth species in the same group of Pyralidae, it was reported that the flight behaviour of males *Ephestia kuehniella*, *Ephestia cautella* and *Plodia interpunctella* is influenced by the pheromone emitted by the female's availability. The pheromone secretion is enhanced by the presence of constant, warm climate, which increases the flight activity of the moths (Levinson and Buchelos, 1981). The observation conducted in the current study was aimed to see the differences in the flight time among different sexes of *T. mundella*, and as such, details on the information related to pheromone secretion is not covered within the scope of this study, but still, in future studies, it is useful to consider this aspect of moths' behaviour.

Meanwhile, in the trial in Location B, three trap designs were evaluated for their attractiveness in mass-trapping the adult *Tirathaba* moths. Based on the results from the first phase of the trial at Location A, three trap designs with the highest number of captures were selected for the second phase of the trial at Location B, explaining the different number of traps deployed at the two study sites (*Table 5*). No significant differences were observed in the number of total moths captured among the traps tested. Similarly, no significant differences were observed in the number of females captured. However, when categorised according to its gender, it was found that Trap 2 (12.6667 individuals) significantly attracted more males than Trap 3 (3.3333 individuals). Trap 1 yielded a balanced number of males and females captured, while Trap 3 (9.333) was seen to be more attractive to the female individuals.

Trap 2 in Location B yielded the highest number of captures among the traps deployed. Trap 1, which was similar to Trap 6 in Location A (the trap design with significantly highest number of *Tirathaba* moths trapped), only managed to trap a mean total capture of 10 individuals, a distinct result compared to the first phase of the trial. It was assumed due to the placement of the light traps in Location A was under a shade by the tarpaulin PE Sheet, which acted as shelter from the wind. Trap 1 in Location B, was set up without any conditioning of shade. Kammar *et al.* (2020) mentioned that, it is possible to set up the trap where it is sheltered from wind. Best position for the light trap operators is with their backs to the wind as the insects fly upwind. The observation confirms earlier findings that the number of captures can be influenced by wide variety of factors, and does not depend on the trap design alone. A trap design, while seemingly working wonders on one night, does not necessarily guarantee a high number of captures in other nights. For example, the light intensity might affect the luminance, and thus the attractiveness of the trap. Increases in mean illuminance and wind speed were associated with decreased light-trap catch. Increase in mean temperature was associated with increased catch (McGeachie, 1989). The number of individuals caught in the light trap increased with temperature but decreased with the fullness of the moon (Yela *et al.,* 1997). Hsia (1972) also discussed on the insect behaviour in relation to light traps and categorising it into 'near' and 'far' phases. The 'near' phase (near the light source) is usually manifested in the number of captures, meanwhile the 'far'-phase influences behaviour of insect at farther distance at which the light traps are deployed. Various estimations were made on the distances at which insects appeared to respond to radiation from the light traps, varying from 50-250 m (Agee, 1972; Plaut, 1971; Stewar *et al.,* 1967). Thus, to optimise the light trap effectiveness, all of these aspects need to be factored in for future studies.

The number of moths trapped in the second time interval was significantly higher (18.3333 individuals) than the later intervals (6.3333 individuals). No significant differences were observed in the number of males captured in the three periods, however, in females, earlier time intervals (Intervals 1 and 2) had a significantly higher number (8 and 9.6667 individuals) of trapped moths compared to the final time interval (2 individuals), which was opposite to the observations made in Location A, at which the final intervals yielded significantly greater number of females than earlier intervals.

The difference in the appearance time between the two study locations can be attributed to the other environment factors (*i.e.* ambient temperature, moon phase and humidity), which were not recorded during the sampling time. Although no prior studies were conducted to specifically light-trap adult *T. mundella*, but based on previous studies, the number of individuals captured by insect traps can be influenced by the placement of the traps, as well as the trap colour (Taha *et al*., 2012; Hoback *et al*., 1999). Moreover, in addition to the trap location, the height of the trap placement might affect the number of captures (Bowie, 1999). In order to increase its effectiveness, these factors must be taken into consideration for future trapping. According to Zhong *et al.* (2017), *Tirathaba* sp. activity and rate of growth development are very much

influenced by temperature. During this trial, the ambient temperature and relative humidity at the peak activity period were not recorded, but it was possible that during the trappings, the temperature was favourable for the moths' activity.

Similar distinctive pattern of appearance between the sexes of *T. mundella* was not observed in Location B (*Table 6*). More females were captured during the first interval compared to similar interval at Location A (*Table 4*). The differences in the pattern is attributable to environmental factors, such as temperature and humidity. As reported by Williams (1961) and Willams and Osman (1960), for a large group of insect taxonomic groups, the insect activity increases with the increase in temperature, from 18°C to the optimum temperature of 29°C. Temperature exceeding the optimum threshold resulted in declining insect activity. Similarly, less activity was detected on temperatures below the minimum threshold. Study by Hrdý *et al.* (1996) and Pinault *et al.* (2012) mentioned that the difference in flight behaviour could be due to temperature, which modulates the activity of nocturnal moths. Kammar *et al.* (2020) suggested that the best nights for insect trapping are warm, humid with cloud cover and little wind. Different species are active at different times of the year and night: some are trapped at dusk, others during the night and some others as daylight appears. Factors such their wing shape or flight times influence the likelihood of moths being captured (Lintott *et al.*, 2014; Fuentes-Montemayor *et al.*, 2012; Beck *et al.*, 2011; Beck and Linsenmair, 2000). As such, these factors should also be considered in future studies.

CONCLUSION

The findings from this study has provided preliminary information on the efficiency of different light sources in light trapping of *T. mundella*. Additionally, patterns of night flight behaviour of the pest were also observed. The information obtained from this study is certainly useful for future studies

TABLE 4. TOTAL CAPTURES AND SEXED-CAPTURES IN LOCATION A ACCORDING TO THE TRAPPING TIME INTERVAL

Time of trapping	N	Mean total captures		Mean male captures		Mean female captures	
		Mean	P-value	Mean	P-value	Mean	P-value
1	3	10.1667a	0.082	7.6667a	0.839	2.5000b	0.027
2	3	18.5000a		10.0000a		8.5000ab	
3	3	26.0000a		10.0000a		16.0000a	

Note: The same letter after numbers in the same column did not indicate a significantly different by Tukey's test at significant level 95%.

TABLE 5. TOTAL CAPTURES IN LOCATION B ACCORDING TO TRAP TYPES

Types of trap	N	Mean total captures		Mean male captures		Mean female captures	
		Mean	P-value	Mean	P-value	Mean	P-value
1	3	10.0000a	0.135	5.0000ab	0.043	5.0000a	0.048
2	3	18.0000a		12.6667a		5.3333a	
3	3	12.6667a		3.3333b		9.3333a	

Note: The same letter after numbers in the same column did not indicate a significantly different by Tukey's test at significant level 95%.

TABLE 6. TOTAL CAPTURES IN LOCATION B ACCORDING TO THE TRAPPING TIME INTERVAL

Time of trapping	N	Mean total captures		Mean male captures		Mean female captures	
		Mean	P-value	Mean	P-value	Mean	P-value
1	3	16.0000ab	0.037	8.0000a	0.294	8.0000a	0.008
2	3	18.3333a		8.6667a		9.6667a	
3	3	6.3333b		4.3333a		2.0000b	

Note: The same letter after numbers in the same column did not indicate a significantly different by Tukey's test at significant level 95%.

in monitoring the pest population in the field, and subsequently, will provide the oil palm plantations management another method to suppress the pest population. From this study, it was observed that different types of light source influenced the number of moths captured. Light-trapping by using fluorescent bulb has resulted in significantly higher number of captures, especially during the first phase of the study in Location A, whereas in the subsequent phase of the study, no significant differences in terms of the number of captures were observed. In this study, it was also observed that the different sexes of *T. mundella* have distinct flight night behaviour, although the observations in both phases of our study yielded inconclusive information. Based on this study, several improvements can be made for future studies related to this topic. It is suggested data such as ambient temperature, humidity, moon phase, and wind speed need to be comprehensively incorporated together for better understanding of the behavioural pattern prediction and pest population monitoring in oil palm plantations. Thus, light trapping of the adult moths of *T. mundella* can be practically applied in the oil palm plantations and can serve as alternative or complementary practices to the current method in controlling the pest population.

ACKNOWLEDGEMENT

The authors would like to extend our gratitude to the Director-General of MPOB for the permission to publish this article. We would like to thank the staff of the Entomology and Integrated Pest Management Unit at MPOB Research Station Sessang, Sarawak who assisted us during this study. Our appreciation also goes to the management of Ta Ann Holdings Bhd., especially Mr. Siaw Ting Chuan and WFM Plantations Bhd. for allowing us to conduct the trial at their estate and lending us the tools required for the trials. We would also like to express our gratitude to the management of Pelitama Estate, Daro, Sarawak (Mr. Marcus, Mr. Merang and Mr. Thien) and Tabaruk Abadi Estate, Sri Aman, Sarawak (Mr. Richard) and the field staff of each estate for the invaluable assistance rendered during the trial.

REFERENCES

Altaf, H S K; Moni, T; Rita, B and Khusboo, B (2016). Light trap and insect sampling: An overview. *Int. J. Curr. Res.*, *8(11)*: 40868-40873.

Agee, H R (1972). Sensory response of the compound eye of adult *Heliothis zea* and *H. virescen* to ultraviolet stimuli. *Ann. Entomol. Soc. Am.*, *65*: 701-705.

Banerjee, A C (1967). Flight activity of the sexes of crambid moths as indicated by light trap catches. *J. Econ. Entomol.*, *60*: 383-390.

Basri, M W; Mukesh, S and Norman, K (1991). Field evaluation of insecticides and cultural practice against the bunch moth, *Tirathaba rufivena* (Lepidotera: Pyralidae) in a mature oil palm plantation. *Elaies, 3(2)*: 355-362.

Basri, M W and Norman, K (2000). Insect pests, pollinators and barn owl. *Advances in Oil Palm Research* (Yusof, B; Chan, K W and Jalani, B S eds.). MPOB, Bangi. p. 466-541.

Beck, J and Linsenmair, K E (2000). Feasibility of light-trapping in community research on moths: Attraction radius of light, completeness of samples, nightly flight times and seasonality of Southeast-Asian hawkmoths (Lepidoptera: Sphingidae). *J. Res. Lepid., 39:* 18-37.

Beck, J; Brehm, G and Fiedler, K (2011). Links between the environment, abundance and diversity of Andean moths. *Biotropica, 43:* 208-217.

Bowden, J (1982). An analysis of factors affecting catches of insects in light-traps. *Bull. Entomol. Res., 72*: 535-556.

Bowie, M H (1999). Effects of distance from field edge on aphidophagous insects in a wheat crop and observations on trap design and placement. *Int. J. Pest Manag., 45(1)*: 69-73.

Brehm, G (2017). A new LED lamp for the collection of nocturnal Lepidoptera and a spectral comparison of light-trapping lamps. *Nota Lepidopterol., 40*: 87.

Cheng, W J; Zheng, X L; Wang, P; Lei, C L and Wang, X P (2011). Sexual difference of insect phototactic behavior and related affecting factors. *J. Appl. Ecol., 22*: 3351-3357.

Cheng, W J; Zheng, X L; Wang, P; Zhou, L L; Si, S Y and Wang, X P (2016). Male-biased capture in light traps in *Spodoptera exigua* (Lepidoptera: Noctuidae): Results from the studies of reproductive activities. *J. Insect Behav., 29(4)*: 368-378.

Cross, J V; Hesketh, H; Jay, N; Hall, D R; Innocenzi, P J; Farman, D I and Burgess, C M (2006). Exploiting the aggregation pheromone of strawberry blossom weevil *Anthonomus rubi* Herbst (Coleoptera: Curculionidae): Part 1. Development of lure and trap. *Crop Prot., 25*: 144-154.

Darus, A and Basri, M W (2000). Intensive IPM for management of oil palm pests. *Oil Palm Bulletin, 41*: 1-14.

Fountain, M T; Baroffio, C; Borg-Karlson, A K; Brain, P; Cross, J V; Farman, D I; Hall, D R; Ralle, B; Rendina, P; Richoz, P; Sigsgaard, L; Storberget, S; Trandem, N and Wibe, A (2017). Design and deployment of semiochemical traps for capturing *Anthonomus rubi* Herbst (Coleoptera: Curculionidae) and *Lygus rugulipennis* poppius (Hetereoptera: Miridae) in soft fruit crops. *Crop Prot.*, *99*: 1-9.

Fuentes-Montemayor, E; Goulson, D; Cavin, L; Wallace, J M and Park, K J (2012). Factors influencing moth assemblages in woodland fragments on farmland: Implications for woodland management and creation schemes. *Biol. Conserv., 153*: 265-275.

Hoback, W W; Svatos, T M; Spomer, S M and Higley, L G (1999). Trap color and placement affects estimates of insect family-level abundance and diversity in a Nebraska salt marsh. *Entomol. Exp. Appl., 91(3)*: 393-402.

Hrdý, I; Kocourek, F; Beránková, J and Kuldoza, J (1996). Temperature models for predicting the flight activity of local populations of *Cydia funebrana* (Lepidoptera: Tortricidae) in Central Europe. *Eur. J. Entomol., 93*: 569-578.

Hsia, O H S (1972). *Attraction of Moths to Light and to Infrared Radiation*. San Fransisco Press Ltd. 89 pp.

Infusino, M; Brehm, G; Di Marco, C and Scalercio, S (2017). Assessing the efficiency of UV LEDsas light sources for sampling the diversity of macro-moths (Lepidoptera). *Eur. J. Entomol.*, *114*: 25-33.

Ismail, B S; Maslinda, M and Zuriati, Z (2012). Effects of temperature, soil moisture content and soil type on the degradation of cypermethrin in two types of Malaysian agricultural soils. *World Appl. Sci. J., 17(4)*: 428-432.

Kammar, V; Rani, A T; Kumar, K P and Chakravarthy, A K (2020). Light trap: A dynamic tool for data analysis, documenting and monitoring insect populations and diversity. *Innovative Pest Management Approaches for the 21st Century.* Springer, Singapore. p. 137-163.

Keszthelyi, S; Nowinszky, L and Szeőke, K (2016). Different catching series from light and pheromone trapping of *Helicoverpa armigera* (Lepidoptera: Noctuidae). *Biologia*, *71*(7): 818-823.

Khoo, K C; Peter, A C O and Ho, C T (1991). *Crop Pest Management in Malaysia*. Tropical Press Sdn. Bhd. Kuala Lumpur. 242 pp.

Kim, K N; Yun, C N; Sin, U C; Huang, Z J; Huang, Q Y and Lei, C L (2018a). Green light and light stress in moth: Influence on antioxidant enzymes in the oriental armyworm, *Mythimna separata* (Lepidoptera: Noctuidae). *Environ. Sci. Pollut. Res.*, *25(35)*: 35176-35183.

Kim, K N; Song, H S; Li, C S; Huang, Q Y and Lei, C L (2018b). Effect of several factors on the phototactic response of the oriental armyworm, *Mythimna separata* (Lepidoptera: Noctuidae). *J. Asia-Pac. Entomol., 21*: 952-957.

Levinson, H Z and Buchelos, C T (1981). Surveillance of storage moth species (Pyralida, Gelechiidae) in a flour mill by adhesive traps with notes on the pheromone-mediated flight behaviour of male moths. *Zeitschrift fur Angewandte Entomol., 92*: 233-251.

Lim, K H (2012). Integrated pest management of *Tirathaba* bunch moth on oil palm planted on peat. *The Planter, 88(1031)*: 97-104.

Lintott, P R; Bunnefeld, N; Fuentes-Montemayor, E; Minderman, J; Blackmore, L M; Goulson, D and Park, K J (2014). Moth species richness, abundance and diversity in fragmented urban woodlands: Implications for conservation and management strategies. *Biodivers. Conserv., 23*: 2875-2901.

McGavin, G C (2007). Expedition field techniques: Insects and other terrestrial arthropods. Geography Outdoors: The centre supporting field research, exploration and outdoor learning. Royal Geographical Society Kensington Gore, London.

McGeachie, W (1989). The effects of moonlight illuminance, temperature and wind speed on light-trap catches of moths. *Bull. Entomol. Res., 79(2)*: 185-192. DOI: 10.1017/S0007485300018162.

Mulder, P; Reid, W; Stafne, E T and Grantham, R A (2007). Monitoring adult weevil populations in pecan and fruit trees in Oklahoma. Extension Service Fact Sheet F-7190. Oklahoma State University, USA. p. 1-8.

Ming, S C; Fah, J B C and Khairulmazmi, A (2016). Field ablation as cultural control for bunch moth *Tirathaba mundella* infestation in young mature oil palm. *J. Oil Palm Res., 28(4)*: 463-470.

Mohamad, S A; Zulkefli, M; Ramle, M; Sulaiman, M R; Ming, S C; Siaw T C, Norman, K; Siti Ramlah, A A and Ahmad, S N (2017). Biological agents

and insecticides to control bunch moth, *Tirathaba rufievena* in oil palm estates in Sarawak, Malaysia. *J. Oil Palm Res., 29(3)*: 323-332.

Moore, D (2001). Insects of palm flowers and fruits. *Insects on Palms* (Howard, F W; Moore, D; Giblin-Davis, R M and Abad, R G eds.). CABI Publishing, Wallingford, Oxon, United Kingdom. p. 233-266.

MPOB (2020a). The oil palm planted area summary. http://bepi.mpob.gov.my/images/area/2019/area_summary.pdf., accessed on 18 May 2020.

MPOB (2020b). Monthly export of oil palm products. http://bepi.mpob.gov.my/index.php/en/export/export-2019/monthly-export-of-oil-palm-products-2019.html, accessed on 18 May 2020.

Norman, K; Idris, A S and Mohamed Mazmira, M M (2019). Prospects in sustainable control of oil palm pests and diseases through the enhancement of ecosystem services - The way forward. *J. Oil Palm Res., 31(3)*: 381-393.

Omar, W; Abd Aziz, N; Mohammed, A T; Harun, M H and Din, A K (2010). Mapping of oil palm cultivation on peatland in Malaysia. *MPOB Information Series No. 473.*

Park, J H and Lee, H S (2017). Phototactic behavioural response of agricultural insects and stored-products insects to light-emitting diodes (LED). *App. Biol. Chem., 60*: 137-144.

Parveez, G K A; Elina, H; Soh, K L; Meilina, O A; Kamalrudin, M S; Bidin, M N I Z; Sundram, S; Hasan, Z A A and Idris, Z (2020). Oil palm economic performance in Malaysia and R&D progress in 2019. *J. Oil Palm Res., 32(2)*: 159-190.

Pinault, L; Guy, J; Vincent, M; Carrat, L and Quiring, D (2012). Temperature and humidity have limited effects on the daily activity patterns of adult pale-winged gray moths in nature (Lepidoptera: Geometridae). *J. Acadian Entomol. Soc., 8*: 61-67.

Plaut, H N (1971). Distance of attraction of moths of *Spodoptera littoralis* to BL radiation, and recapture of moths released at different distances of an ESA blacklight standard trap. *J. Econ. Entomol., 64*: 1402-1404.

Prasetyo, A E and Susanto, A (2012). *Serangga penyerbuk kelapa sawit* Elaeidobious kamerinicus *Faust*: *Agresivitas dan dinamika populasi di Kalimantan Tengah*. *Jurnal Pusat Penelitian Kelapa Sawit, 20(3)*: 103-113.

Prasetyo, A E; Sunindyo, D and Susanto, A (2013). *Pengaruh beberapa jenis bahan aktif insektisida terhadap mortalitas dan kemunculan kumbang baru* Elaiedobius kamerunicus *Faust. Jurnal Pusat Penelitian Kelapa Sawit, 21(3)*: 105-114.

Prokopy, R J; Chandler, B W; Leskey, T C and Wright, S E (2000). Comparison of traps for monitoring plum curculio adults (Coleoptera: Curculionidae) in apple orchards. *J. Entomol. Sci., 35(4)*: 411-420.

Prokopy, R J; Phelan, P L; Wright, S E; Minalga, A J; Barger, R and Leskey, T C (2001). Compounds from host fruit odor attractive to adult plum curculios (Coleoptera: Curculionidae). *J. Entomol. Sci., 36(2)*: 122-134.

Riley, D G and Schuster, D J (1994). Pepper weevil adult response to coloured sticky traps in pepper fields. *Southwest. Entomol., 19*: 93-107.

Sridhar, V and Senthil Kumaran, G (2018). Light trap, an effective component of integrated management of *Tuta absoluta* (Lepidoptera: Gelechiidae) on tomato. *J. Hortic. Sci., 13(1)*: 126-128.

Spalding, A and Parsons, M (2004). Light trap transects – A field method for ascertaining the habitat preferences of night-flying Lepidoptera, using *Mythimna turca* (Linnaeus 1761) (Lepidoptera: Noctuidae) as an example. *J. Insect Conserv., 8:* 185-190.

Stewar, P A; Lam, J J J R and Hoffman, J D (1967). Activity of tobacco hornworm and corn earworm moths as determined by traps equipped with blacklight lamps. *J. Econ. Entomol., 60*: 1520-1522.

Sudharto, P S (2004). *Hama dan penyakit kelapa sawit.* Pusat Penelitian Kelapa Sawit, Medan, Indonesia.

Taha, A M; Homam, B H; Afsah, A F E and El Sharkawy, F M (2012). Effect of trap colour on captures of *Tuta absoluta* moths (Lepidoptera: Gelechiidae). *Int. J. Environ. Sci. Eng., 3*: 43-48.

Taylor, L R and Brown, E S (1972). Effects of light-trap design and illumination on samples of moths in the Kenya highlands. *Bull. Ent. Res., 62*: 91-112.

Taylor, L R and French, R A (1974). Effects of light trap design and illumination on samples of moths in an English woodland. *Bull. Ent. Res., 63*: 583-594.

Williams, C B (1961). Studies in the effect of weather conditions on the activity and abundance of insect populations. *Phil. Trans. B, 244*: 331-378.

Williams, C B and Osman, M F H (1960). A new approach to the problem of the optimum temperature for insect activity. *J. Anim. Ecol., 29*: 187-190.

Wood, B J and Ng, K Y (1974). Studies on boilogy and control of the oil palm bunch moth *Tirathaba rufivena* (Walker) (Lepidoptera: Pyralidae). *Malaya Agriculture J., 49*: 301-331.

Wölfling, M; Becker, M C; Uhl, B; Traub, A and Fiedler, K (2016). How differences in the settling behaviour of moths (Lepidoptera) may contribute to sampling bias when using automated light traps. *European J. Entomology*, *113*: 502 pp.

Yaakop, S and Shafariza, M A M (2015). The bunch moth of the *Tirathaba* species as hidden pest on the peat soil of oil palm plantations: Implications of biological life cycles, the DNA barcoding approach, and infestation pattern detection. *Proc. of the 3rd International Conference on Chemical, Agricultural and Medical Sciences* (CAMS-2015). Singapore. 10-11 December 2015.

Yela, J L and Holyoak, M (1997). Effects of moonlight and meteorological factors on light and bait trap catches of noctuid moths (Lepidoptera: Noctuidae). *Environ. Entomol.*, *26(6)*: 1283-1290.

Zhong, B; Lu, C and Qin, W (2017). Effect of temperature on the population growth of *Tirathaba rufivena* on *Areca catechu* (Arecaceae). *Florida Entomologist, 100(3)*: 578-582. DOI:10.1653/024.100.0314.

Zulkefli, M; Norman, K; Ramle, M and Basri, M W (2012). Integrated pest management of termite and bunch moth in oil palm planted on peat in Malaysia. *Proc. of the Fourth MPOB-IOPRI International Seminar: Existing and Emerging Pests and Diseases of Oil Palm Advances in Research and Management*. Bandung, Indonesia, 13-14 December 2011.

Zulkefli, M; Alindra, G S; Saharul, A M; Norman, K; Siti Ramlah, A A; Siaw, T C; Ramle, M and Siti Nurulhidayah, A (2015). Evaluation of chemical insecticides and biological agents to control bunch moth, *Tirathaba rufivena* in young oil palm area in Sarawak, Malaysia. *Proc. of the PIPOC 2015 International Palm Oil Congress and Exhibition - Oil Palm: Powering the World, Sustaining the Future*. MPOB, Bangi.

Journal of Oil Palm Research Vol. 33 (3) September 2021 p. 425-435
DOI: https://doi.org/10.21894/jopr.2020.0099

IDENTIFICATION AND DETERMINATION OF THE SPECTRAL REFLECTANCE PROPERTIES OF LIVE AND DEAD BAGWORMS, *Metisa plana* WALKER (Lepidoptera: Psychidae) USING VIS/NIR SPECTROSCOPY

MOHD NAJIB AHMAD[1,2]*; ABDUL RASHID MOHAMED SHARIFF[2]; ISHAK ARIS[2]; IZHAL ABDUL HALIN[2] and RAMLE MOSLIM[1]

ABSTRACT

The bagworm is one of main and serious leaf eating insect pest threats of the oil palm plantations in Malaysia. The economic impact from a moderate bagworm attack of 10%-50% leaf damage may cause 43% yield loss. The population of bagworms without control often increases to above its threshold limits, thereby causing a serious outbreak. Monitoring and detection of the oil palm bagworm population is required to ensure proper planning of any control actions in the infested areas. Hence, a study on the determination of the spectral signature of the bagworm species of Metisa plana *Walker was initiated by using Visible/Near Infrared (Vis/NIR) spectroscopy. Live and dead bagworm spectral properties were determined under the Vis/NIR wavelength regions, 350-1050 nm to provide specific infrared detector and band filter for development of an automated counter of the bagworms. The results showed that the live and dead bagworms had specific reflectance spectra at a specific wavelength in the NIR range spectral, ranging from 1032-1051 nm and these were statistically confirmed using the Student's t-Test with two tailed distributions. A principal component analysis (PCA) resulted that the first two principal components, F1 and F2 have eigenvalues greater than 1, at 2.11 and 1.24, respectively. Using a Boxplot Quantiles, the results showed that the lowest and highest means of the reflectance spectra observed for the live bagworms were approximately 3.43% and 26.42%, respectively. Meanwhile, for the dead bagworms, the lowest and highest reflectance spectra observed were 4.02% and 34.29%, respectively. These spectral data were important to determine the suitable infrared (IR) instrumentation for detection of every stage of the live and dead bagworms. This information will be useful, important and crucial for development of an automated detector of insect pest in the future.*

Keywords: *Metisa plana*, spectroscopy, spectral reflectance properties, Vis/NIR.

Received: 13 July 2020**; Accepted:** 24 September 2020**; Published online:** 12 November 2020.

INTRODUCTION

The major insect pests of oil palm capable for causing outbreaks are bagworms. The population of bagworms without control often increases to above its threshold limits, thereby causing serious outbreaks. There are three major species of bagworm pests of oil palm that have been reported, namely, *Metisa plana* Walker, *Pteroma pendula* Joannis and *Mahasena corbetti* Tams. In fact, the bagworms are native species that usually eat indigenous plants, nevertheless, they have changed and adapted to the hosted African oil palm, *Elaeis guineensis* Jacquin (Wood, 1976; Cheong and Tey, 2012). Norman and

[1] Malaysian Palm Oil Board, 6 Persiaran Institusi, Bandar Baru Bangi, 43000 Kajang, Selangor, Malaysia.

[2] Faculty of Engineering, Universiti Putra Malaysia, 43400 UPM Serdang, Selangor, Malaysia.

* *Corresponding author e-mail: mnajib@mpob.gov.my*

Basri (2007) reported that bagworms of the species *M. plana* and *P. pendula* are most of the cases found in Peninsular Malaysia. Meanwhile, *M. corbetti* is the most common in Eastern Sabah (Wood and Nesbit, 1969). Generally, the bagworm in the larval stage survives inside the bag or case until reaching maturity. Different species have their cases in different shapes and sizes, with variation from a narrow hose to an expansive sac (Cheong and Tey, 2012). Furthermore, *M. plana* Walker has seven larval instars or stages based on its life cycle. They create their own bags which are dissimilar in colour and size but the same in structure and shape (Basri and Kevan, 1995). Realising the importance to monitor and detect the bagworm attacks and infestation levels, the spectral properties or spectral signatures of the bagworm, *M. plana*, have been selected and found to be practical and crucial as compared to two other species of the bagworms, due to the *M. plana* species having a long life cycle and survival ability.

The selectivity and specificity of the spectroscopic approaches move towards appropriate early insect infestation detection in crops (Anielle *et al.*, 2017). Basically, the near-infrared or NIR wavelength region in the electromagnetic spectra includes the spectrum range from 780-2500 nm. Besides that, it is known that the photon energy covered under the NIR region ranges from 2.65 x 10^{-19} to 7.96 x 10^{-20} J, with wavenumbers ranging from 13 300 to 4000 cm^{-1}. Initially, the discovery of the first unseen region of light was found by German born British astronomer and music composer, Fredrick William Herschel in the 1800s. Expansion of the NIR spectrum application happened within three decades ago, as well as the instrumentation and spectral analysis method, by using NIR spectroscopy. This may also expand and widen the application scopes into chemical and food product analyses, chemical content determination and many others (Manickavasagan and Jayasuria, 2014). The basic fundamental of the NIR spectroscopy is based on the illumination of materials by electromagnetic emission within the NIR region. This involves the absorption of light within the NIR range by the molecules of the materials, followed by vibrations at specific frequencies relying on the chemical compound inside the materials (Murray and Williams, 1987). Based on the internal chemical interaction, an existing simple molecule grouping attached with strong interatomic bonds, such as carbon-hydrogen, oxygen-nitrogen or nitrogen-hydrogen, will generate a NIR spectrum (Manley *et al.*, 2008).

In general, the NIR spectroscopy has several advantages including fewer requirements for sample preparation and a broad scope of applications. Furthermore, the NIR spectroscopy can assist in providing important data on the chestnut kernel or the outside part by penetrating more than 9 mm, provided there has been proper sample preparation and a suitable wavelength region (Liu *et al.*, 2011). Moreover, the NIR spectroscopy is user friendly, has a quick response, and is environmentally benign and suitable for online assessment (Pasquini, 2003; Wang *et al.*, 2010). It has been proven that this technique is effective and has met the requirements to detect insect pests or insect-damage in food merchandise and seeds. The related research works on the NIR spectroscopy are listed in *Table 1* which include blueberries (Peshlov *et al.*, 2009), cherry fruit (Xing and Guyer, 2008; Xing *et al.*, 2008), fig trees (Burks *et al.*, 2000), flour products (Wilkin *et al.*, 1986), green soyabean vegetables (Sirisomboon *et al.*, 2009), jujube fruit (Wang *et al.*, 2010; Wang *et al.*, 2011) wheat products (Chambers *et al.*, 1992; Baker *et al.*, 1999), Larix species seeds (Tigabu and Oden, 2004), *Picea abies* seeds (Tigabu *et al.*, 2004), *Cordia africana* seeds (Tigabu and Oden, 2002) and other studies. In the case of insects and larvae, they are easily traced because of their internal hemolymph and/or chitin content (Rajendran, 2005) or, incidentally, due to inside damage, dryness or fungi contamination (Wang *et al.*, 2011). Besides that, the effect of different types of spectra measurements to investigate insect-damage by using Vis/NIR spectroscopy was studied by Wang *et al.* (2011) and Moscetti *et al.* (2014).

The objective of this study was to determine the spectral properties of the bagworm, *M. plana* Walker (Lepidoptera: Psychidae) by using Vis/NIR spectroscopy based on the reflectance of light at precise wavelengths in the Vis/NIR wavelength region (350-1050 nm) with the optimum intolerant capacity. The results of this study are important because they can be used to select the best IR instrumentation for bagworm detection based on their spectral reflectance properties, instead of manual observation.

MATERIALS AND METHODS

The live and dead larvae of *M. plana* Walker were collected from all the seven stages of the larval instars of *M. plana*, including the pupal stage (*Figure 2*). The sample size used per stage was 30 larvae/pupae, including live and dead bagworms (n=480). The larvae and pupae were collected and sampled at the smallholding areas in Mukim Chaah (2.207387, 103.038529), Johor and Tanah Mas smallholdings (4.1433155, 101.2665813) in Perak, Malaysia. The locations were varied to study the characteristic of morphology of the bagworm from different environment and insect pest management practices. Collection of the bagworm samples was specific to the *M. plana* species due to its long life cycle and survival ability. The collected bagworms

TABLE 1. RELATED RESEARCH WORKS ON NEAR INFRARED (NIR) SPECTROSCOPY

Researchers	Type of insect detected	Type of food infected	Instrument used	Range of wavelength	Results
Liu *et al.* (2011)	N/A	Chestnut (*Castanea*)	Vector33 NIR spectrometer	833-2 500 nm	The assessment of chestnut quality by NIR spectroscopy. The correlation coefficients of the optimised models for sugar were 0.90 for peeled samples and 0.83 for intact samples.
Wang *et al.* (2011)	Insect, *Ancylis sativa* Liu	Jujube fruit	Handy Lambda II and Lambda NIR2.2t2	400-1 000 nm and 1 000-2 000 nm	The interactance and reflectance in the Vis/SW-NIR wavelength range exhibited higher classification accuracies in sorting severely damaged jujubes from slightly infested and intact samples.
Wang *et al.* (2010)	N/A	'Lizao' jujubes (*Hovenia acerba Lindl.*)	(Handy Lambda II and Solid Lambda NIR2.2t2	310-1 100 nm 1 000-2 150 nm	The abilities of the interactance, reflectance, and transmission modes of visible and near-infrared (Vis/NIR) spectroscopy in detecting internal insect-infested jujubes. The highest correct classification rates obtained from the above modes were 100%, 90.0% and 97.0%, respectively.
Peshlov *et al.* (2009)	Larvae	Wild bluberries	Ocean optics SD2000	650-1 100 nm	The scanning spectrophotometers demonstrated higher signal-to-noise ratios with infestation prediction accuracies of 82.0% and 76.9% compared to the imaging spectrograph with 58.9% accuracy.
Sirisomboon *et al.* (2009)	Worm	Fresh green soyabean	FQA–NIR Gun	600-1 100 nm	The average raw visible and NIR reflectance spectra of good and defective pods of green soyabean showed a similar profile to absorption maximum at 650 (chlorophyll band) and 960 nm (water band).
Xing and Guyer (2008)	Larvae	Tart cherry (*Montomorency*)	FSFR FieldSpec, Analytical Spectral Devices	550-950 nm	The transmittance works slightly better than reflectance in terms of the total classification accuracy.
Tigabu and Oden (2004)	*Petrova perangustana* and *Dioryctria abietella*	Larix species seeds	1225 Infratec analyser	850-1 048 nm	A 100% recognition of infested and empty seeds in the test set by 3-factor PLS models computed based on calibration sets of each species and combined spectra of all species.
Tigabu *et al.* (2004)	*Plemeliella abietina Seitn* (Hymenoptera, Torymidae) larvae	*Picea abies* seeds	NIR Systems Model 6500 spectrometer	1 100-2 498 nm	Discriminant analyses performed with selected NIR absorption bands also gave nearly 100% classification rate for new samples.
Tigabu and Oden (2002)	Hymenoptera, Torymidae larvae	*Cordia africana* seeds	NIR Systems Model 6500 spectrometer	1 100-2 498 nm	Possibility of using NIR spectroscopy in the seed cleaning process in the future provided that appropriate sorting instruments are developed.
Burks *et al.* (2000)	Worm and pupae	Fig trees	Diode-array NIR spectrometer	400-1 700 nm	100 passable figs and 100 figs each for the infested, rotten, sour, and dirty defect categories were examined using NIRS. Correct classifications for these varieties ranged from 83%-100%.
Baker *et al.* (1999)	*Anisopteromalus calandrae* (Howard)	Wheat products	Diode-array NIR spectrometer	400-1 700 nm	With the appropriate integration of NIR spectroscopy and seed-sorting instrumentation, kernels containing parasitoid pupae could be automatically collected from cultures of *A. calandrae* during the mass rearing ofthis beneficial insect.
Wilkin *et al.* (1986)	Flour mite, *Acarus siro* L.	Flour products	Neotec 6350 Mk. 1 Research Composition Analyser	1 100-2 500 nm	Infested samples mite haemolymph caused the absorbance maximum for water to be shifted towards the visible end of the spectrum.

were kept in a 500 ml cylindrical transparent plastic cage and brought back to the Entomology Laboratory at the Malaysian Palm Oil Board (MPOB) Bangi, Selangor for rearing. The live and dead bagworms were sorted out prior to being transferred into Petri dishes, each layered with a Whatman filter paper. The live and dead bagworms were sorted and determined by pinching their bags due to some bagworms were still alive but were parasitised and they were considered as the live bagworms. When pinching the bag of the bagworms, the living bagworms produced liquid at the anterior end of the bag, whilst the bag of the dead bagworms was empty and did not produce any liquid.

Identification of the spectral reflectance properties of live and dead bagworms, *M. plana*, was conducted indoors using a spectroradiometer (GER 1500, USA) (*Figure 1a*) based on the reflectance of light at precise wavelengths in the Vis/NIR wavelength region (350-1050 nm) with the optimum intolerant capacity. The live and dead bagworms were distinguished based on the probe signal (*Figure 1b*), where reflectance spectra differences were plotted for every live and dead bagworm. All sample were analysed 30 times repetition by the spectroradiometer in one round of probe detection and repeated three rounds, n=90. Next, the processing of the data was carried out to select the significant wavelength through a statistical analysis (Izzuddin, 2009). A Student's t-Test with a two-tailed distribution analysis was used for a visual difference interpretation and identifying those wavelengths that exhibited significant spectral separability for normally distributed datasets between the live and dead bagworms at every stage. Data acquisition on the reflectance spectra of live and dead bagworms at every stage of their life cycle was determined. Principal component analysis (PCA), as an unsupervised method, was applied using XLStat 2017 software to quantify cluster separation at different stage of the bagworms that measured variance across all observations in the spectral data (Aaron and Michael, 2011). Boxplot Quantiles were used to compute the boxplot of five summary statistics comprised of three sample quartiles Q1, Q2 and Q3 based on the Tukey statistical analysis (Hyndman and Fan, 1996). The computation was carried out to determine whether the spectral reflectance of every bagworm stage was overlapping each other or the spectral reflectances differed significantly between all stages.

RESULTS

Different values of the reflectance spectra were observed under the Vis/NIR wavelength regions. The results of the reflectance spectra for all of the datasets are illustrated in *Figures 3-10*. The reflectance spectra for the live larvae of the seven instars of *M. plana* were lower as compared to the dead larvae, including the pupal stages.

From the results, PCA scores plot was used to quantify the cluster separation based on the PC1/F1 and PC2/F2 scores, which corresponded to the coordinates for the projection of each observation onto the first two, principal components. The first two principal components, F1 and F2 have eigenvalues



Figure 1. Instrument used in this study (a) a complete set of spectroradiometer, GER 1500 and (b) Spectral reflectance measurement for live and dead bagworms using calibrated probe; only one bagworm positioned on the probe during spectral measurement.

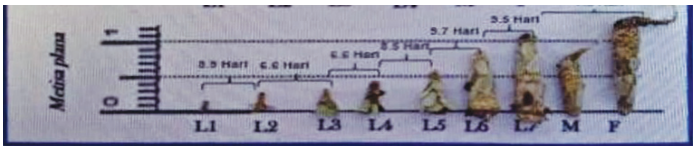


Figure 2. Image of each M. plana *stages.*

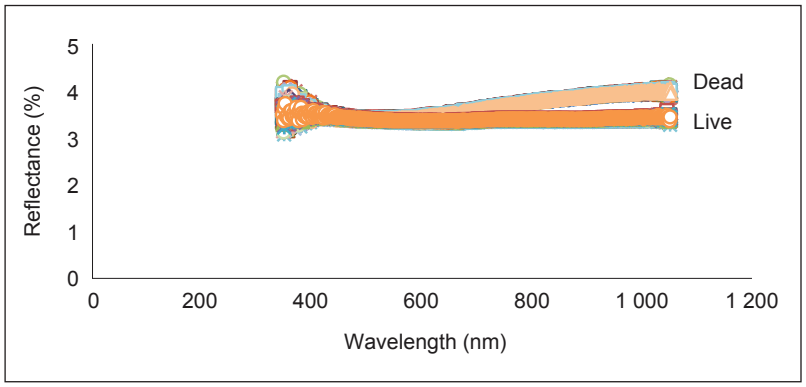


Figure 3. Spectral properties of live and dead stage 1 larval instar of M. plana.

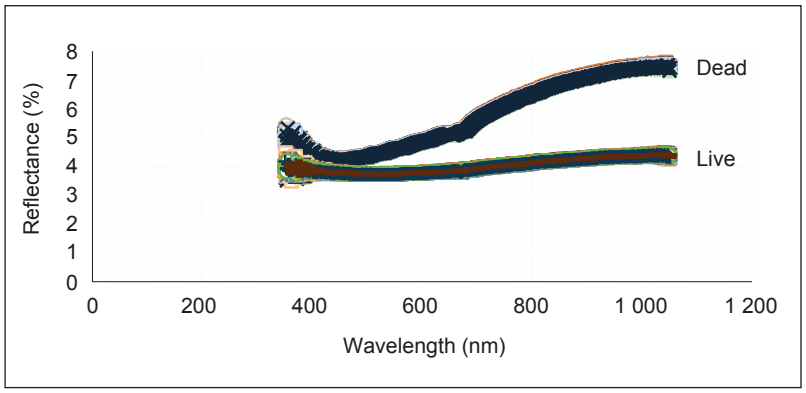


Figure 4. Spectral properties of live and dead stage 2 larval instar of M. plana.

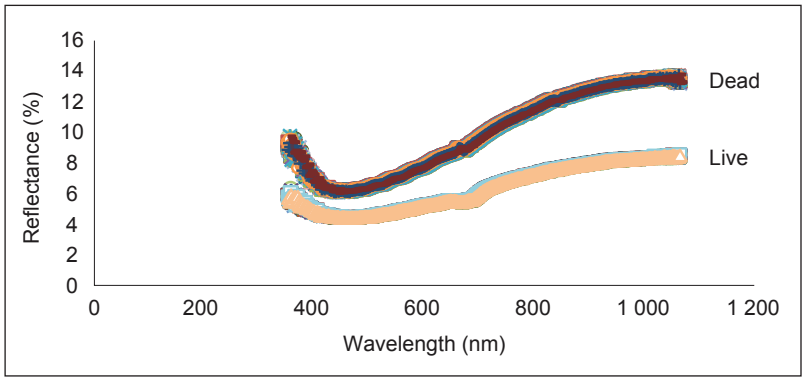


Figure 5. Spectral properties of live and dead stage 3 larval instar of M. plana.

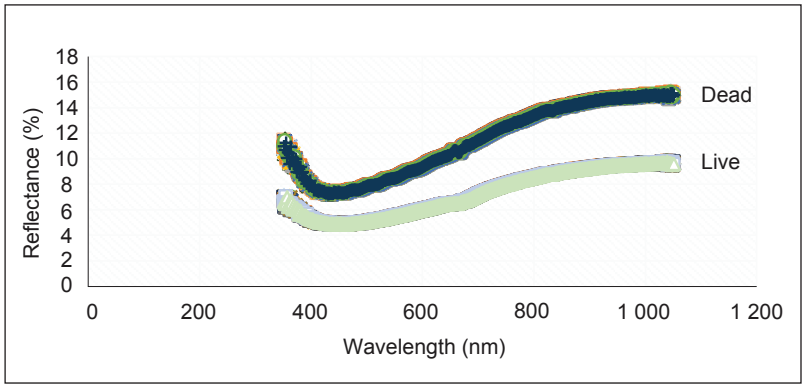


Figure 6. Spectral properties of live and dead stage 4 larval instar of M. plana.

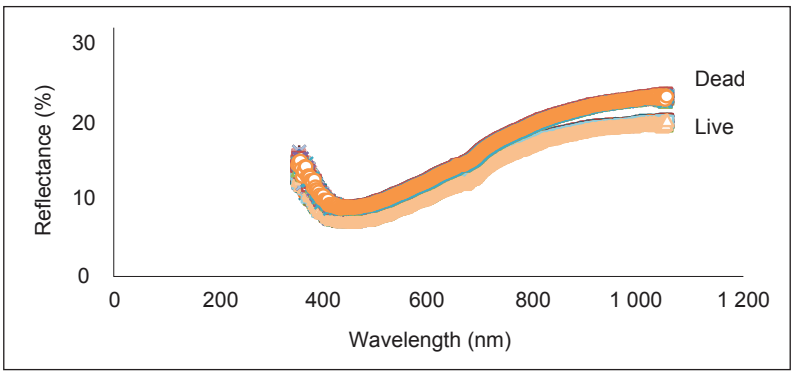


Figure 7. Spectral properties of live and dead stage 5 larval instar of M. plana.

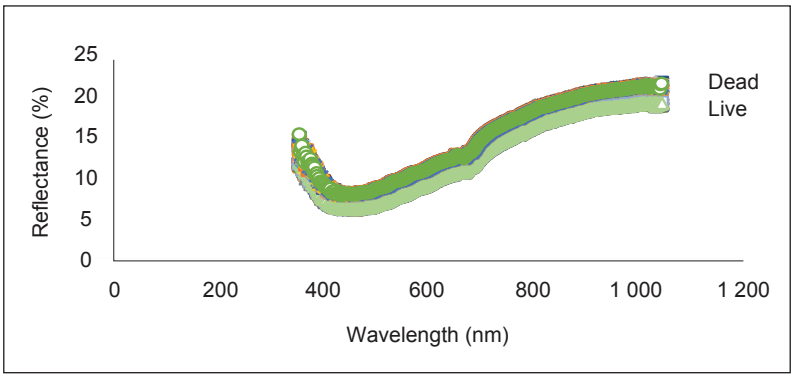


Figure 8. Spectral properties of live and dead stage 6 larval instar of M. plana.

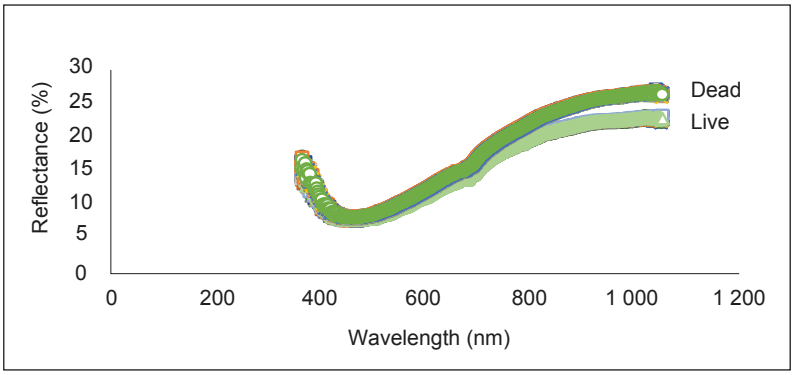


Figure 9. Spectral properties of live and dead stage 7 larval instar of M. plana.

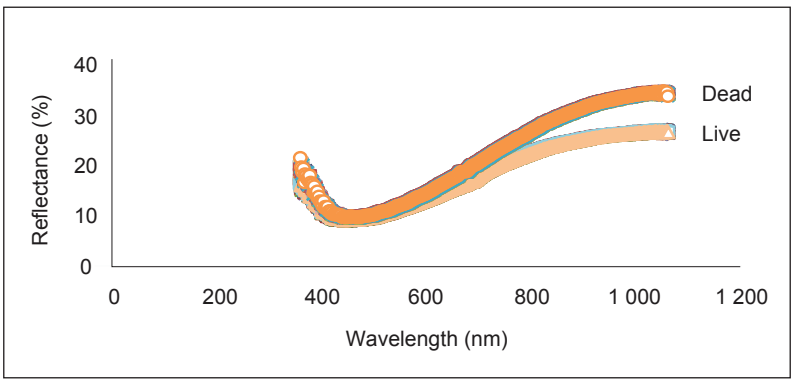


Figure 10. Spectral properties of live and dead pupal stage of M. plana.

greater than 1, at 2.11 and 1.24, respectively. These two components explained 41.8% of the variation in spectral wavelength of the bagworms to separate the *M. plana* stages. Referring to *Figure 10*, the scores and loadings biplot showed that the larval stages 1 (0.139), 2 (0.561), 5 (0.429), 6 (0.455) and 7 (0.603) have large positive loadings on principal component, F2. Therefore, F2 focused on early and late larval stage of *M. plana*, with majority distribution of spectral wavelength from 1032, 1039, 1046, 1048 and 1051 nm. Meanwhile, the larval stages 3 (0.455), 4 (0.709) and pupal stage (0.624) had large positive loadings on principal component, F1. Subsequently, F1 focused on middle and pupal stage of *M. plana*. A statistical test, Student's t-Test, was used to evaluate the significance of the difference between spectral reflectance means and to determine statistically significant of the cluster separation in the PCA scores plot (Aaron and Michael, 2011). Besides that, the maximum difference of the reflectance between the live and dead larval and pupal stages of *M. plana* is shown in *Table 2*. Indeed, there was a significant difference in spectral reflectance of live (Mean = 3.43, SD = 0.045) and dead (Mean = 4.02, SD = 0.043) of first larval instars of *M. plana*, where t (58) is 2.63×10^{-50}; $p<0.05$. The same results were observed for other bagworm stages.

The average reflectance spectra corresponding to every larval instar of the bagworm were obviously different and did not overlap with each other through the boxplot quantiles, implying that every larval instar had a specific reflectance spectra at a specific wavelength in the NIR range (*Figure 11*). The lowest and highest means of the reflectance spectra observed for the live bagworms were approximately 3.43% and 26.42%, respectively. Meanwhile, for the dead bagworms, the lowest and highest reflectance spectra observed were 4.02% and 34.29%, respectively (*Figure 12*).

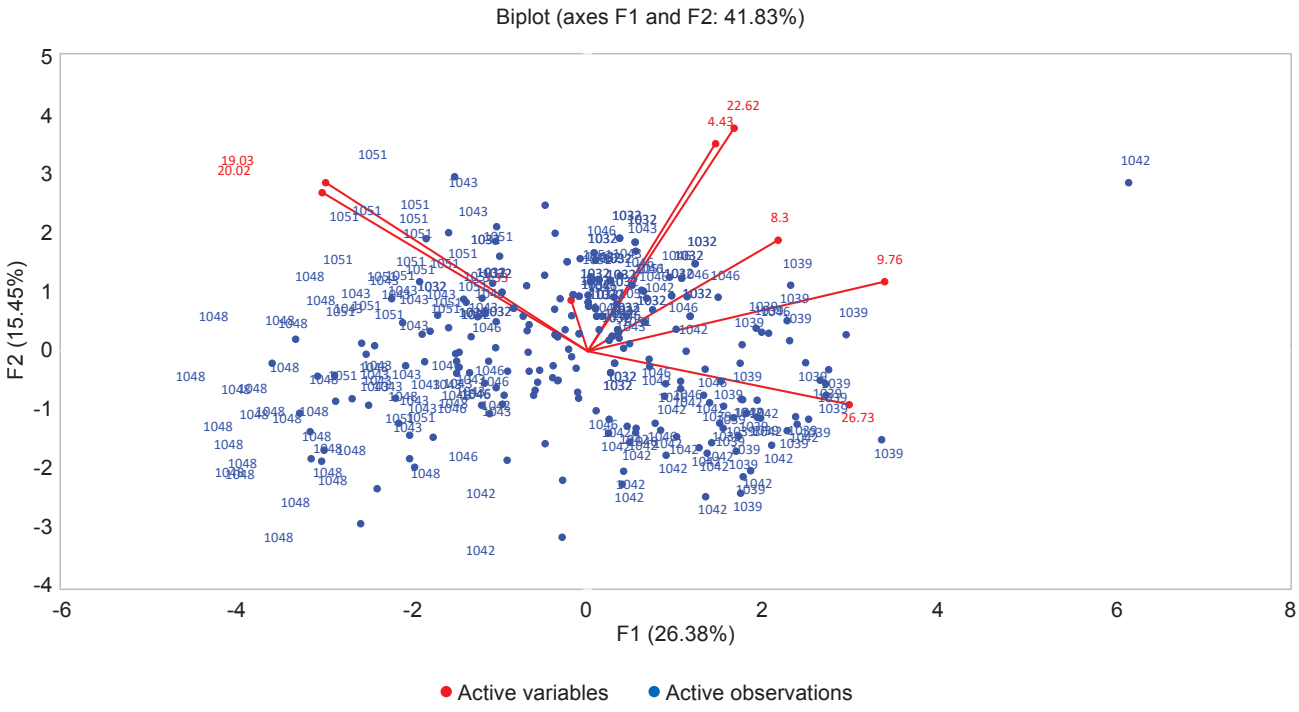
DISCUSSION

Based on the reflectance spectra data, the live larvae and pupae had higher absorbance values in the NIR ranges in the reflectance measurements than the dead larvae and pupae due to the decreased reflectance of the live larval and pupal stages of *M. plana*. This contributed to more incident light to be absorbed and transmitted to the live larvae and pupae due to water content inside their bodies, which resulted in an increase in the reflectance difference between the live and dead larvae and pupae as the wavelength was augmented in the NIR range. The remitted light collected in reflectance measurements contained much more chemical and physical information about the outer surface layers of the dead larvae and pupae than about the internal tissue of the live bagworm. The same result was reported by Wang *et al.* (2010) when detecting infested jujubes

TABLE 2. SPECTRAL PROPERTIES OF BAGWORM, *Metisa plana* USING GER 1500, USA

Bagworm stage	Significant wavelength* (nm)	Reflectance (%)						Reflectance range (%)		Sig. (2-tailed) value
		Min		Max		Mean ± SD				
		Live	Dead	Live	Dead	Live	Dead	Live	Dead	
1	1046 ± 3	3.33	3.97	3.52	4.14	3.43 ± 0.04	4.02 ± 0.04	3.33–3.52	3.97–4.14	2.63 × 10-50
2	1032 ± 15	4.37	7.41	4.47	7.55	4.40 ± 0.02	7.45 ± 0.03	4.37–4.47	7.41–7.55	1.36 × 10-104
3	1039 ± 12	8.29	13.15	8.44	13.35	8.36 ± 0.03	13.23 ± 0.06	8.29–8.44	13.15–13.35	9.46 × 10-103
4	1032 ± 13	9.69	14.88	9.81	15.10	9.74 ± 0.03	14.99 ± 0.05	9.69–9.81	14.88–15.10	1.55 × 10-106
5	1051 ± 11	19.95	23.20	20.56	23.86	20.24 ± 0.12	23.48 ± 0.17	19.95–20.56	23.20–23.86	1.18 × 10-62
6	1048 ± 3	18.91	20.75	19.30	21.38	19.06 ± 0.08	21.03 ± 0.17	18.91–19.30	20.75–21.38	9.48 × 10-53
7	1039 ± 12	22.43	26.67	22.97	27.10	22.69 ± 0.16	26.87 ± 0.11	22.43–22.97	26.67–27.10	2.60 × 10-70
pupa	1043 ± 6	26.16	34.0	26.58	34.52	26.42 ± 0.12	34.29 ± 0.11	26.16–26.58	34.0–34.52	1.70 × 10-91

Note: *The significant wavelengths are determined and validated by statistical analysis through Student's t-Test with two–tailed distributions, where p<0.01. Max and min value of reflectance mode for live and dead bagworm at every stages are used to search for max reflectance difference at specific wavelength and validated using Student's t-Test. Degrees of freedom (df) for all bagworm stages is 58.



Note: Variables in red representing; 3.33 = larval stage (LS) 1, 4.43 = LS 2, 8.3 = LS 3, 9.76 = LS 4, 20.02 = LS 5, 19.03 = LS 6, 22.62 = LS 7 and 26.73 = pupal stage.

Figure 11. Scores and loadings biplot for spectral data separation; F1 vs. F2 factor scores.

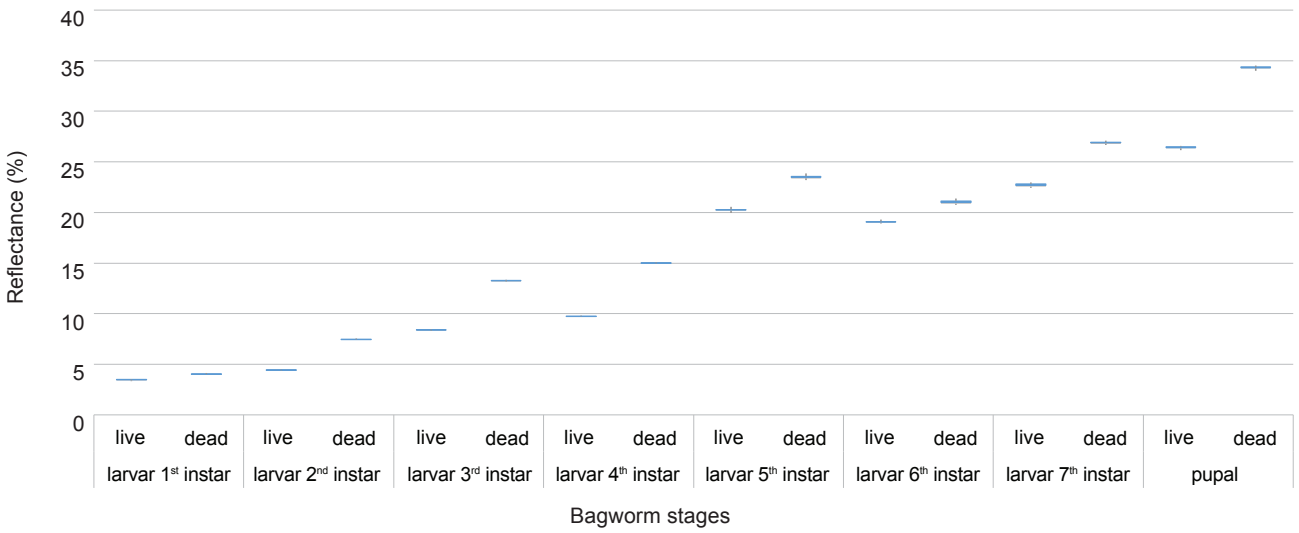


Figure 12. Visualisation of different reflectance spectra for different larval instar and pupal stages of oil palm bagworms, M. plana *by using boxplot quantiles.*

and intact fruits in the visible/Short-wave near infrared (Vis/SW-NIR) range. Dowell *et al.* (1999) reported that wavelengths of 450-700 nm, 900-1400 nm and 1400-1700 nm were related to insect species rather than other wavelengths. Besides that, the epicuticular lipids of the insects consisted of methyl (CH_3) and methylene (CH_2) chemical components, which are positioned at 900-1400 nm and 1400-1700 nm, respectively. Whereby, the effective wavelength for the live and dead of the larvae and pupae of *M. plana* was positioned at 1030-1050 nm. This result was aligned with Dowel *et al.* (1999) finding. Lockey (1988) reported that ketones, fatty acids, aldehydes, alcohols, sterols, hydrocarbons and glycerides were

the main components of the insect cuticular lipids. Moreover, in insects, the long-chain hydrocarbons were the main composition of cuticular lipids but they could differ broadly, from 3%-95% of the overall lipid content. As an example, rice weevils contain 32% hydrocarbon of the overall lipids (Baker *et al.*, 1984). The specific wavelengths of different larval instars of *M. plana*, including the pupal stages, were obtained in the Vis/NIR ranges. This finding supported Dowell *et al.* (1999) and Lockey (1988) statements and proved that the Vis/NIR range is the correct wavelength range for all instars of *M. plana*. From *Table 2*, it was found that the effective wavelengths for the majority of the larvae and pupae were identified at around 1030-1050 nm and the peak around 1000 nm was generally attributed to water or OH functional groups (Wang *et al.*, 2010). According to Najib *et al.* (2018) by using the Ocean-Optics spectrometer, the maximum reflectance difference between the live and dead of the sixth larval instar of *M. plana* was detected at 715 nm. The low values in the reflectance modes for the dead sixth larval instar of *M. plana* could be ascribed to the signal-to-noise ratios that caused inefficiency to interpret the data. These two different results from the authors' current study and Najib *et al.* (2018) revealed that the bagworms could be detected by using NIR spectroscopy at definite region of wavelength under reflectance mode. The characteristic of morphology of the bagworm from different environment was not significantly affected the results because they were seem to be similar and uniform in size. This led to exhibition of same reflectance value at same region of wavelength. Furthermore, in this study, the mean of the reflectance spectra increased with the increase of the larval instar of *M. plana*, except for the sixth larval instar due to the unstable larvae positioning on the probe glass during the experiment. The surface areas of the late larval stages (fourth, fifth, sixth and seventh instar) were larger than the early larval stages (first, second and third instar), subsequently, this was attributed to the higher average reflectance spectra obtained at the effective wavelength (*Table 2*). According to Lockey (1988) each insect species has a cuticle with a specific and unique chemical structure, which leads to different absorbance characteristics that could be differentiated via NIR spectroscopy. Moreover, the effect of unique or specific chemical structures leads to the vibration of the molecules at specific frequencies, subsequently, resulting in the absorption of NIR energy parallel to the specific frequencies (Murray and Williams, 1987). The findings in *Figure 11* generally agree with those reported by Lockey (1988) on differentiating insect species. Moreover, Siegwart *et al.* (2015) reported that the NIR spectroscopy could differentiate between *Cydia pomonella* (L.) and *Cydia molesta* (Busck) (Lepidoptera: Tortricidae) larvae in the wavelengths between 1142 nm and 1338 nm. Jia *et al.* (2014) also proved that the two species of cotton pests, *Gossypium hirsutum* L.; the tobacco budworm, *Heliothis virescens* and the corn earworm, *Helicoverpa zea* could be differentiated at early evolving stages, including egg and young larval stages, by using NIR spectroscopy, resulting in up to a 95% accuracy.

CONCLUSION

The Vis/NIR spectroscopy has been proven as a powerful instrument for quantitative and qualitative analyses which can recognise essential vibrations of the hydroxyl, amine and aldehyde functional groups within the NIR spectra. Determination of the spectral properties of oil palm bagworms is important in order to monitor and detect bagworm populations in the oil palm plantations. The reflectance spectra obtained in the Vis/NIR wavelength range using the spectroradiometer revealed that bagworms can be detected using NIR spectroscopy. Furthermore, these findings are found to be novel and provide new information in the spectroscopy technique, which can be used for inventing specific tools or devices for monitoring bagworm infestations in oil palm plantations worldwide. To meet the mission, data on spectral reflectance properties of the bagworms is used to integrate with suitable band filter specification, in terms of specific wavelength value for particular larval stages. The band filter is located or positioned on the camera lens for filtering red green blue (RGB) image and converted into infrared format, and finally searched for the targeted band of the larval instars of *M. plana* on the fronds.

ACKNOWLEDGEMENT

The authors would like to thanks the Director-General of the MPOB for permission to publish this article, the financial support and patenting of all data under pending patent filing with PI No.: 2017702195. Thanks also to Universiti Putra Malaysia for technical and supervisory support throughout the study.

REFERENCES

Aaron, M and Michael, A K (2011). Quantification and statistical significance analysis of group separation in NMR-based metabonomics studies. *Chemometrics and Intelligent Laboratory Systems, 109*: 162-170.

Anielle, C R; Renan, A R and Aida, B M (2017). Evaluation of the nutritional changes caused by

Huanglongbing (HLB) to citrus plants using laser-induced breakdown spectroscopy. *Appl. Spectrosc., 71(7)*: 1471-1480.

Baker, J E; Dowell, F E and Throne, J E (1999). Detection of parasitized rice weevils in wheat kernels with near-infrared spectroscopy. *Biol. Control, 16*: 88-90.

Baker, J E; Woo, S M; Nelson, D R and Fatland, C L (1984). Olefins as major components of epicuticular lipids of three Sitophilus weevils. *Comp. Biochem. Physiol. B., 77*: 877-884.

Basri, M W and Kevan, P G (1995). Life history and feeding behaviour of the oil palm bagworm, *Metisa plana* Walker (Lepidoptera: Psychidae). *Elaeis, 7(1)*: 18-35.

Burks, C S; Dowell, F E and Xie, F (2000). Measuring fig quality using near-infrared spectroscopy. *J. Stored Prod. Res., 36*: 289-296.

Chambers, J; Cowe, I A; Van Wyk, C B; Wilkin, D R and Cuthbertson, D C (1992). Detection of insects in stored products by NIR. *Near-Infra-Red Spectroscopy: Bridging the Gap between Data Analysis and NIR Applications* (Hildrum, K I; Isaakson, T; Naes, T and Tandberg, A eds.). Ellis Horwood, New York. p. 203-208.

Cheong, Y L and Tey, C C (2012). Understanding pest biology and behaviour for effective control of oil palm bagworm. *The Planter, 88*: 699-715.

Dowell, F E; Throne, J E; Wang, D and Baker, J E (1999). Identifying stored-grain insects using near-infrared spectroscopy. *J. Econ. Entomol., 92(1)*: 165-169.

Hyndman, R J and Fan, Y (1996). Sample quantiles in statistic packages. *The Amer. Statisticians, 50(4)*: 161-165.

Izzuddin, M A (2009). *Early detection of* Ganoderma *disease in oil palms using hyperspectral remote sensing*. M.Sc thesis, Universiti Putra Malaysia.

Jia, F; Maghirang, E; Dowell, F; Abel, C and Ramaswamy, S (2014). Differentiating tobacco budworm and corn earworm using near-infrared spectroscopy. *J. Econ. Entomol., 100(3)*: 759-764.

Liu, J; Li, X; Li, P; Wang, W; Zhang, J; Zhou, W and Zhou, Z (2011). Non-destructive measurement of sugar content in chestnuts using near-infrared spectroscopy. Comput. *Comput. Technol. Agric. IV., 347*: 246-254.

Lockey, K H (1988). Lipids of the insect cuticle: Origin, composition and function. *Comp. Biochem. Physiol. B., 89*: 595-645.

Manickavasagan, A and Jayasuriya, H (2014). *Imaging with Electromagnetic Spectrum*. Springer-Verlag Berlin Heidelberg, Germany. 209 pp.

Manley, M; Downey, G and Baeten, V (2008). Spectroscopic technique: Near-infrared (NIR) spectroscopy. *Modern Techniques for Food Authentication* (Sun, D W ed.). First edition. Academic Press, New York. p. 65-115.

Moscetti, R; Haff, R P; Saranwong, S; Monarco, D; Cecchini, M and Massantini, R (2014). Nondestructive detection of insect infested chestnuts based on NIR spectroscopy. *Postharvest Biol. Technol., 87*: 88-94.

Murray, M I and Williams, P C (1987). Chemical principles of near-infrared technology. *Near Infrared Technology in the Agricultural and Food Industries* (Williams, P and Norris, K eds.). First edition. American Association of Cereal Chemists Inc, St. Paul, Minnesota. p. 17-34.

Najib, M A; Rashid, A M S; Ishak, A; Izhal, A H and Ramle, M (2018). Monitoring insect pest infestation via different spectroscopy techniques. *Appl. Spectrosc. Rev., 53(10)*: 836-853.

Norman, K and Basri, M W (2007). Status of common oil palm insect pests in relation to technology adoption. *The Planter, 83*: 371-385.

Pasquini, C (2003). Near infrared spectroscopy: Fundamentals, practical aspects and analytical applications. *J. Braz. Chem. Soc., 14*: 198-219.

Peshlov, B N; Dowelt, F E; Drummond, F A and Donahue, D W (2009). Comparison of three near infrared spectrophotometers for infestation detection in wild blueberries using multivariate calibration models. *J. Near Infrared Spectrosc., 17*: 203-212.

Rajendran, S (2005). Detection of insect infestation in stored foods. *Adv. Food Nutr. Res., 49*: 163-232.

Siegwart, M; Bouvier, F; Maugin, S; Lecomte, A and Lavigne, C (2015). Differentiating oriental fruit moth and codling moth (Lepidoptera: Tortricidae) larvae using NIR spectroscopy. *J. Econ. Entomol., 108(1)*: 219-227.

Sirisomboon, P; Hashimoto, Y and Tanaka, M (2009). Study on non-destructive evaluation methods for defect pods for green soybean processing by near-infrared spectroscopy. *J. Food Eng., 93*: 502-512.

Tigabu, M and Odén, P C (2002). Multivariate classification of sound and insect infested seeds of a tropical multipurpose tree, *Cordia africana*, with near infrared reflectance spectroscopy. *J. Near Infrared Spectrosc., 10*: 45-51.

Tigabu, M and Odén, P C (2004). Simultaneous detection of filled, empty and insect infested seeds of three Larix species with single seed near-infrared transmittance spectroscopy. *New For., 27*: 39-53.

Tigabu, M; Odén, P C and Shen, T Y (2004). Application of near-infrared spectroscopy for the detection of internal insect infestation in Picea abies seed lots. *Can. J. For. Res., 34*: 76-84.

Wang, J; Nakano, K and Ohashi, S (2011). Non-destructive detection of internal insect infestation in jujubes using visible and near-infrared spectroscopy. *Postharvest Biol. Technol., 59(3)*: 272-279.

Wang, J; Nakano, K; Ohashi, S; Takizawa, K and He, J G (2010). Comparison of different modes of visible and near-infrared spectroscopy for detecting internal insect infestation in jujubes. *J. Food Engineering, 101(1)*: 78-84.

Wilkin, D R; Cowe, I A; Thind, B B; McNicol, J W and Cuthbertson, D C (1986). The detection and measurement of mite infestation in animal feed using near infra-red reflectance. *J. Agric. Sci., 107(2)*: 439-448.

Wood, B J and Nesbit, D P (1969). Caterpillar outbreak on oil palms in Eastem Sabah. *The Planter, 45*: 285-299.

Wood, B J (1976). Pest - Introduction and ecological consideration. *Oil Palm Research* (Corley, R H V; Hardon, J J and Wood, B J eds.). Amsterdam. *Elsevier, 17*: 333-345.

Xing, J and Guyer, D (2008). Comparison of transmittance and reflectance to detect insect infestation in Montmorency tart cherry. *Comput. Electron. Agric., 64(2)*: 194-220.

Xing, J; Guyer, D; Ariana, D and Lu, R (2008). Determining optimal wavebands using genetic algorithm for detection of internal insect infestation in tart cherry. *Sens Instr. Food Qual. Saf., 2(3)*: 161-167.

Journal of Oil Palm Research Vol. 33 (3) September 2021 p. 436-446
DOI: https://doi.org/10.21894/jopr.2020.0107

OIL PALM MALE MEIOSIS PROFILING: FROM FIELD OBSERVATION TO CYTOGENETICS ANALYSIS

NORDIANA, H M N[1]; MADON, M[1,2]; SINGH, R[1]; SRITHARAN, K[3]; MUHAMMAD AZWAN, Z[1] and ZAKI, N M[1]*

ABSTRACT

Male meiosis is a principal process in microsporogenesis, important for male fertility and gamete viability in higher plants. This division ensures genome stability of sexually reproducing organisms and creates genome variation enabling diversity in a species. We present a structured profiling of male meiosis in the interspecific oil palm hybrid, Elaeis oleifera × Elaeis guineensis *(OxG), for an in-depth understanding of the process. In the pollen mother cells (PMC), interaction between the parental genomes was observed in early prophase I, via genomic* in situ *hybridisation (GISH). At this meiosis I stage, the chromosome pairing revealed 16 complete bivalents, confirming the homologous pairing of each* E. guineensis *and* E. oleifera *chromosomes. Interestingly, we found that the* E. guineensis *and* E. oleifera *pollens had distinct morphologies, which represents another feature that differentiates the two species. This could also be used as a basis diagnostic tool to evaluate sterility in oil palm interspecific hybrids.*

Keywords: chromosome pairing, meiosis, oil palm pollen.

Received: 17 August 2020; **Accepted:** 21 October 2020; **Published online:** 4 December 2020.

INTRODUCTION

Oil palm is from the genus *Elaeis* (Arecaceae), a perennial monocot with a single apical meristem. The genus has two interfertile species - the African *E. guineensis* Jacq. and Central/South American *E. oleifera*. Both species are diploid (2n=32), apparently evolved from an ancient tetraploid species (Madon *et al.*, 2005; Singh *et al.*, 2013). Their genome structure and organisation appear quite similar (Singh *et al.*, 2013). *E. guineensis* is planted commercially in most oil palm growing countries, due to its higher yield, while *E. oleifera* only in places where disease(s) devastates *E. guineensis*. Nevertheless, *E. oleifera* has interesting traits that benefit the *E. guineensis* - slower growth, resistance to certain diseases and less saturated oil with higher carotene (Hardon, 1969; Meunier, 1987; Choo *et al.*, 1997; Choo and Yusof, 1996; Amiruddin *et al.*, 2004) - and it has been the ultimate aim to introgress them into *E. guineensis* (Hardon, 1969; Rajanaidu *et al.*, 1995; Escobar and Alvorado, 2003; Amiruddin *et al.*, 2004).

Both monoecious species produce separate male and female inflorescences in alternating phases, influenced by both genetic and environmental factors. The main abiotic factor that influences the sex determination is stress. Anything that detracts from photosynthesis producing more carbohydrates for greater vigour, such as too much/little water and high-density planting, will favour the production of male inflorescences (Corley and Gray, 1976; Barcelos *et al.* 2015). The sex ratio of a palm (number of female inflorescences: total inflorescences)

[1] Malaysian Palm Oil Board,
6 Persiaran Institusi, Bandar Baru Bangi,
43000 Kajang, Selangor, Malaysia.

[2] 9, Jalan BM 5/12, Bandar Bukit Mahkota,
43000 Kajang, Selangor, Malaysia.

[3] United Plantations Berhad, Jenderata Estate,
36009 Teluk Intan, Perak, Malaysia.

* *Corresponding author e-mail: hariza@mpob.gov.my*

(Corley and Tinker, 2003) is an important criterion that determines its yield. A higher sex ratio is generally better for producing more fruit bunches, but excessively high ratios would mean a dearth of male inflorescence/pollen, and denying the female inflorescences of their wherewithal for pollination and fruiting. There has to be a delicate balance in the sex ratio, at any one time, for the desired yield to be realised. A detailed examination of the basic biological process that produce both male and female sex cells in oil palm will be helpful to strategise for higher level of productivity.

The reproductive cells in plants are produced via meiosis, a fundamental inheritance process that occurs in the anthers of male and ovaries of female flowers. In meiotic prophase I, two distinct events occur - homologous chromosome pairing and synapsis, in which the bivalent chromosomes become condensed and distinguishable (Hurel *et al.*, 2018).

Genomic *in situ* hybridisation (GISH) allows visualisation of the homoeologous and homologous chromosome pairing at meiosis, especially in prophase I. The technique further allows detection of chromosome rearrangement, or translocation, and commonly used to evaluate chromosome pairing during meiosis (Schubert *et al.*, 2001; Maluszynska and Hasterok, 2005; Gao *et al.*, 2016). GISH involves labeling of chromosomes or an entire genome in plant hybrids, where total genomic deoxyribonucleic acid (DNA) is used as a probe on chromosome spreads (Anamthawat-Jonsson and Heslop-Harrison, 1995). The technique is generally useful in distinguishing parental genomes in both intergeneric (Leitch *et al.*, 1991; Belandres *et al.*, 2015) and interspecific hybrid plants (Schwarzacher *et al.*, 1992; Abd El-Twab and Kondo, 2007).

Principally, pollen is the end product of meiosis in the male gametic cell, after recombination and reassertion of the chromosomes. Microspores (immature pollen) and pollen are derived from the pollen mother cells (PMC) in pollen sacs. Oil palm belongs to the tribe Cocoaeae, subfamily Arecoideae. Generally, pollen morphology is known to be distinctive for each tribe. The primary aperture type found in this subfamily is monosulcate while trichotomosulcate pollen is only found in *E. guineensis* (Rasheed *et al.*, 2016). The pollen of *E. oleifera* has yet to be described, especially its differences, if any, with that of *E. guineensis* pollen. As plant hybridisation has been known to affect the pollen features, it is anticipated that the pollen morphology of oil palm hybrid might be different than the parental types.

Despite the many studies on meiosis and pollen in other plants, similar researches on oil palm are not many. Hardon and Tan (1969) had reported on the meiotic cytology of interspecific hybrids (*E. guineensis* x *E. oleifera*) and showed that the pachytene chromosomes were normally paired except for the occasional segments. Subsequently, Madon *et al.* (2005) described the basic cytology of *E. guineensis* PMC in an effort to identify two important stages: pachytene and uninucleate stages that will facilitate research. Similarly, apart from histo-anatomical analysis on the *E. oleifera* reproductive system, De Farias *et al.* (2018) also observed the different meiosis and pollen stages, but did not describe the pollen morphology.

This study aims to provide graphical information on male meiosis in oil palm interspecific hybrids. The pairing of the homologous chromosomes of both parental species was observed. In addition, the distinct pollen shapes in the genus *Elaeis* and its interspecific hybrid are also described for the first time. Our findings will provide basic but important information on meiotic recombination in oil palm, apart from the pollen morphology, which can assist in making informed decisions in interspecific breeding of oil palm.

MATERIALS AND METHOD

Plant Materials

Young and mature male inflorescences (*Figure 1*) from *E. guineensis* and *E. oleifera* were sampled from MPOB Kluang, Johor, Malaysia. The inflorescences harvested were still enveloped in their spathes and were identified based on morphological criteria as described by Latif *et al.* (2014). The particular inflorescence to be harvested (whether containing PMC or microspores) was determined based on the description by Madon *et al.* (2005). Generally, the younger inflorescences with whitish buds of soft texture bear PMC, while those mature, with slightly yellowish hard buds should contain microspores.

The PMC are the precursors of microspores which then develop into pollen. The younger inflorescences, subtended by frond numbers 12-17 will have PMC, and those from frond numbers 18-25 bear microspores to pollen (Madon *et al.*, 2005; Latif *et al.*, 2014). The desired inflorescences were selected based on their subtending frond numbers and morphology. However, De Farias *et al.* (2018) had suggested that most meiotic stages in *E. oleifera* could be found in the inflorescence on frond 14, of which, this criterion was not used in the study.

For meiotic chromosome pairing analysis, male inflorescences from an oil palm interspecific hybrid (OxG) created from a cross between a Colombian *oleifera* and Nigerian *guineensis*, were harvested from United Plantations, Teluk Intan, Perak, Malaysia. Spear leaves of the parental palms were provided by the Genomics Laboratory, MPOB.

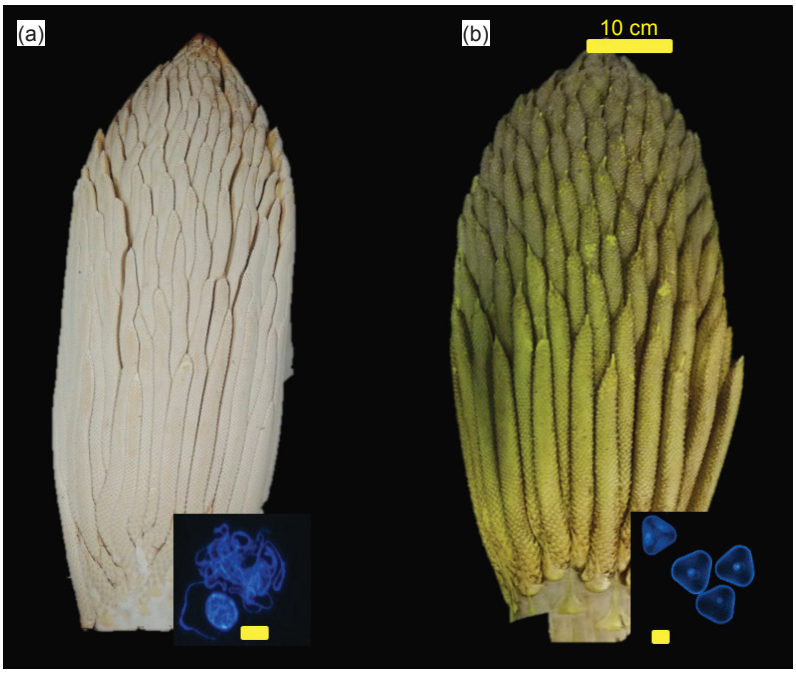


Figure 1. Oil palm male inflorescences (a) young OxG hybrid inflorescence (left) bearing pollen mother cells (PMC) (left inset), and (b) mature E. guineensis *inflorescence (right) bearing microspores (right inset) (inset bar = 20 µm).*

Microspores and Chromosome Staining with 4',6-diamidino-2-phenylindole (DAPI)

The process from harvesting of the male inflorescence to the preparation of the chromosomes spreads is shown in *Figure 2*. The young spikelet with whitish immature buds appeared crisp while the older ones with mature buds are somewhat stringy. A bud from the spikelet was put on a pre-cleaned microscope slide with a 12 µl drop of 1.25 µg ml^{-1} DAPI (Sigma, USA), then squashed with a tweezer. The husk debris was then removed and a clean coverslip was applied to cover the 'suspension'.

Chromosome Preparation

The desired meiosis stage that was stained with DAPI was observed under a fluorescent microscope. Male flower buds at the approximate desired meiotic stage were fixed in ethanol-glacial acetic acid (3:1 v/v) and stored at 4ºC for up to several months. Meiotic preparation was carried out according to Nordiana *et al.* (2016) with minor modification. Anthers from the fixed buds were thoroughly washed with distilled water and 1× citrate buffer (10× citrate buffer consists of 100 mM citric acid and 100 mM tri-sodium citrate, pH 4.6) for 10 min and then digested in 50 µl of enzyme solution containing 1% (w/v) cellulase from *Aspergiller niger* (Sigma Aldrich, USA, C-1184): 1% (w/v) pectolyase from *Aspergiller japonicus* (Sigma Aldrich, USA, P-3026): 1% (w/v) cytohelicase from *Helix pomatia* (Sigma Aldrich, USA, C-8274) for 4 hr at 37ºC. Following the digestion, the anthers were thoroughly rinsed with 1× citrate buffer for 15 min. Two anthers were macerated on a pre-cleaned glass slide in a drop of 60% acetic acid. The PMC were released and dispersed using the squashing technique after applying the coverslip on the suspension. The prepared slides were frozen, the coverslips were removed and the slides were air-dried before use for GISH analysis.

Preparation of Total Genomic Probe and Block

Total genomic DNA of the parental palms, *E. oleifera* (UP1026) and *E. guineensis* (T128), was extracted from their spear leaves using the modified cetyl trimethylammonium bromide (CTAB) method described by Doyle and Doyle (1990), and the quality of the DNA was evaluated as described by Rahimah *et al.* (2006). The DNA of *E. oleifera* (1 µg) was directly labelled with biotin molecules using the BioPrime™ DNA Labelling System Kit (Invitrogen, USA) for use as probe. The DNA of *E. guineensis* was fragmented by autoclaving for 5 min at 15 psi for use as block, as the quantity needed was 140X (140 µg) more than the probe. The autoclaved DNA was stored at -20ºC before use.

Genomic *in situ* Hybridisation (GISH)

GISH was performed according to Madon *et al.* (1999) and Schwarzacher and Heslop-Harrison (2000) with slight modifications. The prepared slides were pre-treated with RNase A [100 µg ml^{-1} RNase A in 2× saline sodium citrate (SSC) at 37ºC for 1 hr,



Figure 2. Isolation of pollen mother cells (PMC) and microspores – from field to microscope. (a) Selection (mentioned in materials above) and harvesting of male inflorescence (left to right) (b) harvested male inflorescence brought to laboratory and processed (left to right) (c) preliminary screening by 4',6-diamidino-2-phenylindole (DAPI) staining viewed under microscope. Spikelet and buds with desired stages fixed for use (left to right).

and then soaked in 0.01M hydrochloric acid (HCl) for 2 min. The slides were then treated with pepsin solution for 10 min at 37ºC and washed in 2× SSC for 5 min. The slides were then post-fixed with 4% paraformaldehyde, washed with 2× SSC, dehydrated in different concentrations of ethanol (70%, 85% and 100%) and left to air dry. A total of 40 µl of probe and block hybridisation mixture with final concentration of 5 µg ml^{-1} was prepared per slide, containing 50% (v/v) formamide, 10% (w/v) dextran sulphate, 2× SSC, 0.125% (w/v) sodium dodecyl sulphate, 0.125 mM ethylenediamine-tetraacetic acid. The mixture was denatured for 10 min at 70ºC, then immediately cooled on ice for another 10 min. A total of 40 µl of hybridisation mixture was dropped on one slide and a plastic coverslip was applied. The hybridisation mixture and chromosomal DNA (the slides) were denatured together on Hybaid Omnislide thermal cycler (Fisher Scientific, USA) at 80ºC for 13 min, 58ºC for 35 min and allowed to cool to the hybridisation temperature of 37ºC overnight (up to 20 hr).

The following day, the slides were washed in 2× SSC for 3 min at 42ºC, rinsed twice for 5 min at 42ºC in 20% (v/v) formamide in 0.1× SSC, twice for 5 min at 42ºC in 0.1x SSC, once for 5 min in 2× SSC at room temperature (RT) and twice for 5 min in detection buffer (4x SSC/0.2% Tween) at RT. Blocking solution [5% (w/v) bovine serum albumin (BSA) in detection buffer] was applied to the slides for 5 min at RT. The biotin-labeled probe was detected with 2 µl streptavidin-CF594 conjugate antibody, 200 µg ml^{-1} (Biotium, USA) in blocking solution. Slides with

the antibody were incubated in a moist chamber at 37ºC for 1 hr. The slides were subsequently washed in detection buffer three times for 5 min each, to remove the surplus antibody at RT. A drop of 10 µl ready-to-use EverBrite™ mounting medium with DAPI (Biotium, CA, USA) was used to counterstain the chromosomes after which they were covered with a glass coverslip.

All the chromosomes slides were viewed and captured under a Leica DMRA fluorescent microscope (Leica Microsystems, Germany) with an Olympus DP73 camera and the images analysed using Olympus CellSens Dimension Imaging Software Version 1.14 (Olympus Corp., Japan).

RESULTS AND DISCUSSION

Male Meiosis Profile of Oil Palm Interspecific Hybrid

We successfully identified all the essential stages of meiosis in oil palm hybrid male inflorescences, occurring as in angiosperms (*Figure 3*). *Figures 3a-e* show prophase 1 with its five known substages - leptotene, zygotene, pachytene, diplotene and diakinesis. Synapsis (pairing) of the chromosome homologues was clearly observed at zygotene, followed by the chromosomes continuing to shorten and thicken at pachytene. The homologous recombination between the parental chromosomes occurs at this stage. The pachytene stage of early meiotic prophase has been extensively studied by cytologists as it provides a unique view of the organisation of haploid genomes (Murphy and Bass, 2012). Using GISH assay, De Farias *et al.* (2018) observed high homology between the chromosomes of the two species when the *E. guineensis* genome was hybridised on *E. oleifera* pachytene chromosomes. The elongated, synapsed fibres at this stage have been applied to assess the organisation of the rice genome (Kim *et al.*, 2005) and to build fluorescence *in situ* hybridisation (FISH) cytogenetic maps, which are ideal for comparative mapping studies and evaluating the quality of the genome sequence assembly in tomato, maize, cucumber and barley (Zhong *et al.*, 1996; Figueroa and Bass, 2012; Lou *et al.*, 2013; Phillips *et al.*, 2013). The transition from pachytene to early diplotene occurs when the elongated chromosomes transform to a compact spindly-looking bivalent fibre configuration. The bivalent fibres continue to separate along their length and eventually become detached. Further chromosome compaction occurs in the transition to diakinesis. The bivalent chromosomes at this stage have been used to study meiotic pairing, as in the intergeneric hybrids of *xBrassicoraphanus*, where the pairing of their parental genomes was observed (Belandres *et al.*, 2015).

The bivalent chromosome pairs align during metaphase I at the equator of the cell (*Figure 3f*). The PMC are in uninucleate, or one-nucleus state. Gao *et al.* (2016) evaluated the chromosome pairing in two population of *Roegneria sinica* var. *media* where it occurred mainly between homologous chromosomes. The homologous chromosomes then separate, and the two sets move to opposite poles of the cell in anaphase I (*Figure 3g*). At telophase I, the chromosome sets arrive at their respective poles and nuclear membrane reappear resulting in two daughter nuclei. A cleavage line appears and gradually divide into two daughter cells (dyad) known as successive cytokinesis (*Figure 3h*).

Following the formation of two daughter cells, the meiotic II division starts which essentially is a mitotic division. In metaphase II, the chromosomes once again orientate on the equatorial plane and divide (*Figure 3i*). The chromatids are then pulled to their respective opposite poles. At the end of telophase II, tetrad eventually gives rise to immature pollen with haploid chromosome number (n=16), also known as microspores (Madon *et al.*, 2005).

Immature pollens from the PMC are known as uninucleate microspores. Their transition to binucleate occurs through mitosis (*Figures 3l-3n*) (Latif *et al.*, 2014). At the end, these two nuclei have different functions, one as a vegetative and the other as a generative nucleus. Microspore culture has been carried out to develop haploid plants, such as in barley, hazelnut and pepper (Li and Devaux, 2001; Karasawa *et al.*, 2016; Ata *et al.*, 2019). This was also attempted for oil palm from uninucleate and binucleate microspores, but oil palm turned out to be recalcitrant to microspore culture, especially in the induction of embryogenesis (Latif *et al.*, 2013).

According to De Farias *et al.* (2018), *E. oleifera* meiosis occurs acropetally, from base to apex. A similar acropetal pattern of meiosis development was also observed for *E. guineensis* and OxG hybrids. Thus, both *Elaeis* sp. and their hybrids go through a similar meiosis pattern (Madon *et al.*, 2005; De Farias *et al.*, 2018). This also occurs in *Arabidopsis* sp. and *Triticum aestivum* (Armstrong *et al.*, 2009; Higgins *et al.*, 2014; Able *et al.*, 2009).

Chromosome Pairing in Early Prophase I in OxG Hybrid

Previously, GISH had differentiated 16 *E. oleifera* and 16 *E. guineensis* chromosomes on the mitotic metaphase spread of an OxG hybrid (Madon *et al.*, 2005). However, the composition of the parental chromosomes varied in the backcross one (BC_1) progenies (Madon *et al.*, 2018). In early meiotic prophase I, the maternal and paternal homologues of each chromosome undergo exact pairing into bivalents. In this study, bivalents are

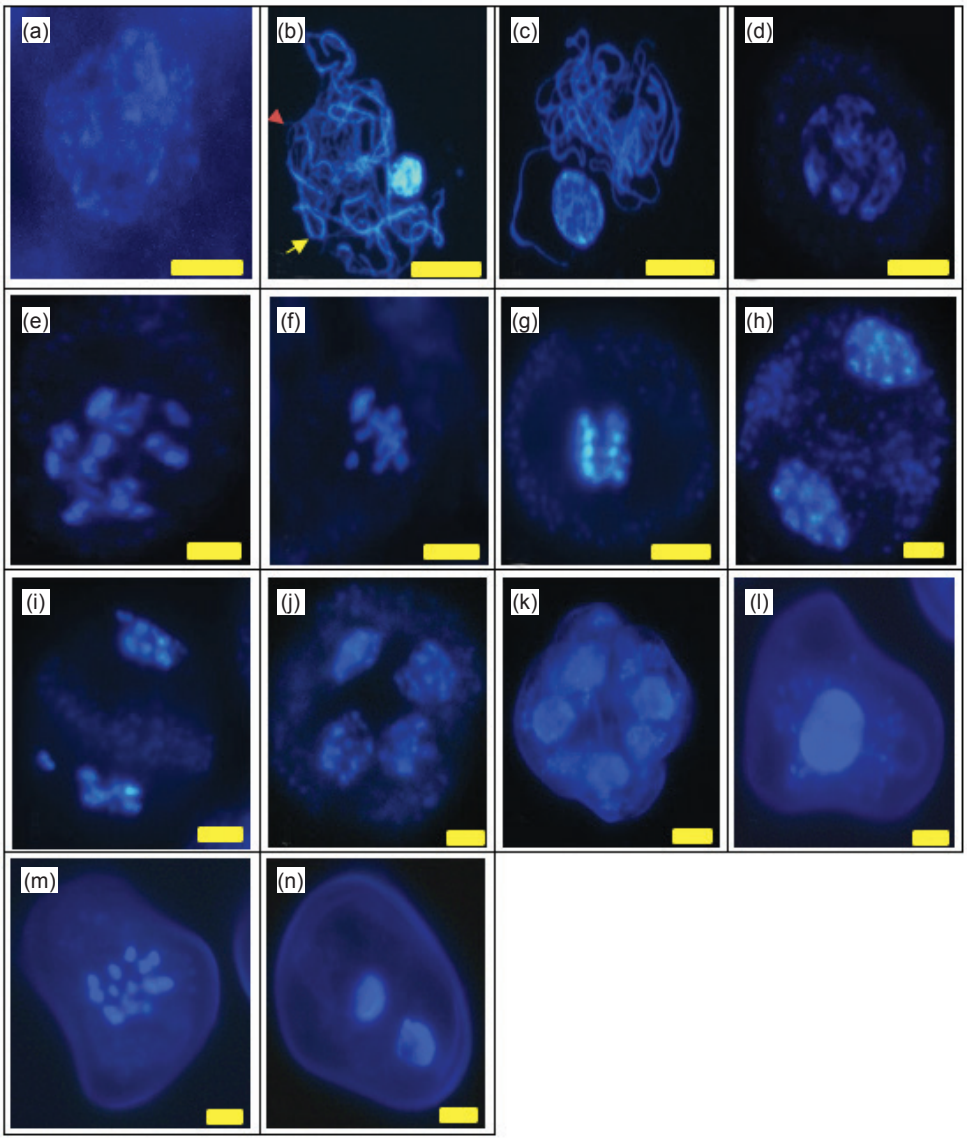


Figure 3. Cytology of male meiosis in oil palm interspecific hybrid. (a) Premeiotic interphase, (b) zygotene with paired (yellow arrow) and unpaired (red arrowhead) chromosomal regions, (c) pachytene with complete paired chromosomes, (d) diplotene, (e) diakenesis showing unaligned bivalents, (f) metaphase i, (g) anaphase i, (h) prophase ii (two daughter cells formation), (i) metaphase ii, (j) tetrad, (k) unreleased microspores, (l) uninucleate (one nucleus state) microspore (m) microspores with 16 chromosomes (n) mid-binucleate microspores with two nuclei. DNA counterstained with 4',6-diamidino-2-phenylindole (DAPI) (bar = 20 µm).

regularly observed on the chromosome spreads. GISH clearly differentiated the 16 bivalent pairs, each pair containing the red fluorescence signals of the *E. oleifera* genomic DNA used as probe, while the *E. guineensis* contributed the blocking DNA. *Figure 4* shows the homologous pairing between two chromosomes at diakinesis, one coming from each parent, forming 16 bivalents in all. These reflect the close homology between the *E. oleifera* and *E. guineensis* chromosomes. Hardon and Tan (1969) had reported the frequent formation of bivalents in meiosis I in *E. guineensis* × *E. oleifera* F1 hybrids, but there has been no information on the pairing of the parental genomes in early meiosis until now.

Cytogenetic studies on meiotic chromosome pairing have been done on other plants, for example, high frequency bivalent formation and regular meiosis in *Lolium perenne* × *Festuca pratensis* hybrids by Thomas and Thomas (1973), while Belandres *et al.* (2015) discriminated 10 pairs of *Brassica* bivalent chromosomes in a new synthetic intergeneric hybrid ×*Brassicoraphanus* line. In a related study, Fukuhara *et al.* (2016) observed frequent formation of bivalents in an interspecific hybrid of Jatropha, suggesting the presence of homoeologous chromosomes in the *Jatropha curcas* × *J. integerrima* hybrid.

Pollen Morphology of *Elaeis* sp. and OxG Hybrid

The pollen of both oil palm species have distinct shapes (*Figure 5*). *E. guineensis* pollen is triangular and *E. oleifera* pollen ellipsoid, in symmetric and asymmetric forms. The OxG pollen is a hodgepodge of the two, being triangular-ellipsoidal. Ravi Kumar

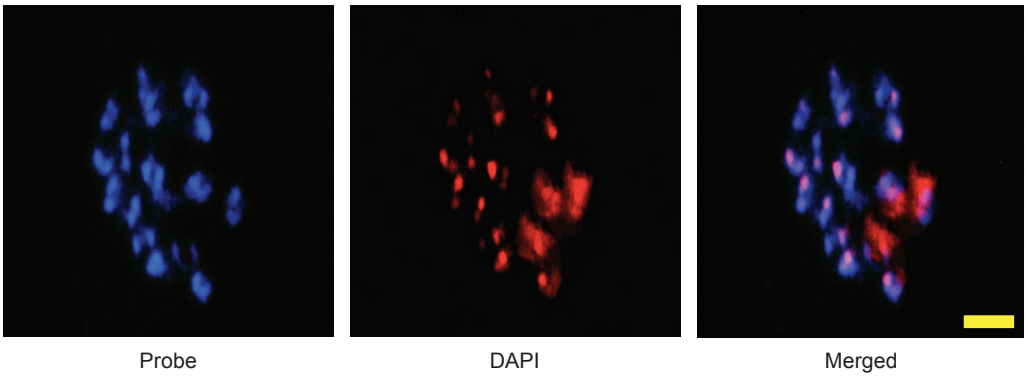


Figure 4. The genomic in situ *hybridisation (GISH) on meiotic chromosomes, probed with BioPrime-labeled total genomic DNA (1 µg) from UP1026, and detected with fluorescent dye CF594 (red) and 140X blocking DNA of T128 counterstained with 4',6-diamidino-2-phenylindole (DAPI) (blue). In the merged image, there are 16 bivalents, each the pairing of one* oleifera *(red) and one* guineensis *(blue) chromosome (bar = 20 µm).*

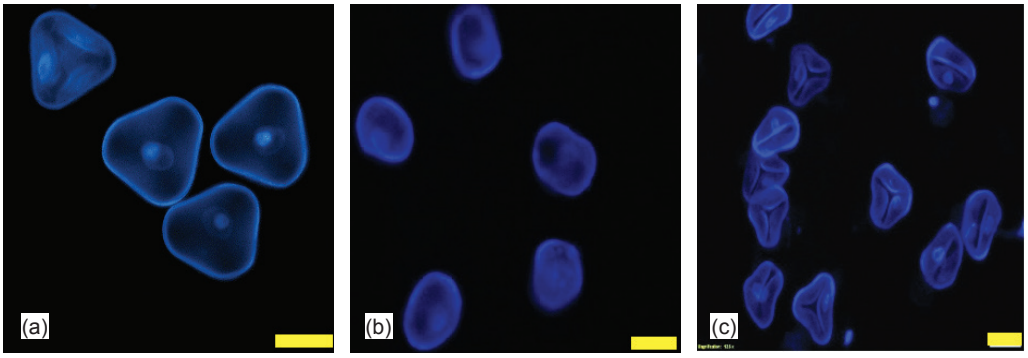


Figure 5. Pollen in (a) E. guineensis *showing triangular shape (b)* E. oleifera *showing ellipsoid shape, and (c) OxG hybrid showing a hodgepodge of both parental morphologies (bar = 50 µm).*

and Nair (1986) reported the pollen shapes in three *Gloriosa* sp. and three of their hybrids (including the reciprocal crosses). In the hybrids, 70%-100% of their pollen resembled those of their respective female parent, suggesting a strong maternal influence on the pollen shape. Similarly, Rhee *et al.* (2005) observed that the pollen morphology of interspecific hybrids of lilies after chromosome doubling highly resembled those of their mother plants. In weeds, the size of *Amaranthus* hybrid pollen was similar to that of the maternal parent but had intermediate aperture numbers between both parents (Franssen *et al.*, 2001), also suggesting a strong maternal influence.

The pollen of both species are aperturate, *i.e.*, having clear apertures on their pollen wall. Harley and Baker (2001) opined that pollen shape is often related to their aperture type, for example, monosulcate aperture (only one opening) with ellipsoidal pollen, as in *E. oleifera* and trichotomosulcate aperture (with three openings) often with trianguloid pollen, as in *E. guineensis* (*Figure 6*). In the tribe Cococeae, Rasheed *et al.* (2016) described the pollen shape are frequently elliptical, but occasionally oblate-triangular pollen are also observed. In some species, the aperture of monosulcate, and, at times, trichotomosulcate pollen can range from being symmetric to asymmetric.

E. guineensis and *Cocos nucifera* (coconut) pollen are easily distinguished by their aperture and exine pattern. *C. nucifera* has monosulcate pollen and *E. guineensis* trichotomosulcate. Cluster analysis revealed that *E. guineensis* is not in the same clade as other aeroids because of its trichotomosulcate pollen (Rasheed *et al.*, 2016). However, the triangular *E. guineensis* pollen does have some similarity with that of *Sclerosperma* sp. (Arecaceae) as described by Grimsson *et al.* (2018). Although no observation of aperture pattern was made on *E. oleifera* by Rasheed *et al.* (2016), this study found that the aperture pattern and subsequent pollen shape are similar to those in *C. nucifera*. Furthermore, the date palm (Arecaceae family) also produces elliptical-oblate and monosulcate pollen (Jazinizadeh *et al.*, 2017).

Nair (1969) suggested that the shapes of pollen could be associated to their functions, hence selection based on morpho-physiological traits may assist in breeding efforts. In *Lilium* sp., a malformed pollen shape was observed in a sterile F1 (Rhee *et al.*, 2005). Interestingly, a similar abnormality was also found in sterile interspecific hybrids of *Lagerstroemia indica* and *L. speciose* (Ju *et al.*, 2019). Hence, the distinct pollen shapes and features identified in this study could form a basis in the development of a diagnostic tool to evaluate sterility in interspecific hybrids of oil palm.

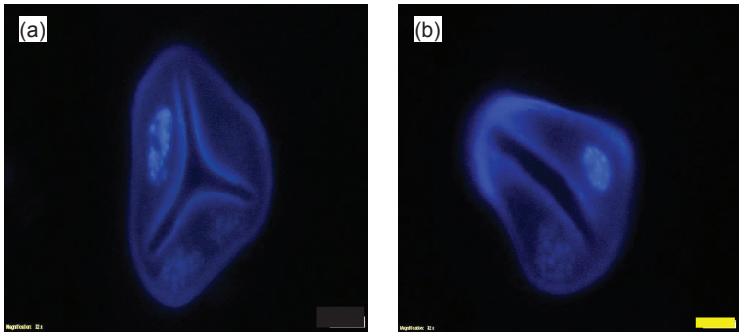


Figure 6. Trichotomosulcate pollen aperture in E. guineensis *(a), and monosulcate pollen aperture in* E. oleifera *(b) (bar = 20 µm).*

CONCLUSION

This study delves into the basic male meiosis process in an oil palm interspecific hybrid, recording its different stages. The meiosis profile of the oil palm interspecific hybrid was consistent with that observed in other plants species, including *E. guineensis* and *E. oleifera*. The information, especially the clear delineation of the different stages, will facilitate other applied experiments, such as *in situ* hybridisation of chromosomes at the particular stages in oil palm breeding. The preliminary results reported will be a spring board for future more in-depth studies on the topic. Moreover, the different pollen morphologies will greatly assist in differentiating the different oil palm types. As expected, the aperture numbers in pollen differed between *E. oleifera* (only one) and *E. guineensis* (three). Hybrid pollen was a hodgepodge of shapes between the two parental types, but more work is required to ascertain the maternal effect on the pollen shape.

ACKNOWLEDGEMENT

The authors would like to thank the Director-General of MPOB for permission to publish this article. Thanks also to the MPOB Cytogenetics Laboratory (SitogenLab) Research Assistants, in particular, Zainab Anip and Mohamad Razali Mohd Noor, for their assistance.

REFERENCES

Abd El-Twab, M H and Kondo, K (2007). Meiotic chromosome organization and segregation in F1 intergeneric hybrid between *Chrysanthemum horaimontanum* and *Nipponanthemum nipponicum* by GISH identification. *Chromosome Botany, 2*: 121-125.

Able, J A; Crismani, W and Boden, S A (2009). Understanding meiosis and the implications for crop improvement. *Funct. Plant Biol., 36*: 575-588.

Amiruddin, M D; Kushairi, A; Rajanaidu, N; Isa Zainol, M A; Noh, A and Junaidah, J (2004). *Elaeis oleifera* oil – A potential source of carotene. Paper presented at the Oils and Fats International Congress (OFIC) 2004. 29 September-2 October 2004. Putra World Trade Centre (PWTC), Kuala Lumpur.

Anamthawat-Jonsson, K and Heslop-Harrison, J S (1995). Establishing relationships between closely related species using total genomic DNA as a probe. *Methods in Molecular Biology Species Identification Species Diagnostics Protocols* (Clapp, J P ed.). *Humana Press, Totowa, 50*: 209-225.

Armstrong, S J; Sanchez-Moran, E and Franklin, F C H (2009). Cytological analysis of *Arabidopsis thaliana* meiotic chromosomes in *Meiosis, Vol. 2: Cytological Methods* (Scott, K ed.). *Humana Press, 558*: 131-145. DOI: 10.1007/978-1-103-5_9.

Ata, A; Keles, D; Taskin, H and Buyukalaca, S (2019). Effects of season, genotype and nutrient medium on pepper anther culture and microspore development. *Turk. J. Agric. For., 43*: 123-137.

Barcelos, E; Rios, S A; Cunha, R N V; Lopes, R; Motoike, S Y; Babiychuk, E; Skirycz, A and Kushnir, S (2015). Oil palm natural diversity and the potential for yield improvement. *Front. Plant Sci., 6: 190*. DOI: 10.3389/fpls.2015.00190.

Belandres, H R; Waminal, N E; Hwang, Y-J; Park, B-S; Lee, S-S; Huh, J H and Kim, H H (2015). FISH karyotype and GISH meiotic pairing analyses of a stable intergeneric hybrid *xBrassicoraphanus* line BB#5. *Korean J. Hortic. Sci. Technol., 33(1)*: 83-92.

Choo, Y M and Yusof, B (1996). *Elaeis oleifera* palm for the pharmaceutical industry. *PORIM Information Series No. 42*.

Choo, Y M; Ma, A N and Yap, S C (1997). Carotenes, vitamin E and sterols in oils from *E. guineensis*, *E. oleifera* and their hybrids. *Palm Oil Developments, 27*: 1-9.

Corley, R H V and Gray, B S (1976). Growth and morphology. *Development in Crop Science Vol. 1* (Corley, R H V; Hardon, J J and Wood, B J eds.). Elsevier, Amsterdam. p. 493-503.

Corley, R H V and Tinker, P B (2003). *The Oil Palm*. Fourth edition. Blackwell Science Ltd, Oxford. 592 pp.

De Farias, M P; De Capdeville, G; Falcao, R; De Moraes, P B; Leao, A P; Camillo, J; Da Cunha, R N V; Alves, A A and Junior, M T S (2018). Microscopic characterization of American oil palm (*Elaeis oleifera* (Kunth) Cortes) floral development. *Flora, 243*: 88-100.

Doyle, J J and Doyle, J L (1990). Isolation of plant DNA from fresh tissue. *Focus, 12*: 13-15.

Escobar, R and Alvarado, A (2003). Strategies in the production of oil palm compact clones and seeds. *Proc. of the PIPOC 2003 International Palm Oil Congress – Agriculture Conference*. MPOB, Bangi. p. 75-90.

Figueroa, D M and Bass, H W (2012). Development of pachytene FISH maps for six maize chromosomes and their integration with other maize maps for insights into genome structure variation. *Chromosome Res., 20(4)*: 363-380. DOI:10.1007/s10577-012-9281-4.

Franssen, A S; Skinner, D Z; Al-Khatib, K and Horak, M J (2001). Pollen morphological differences in *Amaranthus* species and interspecific hybrids. *Weed Sci., 49(6)*: 732-737.

Fukuhara, S; Muakrong, N; Kikuchi, S; Tanya, P; Sassa, H; Koba, T and Srinives, P (2016). Cytological characterization of an interspecific hybrid in *Jatropha* and its progeny reveals preferential uniparental chromosome transmission and interspecific translocation. *Breed. Sci., 66(5)*: 838-844. DOI: 10.1270/jsbbs.16069.

Gao, A; Shi, J and Liang, X (2016). Research on meiotic chromosome pairing in *Roegneria sinica* var. *media* evaluated using genomic *in situ* hybridization. *Plant Biotechnol. Rep., 10*: 129-139.

Grimsson, F; Van Valkenburg, J L C H; Wieringa, J J; Xafis, A; Jacobs, B N and Zetter, R (2018). Pollen morphology of the African *Sclerosperma* (Arecaceae). *Grana, 58(2)*: 99-113.

Hardon, J J (1969). Interspecific hybrids in the genus *Elaeis*. II. Vegetative growth and yield of F1 hybrids *E. guineensis* x *E. oleifera*. *Euphytica, 18*: 380-388.

Hardon, J J and Tan, G Y (1969). Interspecific hybrids in the genus *Elaeis* I. Crossability, cytogenetics and fertility of F1 hybrids of *E. guineensis* x *E. oleifera*. *Euphytica, 18*: 372-379.

Harley, M M and Baker, W J (2001). Pollen aperture morphology in Arecaceae: Application within phylogenetic analyses, and a summary of record of palm-like pollen the fossil. *Grana, 40(1-2)*: 45-77. DOI: 10.1080/001731301591877.

Higgins, J D; Wright, K M; Bomblies, L and Franklin, F C H (2014). Cytological techniques to analyze meiosis in *Arabidopsis arenosa* for investigating adaptation to polyploidy. *Front. Plant Sci., 4*: 546. DOI: 10.3389/fpls.2013.00546.

Hurel, A; Phillips, D; Vrielynck, N; Mezard, C; Grelon, M and Christophorou, N (2018). A cytological approach to studying meiotic recombination and chromosome dynamics in *Arabidopsis thaliana* male meiocytes in three dimensions. *Plant J., 95*: 385-396.

Jazinizadeh, E; Majd, A and Pourpak, Z (2017). Anther development and microsporogenesis in date palm (*Phoenix dacylifera* L.). *Pak. J. Bot., 49(1)*: 331-335.

Ju, Y-Q; Hu, X; Jiao, Y; Ye, Y-J; Cai, M; Cheng, T-R; Wang, J; Pan, H-T and Zhang, Q-X (2019). Fertility analyses of interspecific hybrids between *Lagerstroemia indica* and *L. speciose*. *Czech J. Genet Plant Breed., 55(1)*: 28-34.

Karasawa, M M G; Chiancone, B; Gianguzzi, V; Abdelgalel, A M; Botta, R; Sartor, C and Germana, M A (2016). Gametic embryogenesis through isolated microspore culture in *Corylus avellana* L. *Plant Cell, Tiss. Organ Cult., 124(3)*: 635-647.

Kim, J S; Islam-Faridi, M N; Klein, P E; Stelly, D M; Price, H J; Klein, R R and Mullet, J E (2005). Comprehensive molecular cytogenetic analysis of sorghum genome architecture: Distribution of euchromatin, heterochromatin, genes and recombination in comparison to rice. *Genetics, 171*: 1963-1976.

Latif, A M; Zaki, N M; Nordiana, H M N; Marjuni, M; Che Radziah, C M Z and Madon, M (2014). Correlation of microspore nuclear development with male inflorescence morphology in *Elaeis oleifera*, *Elaeis guineensis* and the OxG hybrid. *J. Oil Palm Res., 26(1)*: 104-108.

Latif, M A; Nordiana, H M N; Zaki, N M; Marjuni, M; Che Radziah, C M Z; Riksen, T; Custers, J and Madon, M (2013). Oil palm microspore culture: MPOB's experience. *Proc. of the PIPOC 2013 International Palm Oil Congress – Agriculture, Biotechnology and Sustainability Conference*. MPOB, Bangi.

Leitch, A R; Schwarzacher, T; Mosgoller, W; Bennet, M D and Heslop-Harrison, J S (1991). Parental

genomes are separated throughout the cell cycle in a plant hybrid. *Chromosoma, 101*: 206-213.

Li, H and Devaux, P (2001). Enhancement of microspore culture efficiency of recalcitrant barley genotypes. *Plant Cell Rep., 20*: 475-481.

Lou, Q; He, Y; Cheng, C; Zhang, Z; Li, J; Huang, S and Chen, J (2013). Integration of high-resolution physical and genetic map reveals differential recombination frequency between chromosomes and the genome assembling quality in cucumber. *PLoS ONE, 8(5)*: e62676.

Madon, M; Arulandoo, X; Sritharan, K; Nordiana, H M N; Muhammad Azwan, Z and Zaki, N M (2018). Short communication: Genomic constitution of oil palm interspecific hybrid crosses monitored by genomic *in situ* hybridization (GISH). *J. Oil Palm Res., 30(2)*: 338-344.

Madon, M; Clyde, M M and Cheah, S C (1999). Application of genomic *in situ* hybridization (GISH) on *Elaeis* hybrids. *J. Oil Palm Res., (Special Issue)*: 74-80.

Madon, M; Heslop-Harrison, J S; Schwarzacher, T; Mohd Rafdi, M H and Clyde, M M (2005). Cytological analysis of oil palm pollen mother cells (PMC). *J. Oil Palm Res., 17*: 176-180.

Maluszynska, J and Hasterok, R (2005). Identification of individual chromosomes and parental genomes in *Brassica juncea* using GISH and FISH. *Cytogenet. Genome Res., 109*: 310-314.

Meunier, J (1987). Prospects of *E. oleifera* x *E. guineensis* interspecific hybrids. IRHO results. *Proc. of ISOPB/PORIM Workshop on Prospects of Interspecific Hybrids* (Soh, A C and Rajanaidu, N eds.). p. 11-15.

Murphy, S P and Bass, H W (2012). Genetics and cytology of meiotic chromosome behavior in plants. *Plant Cytogenetics, Plant Genetics and Genomics: Crops and Models 4* (Bass, H W and Birchler, J A eds.). 345 pp. DOI:10.1007/978-0-387-70869-0_8.

Nair, P K K (1969). The thesis of pollen based plant research. *J. Palynol., 5(1)*: 49-50.

Nordiana, H M N; Muhammad Azwan, Z; Arulandoo, X; Sritharan, K and Madon, M (2016). Development of meiotic pachytene chromosomes preparation technique in oil palm interspecific hybrid and backcross (BC_2). *Transactions of Persatuan Genetik Malaysia Vol. 3*. Genetics Society of Malaysia. p. 143-146.

Phillips, D; Wnetrzak, J; Nibau, C; Barakate, A; Ramsay, L; Wright, F; Higgins, J D, Perry, R M and Jenkins, G (2013). Quantitative high resolution mapping of *HvMLH3* foci in barley pachytene nuclei reveals a strong distal bias and weak interference. *J. Exp. Bot., 64(8)*: 2139-2154. DOI: 10.1093/jxb/ert079.

Rahimah, A B; Cheah, S C and Singh, R (2006). Freeze-drying of oil palm (*Elaeis guineensis*) leaf and its effect on the quality of extractable DNA. *J. Oil Palm Res., 18*: 296-304.

Rajanaidu, N; Chin, C W and Jalani, B S (1995). Performance of *Elaeis oleifera* (Surinam) x *E. guineensis* hybrids. ISOPB International Seminar. Barranquilla, Colombia.

Rasheed, A A; Perveen, A; Abid, R and Qaiser, M (2016). Pollen morphology of the subfamily Arecoideae Griff. (family-Arecaceae) from Pakistan and Kashmir. *Pak. J. Bot., 48(3)*: 1051-1060.

Ravi Kumar, C and Nair, P K K (1986). Inheritance of exine ornamentation and pollen shape in the interspecific tetraploid hybrids of *Gloriosa*. *Can. J. Bot., 64*: 3134-3140.

Rhee, H K; Cho, H R and Kim, K S (2005). Comparison of pollen morphology in interspecific hybrid lilies after *in vitro* chromosome doubling. *Proc. of the IXth International Symposium on Flower Bulbs. Acta Hortic., 673*: 639-643.

Schubert, I; Fransz, P F; Fuchs, J and De Jong, J H (2001). Chromosome painting in plants. *Methods Cell Sci., 23(1-3)*: 57-69.

Schwarzacher, T and Heslop-Harrison, J S (2000). Practical *in situ* hybridization. BIOS Scientific Publishers Ltd., Abindgdon, United Kingdom. 250 pp.

Schwarzacher, T; Anamthawat-Jonsson, K; Harrison, G E; Islam, A K; Jia, J Z; King, I P; Leitch, A R; Miller, T E; Reader, S M; Rogers, W J; Shi, M and Heslop-Harrison, J S (1992). Genomic *in situ* hybridization to identify alien chromosomes and chromosome segments in wheat. *Theor. Appl. Genet., 84*: 778-786.

Singh, R; Ong-Abdullah, M; Low, E T L; Manaf, M A A; Rosli, R; Rajanaidu, N; Ooi, L C L; Ooi, S E; Chan, K-L; Ab Halim, M A; Azizi, N; Jayanthi, N; Bacher, B; Lakey, N; Steven, W S; He, D; Hogan, M; Budiman, M A; Lee, E K; Desalle, R; Kudma, D; Goicoechea, J L; Wing, R A; Wilson, R K; Fulton, R S; Ordway, J M; Martienssen, R A and Sambanthamurthi, R (2013). Oil palm genome sequence reveals divergence of interfertile species in Old and New worlds. *Nature, 500*: 335-339.

Thomas, P T and Thomas, H (1973). *Annual Report of the Welsh Plant Breeding Station for 1973*. Aberystwyth, Cambrian News. 85 pp.

Zhong, X B; De Jong, J H and Zabel, P (1996). Preparation of tomato meiotic pachytene and mitotic metaphase chromosomes suitable for fluorescence *in situ* hybridization (FISH). *Chromosome Res.*, *4*: 24-28.



Journal of Oil Palm Research Vol. 33 (3) September 2021 p. 447-457
DOI: https://doi.org/10.21894/jopr.2020.0113

MOLECULAR CLONING OF *Elaeis guineensis* PHYTOENE SYNTHASE (*Egpsy*) AND ITS EXPRESSION IN MESOCARP TISSUES

WAN NUR SYUHADA, W S[1]*; RASID, O A[1] and GHULAM KADIR AHMAD PARVEEZ[1]

ABSTRACT

Phytoene synthase (psy) *gene is responsible for the synthesis of carotenoids in plants. In this study complimentary deoxyribonucleic acid (cDNA) and genomic sequences of* psy *were isolated by rapid amplification of cDNA ends and polymerase chain reaction (PCR) using ribonucleic acid (RNA) and DNA isolated from the mesocarp tissues of oil palm* (Elaeis guineensis). *The size of the full-length cDNA was 2233 bp. The open reading frame (ORF) was 1299 bp and encoded 433 deduced amino acid (AA) residues. The transcript profile revealed that* psy *was expressed at a maximum level at 12 weeks after anthesis (WAA). The lowest expression of* psy *was at 13 WAA, which was speculated as the transition of the leaf-like carotenoid to the formation of storage carotenoids. The AA sequence deduced from the cDNA was 70%-78% identical to PSY from other higher plants. The genomic sequence analysis revealed that the* psy *gene contains six exons and five introns. Southern blot analysis indicated that oil palm has only one copy of the* psy *gene in its genome.*

Keywords: carotenoids, oil palm, phytoene synthase (*psy*).

Received: 5 August 2020; **Accepted:** 21 October 2020; **Published online:** 17 December 2020.

INTRODUCTION

In 2018, palm oil was a major edible vegetable oil, contributing about 34% of the world's vegetable oils consumption and produced mostly in Malaysia and Indonesia (Kushairi *et al.,* 2019). Crude palm oil is considered as the world's richest natural plant source of carotenoids. Malaysian crude palm oil contains typically 500-700 parts per million (ppm) of carotenoids (Mustapa *et al.*, 2011). Carotenoids such as β-carotene, lycopene and lutein found in vegetable oils, possess anti-oxidant, anti-carcinogenic activities (Uenojo *et al.*, 2007) and provide a primary dietary source of provitamin A in human diets (Tanaka and Ohmiya, 2008). Its deficiency could lead to blindness and premature death (Mayne, 1996). Besides their health-promoting roles, carotenoids are economically important natural products used mainly in food, animal feed, pharmaceutical, nutraceutical and cosmetic industries. In higher plants, carotenoids are essential for providing photoprotective functions during photosynthesis and as precursors for abscisic acid (ABA) biosynthesis.

Gene cloning and functional research of the carotenoid biosynthesis pathway have been extensively carried out in many photosynthetic and non-photosynthetic organisms. The pathway of carotenoid biosynthesis was elucidated in 1987, starting with phytoene synthase (*psy*) in tomato (Zhang *et al.*, 2016). The enzyme catalyses the first step in the synthesis to produce phytoene from geranylgeranyl pyrophosphate (*ggpp*). Phytoene undergoes a series of four desaturations that result in the formation of lycopene. In higher plants, these steps are catalysed by two enzymes, phytoene desaturase (*pds*) and ξ-carotene desaturase. Lycopene undergoes cyclisation by lycopene epsilone cyclase (*lcye*) and lycopene β-cyclase

[1] Malaysian Palm Oil Board,
6 Persiaran Institusi, Bandar Baru Bangi,
43000 Kajang, Selangor, Malaysia.

* *Corresponding author e-mail: syuhada@mpob.gov.my*

(*lcyb*) to produce α- and β-carotenes. Subsequent hydroxylation reactions produce zeaxanthin and lutein (Nisar *et al.*, 2015).

The molecular basis of oil palm carotenoid synthesis has received little attention compared to other higher plants such as tomato (*Solanum lycopersicum*). Tomato is a well-established model plant for carotenoid biosynthesis in fleshy fruit. It has the wealth of genome resources and genetic transformability. However, it is not considered as a comparative reference to study the transcriptional regulation of carotenoid synthesis pathway especially in oil fruits such as oil palm (Tranbarger *et al.*, 2011). The oil palm (*Elaeis guineensis*) genome has been reported (http://genomsawit.mpob.gov.my/). The genome data will be a helpful resource to identify key genes involved in its carotenoid metabolism (Singh *et al.*, 2013). To date, only seven of the oil palm carotenoid genes have been reported, namely, *pds* (Rasid *et al.*, 2005), *lcyb* (Rasid *et al.*, 2003; 2009), 1-deoxy-D-xylulose 5-phosphate synthase (*dxs*) and 1-deoxy-D-xylulose 5-phosphate reductoisomerase (*dxr*) (Khemvong and Suvachittanont, 2005), zeta-carotene desaturase (*zds)* (Rasid *et al.*, 2005), full length of *lcye* (Rasid *et al.*, 2009) and *psy* from *Elaeis oleifera* (Wan Nur Syuhada *et al.*, 2012; Rasid *et al.*, 2008).

Geranylgeranyl pyrophosphate (*ggpp*) is the main precursor for carotenoid biosynthesis in plants. However, this precursor is also shared with other vital metabolic pathways including the synthesis of gibberellic acid, chlorophylls, plastoquinones and tocopherols. Therefore, modifying the carotenoid content and/or composition could have potential negative effects on plant growth (Tanaka and Ohmiya, 2008). Since *ggpp* serves as a precursor for other metabolic pathways, PSY plays an important role in controlling the flux (of carbon) in the carotenoid biosynthetic pathway (Lopez-Emparan *et al.*, 2014). The transcription of *psy* genes has been shown to respond to ABA, salt, light, temperature, drought, photoperiod, development cues and post-transcriptional feedback regulation (Cazzonelli and Pogson, 2010). This enzyme has been isolated previously from a range of plant species including tomato (Ray *et al.*, 1992; Fray and Grierson, 1993; Giuliano *et al.*, 1993; Misawa *et al.*, 1994; Fraser *et al.*, 1995), *Arabidopsis thaliana* (Scolnik and Bartley, 1994), tobacco (Busch *et al.*, 2002), maize (Buckner *et al.*, 1996; Wong *et al.*, 2004), melon (Karvouni *et al.*, 1995), citrus (Kim *et al.*, 2001; Kato *et al.*, 2004; Rodrigo *et al.*, 2004), pepper (Huh *et al.*, 2001), sunflower (Salvini *et al.*, 2005) and banana (Mlalazi *et al.* 2012). The modification of this gene could be effective and useful for increasing carotenoid content in industrial crops. In order to study metabolic pathways especially the carotenoid pathway, genes are usually organised in operons. This operon will be inserted into plastid deoxyribonucleic acid (DNA) and then coexpressed as polycistronic transcripts. These transcripts are often processed further into monocistronic messenger ribonucleic acid (mRNA). For example, Golden rice 2 was developed by introducing maize *psy* in combination with *Erwinia uredovora* carotene desaturase (*crtl*). The amount of β-carotene in the endosperm was increased up to 37 μg g^{-1} of the 31 μg g^{-1} of carotenoids. It is equivalent to the recommended level of vitamin A for a day (Paine *et al.*, 2005).

Manipulation of *psy* in oil palm could potentially increase its carotenoid content as well as alter its composition. However, the molecular basis for the oil palm *psy* is currently unknown especially in *E. guineensis*. Thus, isolation of this gene will enable the investigation of its role in the carotenoid biosynthesis pathway. In this article, we report the isolation and characterisation of *psy* gene from oil palm (*E. guineensis*). The full length of *psy* complimentary DNA (cDNA) and its genomic sequence were successfully isolated and characterised. The molecular phylogeny of *psy* and its expression in mesocarp tissues at different developmental stages were determined.

MATERIALS AND METHODS

Plant Materials

Oil palm fruits were collected from a field at Malaysian Palm Oil Board (MPOB), Bangi, Selangor, Malaysia. The mesocarp tissues at different fruit developmental stages, namely at 5, 7, 9, 11, 13, 15, 17 and 19 weeks after anthesis (WAA), were harvested for ribonucleic acid (RNA) isolation. Total RNA was extracted from the mesocarp tissues of oil palm according to Zeng and Yang (2002). Total DNA from mesocarp tissue was extracted using the modified cetyl trimethylammonium bromide (CTAB) method (Stewart and Via, 1993). The concentration and quality of the RNA and DNA were determined by spectrophotometer and agarose gel analysis. The DNA and RNA samples were stored at -20ºC and -80ºC, respectively, prior to further analysis.

Reverse Transcription of mRNA and Reverse Transcription Polymerase Chain Reaction (RT-PCR)

The first-strand cDNA was synthesised from 1 μg of total RNA sample using the SMART™ RACE cDNA Amplification Kit (Clontech, USA) according to the manufacturer's instructions. The synthesised cDNA was stored at -20°C for PCR amplification.

The primers used in the initial reverse transcription PCR (RT-PCR) amplification were designed by using the COnsensus- DEgenerate Hybrid Oligonucleotide Primer (CODEHOP) (Rose *et al.*, 2005). The software is available at http://blocks.fhrcc.org/codehop.html. Primer sequences were as follows: the sense primer: 5′-GGTGTACAACGTGGTGCTGAARCARGCN GC-3′ and the antisense primer: 5′-TGAA GTTGTTGTAGTCGTTGGCYTCDATYTC-3′. RT-PCR amplifications were performed using AccuPrime™ *Taq* DNA Polymerase System Kit (Invitrogen). The amplifications were carried out in a PTC-100 Thermocycler (MJ Research, USA), in 30-35 sequential cycles programmed as follows: initial denaturing cycle at 94ºC for 30 s, 30 s annealing at 55ºC-60ºC, 2 min elongation at 68ºC and a final cycle of 7 min at 68ºC.

The 5′ RACE primers (PSY15, 5′-TTGGCATA CTCTGCACAGACTTC-3′ and PSY19, 5′-TA GCCGAAGGCGTAATGTGAGAAGC-3′) were designed and synthesised based on the partial sequence of the initial amplified product. Then, the 5′ RACE PCR was performed according to the protocol of the SMART™ RACE cDNA Amplification Kit (Clontech, USA). The first-round PCR was carried out with PSY15 and Universal Primer Mix (UPM) primer set, and the nested-PCR with PSY19 and nested UPM (NUPM) primer set. The nested-PCR product was purified and cloned into PCRII-TOPO vector (TOPO TA Cloning Kit, Invitrogen, USA) and sequenced.

End-to-end PCR was performed to amplify the complete cDNA and genomic sequence of *psy* using the gene-specific primers (PSYA1 and PSYAB4) that were designed based on 5′ and 3′ regions.

Bioinformatics Analysis

The AA sequence analyses were performed using open reading frame (ORF) Finder (http://www.ncbi.nlm.nih.gov/gorf/gorf.html). Comparison of the sequence was performed by using BLAST of GenBank (http://www.ncbi.nlm.nih.gov/BLAST/). Multiple sequence alignment was carried out using Vector NTI software. Predictionof signal peptide was performed with SIGNALP. Full sequences were aligned using ClustalW ver. 2.1, while phylogenetic analysis was done using RAxML (General time reversible nucleotide substitution model with gamma distributed rate variation among sites and Felsenstein's bootstraps) visualisation with ClustalW by ETE3. Protein localisation site was predicted by Wolf PSORT program (Horton *et al.*, 2007). The presence of transmembrane domain was analysed by TMpred algorithm (http://www.ch.embnet.org/software/TMPRED_form.html).

Southern Blot Analysis

A total of 30 μg of genomic DNA were digested with *Bam*HI, *Hin*dIII, *Eco*RI and *Spe*I, separated on a 0.9% agarose gel and transferred onto Hybond XL membrane (Amersham Bioscience). A specific primed DNA probe was synthesised from the *E. guineensis* phytoene synthase *(Egpsy)* cDNA using the TAKARA random primer (TAKARA) according to the manufacturer's instructions. The membrane was hybridised at 60°C with α-^{32} P-dCTP-labelled probe. After hybridisation, the membrane was washed in 2 × SSC/0.1% SDS at 60°C for 10 min followed by 1 × SSC/0.1% SDS at 60°C for 10 min.

Reverse Transcription Quantitative Real-time PCR (RT-qPCR)

The expression study of oil palm *psy* was performed using reverse transcription quantitative real-time PCR (RT-qPCR) analysis. Total RNA from mesocarp of 5-19 WAA fruits were used in the analysis. Total RNA (10 μg) was reverse transcribed with the High Capacity cDNA Archive Kit (Applied Biosystem) according to the manufacturer's protocol. The cDNA (100 ng) was subjected to qPCR assays in triplicate on an ABI PRISM 7000 Sequence Detection System (Applied Biosystems, USA) using TaqMan Universal PCR mastermix according to the manufacturer's recommendation (Applied Biosystems, USA). The primers for the *psy* gene were CGGATCTAGTGAGTTGTTCTTCGA(forward)and GGAATTATGCTGTATATACCATATCCGCAAT (reverse) and the probe for the gene was FAM-CTCGGAACAACAAGATC-NFQ. Meanwhile, the primers for the GAPDH were ACTGCTACTCAGAAGACTGTTGATG (forward) and TGCTGCTAGGAATGATGTTAAAGCT (reverse) and the probe for the gene was FAM-ACCCCTCCAGTCCTTG-NFQ. PCR cycling parameters were set at one cycle of 50°C for 2 min, 95°C for 10 min and then 40 cycles of 95°C for 15 s and 60°C for 1 min. Data was acquired and analysed by using the ABI PRISM 7000 Sequence Detection System software (Applied Biosystems, USA).

The expression profile of each cDNA was studied by the relative quantification of the mRNA using the comparative $\Delta\Delta C_T$ method (Livak and Schmittgen, 2001). First, the threshold cycle (C_T) value for each sample and its replicates was obtained from the amplification plots. The value represents the cycle at which the signal is first recorded as statistically significant above the background. Then, the average C_T values for the target gene in each of the samples were determined from replicates. This was carried out for both the target genes and the internal control glyceraldehyde 3-phosphate dehydrogenase (GAPDH). These values were normalised against

the average C_T values of the internal control (ΔC_T). The difference in C_T values (ΔC_T) is equal to the difference in expression after being normalised to the endogenous control.

RESULTS AND DISCUSSION

Isolation of *Egpsy*

PSY is located in the chloroplast (Fraser *et al.*, 2000) and it catalyses the first committed step of the carotenoid pathway that converts two molecules of *ggpp* into phytoene. This two-step conversion reaction is considered as a rate-limiting step in the pathway (Cunningham and Gantt, 1998). Consequently, *psy* has become the key target for genetic manipulation in many crop plants to increase the carotenoid content (Fraser *et al.*, 2002; Fray *et al.*, 1995).

In this work, *psy* cDNA was isolated from *E. guineensis* using degenerate primers (PSY5 and PSY6). A full-length cDNA encoding *psy* was obtained and designated as *Egpsy*. The gene reported in this article has been submitted to the PalmXPlore database (http://palmxplore.mpob.gov.my/) under the accession number p5.00_sc00017_p0037. The complete *Egpsy* has an ORF of 1299 bp which is preceded by 346 bases of 5-untranslated region (5-UTR) followed by 588 bases of the 3'- UTR (*Figure 1*). Interestingly, Wan Nur Syuhada *et al.* (2012) also reported that *psy* from *Elaeis oleifera* and *Egpsy* nucleotide sequences were highly conserved at about 98%. The BlastP search results demonstrated that the *Egpsy* clone showed a high sequence identity to PSY from other monocots, such as *Phoenix dactylifera* (91.16%) and Musa AAB Group (79.35%). Overall, the *Egpsy* sequence has a high degree of similarity with various species of plants (80.00%), alga (60.00%) and cyanobacteria (40.00%) but not with bacteria and fungi (16.90%).

The PCR product was also amplified directly from genomic DNA, sequenced on both strands and assembled using standard techniques. The total length of *Egpsy* genomic clone was 4342 bp, consisting of six exons and five introns. The sizes and organisation of the exons and introns are summarised in *Figure 1*. Comparatively, the number of exons and introns in *Egpsy* is similar to the *psy* from wheat and maize (Wang *et al.*, 2009; Li *et al.*, 2008).

Egpsy Sequence Analyses

In plants, the synthesis of carotenoids occurs in plastids. Thus, the enzymes involved in the pathway should contain plastid targeting signal for their transport into the plastids. Therefore, we looked for the plastid targeting signal using SIGNALP software and protein localisation using WoLF PSORT program (Horton *et al.*, 2007). The SIGNALP software predicted a 12-amino acid signal peptide with a molecular mass of 48.83 kDa and an isoeletric point of 9.09. The WoLF PSORT program suggested that *Egpsy* might be localised in chloroplast and the protein feature had a similarity of about 69% with PSY from *Arabidopsis thaliana* (https://www.uniprot.org/uniprot/P37271). This result may indicate that *Egpsy* is needed for photosynthesis and photoprotection function.

In order to examine the properties and conserved domains of the enzyme, the protein sequence was subjected to National Centre for Biotechnology Information (NCBI) Conserved Domain Search. We found that the protein has a single large prenyltransferase catalytic domain that belongs to the Trans-Isoprenyl Diphosphate, Head-to-Head (1'-1) condensation reaction (Trans_IPPS_HH) family (NCBO CDD No. cd00683) (Marchler-Bauer *et al.*, 2011). Analysis of the sequence also indicated the presence of other features corresponding to the Trans-Isoprenyl Diphosphate Synthases family. This domain is present in all PSY, which catalyse the head to head (1'-1) condensation of two *ggpp* molecules to produce phytoene (C30 and C40) (*Figure 2*). The analysis also indicated the presence of major aspartate-rich motifs that are thought to be responsible for substrate binding. This result was also confirmed through transmembrane region analysis of the sequence using TMpred algorithm. The result showed two strong transmembrane helices, in-to-outside from 3-24 residues and out-to-inside from 257-259 residues. The active site of the enzyme is hydrophobic and located within the transmembrane helical bundle where carbocation is generated, leaving the diphosphate group attached (Zviling *et al.*, 2007). Meanwhile, Lopez-Emparan *et al.* (2014) reported *Brassica napus* L. PSY also had a conserved trans-IPP region and several motives

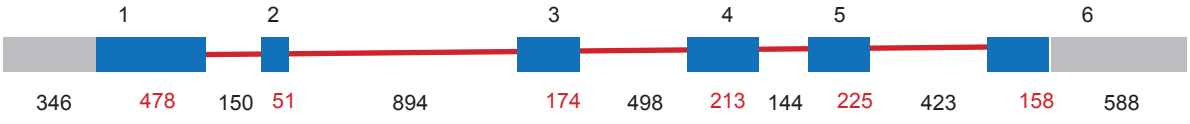


Figure 1. Diagram of exons and introns of Elaeis guineensis *phytoene synthase* (Egpsy). *Grey and blue bars indicate untranslated and coding region, respectively. Meanwhile, thin red lines indicate introns and the number below them indicate their sizes in basepairs.*

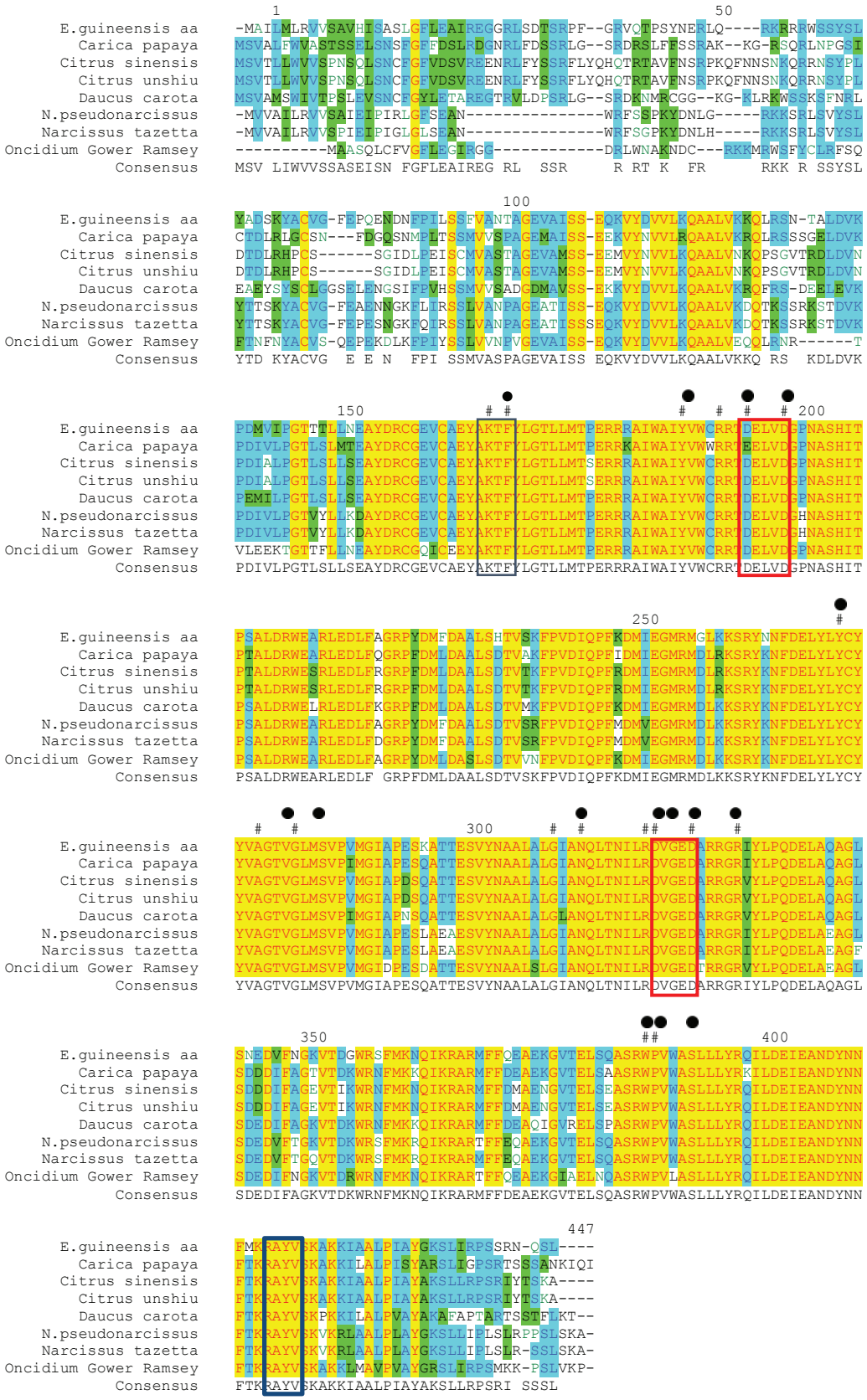


Figure 2. Amino acid sequence alignment of phytoene synthase *(PSY) from oil palm and PSY from several other plants. Yellow colour shows highly conserved amino acid residues. Numbers above the alignment indicate the amino acid positions along the* Egpsy *protein. The two aspartate-rich regions (DXXXD) and substrate-Mg^{2+} binding site are indicated in red box. The active site lid residues are indicated in blue box. The substrate binding pocket are indicated (#). The catalytic residues are indicated (●). The sequences used in this analysis were as follows:* Carica papaya *(GenBank accession No. NW_019019210),* Citrus sinensis *(GenBank accession No. NM_001288886,* Daucus carota *subsp. Sativus (GenBank accession No. NM_001329167),* Narcissus pseudonarcissus *(GenBank accession No. X78814),* Narcissus tazetta *(GenBank accession No. DQ984674,* Oncidium Gower *Ramsey (GenBank accession No. FJ859988).*

such as plastid transit peptide and a putative *psy* active site (DXXXD) with conserved aspartate residues which was similar to *Egpsy*.

The deduced AA sequence for *Egpsy* was also subjected to phylogenetic analysis using ClustalW by ETE3. The sequence was compared with its respective orthologues (*Figure 3*). The phylogeny is rooted on the branch joining the outgroup to other sequences. PSY sequences were shown to fall into three defined clusters. One comprises the enzymes from cyanobacteria. The other clusters comprise of algae and higher plants. *Egpsy* has high identity with PSY sequences from the higher plants. The phylogenetic tree indicates that PSY sequences from higher plants, algae and cyanobacteria have clear divergence from each other. In higher plants, *Egpsy* is categorised into the monocot group together with *Phoenix dactylifera*, commonly known as date palm. This result showed that the PSY sequences from these two palm plants were closely related to each other. Bourgis *et al.* (2011) and Singh *et al.* (2013) also reported that oil palm and date palm nucleotide sequences were highly conserved which was about 92.0%-94.4% identity. Interestingly, these two palms showed a completely different carbon-partitioning pattern with oil palm mesocarp containing mostly lipid while date mesocarp accumulates mostly sugars.

Southern and Expression Analyses

The copy number of *Egpsy* gene in the *E. guineensis* genome was examined by performing Southern blot hybridisation. Using the 1.3-kb coding region of *Egpsy* as a probe, Southern blot analysis revealed the hybridisation pattern of 1-3 bands per lane (*Figure 4*). However, a single major hybridisation band was observed for two of the digestions, namely *Bam*HI (~7 kb) and *Eco*RI (~5 kb). Digestion using *Hind*III and *Spe*I produced two (~3 kb and ~6 kb) and three (~1 kb, ~3 kb and ~4 kb) major hybridisation bands, respectively. The three sites of *Spe*I were located in the intron whereas *Hind*III was in exon 5 (*Figure 1*). Overall, the result

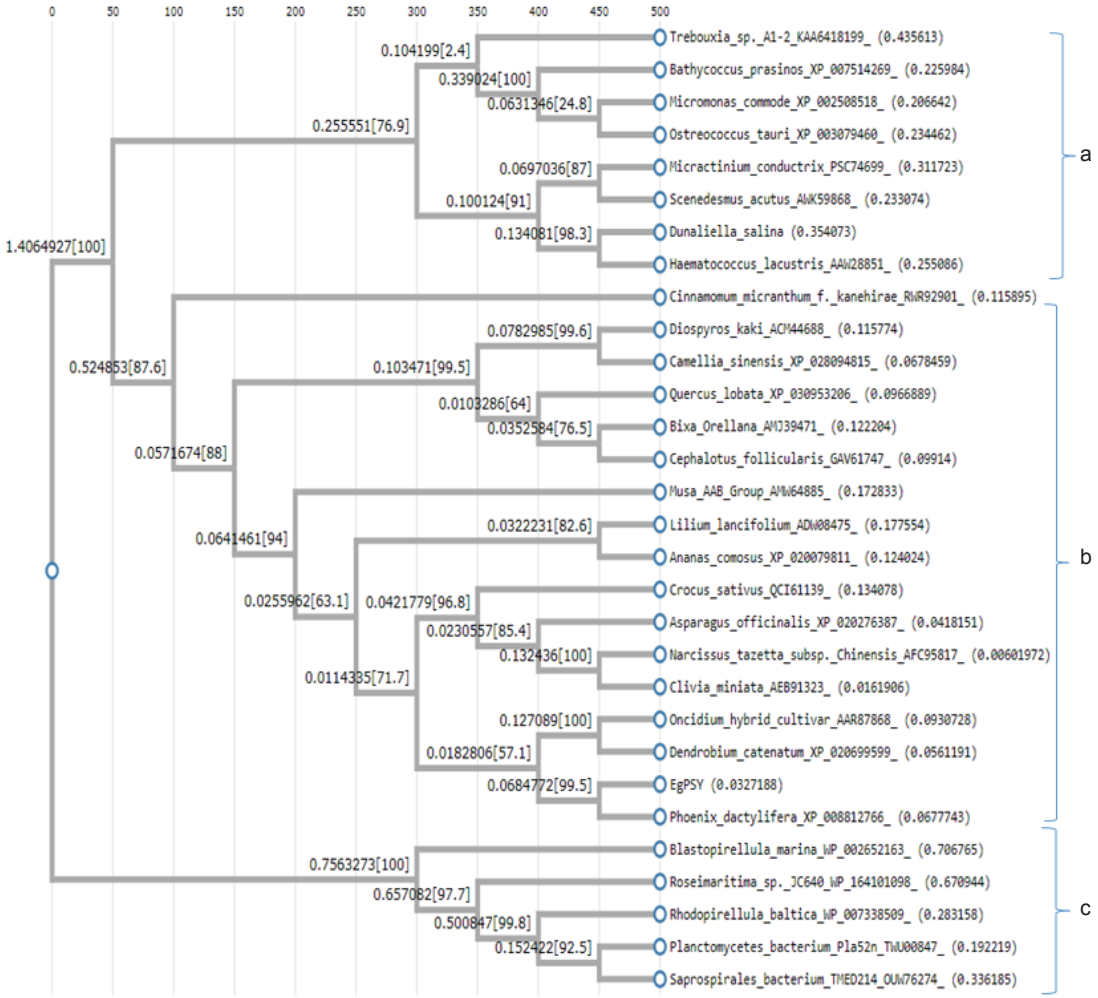


Figure 3. Phylogeny of phytoene synthase *(PSY) amino acid sequences. The value at the nodes and branches represent the length of each branch. The values in bracket indicate the bootstrap support of each branch. The main clades labelled alga (a), plant (b) and cyanobacteria (c). The GenBank accession numbers are indicated at the end of the species names.*

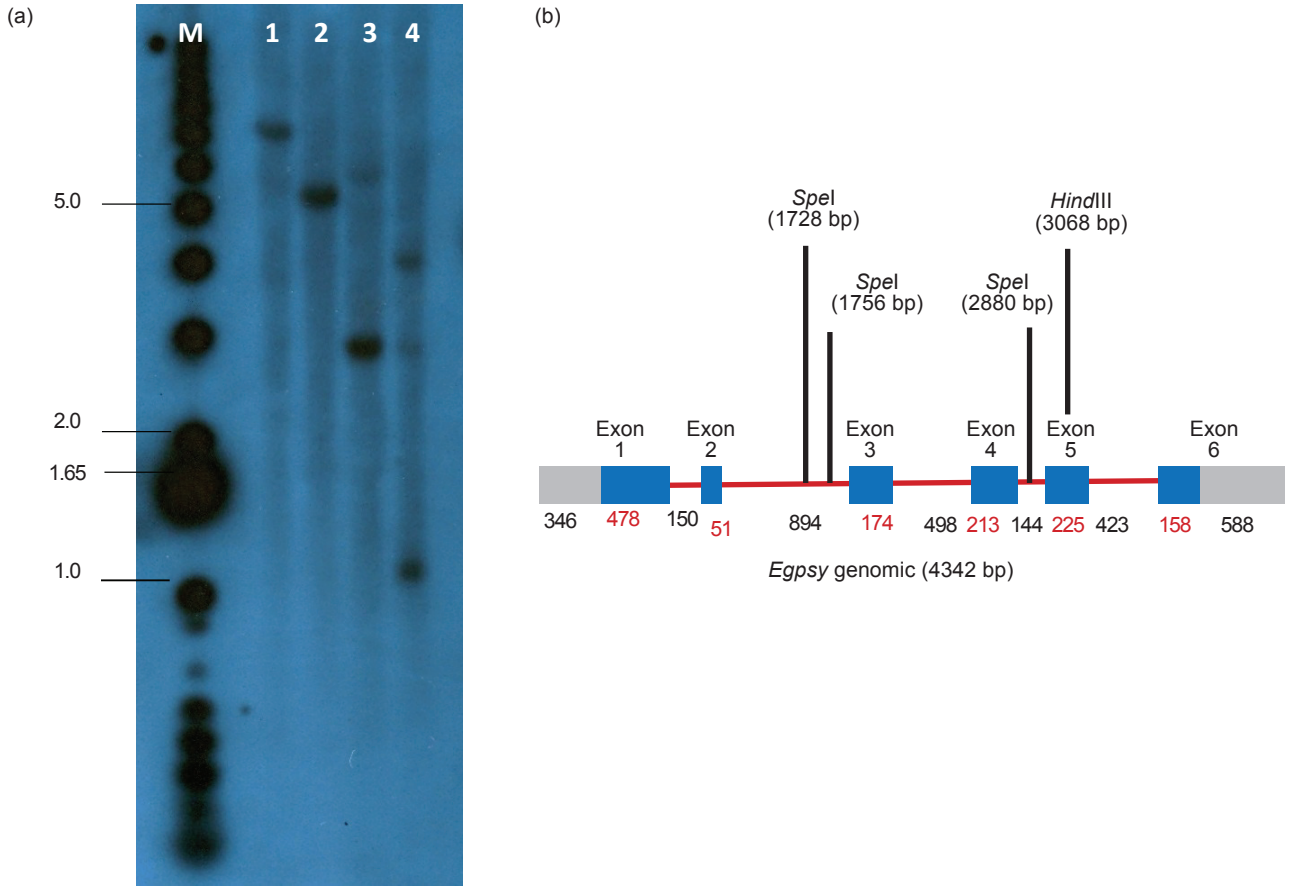


Figure 4. Southern blot analysis of E. guineensis *phytoene synthase* (Egpsy). *(a) Thirty micrograms of total DNA of* E. guineensis *were digested using four different restriction enzymes namely* BamHI, EcoRI, HindIII, *and* SpeI. *Lane 1 is* E. guineensis *DNA digested with* BamHI; *Lane 2,* E. guineensis *DNA digested with* EcoRI; *Lane 3,* E. guineensis *DNA digested with* HindIII; *Lane 4,* E. guineensis *DNA digested with* SpeI. *(b)* SpeI *and* HindIII *restriction sites in the* Egpsy *genomic sequence.*

suggested that there is only one copy of *psy* gene in the genome of *E. guineensis*. The copy number of *psy* gene in *E. guineensis* genome was also examined using the available oil palm genome data (http://genomsawit.mpob.gov.my). The search result indicated that there is a single copy of *psy* gene in *E. guineensis*. The gene was predicted to be located on chromosome 16.

Mesocarp tissue is the storage site of carotenoid accumulation in oil palm. Since PSY is the important control point of flux in carotenoid biosynthesis, the expression of its gene should be highly regulated in this tissue. The expression level of *psy* was examined during oil palm fruit development at weekly-intervals starting from 5 WAA until 19 WAA (*Figure 5*). The expression of *psy* in 5 WAA mesocarp tissue was about 1.72 folds higher than the calibrator (13 WAA). The expression increased to about 2.38 folds at 6 WAA, before decreasing to about 1.7 folds at 7 WAA. The *psy* expression remained at about the same level before decreasing at 10 WAA to about 1.3 folds, rebounded at 11 WAA and reached the peak at about 2.4 folds at 12 WAA. Surprisingly, mRNA level of *psy* decreased to the lowest level at 13 WAA. At 14 WAA, the *psy* expression increased and remained at about the same level thereafter. Overall, *Egpsy* was highly expressed in 6, 11, 12, 17 and 19 WAA as compared to the calibrator. This pattern suggested that *Egpsy* is involved in early and ripening stages of oil palm carotenoid biosynthesis, which is consistent with the findings from *E. oleifera* reported by Rasid *et al.* (2008). Oil synthesis and carotene storage in mesocarp commence at 15 to 16 WAA, reaching a peak at 20 WAA (Kaur and Sambanthamurthi, 2008; Singh *et al.*, 2013). In young and mature tissues, the major product of carotegenesis was leaf-like xanthophylls which is mainly lutein and neoxanthin (Tay and Gwendoline, 2006). However, during fruit ripening, the lutein will decrease drastically and shift to carotene, mainly α- and β-carotene (Kaur and Sambanthamurthi, 2008). The low expression at 13 WAA could possibly be due to the transition from the synthesis of leaf-like carotenoids to the formation of carotenes. The expression pattern observed for *psy* is also quite similar with the expression of a gene encoding phytochrome-interacting factor (*pif*). This protein was shown to repress *psy* and down-regulate the

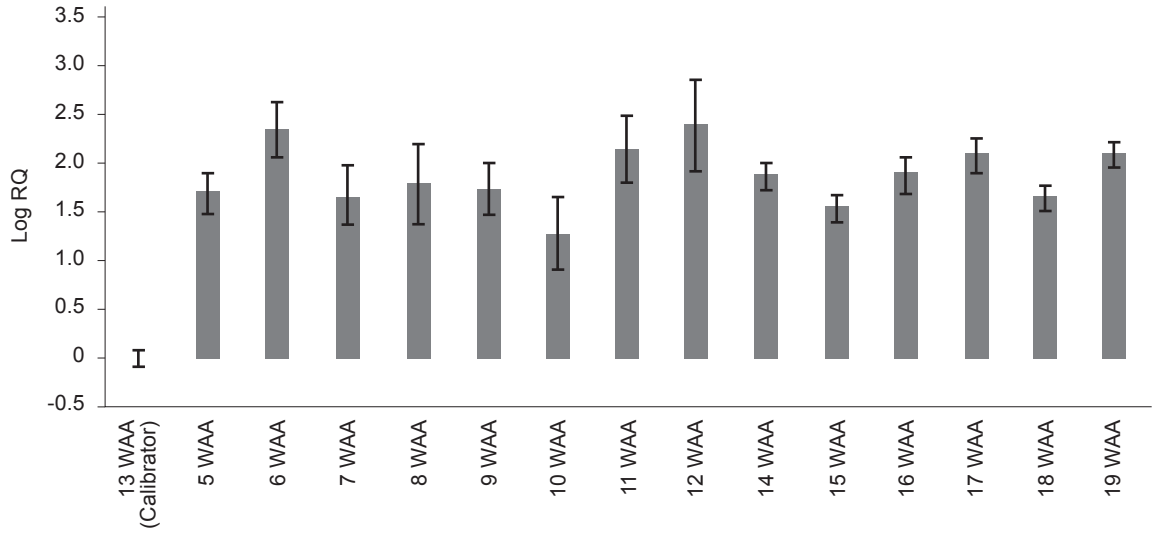


Figure 5. Relative quantities of phytoene synthase *(PSY) mRNA in mesocarp tissue of oil palm fruit at different developmental periods. Each week after anthesis (WAA) sample was individually assayed in triplicates. Values shown represent the log Real-Time Quantitative (RQ) and bars indicate the standard error. The expression in the 13 WAA tissue was used as the calibrator.*

accumulation of carotenoids (Toledo-Ortiz *et al.*, 2010). Interestingly, the *pif* gene was concomitant with the gene encoding phytochromes (*phy*-A, -B, and -C) in oil palm which was reported to be only expressed at 100 DAP (14 WAA) (Tranbager *et al.*, 2011). Therefore, the expression data of *psy* could suggest its important role, possibly along with other regulators, in the accumulation of carotenoids in oil palm fruit.

CONCLUSION

We have isolated a cDNA clone and genomic DNA encoding *E. guineensis psy*. The sequence of this clone was shown to have high identity to *psy* sequences from other plants. We also examined its expression patterns during fruit development. The expression of *psy* was shown to be differentially expressed along the fruit developmental stages. This result suggests that *Egpsy* may regulate the synthesis and accumulation of carotenoids in the *E. guineensis* fruit. In essence, the sequence and expression analyses of the *psy* gene provided useful information for further understanding of its roles in the molecular regulation of carotenoid production and biosynthesis in *E. guineensis*.

ACKNOWLEDGEMENT

The authors would like to thank the Director-General of MPOB for permission to present these results. The authors would also like to thank Dr. Abdul Masani Mat Yunus, Siti Masura Subhi and Nor Hanin Ayob, Advanced Biotechnology and Breeding Center, MPOB for reviewing this manuscript.

REFERENCES

Bourgis, F; Kilaru, A; Cao, X; Ngando-Ebongue, G F; Drira, N; Ohlrogge, J B and Arondel, V (2011). Comparative transcriptome and metabolite analysis of oil palm and date palm mesocarp that differ dramatically in carbon partitioning. *Proc. Natl. Acad. Sci. USA, 108(30)*: 12527-12532.

Buckner, B; Miguel, P S; Janick-Buckner, D and Bennetzen, J L (1996). The y1 gene of maize codes for phytoene synthase. *Genetics, 143(1)*: 479-488.

Busch, M; Sueter, A and Hain, R (2002). Functional analysis of the early steps of carotenoid biosynthesis in tobacco. *Plant Physiol., 128(2)*: 439-453.

Cazzonelli, C I and Pogson, B J (2010). Source to sink: Regulation of carotenoid biosynthesis in plants. *Trends Plant Sci., 15(5)*: 266-274.

Cunningham, F X and Gantt, E (1998). Genes and enzymes of carotenoid biosynthesis in plants. *Annu. Rev. Plant. Physiol. Plant. Mol. Biol., 49*: 557-583.

Fraser, P D; Roemer, S; Shipton, C A; Mills, P B; Kiano, J W; Misawa, N; Drake, R G; Schuch, W and Bramley, P M (2002). Evaluation of transgenic tomato plants expressing an additional phytoene synthase in a fruit-specific manner. *Proc. Natl. Acad. Sci. USA, 99(2)*: 1092-1097.

Fraser, P D; Schuch, W and Bramley, P M (2000). Phytoene synthase from tomato (*Lycopersicon esculentum*) chloroplasts–partial purification and biochemical properties. *Planta, 211(3)*: 361-369.

Fraser, P D; Hedden, P M; Cooke, D T; Bird, C R; Schuch, W and Bramley, P M (1995). The effect of reduced activity of phytoene synthase on isoprenoid levels in tomato pericarp during development and ripening. *Planta, 196*: 321-326.

Fray, R G and Grierson, D (1993). Molecular-genetics of tomato fruit ripening. *Trends in Genetics, 9(12)*: 438-443.

Fray, R G; Wallace, A; Fraser, P D; Valero, D; Hedden, P; Branley, P M and Grierson, D (1995). Constitutive expression of a fruit phytoene synthase gene in transgenic tomatoes causes dwarfism by redirecting metabolites from the gibberellin pathway. *Plant J., 8(5)*: 693-701.

Giuliano, G; Bartley, G E and Scolnik, P A (1993). Regulation of carotenoid biosynthesis during tomato development. *Plant Cell, 5(4)*: 379-387.

Horton, P; Park, K J; Obayashi, T; Fujita, N; Harada, H; Adams-Collier, C J and Nakai, K (2007). WoLF PSORT: Protein localization predictor. *Nucleic Acids Res., 35*: 585-587.

Huh, J H; Kang, B C; Nahm, S H; Kim, S, Ha, K S; Lee, M H and Kim, B D (2001). A candidate gene approach identified phytoene synthase as the locus for mature fruit colour in red pepper (*Capsicum* spp.). *Theor. Appl. Genet., 102*: 524-530.

Karvouni, Z; John, I; Taylor, J E; Watson, C F; Turner, A J and Grierson, D (1995). Isolation and characterisation of a melon cDNA clone encoding phytoene synthase. *Plant Mol. Biol., 27(6)*: 1153-1162.

Kato, M; Ikoma, Y; Matsumoto, H; Sugiura, M; Hyodo, H and Yano, M (2004). Accumulation of carotenoids and expression of carotenoid biosynthetic genes during maturation in citrus fruit. *Plant Physiol., 134(2)*: 824-837.

Kaur, J S and Sambanthamurthi, R (2008). Carotenoid profiles and preliminary investigation on carotenoid biosynthesis in the oil palm (*Elaeis guineensis*) mesocarp. *J. Oil Palm Res., (Malaysia-MIT Biotech Partner Prog.) 2*: 108-117.

Khemvong, S and Suvachittanont, W (2005). Molecular cloning and expression of a cDNA encoding 1-deoxy-D-xylulose 5-phosphate synthase from oil palm *Elaeis guineensis* Jacq. *Plant Sci., 169(3)*: 571-578.

Kim, I J; Ko, K C; Kim, C S and Chung, W (2001). Isolation and expression pattern of a cDNA encoding phytoene synthase in Citrus. *J. Plant Physiol., 158(6)*: 795-800

Kushairi, A; Ong-Abdullah, M; Balu, N; Hishamuddin, E; Izuddin, Z B; Razmah, G; Subramaniam, V; Sundram, S and Parveez, G K A (2019). Oil palm economic performance in Malaysia and R&D progress in 2018. *J. Oil Palm Res., 31(2)*: 165-194.

Li, F; Vallabhaneni, R; Yu, J; Rocheford, T and Wutzel, E T (2008). The maize phytoene synthase gene family: Overlapping roles for carotenogenesis in endosperm, photomorphogenesis and thermal stress tolerance. *Plant Physiol., 147*: 1334-1346.

Lopez-Emparan, A; Quezada-Martinez, D; Zuniga-Bustos, M; Cifuentes, V; Iniguez-Luy, F and Laura, F M (2014). Functional analysis of the *Brassica napus* L. phytoene synthase (*psy*) gene family. *PLoS ONE, 9*: 12.

Marchler-Bauer, A; Lu, S; Anderson, J B; Chitsaz, F; Derbyshire, M K; DeWeese-Scott, C; Fong, J H; Geer, L Y; Geer, R C; Gonzales, N R; Gwadz, M; Hurwitz, D I; Jackson, J D; Ke, Z; Lanczycki, C J; Lu, F; Marchler, G H; Mullokandov, M; Omelchenko, M V; Robertson, C L; Song, J S; Thanki, N; Yamashita, R A; Zhang, D; Zhang, N; Zheng, C and Bryant, S H (2011). CDD: A conserved domain database for the functional annotation of proteins. *Nucleic Acids Res., 39*: 225-229.

Mayne, S T (1996). Beta-carotene, carotenoids, and disease prevention in humans. *FESEB J., 10*: 690-701.

Mlalazi, B; Welsch, R; Namanya, P; Khanna, H; Geijskes, R J; Harrison, M D and Harding, R (2012). Isolation and functional characterisation of banana phytoene synthase genes as potential cisgenes. *Planta, 236*: 1585-1598.

Misawa, N; Truesdale, M R; Sandmann, G; Fraser, P D; Bird, C; Schuch, W and Bramley, P M (1994). Expression of a tomato cDNA coding for phytoene synthase in *Escherichia coli*, phytoene formation *in vivo* and *in vitro*, and functional analysis of the various truncated gene products. *J. Biochem., 116(5)*: 980-985.

Mustapa, A N; Manan, Z A; Mohd Azizi, C Y; Setianto, W B and Mohd Omar, A K (2011). Extraction of b-carotenes from palm oil mesocarp using sub-critical R134a. *Food Chem., 125*: 262-267.

Nisar, N; Li, L; Lu, S; Khin, N C and Pogson, B J (2015). Carotenoid metabolism in plants. *Mol. Plant, 8*: 68-82.

Paine, J A; Shipton, C A; Chaggar S; Howells, R M; Kennedy, M J; Vernon, G; Wright, S Y; Hinchliffe, E; Adams, J L; Silverstone, A L and Drake, R

(2005). Improving the nutritional value of Golden Rice through increased pro-vitamin A content. *Nat. Biotechnol., 23*: 482-487.

Rasid, O A; Parveez, G K A; Ho, C L; Sambanthamurthi, R and Napis, S (2009). Plant carotenoids: molecular genetics and regulation. *J. Oil Palm Res., 21*: 588-601.

Rasid, O A; Wan Nur Syuhada, W S; Nor Hanin, A; Masura, S S; Zulqarnain, M; Ho, C L; Sambanthamurthi, R and Suhaimi, N (2008). RT-PCR amplification and cloning of partial DNA sequence coding for oil palm (*Elaeis oleifera*) phytoene synthase gene. *Asia-Pac. J. Mol. Biol. Biotechnol., 16*: 17-24.

Rasid, O A; Singh, R; Harikrishna, K and Cheah, S C (2003). Isolation of partial DNA sequence codon for lycopene β-cyclas from oil palm. *Proc. of the 2003 MPOB International Palm Oil Congress*. p. 781-788.

Rasid, O A; Singh, R; Sambanthamurthi, R and Cheah, S C (2005). RT-PCR amplification and cloning of partial DNA sequence coding for oil palm (*E. guineensis*) zeaxanthin epoxidase. *Proc. of the 2005 Conference on Biotechnology of Plantation Commodities*. Selangor, Malaysia. p. 553.

Ray, J; Moureau, P; Bird, C; Bird, A; Grierson, D; Mauders, M; Truesdale, M; Bramley, P and Schuch, W (1992). Cloning and characterisation of a gene involved in phytoene synthesis from tomato. *Plant Mol. Biol., 19*: 401-404.

Rodrigo, M J; Marcos, J F and Zacarias, L (2004). Biochemical and molecular analysis of carotenoid biosynthesis in flavedo of orange (*Citrus sinensis* L.) during fruit development and maturation. *J. Agric. Food Chem., 52(22)*: 6724-6731.

Rose, T M (2005). CODEHOP-mediated PCR - A powerful technique for the identification and characterization of viral genomes. *Virol J., 15*: 20.

Salvini, M; Bernini, A; Fambrini, M and Pugliesi, C (2005). cDNA cloning and expression of the phytoene synthase gene in sunflower. *J. Plant Physiol., 162(4)*: 479-484.

Scolnik, P A and Bartley, G E (1994). Nucleotide sequence of an *Arabidopsis* cDNA for phytoene synthase. *Plant Physiol., 104(4)*: 1471-1472.

SIB (2020). TMpred webserver. http://www.ch.embnet.org/software/TMPRED_form.html Swiss Institute of Bioinformatics (SIB), accessed on 13 March 2020.

Singh, R; Ong-Abdullah, M; Low, E T; Manaf, M A; Rosli, R; Nookiah, R; Ooi, L C; Ooi, S E; Chan, K L; Halim, M A; Azizi, N; Nagappan, J; Bacher, B; Lakey, N; Smith, S W; He, D; Hogan, M; Budiman, M A; Lee, E K; DeSalle, R; Kudrna, D; Goicoechea, J L; Wing, R A; Wilson, R K; Fulton, R S; Ordway, J M; Martienssen, R A and Sambanthamurthi, R (2013). Oil palm genome sequence reveals divergence of interfertile species in old and new worlds. *Nature, 500*: 335-339.

Stewart Jr, C N and Via, L E (1993). A rapid CTAB isolation technique useful for rapid fingerprinting and other PCR application. *Biotechniques, 14(5)*: 748-750.

Tanaka, Y and Ohmiya, A (2008). Seeing is believing: Engineering anrhocyanin and carotenoid biosynthetic pathways. *Curr. Opin. Biotechnol., 19(2)*: 190-197.

Tay, B Y P and Gwendoline, E C L (2006). Identification of lutein in crude palm oil and evaluation of carotenoids at various ripening stages of the oil palm fruit. *J. Oil Palm Res., 18*: 189-197.

Toledo-Ortiz, G; Huq, E and Rodrı´guez-Concepcio´n, M (2010). Direct regulation of phytoene synthase gene expression and carotenoid biosynthesis by phytochrome-interacting factors. *Proc. Natl. Acad. Sci. USA, 107(25)*: 11626-11631.

Tranbarger, T J; Dussert, S; Joët, T; Argout, X; Summo, M; Champion, A; Cros, D; Omore, A; Nouy, B and Morcillo, F (2011). Regulatory mechanisms underlying oil palm fruit mesocarp maturation, ripening, and functional specialization in lipid and carotenoid metabolism. *Plant Physiol., 156(2)*: 564-584.

Uenojo, M; Maróstica Júnior, M R and Pastore, G M (2007). Carotenoids: Properties, applications and biotransformation in flavour compounds. *Química Nova, 30(3)*: 616-622.

Wang, J; He, X; He, Z; Wang, H and Xia, X (2009). Cloning and phylogenetic analysis of phytoene synthase 1 (PSY1) genes in common wheat and related species. *Hereditas, 146(5)*: 208-256.

Wan Nur Syuhada, W S; Rasid, O A and Parveez, G K A (2012). Phytoene synthase gene from oil palm (*Elaeis oleifera*) for modification of carotenoid content. *MPOB Information Series No. 600.*

Wong, J C; Lambert, R J; Wutzel, E T and Rocheford, T R (2004). QTL and candidate genes phytoene synthase and zeta-carotene associated with the accumulation of carotenoids in maize. *Theor. Appl. Genet., 108(2)*: 349-359.

Zeng, Y and Yang, T (2002). RNA isolation from highly viscous samples rich in polyphenols and polysaccharides. *Plant Mol. Bio. Rep., 20*: 415-417.

Zhang, L; Zhang, Z; Zheng, T; Wei, W; Zhu, Y; Gao, Y; Yang, X and Lin, S (2016). Characterization of carotenoid accumulation and carotenogenic gene expression during fruit development in yellow and white loquat fruit. *Hortic. Plant J., 2(1)*: 9-15.

Zviling, M; Kochva, U and Arkin, I T (2007). How important are transmembrane helices of bitopic membrane proteins? *Biochim. Biophys. Acta, 1768(3)*: 387-392.

Journal of Oil Palm Research Vol. 33 (3) September 2021 p. 458-472
DOI: https://doi.org/10.21894/jopr.2020.0112

QUALITY IMPROVEMENT OF PALM KERNEL CAKE AS BROILER FEED USING PRE-CLEANING SYSTEM

ROHAYA MOHAMED HALIM[1]*; RIDZUAN RAMLI[1]; CHE RAHMAT CHE MAT[1]; NU'MAN ABDUL HADI[1]; MOHD FIRDAUS OTHMAN[1] and ASTIMAR ABD AZIZ[1]

ABSTRACT

The use of palm kernel cake (PKC) in broiler feed is limited due to high fibrous material contributed mainly by dirt and shell, exceeding 6%. The fibrous component consists of mainly insoluble mannose-based polysaccharides which is not suitable for monogastric animals such as poultry and swine. This study highlights the development of a pre-cleaning system consisting of three-stage winnowing columns to reduce the shell content in kernel by less than 4% prior to oil extraction. In this study, the palm kernels received from 21 palm oil mills were subjected to dirt and shell content analysis. To produce palm kernel with low shell content, the pre-cleaning system was optimised. Further analysis on nutrient values was also carried out for premium grade PKC produced, also known as Purafex, from the clean kernels of low shell content (<4%) after pre-cleaning. A feeding trial was carried out to study the effect of different Purafex inclusion in the dietary treatment on the broilers performance. Results showed that the dirt and shell contents in the kernels varied from 3.48%-5.18%. The nutrient values and quality of Purafex conformed to that of standard specifications by Malayan Edible Oil Manufacturers' Association (MEOMA). Reduction of shell and fibre in kernel reduces the crude fibre in Purafex from ≥15% to ≤12%, which is far below the fibre in commercial PKC, thus, making it digestible for monogastric animals. Better performance in terms of body weight gain (BWG) and feed intake (FI) were exhibited when 15%-30% Purafex were included in feeding trials compared to those of 45% inclusion.

Keywords: dry separation system, palm kernel, palm kernel cake, quality.

Received: 10 June 2020; **Accepted:** 30 September 2020; **Published online:** 14 December 2020.

INTRODUCTION

Malaysia has depended mostly on imported feed, particularly for the non-ruminant sector, such as poultry and swine, where corn and soyabean are the main imported energy and protein feeds (Zahari and Wong, 2009). High demand for imported feed will cause price fluctuation and high production cost. As a result, local resources, such as palm kernel cake (PKC), is considered as an alternative to corn and soyabean for animal feed application. PKC is mechanically produced as by-product using screw press after extracting oil from the palm kernel at the kernel crushing plant. This by-product is easily available throughout the year and non-competitive as human food (Roslan *et al.*, 2015).

Nutritionally, PKC is an ideal feed for most ruminant due to the protein and crude fibre content in the range of 15%-20% (Chong *et al.*, 2008). However, the use of PKC for monogastric animals such as poultry (chickens, ducks, turkeys and geese) is limited owing to high shell and dirt content which exceeded 6% (Rohaya *et al.*, 2005). It also contains 15% lignin (Cerveró *et al.*, 2010) stemming from the shells in PKC (O'mara *et al.*, 1999) and

[1] Malaysian Palm Oil Board,
6 Persiaran Institusi, Bandar Baru Bangi,
43000 Kajang, Selangor, Malaysia.

* *Corresponding author e-mail: rohaya@mpob.gov.my*

18%-21% fibre (Nwokolo *et al*., 1976; Sundu *et al*., 2005a; Lawal *et al*., 2010). The fibrous material in PKC also comprises mainly of insoluble mannose-based polysaccharides. These components are not favourable for nutrients digestibility (Saenphoom *et al*., 2013) particularly for monogastric animals such as broiler. This type of polysaccharide possesses anti-nutritional property which hinders full nutrients utilisation in PKC, resulting in feed conversion ratio depression and reduction in weight gains by 20%-25% in monogastric animals (Dusterhoft and Voragen, 1991).

The quality of PKC is highly dependent on the palm kernel quality. Palm kernel consignment comprises of high dirt and shell content in the range of 6%-11% (Rohaya *et al.*, 2002). Using conventional process, the PKC generated also contains high shell (>12%) and crude fibre (>18%) (Rohaya *et al.*, 2017). The use of PKC as feed meals for poultry is also limited by the presence of shell. During palm kernel processing, the shells are hardly removed from the PKC due to its various sizes, shape irregularity and similar density to that of kernel residues (Roslan *et al.*, 2015). Inefficiency of shell and kernel separation at the mill had resulted in high dirt and shell content in palm kernel, thereby contaminating the PKC at the kernel crushing plant. Several studies have been carried out to enhance the separation of shell from kernel, to obtain PKC with low shell content. Sinurat *et al.* (2013) used sieving method to separate shell from PKC but it was not successful as the particle size of shell was smaller than the sieve pores which used static cling and electrostatic approach (Roslan *et al.*, 2015) to separate shell from PKC, in order to reduce the lignin and fibre content of PKC. A study by Sanni *et al.* (2017) reported the use of saline bath system to replace clay-water batch system in separating the shell from palm kernel. Although the system showed a promising separation efficiency, it has some limitation, in terms of having increased quantity of palm kernel and shell mixtures.

Conventionally, separation of palm kernels and shells from cracked mixture at the mill is conducted using a combination of dry and wet separation system, namely winnowing column, hydrocyclone and clay bath (Rohaya *et al.*, 2009). However, water-based system will contribute to the generation of waste effluent which may jeopardise the environment. Thus, the aim of this study is to highlight the development of a pre-cleaning system to maximise the removal of shell in the PKC and kernels. The pre-cleaning system works based on dry separation process, reducing shell content from palm kernels between 4%-6%, with acceptable kernel losses. Kernel with low shell content was then used as raw material for the production of premium grade PKC, known as Purafex, of superior quality as value-added product for chicken feed application. A feeding trial was carried out to examine the effect of different Purafex inclusion in the dietary treatment on the performance of broilers.

MATERIALS AND METHOD

Materials

The palm kernel consignments were obtained from 21 palm oil mills under Sime Darby Group. Each consignment received from those mills was used as raw materials for the pre-cleaning system developed to verify the range of dirt and shell content.

Pre-cleaning System Development

The pre-cleaning system works based on dry separation process to reduce shell content in the palm kernel consignment from ≥6% to ≤4% with acceptable kernel losses. The system consists of three units of winnowing columns with three different air velocities (24, 22 and 20 amp) to ensure maximum shell removal to achieve the targeted parameter. Two different shell fragments are discharged at two different outlets. Small shell fragments are drawn at Column 1, followed by big shells at Column 3. Palm kernels, whole and broken, were recovered from Column 2 and 3. *Figure 1* depicts the kernels and shells recovered from Column 1, 2 and 3. The kernels obtained after this pre-cleaning system (low shell content) were subsequently used as raw materials for the production of high quality kernel oil and high nutrient value PKC that is highly digestible for monogastric animals.

Each column is designed with different parameters, such as air velocity, column height, inlet and outlet level and feeding ratio to achieve the desired shell and kernel ratio separation at each outlet point. It operates using forced draught (blower concept) where its air flow velocity is adjusted via a device (damper) located at the ground of each separating column (*Figure 2*). This damper allows alteration of the throat diameter of the column to suit the composition of the feed mixture, thus, enhancing the separation of kernel and shell through different specific gravity of the materials.

Evaluation of Pre-cleaning System Performance

The pre-cleaning system was installed at the kernel crushing plant (*Figure 3*). Optimisation of the system was carried out for two months to produce palm kernels with low shell content. The amount of shells in the kernels after pre-cleaning was intensively determined to optimise the most suitable air velocity to cater for different composition of



Figure 1. Palm kernel and shell recovered from three separating columns.



Figure 2. Adjustable damper.



Figure 3. Pre-cleaning system installed at the kernel crushing plant.

of feed materials. Performance of pre-cleaning system was evaluated based on the amount of free shells, *i.e.* small and big shell fragments, half-cracked and whole nuts (uncracked nuts) in kernels.

Determination of dirt and shell content in palm kernels. Approximately 1 kg palm kernel (PK) was taken from each consignment received from 21 palm oil mills for the study. The level of contaminants such as dirt and shell content (small and big shell fragments, half-cracked and whole nuts) prior to oil extraction process was determined following the MPOB Test Method (MPOB, 2005).

The kernel samples were sorted as whole nuts (W_1), half-cracked nuts (W_2), loose shells and debris (W_3) and stones (W_4). Prior to weighing, the whole nuts (W_1) and half-cracked nuts (W_2) were carefully cracked and the shells separately weighed. Total dirt and shell content was calculated in Equation (1) - (5) as follows:

$$W_1(\%) = \frac{weight\ of\ shell\ cracked\ from\ whole\ nut}{weight\ of\ PK} \times 100\% \quad (1)$$

$$W_2(\%) = \frac{weight\ of\ shell\ from\ half\text{-}cracked\ nut}{weight\ of\ PK} \times 100\% \quad (2)$$

$$W_3(\%) = \frac{weight\ of\ loose\ shell\ and\ debris}{weight\ of\ PK} \times 100\% \quad (3)$$

$$W_4(\%) = \frac{weight\ of\ stone}{weight\ of\ PK} \times 100\% \quad (4)$$

$$Total\ dirt\ and\ shell\ content\ (\%) = W_1 + W_2 + W_3 + W_4 \quad (5)$$

Production of Purafex

Purafex, was commercially produced at the kernel crushing plant by processing clean palm kernels with low shell (<4%) after pre-cleaning system as feeding material (*Figure 4*). The overall process flow for commercial production of Purafex using pre-cleaning system is illustrated in *Figure 5*. The nutrient values of this Purafex in terms of oil, crude protein, crude fibre, ash, moisture and shell content were further analysed. The oil content was determined according to the MPOB Test Method (2005) by extracting the Purafex samples with hexane using Soxhlet apparatus. Crude fibre was determined following the ISO6865:2000 method, while crude protein in Purafex samples was determined according to the standard methods described by ISO5983-2:2009. The shell content in Purafex samples was quantified in accordance to the MPOB Test Method (2005) as the main parameter to indicate the performance of the pre-cleaning system without contributing to high kernel losses.

Feeding Trials on Broiler Growth Performance

Birds and housing. In total, 300 of male Cobb broiler chicks (one day old) were obtained from a commercial hatchery and used in this study. The birds were reared inside cages in the Climatic Controlled House (CCH) at Energy and Protein Center, MPOB



Figure 4. Commercial production of Purafex in kernel crushing plant.

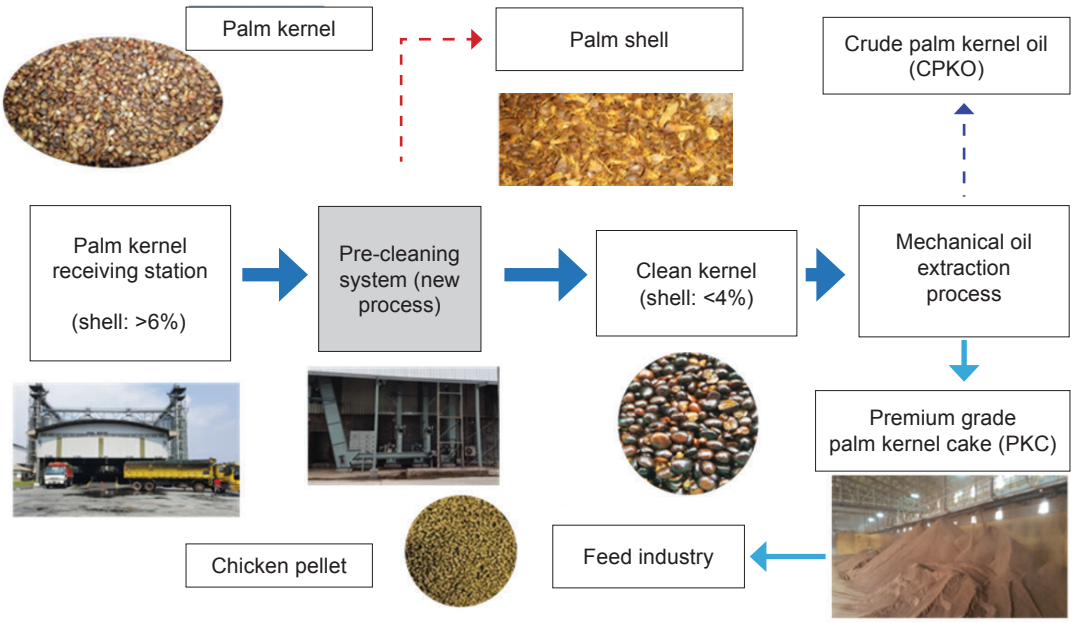


Figure 5. Process flow for commercial production of Purafex using pre-cleaning system.

Keratong, Pahang, Malaysia. The temperature of the house was at ambient temperature and controlled through an evaporative cooling system. All birds were randomly divided into four groups; each group subjected to different Purafex inclusion in the dietary treatment, *i.e.* 0%, 15%, 30% and 45% (*Figure 6*). Each group consisted of three replications with 25 birds in each cage. Water was provided *ad-libitum*, while light was supplied for 16:8 hr (light: dark) daily throughout the experiment. The feeding trial was conducted for 35 days.

Experimental diets. Diets were formulated according to the recommendation by Cobb 500 Management Guide (Cobb-Vantress.com, 2018). The experimental diet consisted of a corn-soyabean meal diet with four levels of Purafex, which was 0%, 15%, 30% and 45%. The formulation also consisted of palm oil, vitamins and minerals to balance the nutrient requirement for broiler growth so that it is isonitrogenous and isocaloric (*Table 1*).

Growth performance analysis. During the broiler experimental period, the body weight and feed intake (FI) of the broiler were recorded daily to determine the body weight gain (BWG), average daily weight gain (ADWG), FI, average daily feed intake (ADFI) and FCR for 35 days. The BWG is measured as the difference between the final and initial weight of birds at each of the weighing periods. FI is determined based on the difference between the amount of feed supplied to the birds

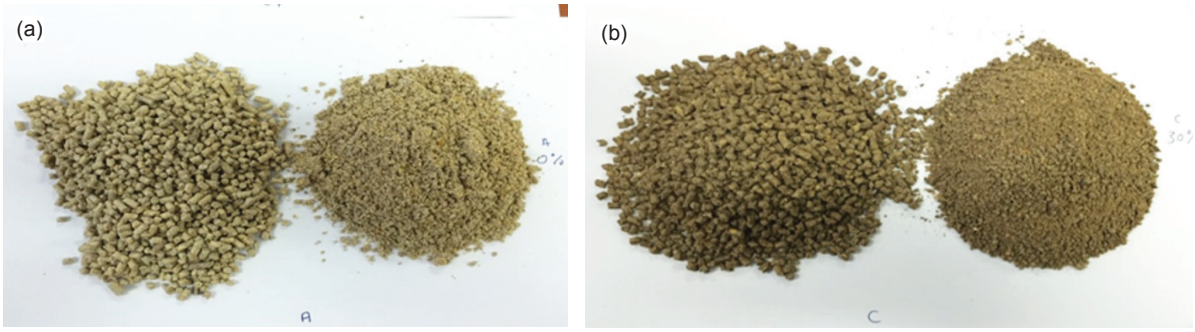


Figure 6. (a) Feed without Purafex as control, (b) feed with 30% Purafex inclusion.

TABLE 1. INGREDIENTS AND CALCULATED ANALYSIS OF EXPERIMENTAL DIETS CONTAINING PURAFEX (palm kernel cake)

Ingredients	Diet (%)			
	0	**15**	**30**	**45**
Purafex (palm kernel cake)	0	15	30	45
Corn	57	47	32.9	21.5
Soyabean meal	24	21.5	21	19.5
Fish meal	10	10.5	11	9.5
Rice bran	3.6	3.2	2.8	2.4
Palm oil	4	1	0.5	0
DiCalcium Phospate	1.5	1.5	1.5	1.5
Vitamin premix	0.1	0.1	0.1	0.1
Mineral	0.1	0.1	0.1	0.1
Methionine	0.2	0.2	0.2	0.2
Lysine	0.1	0.1	0.1	0.1
Total	100.6	100.2	100.2	99.9
Calculated analysis (%)				
Crude protein	22	22	22	22
Fibre	4	5.2	6.3	8.1
Fat	3.5	4.5	6.2	7.3
Ash	7	8.3	8.8	9.5
Metabolisable energy (kcal kg^{-1})	3 850	3 850	3 850	3 850

and the remaining of feed at the end of each feeding period.

Statistical analysis. Data were analysed using the general linear models procedure of SAS (The Statistical Analysis System). Differences among treatments were by the least significant difference at $P<0.05$.

RESULTS AND DISCUSSION

Dirt and Shell Content of Palm Kernels

The crucial quality parameter for palm kernels is the shell and dirt content, which measures the impurities and foreign matters (Nordin *et al.*, 2005). *Figures 7a* and *7b* illustrate the range of dirt and shell content determined in palm kernel consignments received from 21 mills in January and February 2015. Results indicated that the dirt and shell content in the kernels varied from 3.48%-5.18%. Most palm oil mills delivered kernels with dirt and shell content below 5.0%, meeting the specification set by the Malayan Edible Oil Manufacturers' Association (MEOMA).

Quality of PKC highly depended on the quality of palm kernels as raw material. Rohaya *et al.* (2005) emphasised that the main contributing factor to low PKC quality is the inconsistent quality of kernels delivered to the crushing plant. The dirt and shell content was reported to be around 6%-11%, resulting in high dirt content (12%-15%) in PKC produced by the crushing plants. Shell content of more than 10% will result in low kernel oil yield, affecting the PKC feed value and accelerate the machinery wear and tear (Rohaya and Osman, 2002). Eliminating shells in kernels is unachievable due to the various sizes, irregular shapes and similar density between shells and kernels (Roslan *et al.*, 2015). Thus, quality improvement of palm kernels is warranted.

Performance of Pre-cleaning System

Figure 8 illustrates the performance of the pre-cleaning system from October-December 2016. It was found that by applying the correct air velocity in each column, the pre-cleaning system was capable of reducing the amount of free shell in kernel by 50%. The amount of free shell in kernels before pre-cleaning varied from 2.0%-4.0%. However, it was reduced consistently to below 3.0% after pre-cleaning.

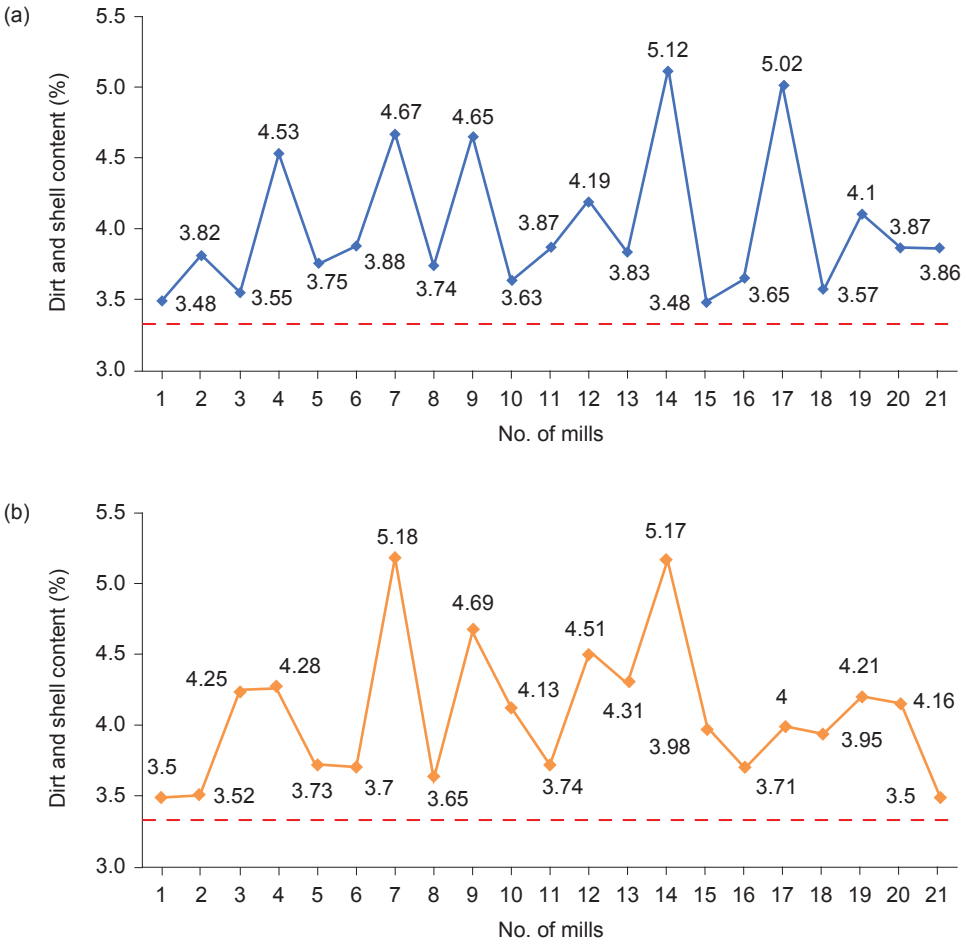


Figure 7. Dirt and shell content in palm kernel consignments for (a) January, and (b) February 2015.

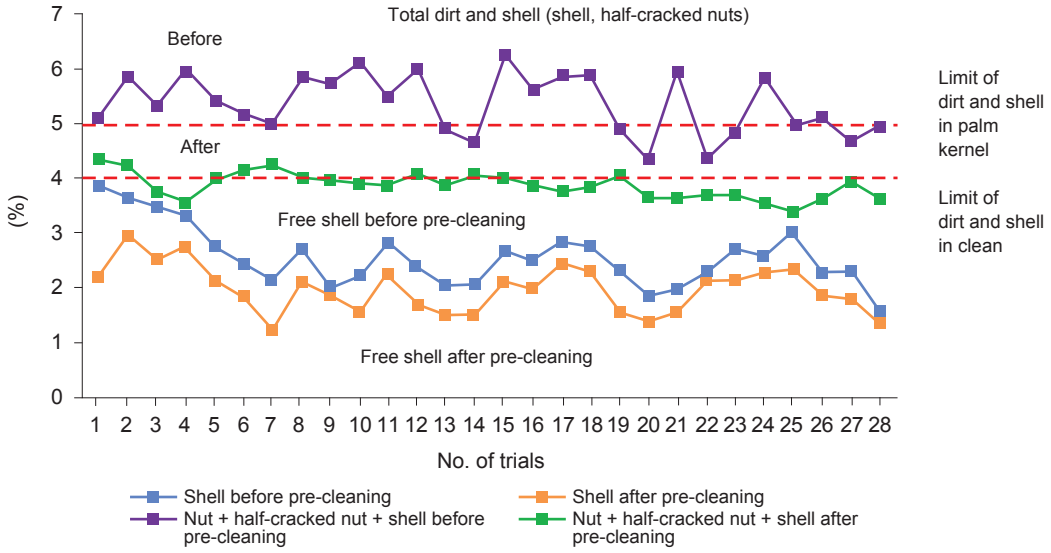


Figure 8. Performance of pre-cleaning system from October-December 2016.

The free small and big shell fragments were effectively removed by the pre-cleaning system with reasonable amount of kernel losses amounting not more than 1.6% of the sample. Kernel losses depended on the amount of small broken kernel received by the kernel crushing plant. However, the presence of high whole (uncracked) and half-cracked nuts due to inefficient cracking performance of the palm nuts at the palm oil mill, contributed to high dirt and shell content in the clean kernels. The total shell stemming from free shell, whole and half-cracked nuts fluctuated from 3.4%-4.4%, slightly higher than the targeted performance (<4.0%). The density of nuts is quite similar to that of kernels, where nuts tends to fall into the kernels.

The performance of the pre-cleaning system was continuously monitored for three months starting from January-March 2017. *Figure 9* illustrates the separation performance of the system for free shell removal in kernels. The results indicated that the amount of free shell after pre-cleaning was maintained below the targeted limit (<4.0%). However, the total amount of shell exceeded the limit (>4.0%) for separation of whole and half-cracked nuts from the kernels. The air velocity applied in Column 2 and 3 was capable of removing some of the whole and half-cracked nuts present in the kernel consignments to minimise kernel losses. Based on the results, it can be concluded that the maximum limit of dirt and shell in palm kernel before pre-cleaning must not exceed 5%, in order to achieve the targeted limit of <4.0% shell in the clean kernel.

The presence of shell and half-cracked nuts together with kernels may increase the dirt and shell content in Purafex. It was observed that the amount of free shell was reduced significantly after pre-cleaning, compared to the half-cracked nuts.

Proximate Values of Purafex

The proximate values of Purafex are illustrated in *Figures 10* and *11*. The Purafex referred to PKC containing lower shell content (≤6%) compared to the commercial PKC (≥12%) and higher crude protein content (≥16%) than commercial PKC (14%). Crude protein content is directly influenced by the amount of shell; high shell content will lower the crude protein content (Rohaya and Osman, 2002). According to MEOMA trade specification for domestic contract (MEOMA, 2000), the minimum level of protein content in PKC is 14%. Purafex also comprised of low crude fibre (≤12%), in align with the nutrients requirement for broilers when the inclusion level of PKC is below 50%. Reduction of shell and fibre in the kernels using pre-cleaning system also reduced the crude fibre in the PKC from ≥18% to ≤10%, which was far below the fibre in the commercial PKC, thus, making it digestible for monogastric animals and ruminants.

From *Figure 11*, it could be seen that the oil content in Purafex fluctuated from 7.5%-10% depending on the efficiency of the screw press during oil extraction process. Another study by Rohaya and Osman (2002) reported that the oil content in PKC from seven conventional crushing plants ranged from 7.5% to as high as 13.2%. The oil content retained in PKC is a good source of energy for feed uses (Nordin *et al.*, 2005); however, it should be reduced to increase the kernel oil recovery as additional income to the crushing plants (Rohaya and Osman, 2002). For domestic trade, the minimum level of oil content in PKC is 8% (Nordin *et al.*, 2005). Similar trend was also observed for moisture content of Purafex ranging from 5.8%-8.7%. Using conventional method, the moisture content of PKC was in the range of

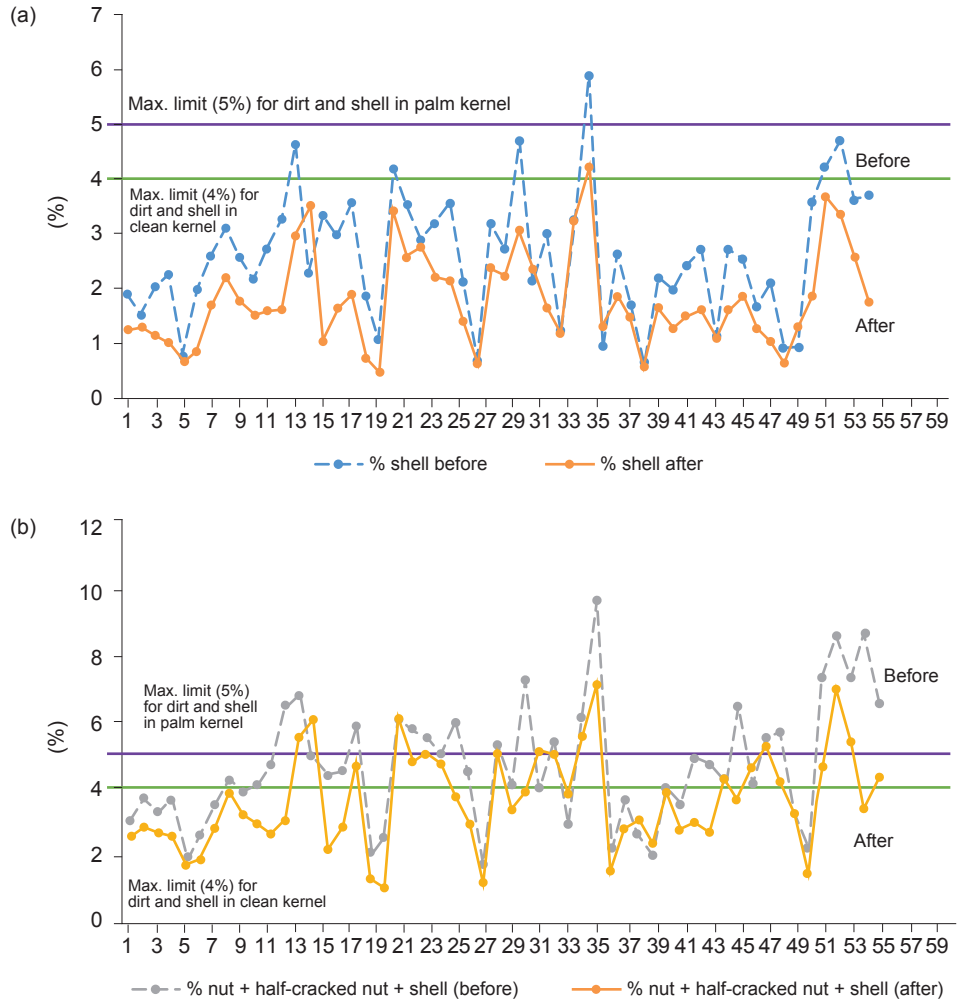


Figure 9. Removal of (a) free shell and (b) whole and half-cracked nuts by pre-cleaning system from January-March 2017.

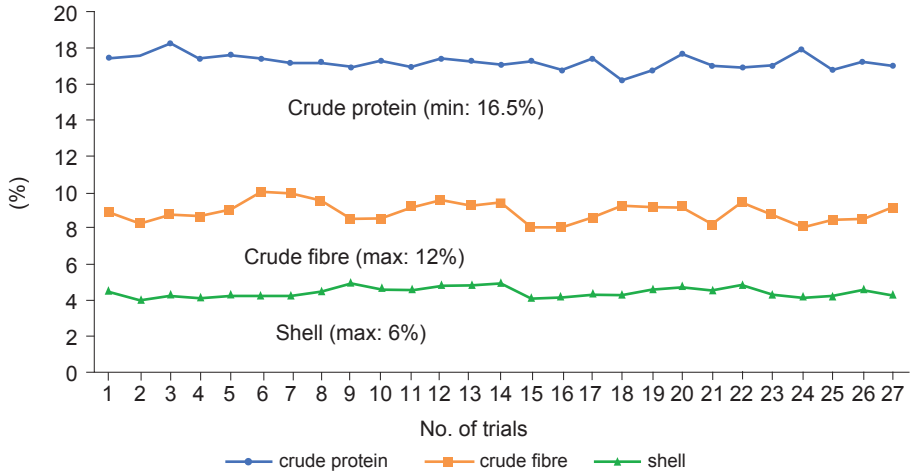


Figure 10. Crude protein, crude fibre and shell content in Purafex.

3.3%-11.5% as reported by Rohaya and Osman (2002). Nordin *et al.* (2005) emphasised that the moisture content in PKC is influenced by moisture content in palm kernels. Hence, the moisture content of raw material must not exceed 10%. The maximum levels of PKC's moisture content stipulated for domestic and export trades are 9.5% and 10% at the point of shipment, respectively (MEOMA, 2000). In addition, the ash content of Purafex was maintained below 5.0% for all trials.

The shell content in Purafex was between 4.0%-5.0%, compared to >12.0% in commercial PKC, meeting the targeted performance of below 6.0%.

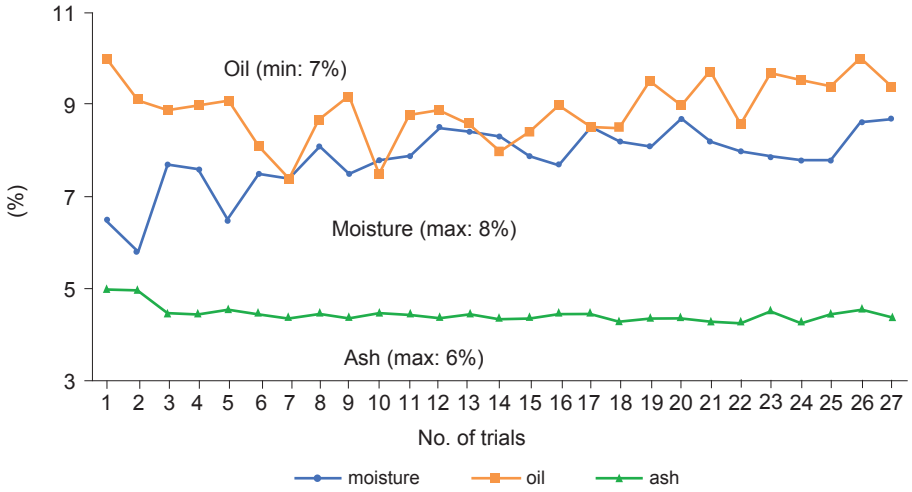


Figure 11. Moisture, oil and ash content in Purafex.

A survey conducted for seven crushing plants using conventional processing recorded the amount of shell in PKC ranging from 6.3%-21.0% (Rohaya and Osman, 2002). The maximum content of shell in PKC should be lower than 15% as stipulated by MEOMA standard specification. The PKC consignment can be rejected for domestic trade if the shell content is higher than 18% (Nordin *et al.*, 2005). Thus, the pre-cleaning system has succeeded in reducing the shell content in Purafex, demonstrating better performance than the conventional separation system.

The crude fibre in Purafex was lower than 12%, indicating better quality than commercial PKC with crude fibre more than 15%. The protein content in Purafex fell within 16.0%-17.8%, compared to <16.0% in the commercial PKC. The comparisons of crude protein, crude fibre and shell content between Purafex and commercial PKC are shown in *Figures 12a-c*. Thus, the Purafex quality produced from the clean kernels with low shell content after pre-cleaning system conformed to the standard specifications by MEOMA.

Effect of Broilers Chicken Fed with Purafex

Table 2 summarises the nutritive values of the broilers fed with 15%-45% Purafex inclusion. The feeds were formulated through combination of energy and protein sources to provide better amino acid balance and sufficient nutrients requirement so it is isonitrogenous and isocaloric. However, the crude fibre content in diet 45% Purafex was slightly higher (7.0%) than the required, which is less than 7% in poultry feed (Varastegani and Dahlan, 2014). Although fibrous components in food may give negative effect on broiler growth performance (Janssen and Carré, 1985), crude fibre should be moderately incorporated in the diets which are beneficial for gizzard activity and bacterial population prevention of broilers (Montagne *et al.*, 2003; Mateos *et al.*, 2012). As a result, this study has limited the inclusion of Purafex up to 45% only.

As can be seen in *Table 2*, the crude protein had negatively correlated with the fibre content. As the inclusion level increased, the crude protein indicated a declining trend. Similarly, the oil content had also increased with the increasing Purafex inclusion. The results are in agreement with that reported by Pushpakumara *et al.* (2017). High shell content stemming from processing method is the prominent factor in limiting the inclusion level of PKC in broiler diets. Hence, it is crucial to improve the separation process of shell and kernels, thus, producing PKC with enhanced quality to be used as broiler feed source.

Growth Performance Analyses of Starter Phase for Broilers Chicks

Figure 13 depicts the growth performance of starter phase for the broiler chicks fed with Purafex formulated diets for 21 days. It was found that the control diet (0% Purafex) had caused the highest body weight of broilers at 0.92 kg, whereas diet 15% Purafex and 30% Purafex showed no significant differences (P>0.05) in body weight of 0.86 and 0.85 kg with the control, respectively. The lowest body weight of 0.74 kg was obtained by diet 45% Purafex. Similar trend was observed in the BWG for diet 15% and 30% Purafex of 0.81 kg and 0.82 kg, respectively, which showed no significant differences (P>0.05) with the control diet, of which BWG was 0.87 kg. This result was in line with findings by Noraini *et al.* (2009) and Mohd Firdaus (2014) that broiler chicks can tolerate up to 30% of PKC in the starter diet. However, broiler chicks fed with 45% Purafex (D) showed the lowest BWG of 0.7 kg although

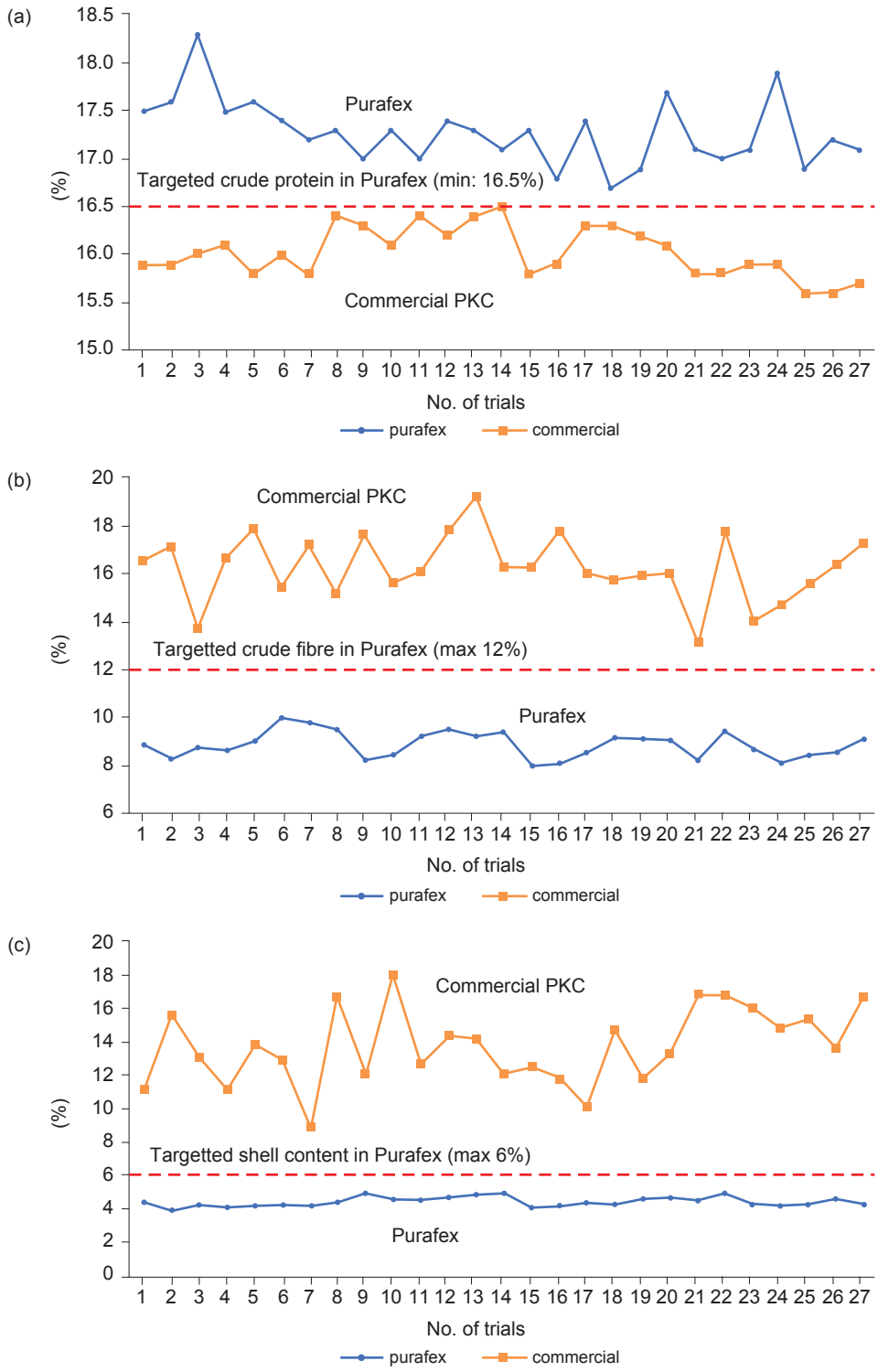
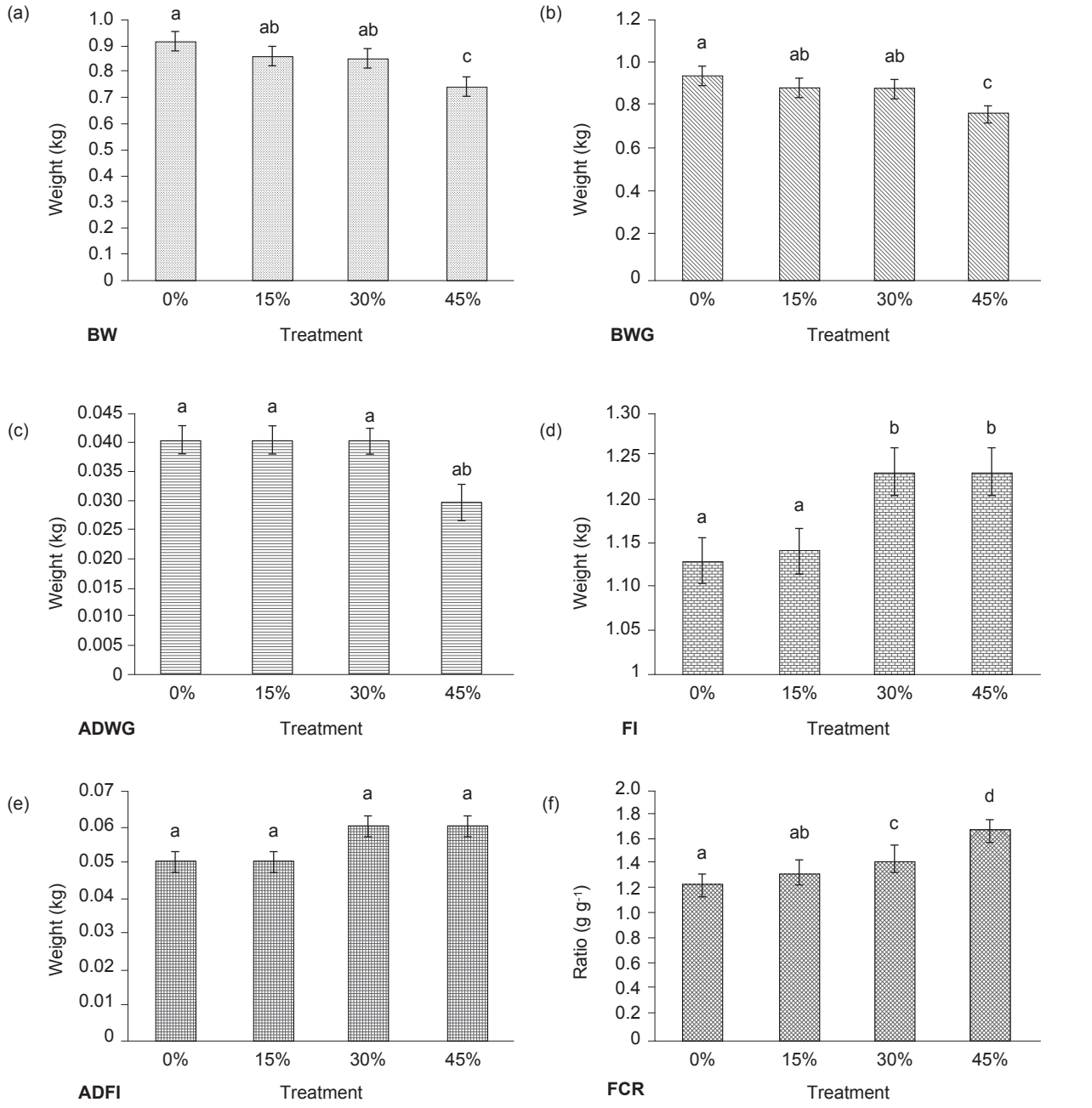


Figure 12. Comparison of (a) crude protein, (b) crude fibre, and (c) shell content in commercial palm kernel cake (PKC) against Purafex.

TABLE 2. NUTRITIVE VALUE OF STARTER BROILERS FEED WITH 15%-45% PURAFEX INCLUSION

Proximate analysis	Control	Purafex 15%	Purafex 30%	Purafex 45%
Moisture content (%)	11.32 ± 0.07	7.83 ± 3.47	9.32 ± 0.03	8.45 ± 0.04
Ash (%)	8.08 ± 0.15	7.51 ± 0.26	7.95 ± 0.50	8.17 ± 0.38
Oil content (%)	4.17 ± 0.03	4.75 ± 0.03	5.48 ± 0.02	6.00 ± 0.02
Crude protein (%)	23.08 ± 0.26	22.18 ± 0.23	21.72 ± 0.29	21.57 ± 0.35
Fibre content (%)	3.70 ± 0.30	3.99 ± 0.09	5.40 ± 0.20	7.00 ± 0.18
Gross energy (kcal kg^{-1})	3 908 ± 15.40	4 002 ± 5.44	4 064 ± 9.86	4 129 ± 7.64



Note: [a,b,c,d] Min with different superscript is significantly different (P<0.05).

Figure 13. Growth performance of broilers during 1-21 days age; (a) body weight (BW), (b) body weight gain (BWG), (c) average daily weight gain (ADWG), (d) feed intake (FI), (e) average daily feed intake (ADFI), and (f) feed conversion ratio (FCR).

the FI was high (1.23 kg). This could be due to the presence of high fibre content in the formulated diet, as the increase in PKC inclusion level will reduce the palatability and availability of amino acids and energy (Onwudike, 1986). Another reason might be that the crude fibre content in diet 45% Purafex was slightly higher (7.0%) than the required, which is less than 7% in poultry feed (Varastegani and Dahlan, 2014).

The FI of diet 30% Purafex and 45% Purafex shared the highest FI at 1.23 kg and were significantly different (P<0.05) from FI of control diet and diet 15% Purafex, (1.13 and 1.14 kg, respectively). In parallel with that, diet 30% and 45% Purafex had the highest ADFI of 0.06 kg, while diet 0% and 15% Purafex shared the same value of 0.05 kg and had no significant difference (P>0.05). These results indicated that broilers will consume more feed that has 30% and 45% Purafex to achieve its targeted body weight.

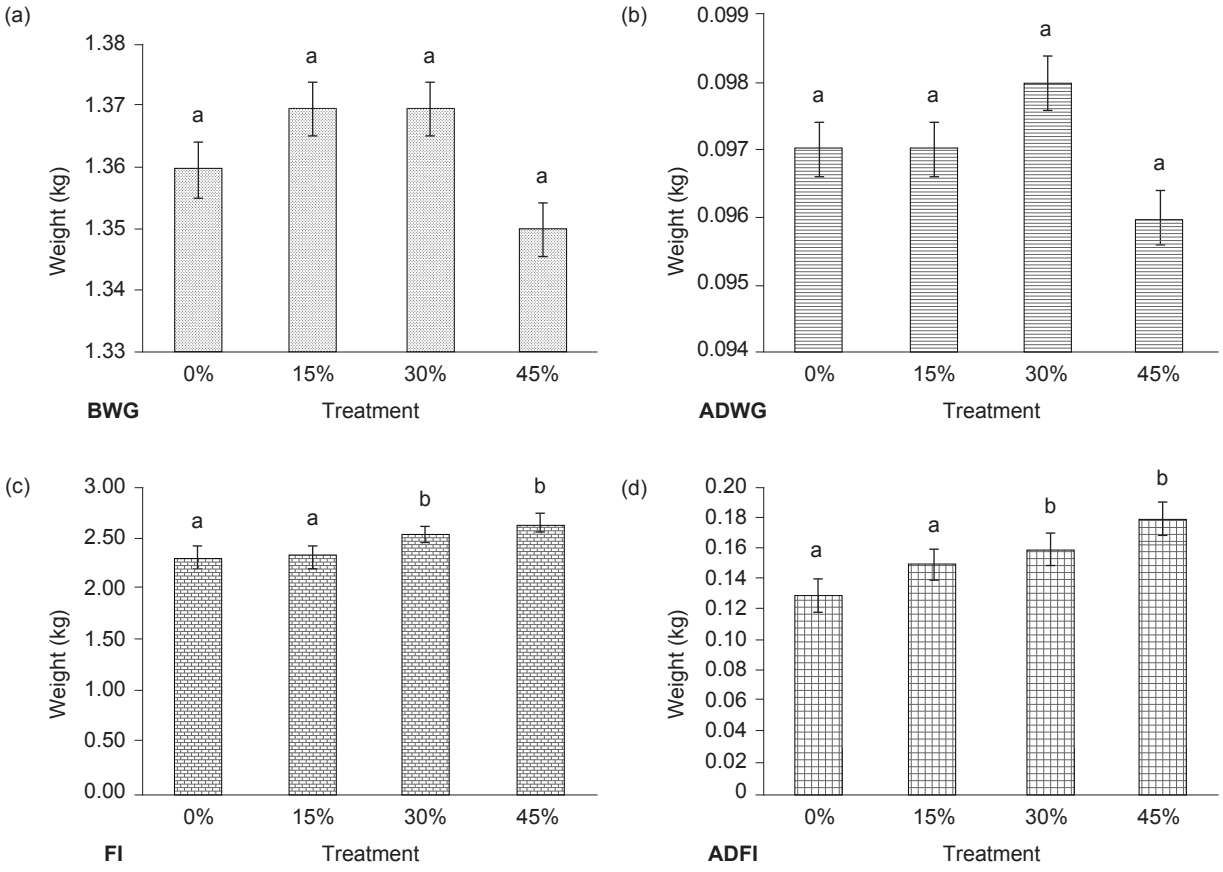
The FCR for control diet and diet 15% Purafex were 1.23 and 1.33, respectively, which did not differ significantly (P>0.05), indicating the efficiency of feed towards broiler's growth which most of the

feed were converted back to body growth of the broiler. Low FI and low FCR but high BWG proved the efficiency of the feed. In addition, diet 30% and 45% Purafex indicated higher FCR of 1.45 and 1.66, respectively and was significantly difference with the control diet at 1.23 ($P<0.05$).

Growth Performance of Finisher Phase for Broilers

Figure 14 shows the growth performance of finisher phase from 22-35 days for broilers fed with 15%, 30% and 45% Purafex in comparison with control (0%). The highest BWG was acquired by control diet, 0% (1.36 kg), 15% (1.37 kg) and 30% (1.37 kg), and followed by diet 45% Purafex (1.35 kg). However, there was no significant difference ($P>0.05$) between the control and the experimental diets in terms of BWG. In fact, the ADWG of broilers fed with 15% (0.097 kg) and 30% Purafex (0.098 kg) were comparable and also have no significant difference ($P>0.05$) to that of control diet (0.097 kg), except for diet 45% Purafex which indicated the lowest ADGW of 0.096 kg. This study confirmed the findings reported by Ezieshi and Olumu (2004); Okuedo *et al.* (2005) and Bello *et al.* (2011), which concluded that inclusion of 45% PKC in the diet caused lower BWG and ADWG compared to that of 30% PKC. In contrast, Navidshad *et al.* (2016) found that even feeding 20% low shell PKC towards broiler at finisher phase gave lower ADWG compared to diet without PKC.

The FI of the broilers has increased significantly when the level of Purafex increased from 30%-45%. Broilers consuming higher Purafex by 30% and 45% in their diets exhibited higher FI of 2.51 kg and 2.59 kg, respectively, which were significantly different ($P<0.05$) to the control diet (2.27 kg) and diet 15% Purafex (2.3 kg), respectively. A similar trend was indicated for ADFI, as it is in parallel with FI. The highest ADFI was consumed by diet 30% and 45% Purafex, with the values of 0.16 kg and 0.18 kg, respectively, which was significantly different ($P<0.05$) with the control (0.13 kg) and diet 15% Purafex (0.15 kg). These findings showed that higher Purafex inclusion in the diets will drive the broilers to consume more feed to achieve the targeted weight. Similar finding was also reported by Sundu *et al.* (2005b) where the FI had increased with the increasing PKC levels in the broiler diets. Nevertheless, increasing the proportion of Purafex in the diets will increase the fibre content, which accounted for poor BWG and depression in acid



Note: [a,b,c,d] Min with different superscript is significantly different ($P<0.05$).

Figure 14. Growth performance of broilers during 22-35 days age; (a) body weight gain (BWG), (b) average daily weight gain (ADWG), (c) feed intake (FI), and (d) average daily feed intake (ADFI).

amino availability. High lignin content also results in poor digestibility in monogastric animals (Jha and Berrocoso, 2015). There was no adverse health effect on animal growth even when Purafex was given up to 45% in the diet.

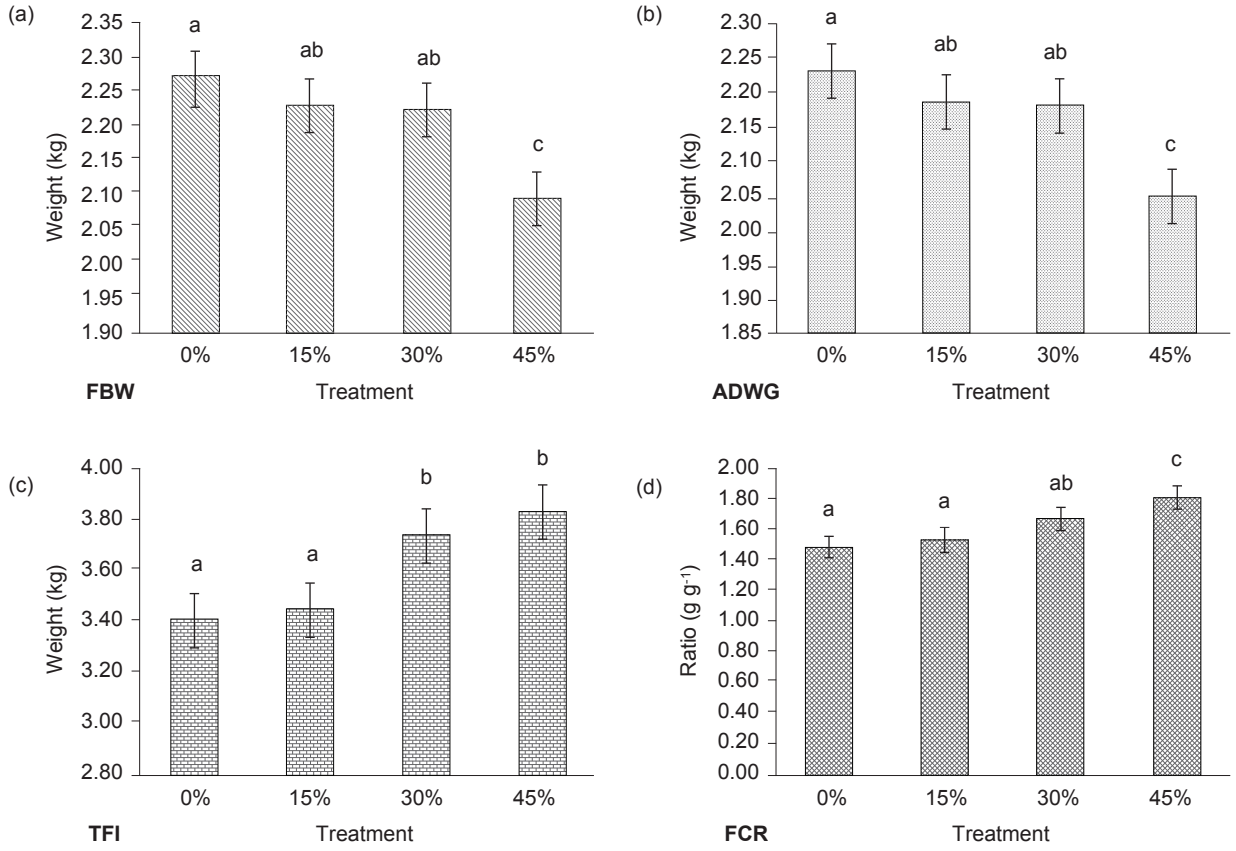
Growth Performance of Full Phases for Broilers

Figure 15 depicts the growth performance of full broiler phase from Day 1 to Day 35. Results showed that all treatments reached commercial targeted minimum of 2 kg live final weight. Diet control (0% Purafex) indicated the highest final body weight (FBW) was 2.27 kg and BWG was 2.23 kg. However, there was no significant difference (P>0.05) in the FBW (2.23 and 2.22 kg) and BWG (2.19 and 2.18 kg) of broilers fed with 15%, 30% Purafex and the control. This finding proved the previous studies by Ezieshi and Olumu (2004), and Iyayi and Davies (2005), that broiler chicken can tolerate up to 30% in the formulation without adverse effects. The lowest FBW and BWG of 2.09 and 2.05 kg, respectively, which were obtained by diet 45% Purafex. According to Ezieshi and Olumu (2004), BWG of broilers fed with 45% PKC were lower than 30% PKC.

Broilers consuming high Purafex diet by 30% and 45% have recorded higher FI of 3.74 and 3.82 kg, respectively, and was significantly different (P<0.05) to that of diet containing 15% Purafex (3.44 kg) and control (3.40 kg). Feed consumed (g) per g of weight gain is taken as FCR (Rasal *et al.*, 2015). The FCR as depicted in *Figure 15* had increased to 1.68 when the substitution of Purafex in the diets was more than 30% (standard set by Tegel Poultry of NZ is 1.56). The FCR of broilers without Purafex was 1.5 and substitution of 15% Purafex in broiler feed indicated an increase in FCR (1.58). Established information on optimal inclusion level of PKC in poultry diet is not available at present; however, different studies have recommended inclusion level to be in the range of 10%-50% depending on the types of PKC used (Fadil *et al.*, 2014).

CONCLUSION

Palm kernels are the sole raw material for PKC production, thus the quality should be given highest priority. Since palm oil millers are unable to improve the kernel quality delivered to the crushing plant, the use of pre-cleaning system prior to oil extraction



Note: [a,b,c,d] Min with different superscript is significantly different (P<0.05).

Figure 15. Growth performance of broilers during 1-35 days; (a) final body weight (FBW), (b) body weight gain (BWG), (c) total feed intake (TFI), and (d) feed conversion ratio (FCR).

is desirable to enhance the quality of end products. Results from the study proved that the pre-cleaning system was capable of reducing the shell content in kernels, thus, enhancing the quality of PKC (Purafex) produced. The nutrient values of Purafex surpassed those of commercial PKC, conforming to the standard specifications by MEOMA. Feeding trials on broilers showed that the inclusions of Purafex between 15%-30% exhibited better performance in terms of BWG and FI compared to those of 45% inclusion. However, increasing the proportion of Purafex in the dietary treatments will increase the crude fibre content, thereby alleviating the digestibility of broilers.

ACKNOWLEDGEMENT

We would like to thank the Director-General and management of MPOB for the continuous support to conduct this research.

REFERENCES

Bello, K M; Oyawoye, E O; Bogoro, S E and Dass, U D (2011). Performance of broilers fed varying levels of palm kernel cake. *Int. J. Poult. Sci., 10(4)*: 290-294.

Cerveró, J M; Skovgaard, P A; Felby, C; Sørensen, H R and Jørgensen, H (2010). Enzymatic hydrolysis and fermentation of palm kernel press cake for production of bioethanol. *Enzyme Microb. Technol., 46(3-4)*: 177-184.

Chong, C H; Zulkifli, I and Blair, R (2008). Effects of dietary inclusion of palm kernel cake and palm oil, and enzyme supplementation on performance of laying hens. *Asian-Australas. J. Anim. Sci., 21(7)*: 1053-1058.

COBB (2018). Cobb 500 Broiler performance and nutrition supplement. Cobb-Vantress.com. https://cobbstorage.blob.core.windows.net/guides, accessed on 4 April 2020.

Dusterhoft, E M and Voragen, A G J (1991). Non-starch polysaccharides from sunflower (*Helianthus annus*) and palm kernel (*Elaeis guineensis*) meal preparation of cell wall material and extraction of polysaccharides fractions. *J. Sci. Food Agric., 55(3)*: 411-422.

Ezieshi, E V and Olomu, J M (2004). Comparative performance of broiler chickens fed varying levels of palm kernel cake and maize offal. *Pak. J. Nutr., 3(4)*: 254-257.

Fadil, M; Alimon, A R; Meng, G Y; Ebrahimi, M and Farjam, A S (2014). Palm kernel cake as a potential ingredient in Muscovy ducks diet. *Ital. J. Anim. Sci., 13*: 112-115.

Iyayi, E A and Davies, B I (2005). Effect of enzyme supplementation of palm kernel meal and brewer's dried grain on the performance of broilers. *Int. J. Poult. Sci., 4(2)*: 76-80.

Janssen, W M M A and Carré, B (1985). Influence of fibre on digestibility of broiler feeds. *Recent Advances in Animal Nutrition* (Cole, D J A and Haresign, W eds.). Butterworths, London, United Kingdom. p. 78-93.

Jha, R and Berrocoso, J D (2015). Review: Dietary fibre utilization and its effect on physiological functions and gut health of swine. *Animal, 9(9)*: 1441-1452.

Lawal, T E; Lyayi, E A; Adeniyi, B A and Adaramoye, O A (2010). Biodegradation of palm kernel cake with multienzyme complexes from fungi and its feeding value for broilers. *Int. J. Poult Sci., 9*: 695-701.

Mateos, G G; Jiménez-Moreno, E; Serrano, M P and Lázaro, R P (2012). Poultry response to high levels of dietary fibre sources varying in physical and chemical characteristics. *J. Appl. Poult. Res., 21(1)*: 156-174.

MEOMA (2000). Malayan Edible Oil Manufacturers' Association Handbook 2000/2001. 39 pp.

Mohd Firdaus, O (2014). *Penghasilan Dedak Isirung Sawit (PKE dan PKC) Terfermentasi Melalui Sistem Fermentasi Keadaan Pepejal oleh Kulat Pencilan Tempatan Rhizopus oryzae ME01*. M.Sc thesis, Universiti Kebangsaan Malaysia.

Montagne, L; Pluske, J R and Hampson, D J (2003). A review of interactions between dietary fibre and the intestinal mucosa, and their consequences on digestive health in young non-ruminant animals. *Anim. Feed Sci. Technol., 108(1-4)*: 95-117.

MPOB (2005). *MPOB Test Methods* (Aini, K; Siew, W L; Tan, Y A; Nor Aini, I; Tang, T S and Nuzul, A I eds). MPOB, Bangi.

Navidshad, B; Liang, J B; Jahromi, M F; Akhlaghi, A and Abdullah, N (2016). Effects of enzymatic treatment and shell content of palm kernel expeller meal on performance, nutrient digestibility and ileal bacterial population in broiler chickens. *J. Appl. Poult. Res., 25(4)*: 474-482.

Noraini, S; Sarah, R; Mohd Fazli, F A; Rosnizah, I and Norham, I (2009). Response of young broiler

chickens fed increasing levels of fermented palm kernel expeller (f-PKE). *Prosiding Seminar Kebangsaan Kedua Agro-Environment 2009*. 24-26 March 2009. Johor Bahru, Johor.

Nordin, A B A; Venugopal, R; Amiruddin, N and Simeh, M A (2005). Palm kernel cake marketing: Constraints and prospects. *Oil Palm Industry Economic J., 5*: 37-46.

Nwokolo, E N; Bragg, D B and Kitts, W D (1976). The availability of amino acids from palm kernel, soybean, cottonseed and rapeseed meal for the growing chick. *Poult. Sci., 55(6)*: 2300-2304.

Okuedo, N J; Eboh, K V; Ndidi, V I and Akanno, E C (2005). Growth rate, carcass characteristics and organoleptic quality of broilers fed graded levels of palm kernel cake. *Int. J. Poult. Sci., 4(5)*: 330-333.

O'Mara, P P; Mulligan, F J; Cronin, E J; Rath, M and Caffrey, P J (1999). The nutritive value of palm kernel meal measured *in vivo* and using rumen fluid and enzymatic techniques. *Livest. Prod. Sci., 60(2-3)*: 305-316.

Onwudike, O C (1986). Palm kernel as feed a feed poultry. 2. Diets containing palm kernel meal for starter and grower pullets. *Anim. Feed Sci. Tech., 16(3)*: 187-194.

Pushpakumara, D M S; Priyankarage, N; Nayananjalie, W A D; Ranathunge, D L and Dissanayake, D M D P (2017). Effect of inclusion of palm (*Elaeis guineensis*) kernel cake in broiler chicken rations. *Int. J. Livest. Res., 7(2)*: 103-109.

Rasal, K D; Shah, T M; Vaidya, M; Jakhesara, S J and Joshi, C G (2015). Analysis of consequences of non-synonymous SNP in feed conversion ratio associated TGF-β receptor type 3 gene in chicken. *Meta Gene, 4*: 107-117.

Rohaya, M H and Osman, A (2002). The quality of Malaysian palm kernel: Effect of shell content and broken kernel on the quality of final products. Paper presented at 2002 National Seminar on Palm Oil Milling, Refining Technology, Quality and Environment. 19-20 August 2002. Kota Kinabalu, Sabah.

Rohaya, M H; Osman, A and Nasrin, A B (2005). Water cooled screw press for production of feed quality palm kernel expeller (PKE) for feedstuff. *MPOB Information Series No. 286*.

Rohaya, M H; Nasrin, A B; Wahid, M B; Choo, Y M; Ridzuan, R; Ma, A N and Ravi, M (2009). Maximising the recovery of dry kernel and shell via a four-stage winnowing column. *MPOB Information Series No. 427*.

Rohaya, M H; Ridzuan, R; Che Rahmat, C M; Nu'man, A H; Nasrin, A B and Astimar, A A (2017). Highly digestible palm kernel cake (PKC) for animal feed. *MPOB Information Series No. 619*.

Roslan, M A H; Norhani, A and Mustafa, S (2015). Removal of shells in palm kernel cake via static cling and electrostatic separation. *J. Biochem. Microbiol. Biotechnol., 3*: 1-16.

Saenphoom, P; Liang, J B; Ho, Y W; Loh, T C and Rosfarizan, M (2013). Effects of enzyme treated palm kernel expeller on metabolizable energy, growth performance, villus height and digesta viscosity in broiler chickens. *Asian-Australas. J. Anim. Sci., 26(4)*: 537-544.

Sanni, L A; Ohiare, T and Ibrahim, R O (2017). Saline bath system for separation of palm kernels from shells. *J. Biochem. Microbiol. Biotechnol., 3*: 1-6.

SAS (2004). SAS Institute Inc., 2002-2003 Version 9.1. Cary, NC, USA.

Sinurat, A P; Purwadaria, T and Pasaribu, T (2013). Improving nutrient values of palm kernel cake (PKC) by reducing shell contamination and enzymes supplementation. *J. Ilmu Ternak dan Vet., 18(1)*: 34-41.

Sundu, B; Kumar, A and Dingle, J (2005a). Comparison of feeding values of palm kernel meal and copra meal for broilers. *Recent Adv. Anim. Nutr. Aust*. p. 15-16.

Sundu, B; Kumar, A and Dingle, J (2005b). Palm kernel meal in broilers diets, effect on chicken performance and health. *World Poult. Sci. J., 62(2)*: 316-325.

Varastegani, A and Ismail, D (2014). Influence of dietary fibre levels on feed utilization and growth performance in poultry. *J. Anim. Sci. Adv., 4(1)*: 422-429.

Zahari, M W and Wong, H K (2009). Research and development on animal feed in Malaysia. *WARTAZOA, 19(4)*: 172-179.

Journal of Oil Palm Research Vol. 33 (3) September 2021 p. 473-481
DOI: https://doi.org/10.21894/jopr.2020.0109

PRODUCTION OF FURFURAL FROM OIL PALM FIBRES

NUR ELIYANTI ALI OTHMAN[1]*; ASTIMAR ABD AZIZ[1]; WAN HASAMUDIN WAN HASSAN[1]; NOR FAIZAH JAILANI[1]; FAZLIANA ABD HAMID[1] and NOORSHAMSIANA ABDUL WAHAB[1]

ABSTRACT

Furfural is a chemical compound produced by biomass rich in pentoses content in the hemicellulose as raw material, in a reaction catalysed in presence of strong acids. This study determines the process parameters for converting xylan, extracted from oil palm empty fruit bunches (OPEFB), into furfural using a two-step process, namely acid hydrolysis, followed by dehydration. Xylan was first extracted from OPEFB using direct alkaline extraction method. The resulting xylan was then treated with a known concentration of sulphuric acid (H_2SO_4) (ranging from 11%-15% v/v) with reaction time (ranging from 30-150 min), with or without presence of sodium chloride (NaCl) as co-catalyst to produce xylose. After dehydration process, xylose was converted into furfural with parameters as in dehydration process. Furfural was characterised using Fourier transform infrared (FTIR) and Proton nuclear magnetic resonance (^{1}H-NMR). FTIR spectrum exhibited a very strong absorption at 1706 cm^{-1}, indicating the presence of the conjugated carbonyl (C=O) group. The highest yield of furfural produced was 9.01% after treatment with 15% H_2SO_4 using NaCl as catalyst for 90 min. However, pentosans only contribute a portion of the total composition of lignocellulose, compared to cellulose which is the largest fraction of lignocellulosic biomass. Therefore, the furfural should be extracted using an integrated value economy method.

Keywords: dilute acid hydrolysis, empty fruit bunch fibre, furfural.

Received: 13 August 2020; **Accepted:** 12 October 2020; **Published online:** 9 December 2020.

INTRODUCTION

Furfural or 2-furaldehyde and its derivatives are considered as a versatile precursor to obtain a wide range of chemicals for various applications (Kamm *et al.*, 2006; Alonso-Fagundez *et al.*, 2012; Sadaba *et al.*, 2011; Mansilla *et al.*, 1998). The furfuryl alcohol produced from hydrogenation of furfural has been used as additive or solvent in the production of resins with different characteristics in chemical industry (Merlo *et al.*, 2009; Vazquez *et al.*, 2007; Mansilla *et al.*, 1998). One of the common and important usage of furfural in gas oil, diesel fuel and petroleum refining industry is as selective solvent for separating saturated and unsaturated compounds (Mansilla *et al.*, 1998). In addition, furfural along with its sister molecule, hydroxymethyl furfural (HMF) can serve as a building block for other potential transportation fuels, including dimethylfuran and ethyl levulinate. These fuels could replace furan from petroleum based maleic anhydride (Shen *et al.*, 2018).

Furfural is produced by acid hydrolysis process and dehydration of pentoses containing (mainly xylose) in lignocellulosic materials. *Figure 1* shows simplified reaction scheme for conversion of lignocellulosic biomass into furfural. Several researchers investigated the production of furfural by hydrolysis of lignocellulosic waste materials in dilute acid, such as hydrochloric acid (Herrera *et al.*, 2004; 2003; Lavarack *et al.*, 2002) nitric acid (Rodriguez-Chong *et al.*, 2004), sulphuric acid (H_2SO_4) (Yat *et al.*, 2008; Rahman *et al.*, 2006; Aguilar *et al.*, 2002; Montane *et al.*, 2002) and phosphoric acid (Lenihan *et al.*, 2010; Vazquez *et al.*, 2007; Gamez *et*

[1] Malaysian Palm Oil Board,
6 Persiaran Institusi, Bandar Baru Bangi,
43000 Kajang, Selangor, Malaysia.

* *Corresponding author e-mail: nureliyanti@mpob.gov.my*

al., 2006). The advantage of acid hydrolysis is that the rate of acid hydrolysis is faster than enzyme hydrolysis but glucose also degrades rapidly under acidic conditions (Cheung and Anderson, 1996).

Acid hydrolysis employs usually H_2SO_4 and hydrochloric acid at concentrations of 1%-15% using moderate temperature (in the range of 100°C -150°C) (Wingren *et al.*, 2003). Dilute acid hydrolysis is generally more desirable compared to concentrated acid because of its lower cost. It also allows the high degradation of lignocellulosic biomass under relatively low reaction temperatures. The H_2SO_4 and hydrochloric acids are the most commonly used catalysts for hydrolysis of lignocellulosic biomass.

The formation of furfural from pentosan can be understood in terms of hydrolysis of pentosan (xylan), followed by dehydration of pentose (xylose). Introduction of water molecule in hydrolysis process is to break the glycosidic bond to form xylose or arabinose, and later in dehydration process, three water molecules are then released from the respective sugars to form furfural. *Figure 2* shows acid hydrolysis and dehydration process of xylose for furfural production.

Several mechanisms have been proposed for furfural formation from xylan. Nimlos *et al.* (2006) favoured closed-chain formation of a dehydrofuranose intermediate by ring contraction of the O2-protonated pyranose (*Figure 3*) in the presence of strong acid such as H_2SO_4.

Furfural can be extracted from lignocellulosic materials, including plant fibre, such as eucalyptus (García-Domínguez *et al.*, 2013), olive tree (Romero *et al.*, 2010), agriculture waste such as rice husks (Suxia *et al.*, 2012), corn cobs (Sánchez *et al.*, 2013), sorghum straw (Vazquez *et al.*, 2007), sugar cane bagasse (Gamez *et al.*, 2006), wheat straw (Yemis and Mazza, 2011) rice straw (Lin *et al.*, 2013) and non-wood fibre such as date palm tree (Bamufleh *et al.*, 2013). For non-wood, the study on the conversion of oil palm fibre into furfural was limited. About 17.34% furfural was produced from oil palm mesocarp fibre when it was subjected to 15% H_2SO_4 (Riansa-Ngawong and Prasertsan, 2011).

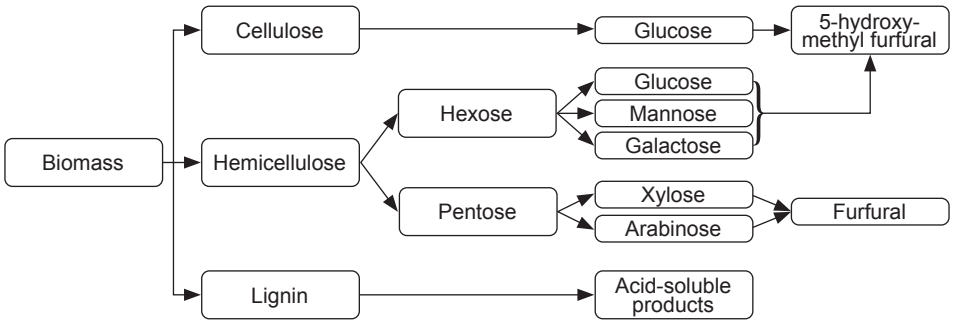
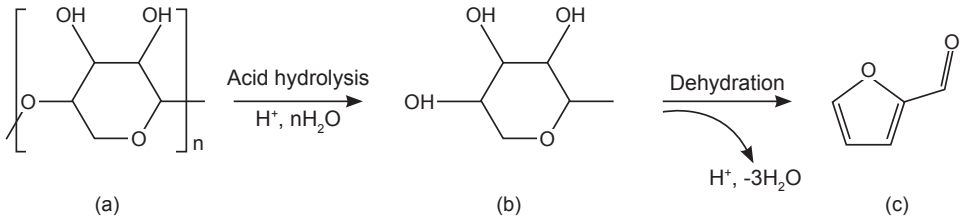


Figure 1. Simplified reaction scheme for conversion of lignocellulosic biomass to furfural.



Source: Riansa-Ngawong and Prasertsan (2011).

Figure 2. (a) Hydrolysis of pentosan (b) followed by dehydration of pentose, (c) to form furfural.

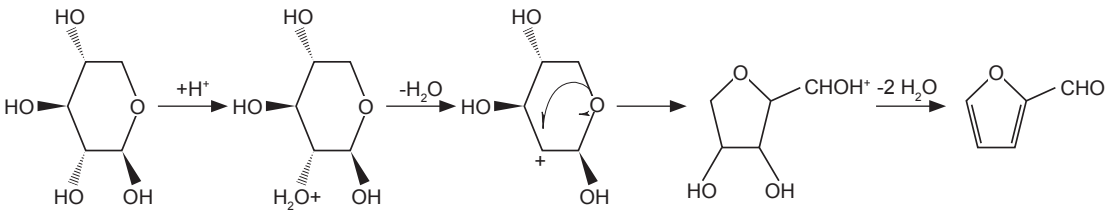


Figure 3. Proposed closed-chain mechanism for furfural formation from xylose.

It is estimated about one third of total pentosans (raw material) can be converted into furfural by existing production processes (Mansilla *et al.*, 1998). In theory, any material containing a large amount of pentose (five carbon) sugars arabinose and xylose can serve as raw material for furfural production. *Table 1* outlines the approximate pentosan content of several plants and agricultural residues potentially suitable for furfural production.

In Malaysia, from 17.16 t ha^{-1} of oil palm fresh fruit bunches produced in 2018, the oil palm industry generates 20%-22% oil palm empty fruit bunches (OPEFB) (Kushairi *et al.*, 2019). The OPEFB biomass with cellulose, hemicelluloses and lignin is estimated to contain about 23%-26% xylan, a sugar polymer made of pentose sugar, xylose (Rahman *et al.*, 2006). Studies available on furfural production from oil palm tree wastes are scarce, relatively old and limited in scope (Rahman *et al.*, 2006; Riansa-Ngawong and Prasertan 2010; 2011; Loi *et al.*, 2011).

The aim of this work is to investigate the production of furfural from OPEFB using H_2SO_4 as catalyst for the process and sodium chloride (NaCl) will be introduced as a co-catalyst or promoter. The effect of acid concentration and reaction time will be investigated and the optimum condition to maximise furfural yield will be determined.

TABLE 1. PENTOSAN CONTENT OF PLANTS AND AGRICULTURAL RESIDUES

Plant material	Pentosan content (%)
Corn cobs	35
Almond husks	30
Rye straw	30
Oat hulls	29
Cottonseed hulls	28
Barley straw	25
Birchwood residues after felling	25
Sugarcane bagasse	25
Sunflower husks	25
Wheat straw	24
Flax shives	23
Hazelnut shells	23
Birchwood logs	22
Eucalyptus wood	20
Rice hulls	17
Maple wood	16
Pinewood	8
Peanut shells	3

Source: O'Brien (2006).

METHODOLOGY

Materials

Shredded OPEFB fibres were collected from the Palm Oil Milling Technology Centre (POMTEC), located in Labu, Negeri Sembilan, Malaysia. After drying, OPEFB fibres were kept in a plastic bag and stored at room temperature. All chemicals used were analytical grade and used without further purification. Xylan from beech wood and 2-furfuraldehyde (furfural) standard reference materials were purchased from Sigma-Aldrich.

Method

OPEFB pretreatment and xylan extraction. Pretreatments of OPEFB fibres were carried out according to ASTM D 1104-56 (1978). Dry EFB-fibre was initially treated by soaking in 24% solution sodium chlorite ($NaClO_2$) in the ratio of 1:10 (w/v) and (ml) 0.01% acetic acid solution, at 70°C for 1 hr. The solid residues were then washed with hot water followed by acetone, to remove water. The treated OPEFB fibres was then dried in an electric oven at 105°C for 3 hr.

The treated OPEFB fibres were then soaked in 3M sodium hydroxide (NaOH) at ratio of 1:10 (w/v) for 4 hr. The solid residue material was then separated from the solution by vacuum filtration. The filtrate was collected and neutralised with 50% acetic acid (v/v). Cold isopropanol was then slowly mixed into the filtrate admixture resulting in a colloidal suspension. After being left overnight, the suspension was then separated into two heterogenous layers containing xylan solid. After filtration, the xylan was washed with 100 ml distilled water and dried in an electric oven at 60 ± 5°C for 6 hr. The yield (%) of xylan was measured as dry weight basis and calculated using the following Equation (1):

$$\text{Yield (\%)} = \frac{\text{Weight of dried xylan}}{\text{Weight of dried OPEFB}} \times 100 \quad (1)$$

Conversion of xylan into furfural. Furfural was converted from xylan using a modified steam distillation method (Sashikala and Ong, 2007). About 1 g dry xylan was placed into a 250 ml round bottomed flask with 100 ml of dilute H_2SO_4. The mixture was constantly stired and heated at 175°C. The vapour produced was condensed and collected in a receiving flask. The distillation process ran for 30-150 min.

Characterisation of xylan and furfural. The extracted xylan was characterised using Fourier transform infrared (FTIR) spectroscopic technique. Furfural was also characterised using FTIR and Proton nuclear

magnetic resonance (^{1}H-NMR). FTIR analysis was performed by Perkin Elmer TG-IR Hyphenation System and ^{1}H-NMR spectra were obtained using JEOL ECZ 600R/S1 spectrometer. The ^{1}H-NMR spectra were measured at 600.17 MHz in deuterium oxide (D_2O).

Amount of furfural in distillate was determined by Ultraviolet visible (UV-Vis) spectroscopy, as furfural has a strong absorption in ultra violet at wavelength of 276 nm (Zhang *et al.,* 2017). The concentration of furfural can be calculated from the calibration graph of commercial furfural. The calibration graph of commercial furfural was obtained based on absorption spectrum of a set of different concentrations at 276 nm. The UV-Vis spectroscopy was carried out using a Thermo Scientific Genesys 10S UV-Vis (*Figure 4*).

RESULTS AND DISCUSSION

Characterisation of Xylan by FTIR Spectroscopy

The xylan yield was about 22%-25% per kg of EFB-fibre processed. From FTIR spectroscopy analysis, spectrum of xylan from EFB was found to be comparable to that of standard commercial xylan (Sigma).

The FTIR spectrum of xylan from OPEFB within the region of 650-4000 cm^{-1} is shown in *Figure 5*. The region of between 850-1200 cm^{-1} is typical for hemicellulose. This indicates that the alkaline extraction did not change the macromolecular structure of xylan. The absence of absorption band at 1710 cm^{-1} which is the finger-print peak for carboxyl groups in lignin, showed that the extracted xylan was pure and clean from lignin residue (Herrera *et al.*, 2003).

Absorption band at 1037 cm^{-1} was due to the C-O-C stretching glycosidic linkages in xylan. The broad absorption band at 3400 and 2400 cm^{-1} were due to the stretching vibrations of OH and C-H respectively. The C-H bending vibration showed absorption bands at 1555 and 1406 cm^{-1} while the OH bending vibration showed absorption bands at 1344 cm^{-1}.

Characterisation of Furfural by FTIR Spectroscopy

The furfural obtained was in liquid form. It was colourless intially but turned yellowish to dark brown when exposed to light and air. Its scent resembled that of bitter almond. Its vapour irritates the eyes. *Figure 6* shows an overlay FTIR spectra of xylan and furfural from OPEFB.

The FTIR spectrum of furfural showed a very strong absorption at 1706 cm^{-1}. This absorption indicates a very significant functional group in furfural which is the conjugated carbonyl (C=O) (Sashikala and Ong, 2007). The absorption wave number was slightly lower than usual, which is around 1740-1720 cm^{-1}, due to internal hydrogen bonding that occurs in conjugated unsaturated aldehydes. However, this peak can be atributed to chemical compounds such as carboxylic acid (COOH), ketone, ester and aldehyde groups. The absence of peak at 1725 cm^{-1} strongly indicates the presence of aldehyde and not ketone group. Furthermore, no broad peak is observed between 3400-2400 cm^{-1} of hydroxyl (OH), as in xylan FTIR spectrum. This confirmed the absence of carboxylic acid group. The presence of aldehyde was proven with the existence of two peaks at 2841 cm^{-1} and 2816 cm^{-1} respectively. These absorptions showed moderate intense stretching of aldehydic C-H, attributed to the resonance between stretching and bending vibration of aldehydic C-H, which appeared at 1389 cm^{-1} in the spectrum. These bands were observed in aldehyde group.

Strong peaks between 1565-1466 cm^{-1} represent stretching of C=C from aromatic ring. Aromatic =C-H bending out of plane peaks were observed from 929-881 cm^{-1}. Two strong peaks at 1016 cm^{-1} and 1077 cm^{-1} indicated the C-O stretching vibration. This FTIR spectrum was comparable to commercial furfural standard reference material FTIR spectrum.

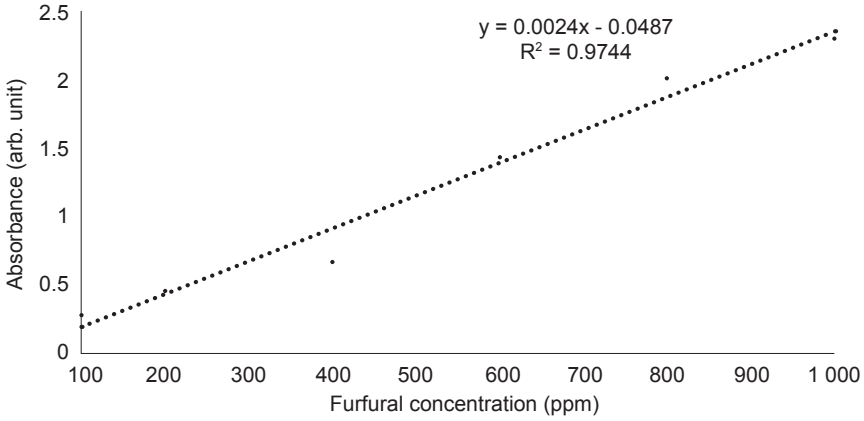


Figure 4. Calibration graph of standard commercial furfural in distilled water at different concentration.

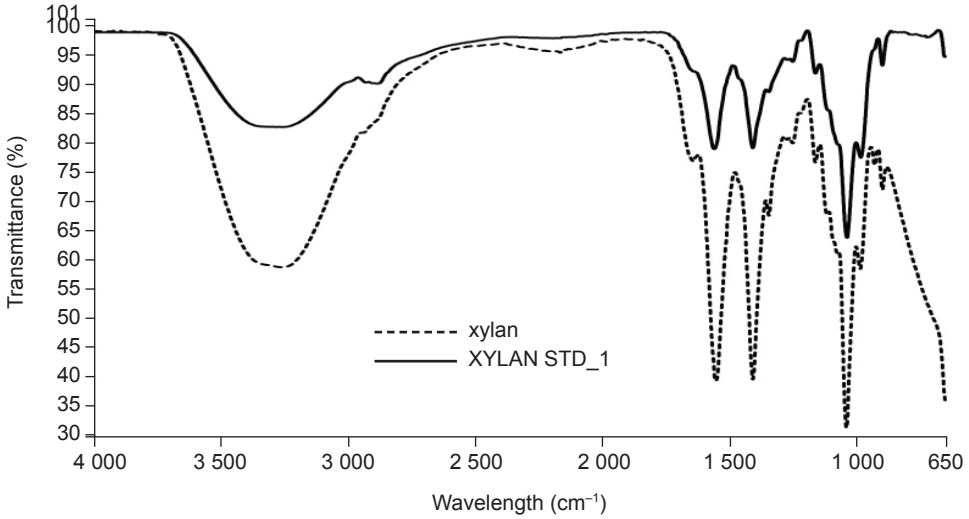


Figure 5. An overlay Fourier transform infrared (FTIR) spectrum of xylan from oil palm empty fruit bunches (OPEFB) and standard commercial xylan from beech wood (Sigma).

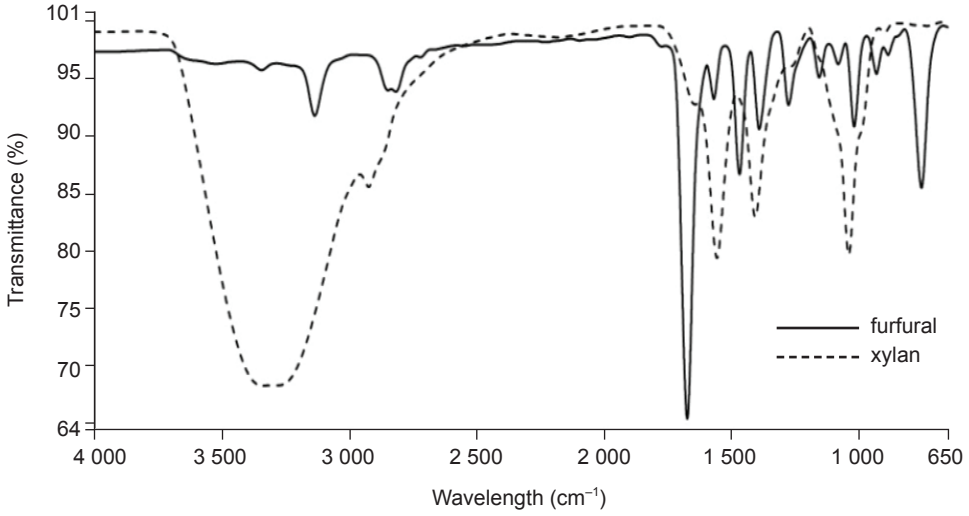


Figure 6. An overlay Fourier transform infrared (FTIR) spectrum of xylan and furfural from oil palm empty fruit bunches (OPEFB).

Characterisation of Furfural by ^{1}H-NMR Spectroscopy

The ^{1}H-NMR spectrum of furfural is shown in *Figure 7*. In this spectrum, both the individual groups and their component lines are well separated and thus the formal analysis is quite straight forward. The spectrum was separated by the coupling of the aldehyde proton to one of the ring protons. The aldehyde proton signal appears in normal low-field signal at δ 9.298 (1H) similar as reported by other researchers at δ 9.63-9.67 (Ismiyarto *et al.*, 2017; Bhaumik and Dhepe 2014).

The ring protons appeared as the three groups signal in region 6.56-7.72 ppm (3H) due to the asymmetric ring structures. On the basis of the chemical shift data, the low field signal would be expected to be that of proton 4. Further, spin-spin coupling constants are known to be very insensitive to substitution. For example, Richards and Schaeffer (1958) have shown that the coupling constant in a series of para-substituted benzenes vary by less than 10% over a whole range of substituent groups. This again supports the assignment of the low field signal in furfural to proton 4 at δ 7.72 (1H). However, the spin-spin coupling between the aldehyde proton and the proton giving the low field signal would normally be expected to be between the aldehyde proton and the nearest neighbouring proton in the ring. On this basis, the low field signal in region 7.38-7.39 ppm would be assigned to proton 2. The chemical shift data as proton 2 and proton 4 in furfural would be expected to be at lower field than hydrogen 3 due to the influence of the electronegative aldehyde group.

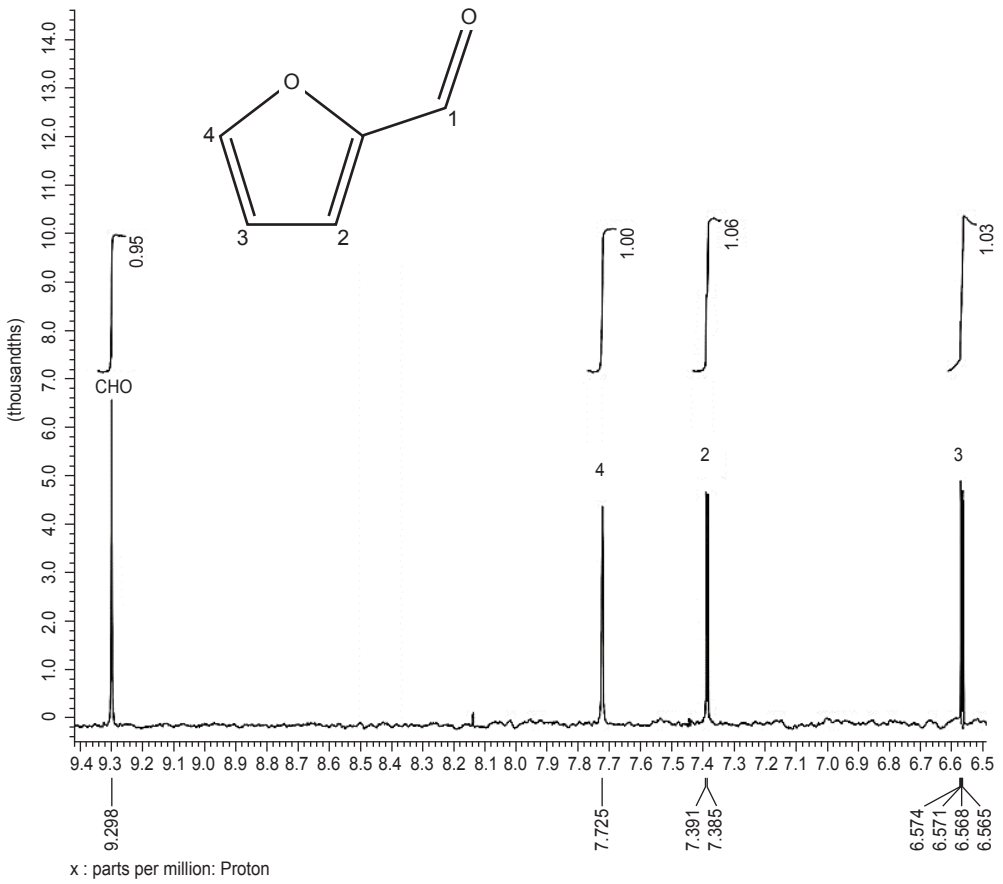


Figure 7. The Proton nuclear magnetic resonance (^{1}H-NMR) spectrum of furfural dissolved in deuterium oxide (D_2O).

Production of Furfural from Xylan

Hydrolysis using dilute acid is very complex, mainly because the substrate was in solid phase while the acid catalyst was in liquid phase. Results showed that the reaction parameters that influence yield of furfural production are acid concentrations, reaction time and presence of NaCl as promoter (*Table* 2). Furfural yield increased with increasing reaction time (up to 120 min) (*Figures 8a* and *8b*) and H_2SO_4 concentration (up to 15% v/v) (*Figures 8a* and *8b*).

The highest amount of furfural production was achived at 90 min reaction time in H_2SO_4 with or without the presence of NaCl. The amount of furfural produced were lowest at 30 min reaction time while the yield of furfural continued to increase until 90 min. From 90-120 min reaction times, yield of furfural produced were high, ranging from 2.99%-9.01%. Beyond 120 min, the furfural's yield started to decrease due to degradation to acetic acid. Gupta *et al.* (2009) and Mansilla *et al.* (1998) reported that the highest concentration of acid for steam distillation was performed with 15% H_2SO_4 as the increment to 20% did not appear to increase furfural yield. Any further increase in acid concentration caused the increase in inhibitor release, resulting in a decrease of furfural concentration in distillate.

Furfural yields were increased with addition of NaCl into reaction with H_2SO_4 compared to without NaCl (*Figure 8*). The highest yield of furfural produced in the presence of NaCl was 9.01% which was achieved in 15% H_2SO_4 and 90 min reaction time (*Figure 8b*). Meanwhile the highest yield of furfural produced without NaCl was about 6.63% in 15% H_2SO_4, and 120 min reaction time (*Figure 8a*). It was found that NaCl and H_2SO_4, which produces an inorganic salt $NaHSO_4$ greatly improved the yield of furfural (0.8%-2.38%) compared to reaction with only H_2SO_4. Similar finding was reported by Yazdizadeh *et al.*, (2016), whereby addition of NaCl into the reaction increased the yield of furfural by 1%-5%.

Furfural yield in this article was lower than a reported yield from oil palm pressed fibre of 17.34% (Riansa-Ngawong and Prasertsan, 2011). This is because only pentosans (xylose and arabinose) contribute a portion of the total composition of lignocellulose to the furfural production, compared to cellulose which is the largest fraction of lignocellulosic biomass. Therefore, the integrated strategies need to be introduced or the sole production of furfural from these residues would be wasteful, inefficient and uneconomic.

TABLE 2. AMOUNT OF FURFURAL PRODUCED IN DIFFERENT ACID CONCENTRATIONS AND WITH DIFFERENT REACTION TIMES

Acid concentration (H_2SO_4)		Without NaCl			With presence NaCl		
		Amount of furfural (%)					
		11%	13%	15%	11%	13%	15%
Reaction time (min)	30	0.42	0.87	3.27	3.28	6.83	7.80
	60	1.11	2.31	5.36	3.37	7.03	8.03
	90	2.80	5.83	6.07	3.70	7.70	9.01
	120	3.12	6.49	6.63	3.92	8.17	6.67
	150	2.72	5.67	4.70	2.88	5.99	5.52

Note: H_2SO_4 - sulphuric acid; NaCl - sodium chloride.

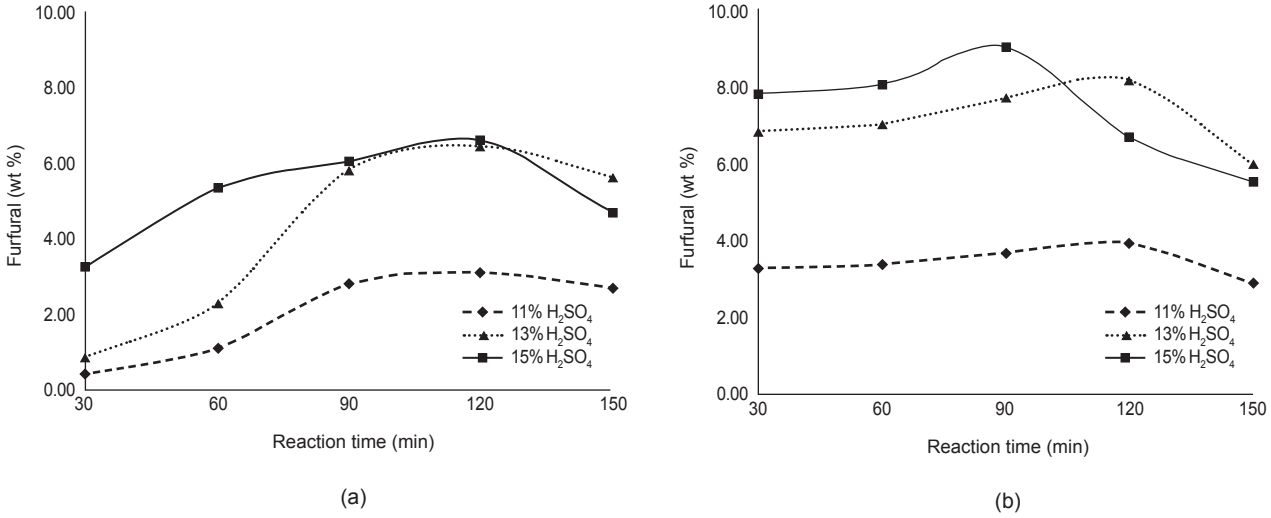


Figure 8. (a) Amount of furfural produced without sodium chloride (NaCl), and (b) with presence of NaCl at different reaction time in different sulphuric acid (H_2SO_4) concentration.

CONCLUSION

Furfural was successfully extracted from OPEFB by two-step process consisted of acid hydrolysis, followed by dehydration with highest yield of 0.90 ± 0.002 g litre^{-1} of dry OPEFB. Xylan was extracted from OPEFB was used as substrate for furfural production. The xylan and furfural extracted were analysed using FTIR spectroscopy for structural confirmations and found to be comparable to commercial standard. The highest yield of furfural produced was 9.01% which achieved at 90 min reaction time in 15% H_2SO_4 in the presence of NaCl. To be economically visible, the production of furfural should be intergrated with cellulose extraction as pentoses (xylose) is just a minor portion of OPEFB chemical composition.

ACKNOWLEDGEMENT

The authors wish to thank the Director-General of MPOB for his permission to publish this article.

REFERENCES

Aguilar, R; Ramirez, J A; Garrote, G and Vazquez, M (2002). Kinetic study of the acid hydrolysis of sugar cane bagasse. *J. Food Eng., 55(4)*: 309-318.

Alonso-Fagundez, N; Lopez Granados, M; Mariscal, R and Ojeda, M (2012). Selective conversion of furfural to maleic anhydride and furan with VOx/Al_2O_3 catalysts. *ChemSusChem., 5(10)*: 1984-1990.

ASTM (1978). Method of Test for Holocellulose in Wood-D1104-56. American Society for Testing and Materials (ASTM) International, West Conshohocken, Pennsylvania, USA.

Bamufleh, H S; Alhamed, Y A and Daous, M A (2013). Furfural from midribs of date-palm trees by sulfuric acid hydrolysis. *Ind. Crops Prod., 42*: 421-428.

Bhaumik, P and Dhepe, P L (2014). Exceptionally high yields of furfural from assorted raw biomass over solid acids. *RSC Adv., 4*: 26215-26221.

Cheung, S and Anderson, B (1996). Ethanol production from wastewater solids. *Water Environ. Technol., 8(5)*: 55-60.

Gamez, S; Gonzalez-Cabriales, J J; Ramirez, J A; Garrote, G and Vazquez, M (2006). Study of the hydrolysis of sugar cane bagasse using phosphoric acid. *J. Food Eng., 74*: 78-88.

García-Domínguez, M T; García-Domínguez, J C; Feria, M J; Gómez-Lozano, D M; López, F and Díaz, M J (2013). Furfural production from *Eucalyptus globulus*: Optimizing by using neural fuzzy models. *Chem. Eng. J., 221*: 185-192.

Gupta, R; Sharma, K K and Kuhad, R C (2009). Separate hydrolysis and fermentation (SHF) of Prosopis juliflora a wood substrate, for the production of cellulosic ethanol by Saccharomyces cerevisiae and Pichia stipitis – NCIM 3498. *Bioresour. Technol., 100(3)*: 1214-1220.

Herrera, A; Tellez-Luis, S J; Gonzalez-Cabriales, J J; Ramirez, J A and Vazquez, M (2004). Effect of the hydrochloric acid concentration on the hydrolysis of the sorghum at atmospheric pressure. *J. Food Eng., 63(1)*: 103-109.

Herrera, A; Tellez-Luis, S J; Ramirez, J A and Vazquez, M (2003). Production of xylose from sorghum straw using hydrochloric acid. *J. Cereal Sci., 37(3)*: 267-274.

Ismiyarto; Ngadiwiyana; Windarti, T; Purbowatiningrum, R S; Hapsari, M; Rafi'ah, F H; Suyanti and Haq, M S (2017). Synthesis of furfural from water hyacinth *(Eichornia croassipes). IOP Conf. Ser.: Mater. Sci. Eng., 172(1):* 012027.

Kamm, B G; Gruber, P R and Kamm, M (2006). *Biorefineries Industrial Processes and Products Status Quo and Future Directions*. Wiley–VCH Verlag GmbH Verlag and Co. KGaA, Weinheim, Germany.

Kushairi, A; Meilina, O; Balu, N; Elina, H; Mohd Noor Izuddin, Z B; Razmah, G; Vijaya, S; Shamala, S and Ghulam Kadir, A P (2019). Oil palm economic performance in Malaysia and R&D progress in 2018. *J. Oil Palm Res., 31(2)*: 165-194.

Lavarack, B P; Griffin, G J and Rodman, D (2002). The acid hydrolysis of sugar cane bagasse hemicelluloses to produce xylose, arabinose, glucose and other products. *Biomass Bioenerg., 23(5)*: 367-380.

Lenihan, P; Orozco, A; O'neill, E; Ahmad, M N M; Rooney, D W and Walker, G M (2010). Dilute acid hydrolysis of lignocelluloses biomass. *Chem. Eng. J., 156(2)*: 395-403.

Lin, K H; Huang, M H and Chang, A C C (2013). Liquid phase reforming of rice straw for furfural production. *Int. J. Hydro. Energy, 38(35)*: 15794.

Loi, C C; Boo, H C; Mohammed, A S and Ariffin, A A (2011). A high performance liquid chromatography method for determination of furfural in crude palm oil. *Food Chem., 128(1)*: 223-226.

Mansilla, H D; Baeza, J; Urzua, S; Maturana, G; Villasenor, J and Duran, N (1998). Acid catalyzed hydrolysis of rice hull: Evaluation of furfural production. *Bioresour. Technol., 66(3)*: 189-193.

Merlo, A B; Vetere, V; Ruggera, J F and Casella, M L (2009). Bimetallic PTSn catalyst for the selective hydrogenation of furfural to furfuryl alcohol in liquid-phase. *Catal. Commun., 10(13)*: 1665-1669.

Montane, D; Salvado, J; Torras, C and Farriol, X (2002). High-temperature dilute-acid hydrolysis of olive stones for furfural production. *Biomass Bioenerg., 22(4)*: 295-304.

Nimlos, M R; Qian, X; Davis, M; Himmel, M E and Johnson, D K (2006). Energetics of xylose decomposition as determined using quantum mechanics modeling. *J. Phys. Chem. A., 110(42)*: 11824-11838.

O'Brien, P (2006). Furfural chemicals and biofuels from agriculture. Report for the Rural Industries Research and Development Corporation. RIRDC Publication No. 06/127. Wondu Business and Technology Services. p. 1-28.

Rahman, S H A; Choudhury, J P and Ahmad, A L (2006). Production of xylose from oil palm empty fruit bunch fibre using sulfuric acid. *Biochem. Eng. J., 30(1)*: 97-103.

Riansa-Ngawong, W and Prasertsan, P (2010). Statistical approach for hemicellulose production from delignified palm pressed fibre and used as a bio-material for one-stage production of furfural. *Int. J. Biotechnol. Biochem., 6(7)*: 1101-1116.

Riansa-Ngawong, W and Prasertsan, P (2011). Optimization of furfural production from hemicellulose extracted from delignified palm pressed fibre using a two-stage process. *Carbohydr. Res., 346(1)*: 103-110.

Richards, R E and Schaeffer, T (1958). Nuclear resonance spectra of some fluorine derivatives of toluene and benzotrifluoride. *Trans. Faraday Soc., 54*: 1447-1453.

Rodriguez-Chong, A; Ramirez, J A; Garrote, G and Vazquez, M (2004). Hydrolysis of sugar cane bagasse using nitric acid: A kinetic assessment. *J. Food Eng., 61(2)*: 143-152.

Romero, I; Ruiz, E; Castro, E and Moya, M (2010). Acid hydrolysis of olive tree biomass. *Chem. Eng. Res. Des., 88(56)*: 633-640.

Sadaba, I; Ojeda, M; Mariscal, R; Fierro, J L G and Lopez Granados, M (2011). Catalytic and structural properties of co-precipitated Mg–Zr mixed oxides for furfural valorization via aqueous aldol condensation with acetone. *Appl. Catal. B Environ., 101(3-4)*: 638-648.

Sánchez, C; Serrano, L; Andres, M A and Labidi, J (2013). Furfural production from corn cobs autohydrolysis liquors by microwave technology. *Ind. Crops Prod., 42(1):* 513-519.

Sashikala, M and Ong, H K (2007). Identification of furfural synthesized from pentosan in rice husk. *J. Trop. Agric. Food Sci., 35(2)*: 305-312.

Shen, Y; Sun, J; Wang, B; Xu, F and Sun, R (2018). Catalytic approaches to the production of furfural and levulinates from lignocelluloses. *Biomass as Renewable Raw Material to Obtain Bioproducts of High-Tech Value*. Elsevier. p. 235-269.

Suxia, R; Haiyan, X; Jinling, Z; Shunqing, L; Xiaofeng, H and Tingzhou, L (2012). Furfural production from rice husk using sulfuric acid and a solid acid catalyst through a two-stage process. *Carbohydr. Res., 359*: 1-6.

Vazquez, M; Oliva, M; Tellez-Luis, S J and Ramirez, J A (2007). Hydrolysis of sorghum straw using phosphoric acid: Evaluation of furfural production. *Bioresour. Technol., 98(16)*: 3053-3060.

Wingren, A; Galbe, M and Zacchi, G (2003). Techno-economic evaluation of producing ethanol from softwood: Comparison of SSF and SHF and identification of bottlenecks. *Biotechnol. Prog., 19(4)*: 1109-1117.

Yat, S C; Berger, A and Shonnard, D R (2008). Kinetic characterization for dilute sulfuric acid hydrolysis of timber varieties and switch grass. *Bioresour. Technol., 99(9)*: 3855-3863.

Yazdizadeh, M; Jafari Nasr, M R and Safekordi, A (2016). A new catalyst for the production of furfural from bagasse. *RSC Adv., 6(61)*: 55778-55785.

Yemis, O and Mazza, G (2011). Acid-catalyzed conversion of xylose: Xylan and straw into furfural by microwave-assisted reaction. *Bioresour. Technol., 102(15)*: 7371-7378.

Zhang, H; Ping, Q; Zhanga, J and Li, N (2017). Determination of furfural and hydroxymethyl furfural by UV spectroscopy in ethanol-water hydrolysate of reed. *J. Bioresour. Bioprod., 2(4)*: 170-174.

Journal of Oil Palm Research Vol. 33 (3) September 2021 p. 482-492
DOI: https://doi.org/10.21894/jopr.2021.0002

DRYING OF OIL PALM LUMBER BY COMBINING FORCED-AIR DRYING AND MODIFIED SUPER-FAST DRYING METHODS

MUHAMMAD NADZIM, M N[1]; EDI, S B[1]; MOJTABA, S[2]; ZAIDON, A[1] and LEE, S H[3]*

ABSTRACT

In this study, super-fast drying (SFD) method was modified by adding forced-air drying (AFD) method in the beginning stage. The modified drying method is called modified super-fast drying (MSFD). This method eliminates the holing process in SFD and makes it more favourable by wood-based manufacturers. Inner and outer portion of oil palm lumber (OPL) were segregated and dried using both SFD and MSFD methods. The drying rate and drying defects of the OPL dried with AFD method were compared with conventional air drying (AD) method. The OPL dried with MSFD were compared with SFD in terms of drying defects, rate, physical and mechanical properties. The results revealed that AFD method exhibited significantly effective drying rate compared to AD by shorten the time needed to achieve desired moisture content (MC). On the other hand, MSFD were found to be able to reduce the outer OPL to 10% within 3 hr. The SFD method reported the same rate of drying performance. However, MSFD did not involve the unfavourable holing process as in SFD method. In addition, OPL dried using MSFD exhibited better mechanical and physical properties than SFD. The findings suggested the MSFD method is an enhanced method compared to SFD method.

Keywords: drying procedure, drying rate, forced-air drying, modification, oil palm lumber.

Received: 2 June 2020**; Accepted:** 27 October 2020; **Published online:** 7 January 2021.

INTRODUCTION

Declining in the supply of traditional high density hardwood has made the attention of manufacturer shifted to other resources, for example, oil palm wood (*Elaeis guineensis*) owing to its enlarging area of plantation in Malaysia. Existing abundantly in the country and readily availability has made oil palm trunk (OPT) a very promising materials for the sustainability of wood-based industry. The total oil palm planted area in Malaysia has seen a steadily increasing trend from the year of 2013-2019. In 2019, the total planted area of oil palm is recorded as 5.90 million hectares, an increase of 13.8% compared to the 5.23 million hectares recorded in the year of 2013 (MPOB, 2020; Mohammad Padzil *et al*., 2020). The main agri-based wastes that existing in the country are oil palm biomass (in the form of fronds, trunks and fibres), paddy straw, rice husk, banana residues, sugarcane bagasse, coconut husk and pineapple waste (Goh *et al*., 2010). Oil palm biomass is the main contributor among these agri-based wastes which accounted for 46 000 kilotonne in the form of fronds and 11 000 kilotonne in the form of trunks. Oil palm biomass has been utilised in producing a wide range of value-added products. Products manufactured using oil palm biomass include medium density fibreboard (Laemsak and Okuma, 2000), particleboard (Lee *et al*., 2015; 2018), fibre reinforce cement board (Zhang *et al*., 2020), fibre plastic composite (Liew *et al*., 2000), plywood (Onoja

[1] Faculty of Forestry and Environment, Universiti Putra Malaysia, 43400 UPM Serdang, Selangor, Malaysia.

[2] Department of Wood and Paper Science and Technology, Islamic Azad University of Chaloos, Noshahr-Chaloos Rd, 46615/397 Mazandaran Province, Iran.

[3] Institute of Tropical Forestry and Forest Products, Universiti Putra Malaysia, 43400 UPM Serdang, Selangor, Malaysia.

* *Corresponding author e-mail: lee_seng@upm.edu.my*

et al., 2018), laminated-veneer lumber (Nordin *et al*., 2004), biochar (Kong *et al*., 2014), concrete (Zawawi *et al*., 2020) and furniture (Ratnasingam and Ioras, 2010). Therefore, effective utilisation of these OPT could be beneficial to the wood-based industry in term of sustainability of raw materials supply.

Nevertheless, before oil palm wood (OPW) could be utilised effectively, drying of the materials is the utmost importance procedure. Minimisation of production costs could be achieved provided that an optimised drying process was adopted for woody materials. In addition, optimised drying process could also prevent productivity and quality lost. It was reported that moisture content (MC) is the highest at the core of oil palm stem and decreased when moving to the outer layer of the stem (Choo *et al*., 2011; 2013). The MC of the oil palm stem could reach to an astonishing 500% as reported by previous studies (Lim and Khoo, 1986; Bakar *et al*., 2008). Green MC of up to 300%-500% and density of 200-700 kg m^{-3} (Anis *et al*., 2007) can be found mainly from the trunk. High MC found in oil palm lumbers (OPL) caused the drying process to be very time-consuming and higher energy is therefore needed to completely dried the lumber. In addition, the variation in MC across the oil palm stem make the drying of OPL have to be adjusted specifically according to lumbers obtained from different parts of the OPT. To date, an optimum drying schedule is yet to be developed for OPL. Thirty to 35 days is needed for drying OPL by using conventional drying method in kiln drier and resulted in many drying defects.

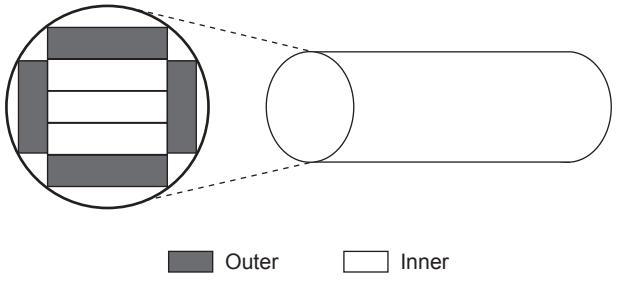
In order to resolve this matter, a drying method for OPL, called Oil Palm Lumber Drying Method and System Thereof, has been developed by Bakar *et al*. (2016). The concept of the method was to increase the evaporation rate of water from the material by using holing technique on the OPL. This method had successfully reduced the drying time of OPL from 30-35 days to approximately 3 hr. The method is called super-fast drying (SFD). The method involved drilling holes, or holing, on the OPL surface to accelerate the moisture reduction, followed by applying light compression to produce defect free board. This method requires high precision on the intermediate MC and therefore the drying process for inner and outer part of OPL are different. The inner portion of OPL requires two higher compressions cycle while the outer portion of OPL only undergoes one cycle with lower compression. Nevertheless, despite its effectiveness in drying OPL in a shorter time, the unattractive holes on the surface has repelled the manufacturers from using this OPL. To make the method more attractive to the wood industry, the drawback mentioned above needs to be solved in order to produce laminated products with two clear surfaces.

A preliminary study demonstrated that the OPL can be dried using SFD without holes provided the initial MC of the green OPW is lowered to less than 200%. Therefore, in this study, the initial MC of the outer and inner OPL were reduced by using forced-air drying (AFD) method prior to dried using SFD method. The new method, a combination of AFD and SFD methods, are called modified super-fast drying (MSFD) method. The MSFD method consist of two stages. The first stage involving the drying of OPL to intermediate MC of 60%, 80% and 100% using AFD method. The second stage involve the drying of OPL from intermediate MC to final target MC of <10% using SFD method. Using the MSFD method, the holing process in SFD method could be eliminated. Nevertheless, the drying rate and drying defects of the OPL using AFD method are still remained unknown. In addition, physical and mechanical properties of the OPL dried using MSFD in comparison to the conventional ai-dried method as well as SFD method have yet been documented. Therefore, the objectives of this study were to identify an optimum drying method without holing process for inner and outer OPL. Conventional air drying (AD) method was compared with the AFD method in terms of drying time, rate and defects.

MATERIALS AND METHOD

Material Preparation

Three 25-years old OPT with length of 4-5 m were purchased from a private company in Bandar Saujana Putra, Selangor, Malaysia. The OPT were cut into 200 cm in length and were sawn into planks of two different thicknesses, namely 3 cm and 5 cm, using modified cant sawing as shown in *Figure 1*. Modified cant sawing is a simpler method compared to polygon sawing and able to make sure a proper separation of inner and outer parts of OPL with higher recovery. The MC of the OPL were determined.



Source: Bakar *et al*. (2006).

Figure 1. Segregation of outer and inner portion of oil palm lumber using modified cant sawing.

Segregation Oil Palm Lumber (OPL)

Prior to drying, OPL were segregated based on the green MC. The OPL with green MC above 200% were regarded as inner part while OPL with green MC below 200% were regarded as outer part (Bakar *et al*., 2016). The lumbers were sawn into two dimensions with different thicknesses, namely 3 cm x 15 cm x 200 cm and 5 cm x 15 cm x 200 cm (thickness x width x length) prior to drying process.

Drying Process

Air drying (AD) and forced-air drying (AFD) of OPL. The OPL samples were dried using AD and AFD method. The set-up of the AD method is shown in *Figure 2*. The set-up of the AFD method is shown in *Figure 3*. A fan was used to charge a direct air flow towards the OPL samples. The velocity of the air slow was set between 6-11 km hr^{-1}, measured by a thermos-anemometer. The OPL stacks dried with both AD and AFD method were consisted of two types of samples with different dimensions, namely 15 cm width x 150 cm length x 3 cm or 5 cm thick and 15 cm width x 40 cm length x 3 cm or 5 cm thick. The former was denoted as large samples while the latter were denoted as small samples.

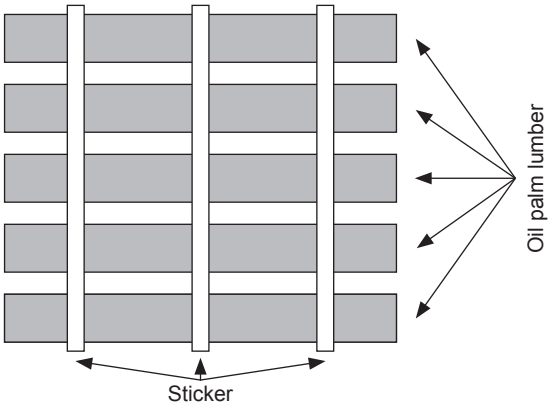


Figure 2. Top view diagram of air drying stacking of oil palm lumber.

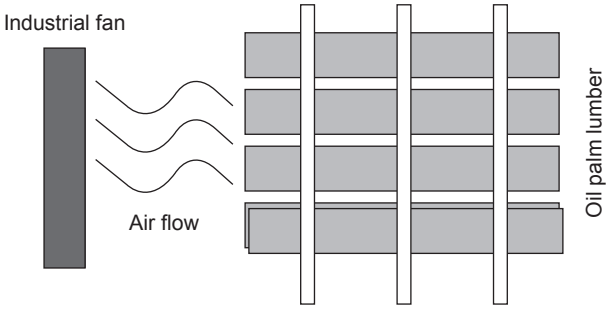


Figure 3. Top view diagram of forced-air drying stacking of oil palm lumber.

Super-fast drying (SFD) of OPL. *Figure 4* shows the drying procedure for inner and outer OPL, respectively. Both inner and outer plank of OPL were undergone holing process prior to Direct Contact Drying (DCD) processing. For outer part, the OPL were subjected to DCD with a compression of 20% at 180°C for 40 min and followed by a High Temperature Drying (HTD) at 100 ± 3°C for 3 hr. As for inner part, the inner OPL were subjected to two cycles of DCD instead of one as in outer OPL. The inner OPL were firstly subjected to 180°C for 40 min with a compression of 20% and then an additional cycle at the same temperature and compression for another 40 min before dried using HTD at 100 ± 3°C for 3 hr.

Modified super-fast drying (MSFD) of OPL. The MSFD method includes AFD in preliminary drying of the OPL where the holing process as in SFD method were omitted. The MSFD method consisted of three phases, namely, AFD process, DCD and HTD as shown in *Figure 5*. The OPL were underwent a preliminary drying of OPL using AFD method to achieve intermediate MC (100%, 80% and 60%). Then the OPL were subject to DCD method with a compression of 20% at 180°C for 40 min and followed by the HTD method at 100 ± 3°C for 3 hr.

Properties Evaluation

Moisture content (MC) and drying rate of OPL. The MC and drying rate of samples underwent AD, AFD and MSFD processes were recorded daily. The weight of the small samples was taken and recorded every day for the determination of MC and drying rate. In addition to that, the drying defects of the OPL under drying were recorded daily.

Drying defects of dried OPL. The drying defect of the AD, AFD and MSFD processes were recorded daily. The type of defects such as mechanical and physical defects were observed and recorded. Types of defects could include honey combing, warping and cracking as well as occurrence of stain and fungi.

Physical and mechanical properties of dried OPL. Physical and mechanical properties of the OPT dried using AD, SFD, MSFD at intermediate MC of 60%, 80% and 100% (MSFD 60, MSFD 80 and MSFD 100) were tested. The bending strength, modulus of rupture (MOR) and modulus of elasticity (MOE), of the lumbers were tested according to the procedures stipulated in EN 310:1993. As the bending strength of the samples are highly dependent on the final board density (Yano, 2001; Yano *et al*., 2000; 1997), specific MOR and specific MOE were measured based on Equation (1) and

(2) to eliminate the effects of density (Garcia *et al*., 2005; Xing *et al*., 2007).

$$SMOR\ (Nmm^{-2}/g\ cm^{-3}) = \frac{MOR}{Density} \quad (1)$$

$$SMOE\ (Nmm^{-2}/g\ cm^{-3}) = \frac{MOE}{Density} \quad (2)$$

As for physical properties, water absorption (WA) and thickness swelling (TS) were evaluated in accordance with EN 317:1993. Samples with dimension of 50 mm width and 50 mm length were soaked into water for 24 hr. The TS and WA of the samples were expressed as a percentage increment of the initial thickness and weight of the sample after 24 hr immersion in the water.

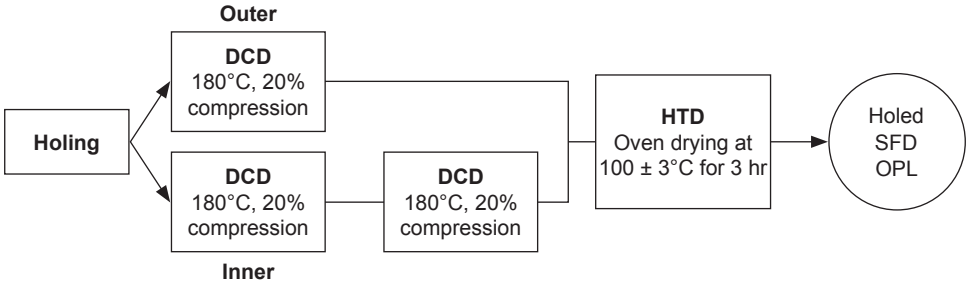
RESULT AND DISCUSSION

Drying Time of AFD and AD

Figure 6 illustrates the drying time of inner OPL using both AFD and AD. Inner parts of OPL with 3 cm and 5 cm thickness exhibits different drying times. Using AFD method, inner part with 3 cm thickness achieves MC of 100%, 80% and 60% at Days 8, 9 and 11, respectively. Meanwhile, 5 cm inner part attains intermediate MC of 100%, 80% and 60% at Days 11, 14 and 16, respectively. As for AD method, 3 cm inner part and 5 cm inner part achieve MC of 100% at Days 21 and 20, respectively and both achieve MC of 80% at Day 23.

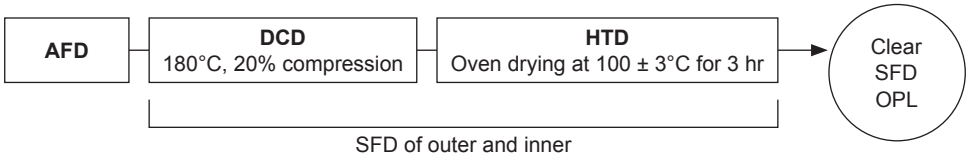
Figure 7 illustrates the drying time of OPL outer parts using both AFD and AD. Due to the fact that outer part has lower initial MC, it achieves targeted MC faster than that of the inner OPL for both AFD and AD method. Six, eight and 10 days were required for both the 3 cm and 5 cm outer OPL to be dried to 100%, 80% and 60%, respectively, using AFD method. As for AD method, the OPL with 5 cm thickness has a green MC of 150% and the 3 cm has lower green MC of 129%. A total of 5 cm OPL attain the targeted MC of 100% at Day 9 while the 3 cm OPL reach at Day 6. At Day 12, the MC of the 5 cm OPL reaches 80% and 60% at Day 18. Meanwhile, 3 cm OPL reaches MC of 80% and 60% at Days 9 and 16, respectively.

The findings were in agreement with Pfeiffer (1957) who recorded around 50% reduction in MC in lumber West Coast hemlock and Douglas fir after a two-weeks drying period using propeller fans. The OPL dried using AFD generally require shorter times to achieve targeted MC. Air flow is needed to transport the moisture away from the OPL. A constant air flow in AFD method gives the surrounding a uniform relative humidity and temperature (Eckelman and Baker, 1976). Equilibrium MC between surroundings and OPL could be achieved in an accelerated manner and making the drying process more efficient.



Note: DCD - direct contact drying; HTD - high temperature drying; OPL - oil palm lumber.

Figure 4. Procedure for super-fast drying (SFD) method.



Note: AFD - forced-air drying; DCD - direct contact drying; HTD - high temperature drying; SFD - super-fast drying; OPL - oil palm lumber.

Figure 5. Procedure for modified super-fast drying method.

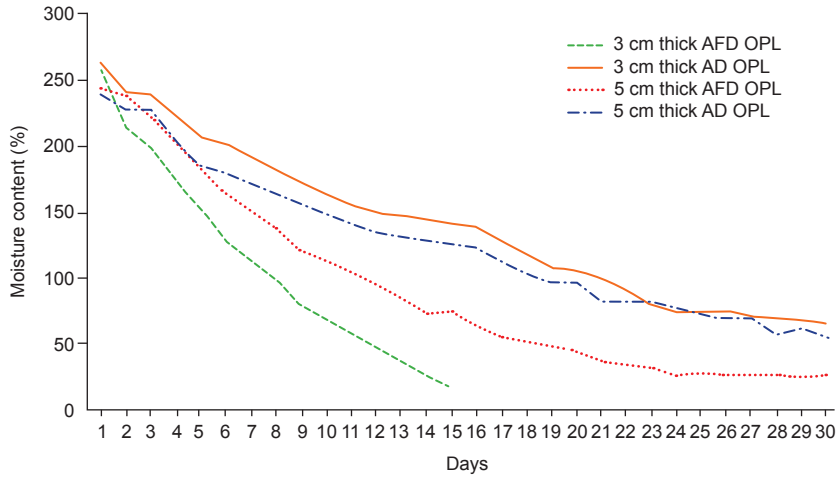


Figure 6. Moisture content reduction of inner oil palm lumber (OPL) dried using air drying (AD) and forced-air drying (AFD) method.

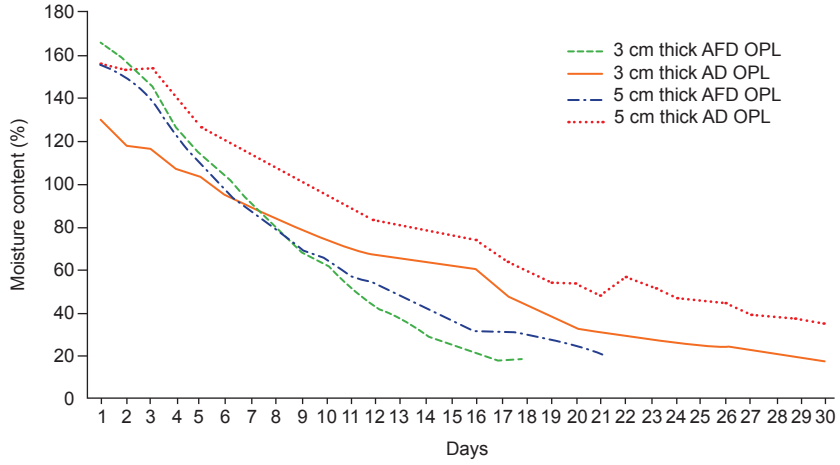


Figure 7. Moisture content reduction of outer oil palm lumber (OPL) dried using air drying (AD) and forced-air drying (AFD) method.

Drying Rate of AFD and AD

The drying rate of the AFD and AD methods are illustrated in *Figure 8*. It can be seen from the figure that AFD process accelerate the drying process significantly. The highest drying rate of 15.18% was recorded in 3 cm inner OPL when AFD was used. Thickness plays a significant role on the AFD method as 5 cm OPL samples generally have lower drying rate than that of the 3 cm OPL. In comparison to AFD, AD resulted in lower drying rate and the influence of thickness is not as significant as AFD. This observation might be due to the fact that AD is an uncontrolled drying where the moisture gradient in the samples is completely dependent on the temperature and relative humidity of the surroundings (Tschernitz and Simpson, 1979).

Table 1 summarises the drying time required for AFD and AD method to achieve target MC of 100%, 80% and 60%. Using AFD method, inner OPL with 3 cm and 5 cm thickness could attain target MC of 60% at Days 11 and 16, respectively. As for outer OPL, it required 10 days for both 3 cm and 5 cm OPL to achieve target MC of 60%. In comparison to the AD method, AFD greatly reduced the drying time needed. It would take 28 and 29 days for 3 cm and 5 cm inner OPL to achieve target MC of 60% using AD method. More than 16 days is needed for outer OPL to achieve 60% MC. In addition, AFD method also helps to decrease the drying defect when compared with AD method. Although some minor defects were also detected in AFD method, it is however, could be overcame during the SFD process where pressure was to be applied to the OPL.

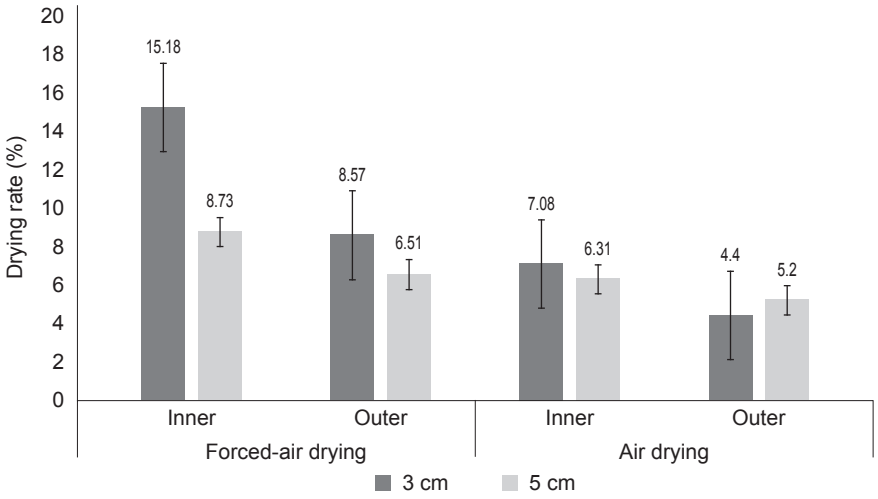


Figure 8. Drying rate of forced-air drying and air drying methods at different portions and thickness of oil palm lumber.

TABLE 1. DRYING TIME REQUIRED FOR FORCED-AIR DRYING AND AIR DRYING METHOD TO ACHIEVE TARGET MOISTURE CONTENT OF 100%, 80% AND 60% FOR THE INNER AND OUTER PORTIONS OF OIL PALM LUMBER (OPL)

Treatments	Target moisture content (days)		
	100%	80%	60%
Forced-air drying			
Inner OPL			
3 cm	8	9	11
5 cm	11	14	16
Outer OPL			
3 cm	6	8	10
5 cm	6	8	10
Air drying			
Inner OPL			
3 cm	21	23	28
5 cm	20	23	29
Outer OPL			
3 cm	6	9	16
5 cm	9	12	18



Figure 9. Warping of inner oil palm lumber.



Figure 10. Cell wall collapse of inner oil palm lumber.

Drying Defect of AFD and AD of OPL

Drying defects could be observed from inner OPL on Day 3 using AFD method. However, the drying defects among samples were relatively low as only 9% of the total defected samples were identified. On the contrary, no defect was found on the outer OPL. From *Figures 9* and *10*, one can see that inner OPL experienced warping and cell wall collapse. Black moss was found on the surface of the OPL where these air-borne fungal spores are quite fine (≤2.5 μm) and settled on the OPL surface during the drying process.

On the other hand, AD method exhibited different observation compared to that of AFD method. Sap stain and fungal decay started to occur at Day 3 at the end butt and various places for both inner and outer OPL (*Figure 11*). The aforementioned defects were found to be more affected inner OPL than outer OPL. After a week, mechanical defect such as cell wall collapse started to be observed. At the end of the process, all the OPL samples were fully covered by the moss and unusable. These

findings are in agreement with Anis *et al*. (2016) who concluded that OPL has a low drying recovery due to high green MC and wide density variation.

Drying Rate of MSFD from Different Initial MC

Figures 12 and *13* exhibits the moisture reduction of outer and inner portion OPL dried using MSFD from three different intermediate MC, namely 100%, 80% and 60%. For outer OPL, it can be observed that MC are able to achieve less than 10% within 3 hr of drying. On the other hand, inner OPL with intermediate MC of 80% and 60% could be dried to less than 10% within 3 hr while inner OPL with intermediate MC of 100% required duration longer than 3 hr to reach MC of less than 10%. The MSFD method is a combination of DCD process and HTD process. The DCD process has facilitated the drying process by reducing the intermediate MC to more than half. Compression level of 20% applied during DCD has created some micro-cracks on the surface of the OPL. These micro-cracks accelerated the water evaporation process and making the entire drying process faster without compromising the quality of OPL. The HTD process were then ensued to bring down the MC of the OPL to less than 10%. As a result, both inner and outer OPL with intermediate MC of 100%, 80% and 60% was able to achieve MC less than 10% within 3-4 hr.

Drying Defect of MSFD from Different Initial MC

Visual appearance of the OPL dried with SFD and MFSD methods are shown in *Figures 14* and *15*. From *Figure 14*, one can see that no visible drying defect was detected during the drying process for both inner and outer OPL. In addition, no spring back or physical alteration was observed from the samples.

Performance of Dried OPL

Physical properties of MSFD of OPL. In this section, the properties of the OPL samples dried with MSFD method at intermediate MC of 60%, 80% and 100% (denoted as MSFD 60, MSFD 80 and MSFD 100) were compared with the samples dried using SFD and AD. The TS and WA of both inner and outer OPL dried using AD, SFD and MSFD methods are shown in *Table 2*.

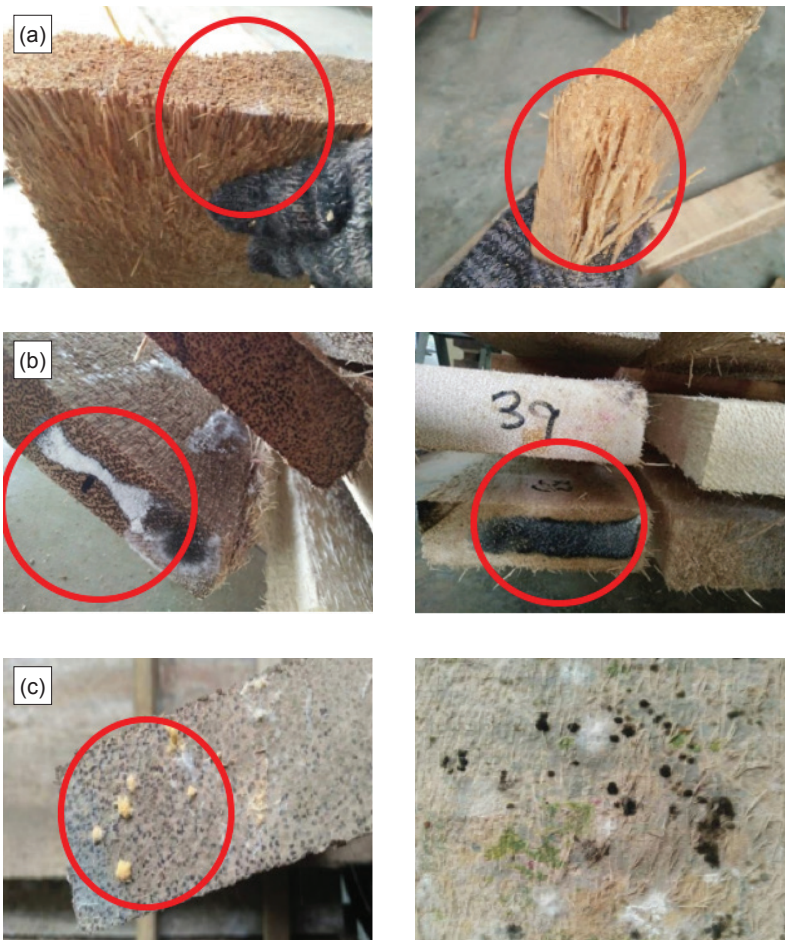
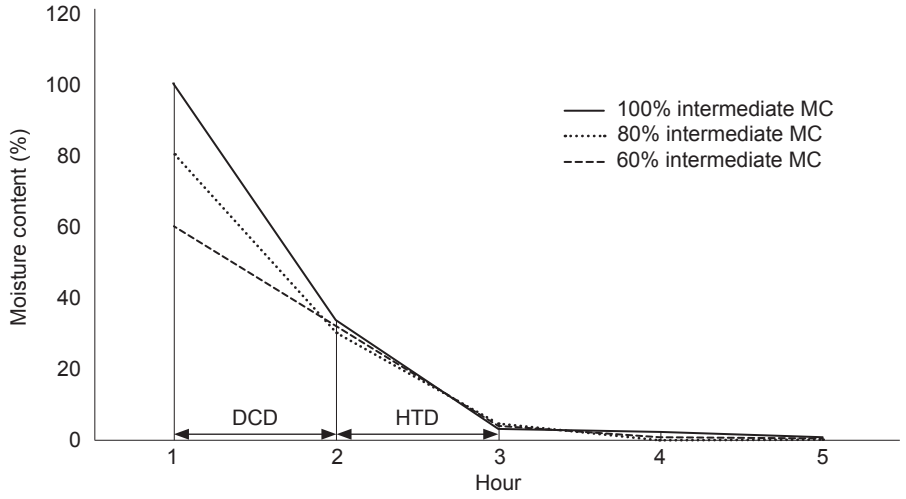
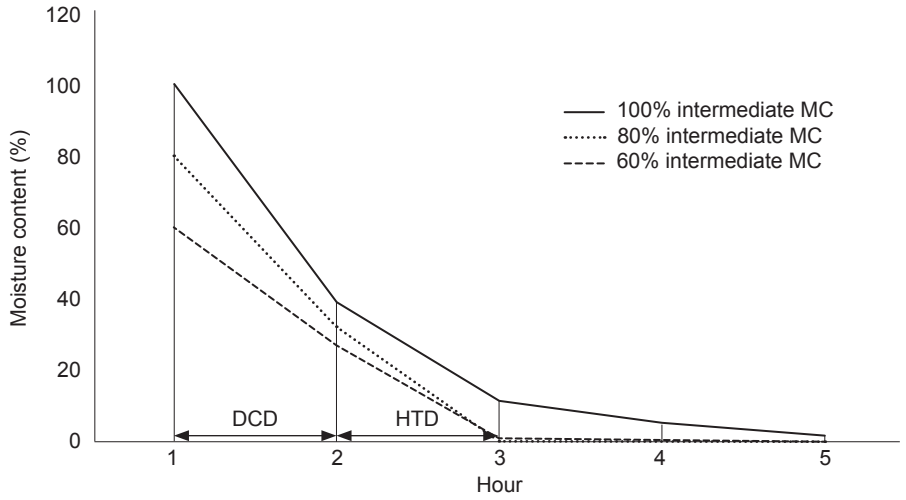


Figure 11. Types of drying defect of oil palm lumber dried with air drying method (a) cell wall collapse, (b) sap stain, and (c) fungal decay.



Note: DCD - direct contact drying; HTD - high temperature drying.

Figure 12. Moisture reduction of outer oil palm lumber using modified super-fast drying from intermediate moisture content (MC) of 100%, 80% and 60%.



Note: DCD - direct contact drying; HTD - high temperature drying.

Figure 13. Moisture reduction of inner oil palm lumber using modified super-fast drying from intermediate moisture content (MC) of 100%, 80% and 60%.



Figure 14. Visual appearance of oil palm lumber samples dried with super-fast drying method.



Figure 15. Visual appearance of oil palm lumber samples dried with modified super-fast drying method (top – outer portion; bottom – inner portion).

Inner OPL dried using AD method has TS and WA of 2.33% and 97.96%, respectively. However, when the inner OPL was dried using SFD, increment in TS (10.42%) and WA (141.10%) was recorded. This phenomenon could be attributed to the holes in the samples dried using SFD method. In order to remove excess MC, an additional step of holing was added to the SFD method. The existence of holes increased the surface area and enables more water to penetrate into the samples and resulted in higher TS and WA. As for MSFD method, samples that dried at intermediate MC of 100% and 80% exhibited lower TS compared to that of SFD but still significantly higher than that of the AD method. However, it is interesting to note that inner OPL samples that dried with MSFD method at intermediate MC of 60% displayed comparable TS value with AD method. The MSFD method has eliminated the holing process as in SFD method and therefore the surface area remained the same as original OPL samples. Nevertheless, pressure was applied to the samples during drying using MSFD method. Therefore, springback might occur during the water immersion and resulted in higher TS compared to that of AD method. Similar trend was also observed for outer OPL.

Mechanical properties of MSFD of OPL. *Tables 3* and *4* show the specific modulus of rupture (SMOR) and specific modulus of elasticity (SMOE) for inner and outer OPL, respectively. For inner OPL, the highest SMOR was recorded in the samples dried with MSFD at intermediate MC of 60%. Air-dried OPL has SMOR and SMOE of 53.73 MPa and 5900.88 MPa, respectively. Meanwhile, SFD samples was recorded to have SMOR of 55.45 MPa and SMOE of 6383 MPa. On the other hand, the highest SMOR was found in the samples dried with MSFD at intermediate MC of 100% for outer OPL. The OPL samples dried using MSFD involved a compression step during DCD. Therefore, the higher SMOR and SMOE could be attributed to the effect of densification. Hamzah *et al*. (2017) reported that the compression process is able to increase the density of the wood which in turn led to improved mechanical properties.

TABLE 2. PHYSICAL PROPERTIES OF OIL PALM LUMBER (OPL) DRIED USING SUPER-FAST DRYING (SFD), MODIFIED SUPER-FAST DRYING (MSFD) AT DIFFERENT PERCENTAGES OF MOISTURE CONTENT (MC) AND AIR DRYING (AD) METHOD

Treatments	Inner OPL		Outer OPL	
	Thickness swelling (%)	Water absorption (%)	Thickness swelling (%)	Water absorption (%)
SFD	10.42 ± 0.62a	141.10 ± 18.49ab	22.61 ± 2.91a	151.69 ± 32.99a
MSFD at 100% MC	8.66 ± 1.90ab	183.05 ± 57.87a	8.72.38 ± 4.07b	88.66 ± 21.39bc
MSFD at 80% MC	7.12 ± 3.02b	136.29 ± 41.10ab	6.46 ± 1.78b	95.46 ± 27.89bc
MSFD at 60% MC	2.73 ± 1.39c	164.10 ± 79.18a	6.14 ± 2.71b	102.79 ± 17.79b
AD	2.33 ± 1.50c	97.96 ± 25.87b	1.78 ± 0.71c	73.25 ± 23.53c

Note: Numbers after ± are standard deviation values; Means followed by the same letter in the same column are not significantly different at P≤0.05.

TABLE 3. SPECIFIC MODULUS OF RUPTURE (SMOR) AND SPECIFIC MODULUS OF ELASTICITY (SMOE) FOR INNER OIL PALM LUMBER (OPL) DRIED USING SUPER-FAST DRYING (SFD), MODIFIED SUPER-FAST DRYING (MSFD) AT DIFFERENT MOISTURE CONTENT (MC) AND AIR DRYING (AD) METHOD

Treatments	Density	SMOR	SMOE
SFD	0.51 ± 0.27a	55.45 ± 28.17a	6 383.33 ± 2 744.32a
MSFD 100% MC	0.24 ± 0.02b	48.45 ± 14.23a	4 906 ± 1 371.02a
MSFD 80% MC	0.25 ± 0.01b	41.71 ± 10.39a	4 736.92 ± 1 538.47a
MSFD 60% MC	0.26 ± 0.02b	60.55 ± 10.66a	6 376.47 ± 1 063.01a
AD	0.29 ± 0.02b	53.73 ± 8.89a	5 900.88 ± 3 126.95a

Note: Numbers after ± are standard deviation values; Means followed by the same letter in the same column are not significantly different at P≤0.05.

TABLE 4. SPECIFIC MODULUS OF RUPTURE (SMOR) AND SPECIFIC MODULUS OF ELASTICITY (SMOE) FOR OUTER OIL PALM LUMBER (OPL) DRIED USING SUPER-FAST DRYING (SFD), MODIFIED SUPER-FAST DRYING (MSFD) AT DIFFERENT MOISTURE CONTENT (MC) AND AIR DRYING (AD) METHOD

Treatments	Density	SMOR	SMOE
SFD	0.43 ± 0.06ab	29.63 ± 4.07c	4 833.09 ± 1 282.84b
MSFD 100% MC	0.45 ± 0.09a	72.38 ± 24.81a	8 450.27 ± 4 192.02a
MSFD 80% MC	0.42 ± 0.07ab	54.71 ± 13.71b	7 056.25 ± 1 306.69ab
MSFD 60% MC	0.38 ± 0.06ab	63.07 ± 11.67ab	7 919.40 ± 1 641.98a
AD	0.34 ± 0.04b	49.26 ± 8.09b	6 271.67 ± 1 323.46ab

Note: Numbers after ± are standard deviation values; Means followed by the same letter in the same column are not significantly different at P≤0.05.

CONCLUSION

Outer and inner OPL were dried using SFD and MSFD. The following conclusions could be drawn based on the current findings:

i) Dissimilar to SFD, MSFD involves AFD at the beginning stage of drying instead of conventional AD method. The AFD method exhibited significantly effective drying rate compared to that of the AD method. Using AFD method, inner OPL achieved MC of 80% in nine days while AD method required 23 days for the inner OPL to attain MC of 80%. In the case of outer OPL, eight days are needed for the samples to be dried to around 80% MC. However, drying to 80% MC using AD method would require 12 days.

ii) MSFD were found to be able to reduce the outer OPL with intermediate MC of 100%, 80% and 60% to less than 10% within 3 hr. As for inner OPL, OPL with intermediate MC of 80% and 60% could be dried to less than 10% within 3 hr while inner OPL with intermediate MC of 100% required longer duration, which is 3-4 hr to reach MC of less than 10%.

iii) In term of physical properties, due to the application of pressure during drying and the springback effect after drying, OPL samples that dried using MSFD displayed higher TS and WA compared to samples dried using AD method. However, due to the inexistence of holes, MSFD has lower exposure area and consequently lower TS and WA in comparison to SFD method.

iv) In term of mechanical properties, inner OPL dried using MSFD at intermediate MC of 60% has the highest SMOR. Meanwhile, outer OPL dried using MSFD at intermediate MC of 100% exhibited the highest SMOR and SMOE.

The findings suggested the MSFD method is an enhanced method compared to SFD method. Without the existence of holes in MSFD method, the dried OPL could be utilised for wider applications.

ACKNOWLEDGEMENT

The authors wish to thank for the financial support provided by Geran Universiti Putra Malaysia (GP) GP/2018/9650000 and Higher Institutions' Centre of Excellence (HICoE), Project Code: UPM/INTROP/100-13/9/3/HICoE/6369107.

REFERENCES

Anis, M; Kamarudin, H and Lim, W S (2007). Challenges in drying of oil palm wood. *Proc. of the 2007 PIPOC International Palm Oil Congress - Empowering Change*. 26-30 August 2007. Kuala Lumpur.

Anis, M; Shamsudin, N A; Muhammad, H and Aziz, A A (2016). Recovery of oil palm lumber production. *Palm Oil Developments*, *64*: 7-10.

Bakar, E S; Febrianto, F; Wahyudi, I and Ashaari, Z (2006). Polygon sawing: An optimum sawing pattern for oil palm stems. *J. Biol. Sci.*, *6(4)*: 744-749.

Bakar, E S; Mohd Hamami, S and H'ng, P S (2008). *A Challenge from the Perspective of Functional Wood Anatomy*. Universiti Putra Malaysia Press, Serdang.

Bakar, E S; Soltani, M; Paridah, M T and Choo, A C Y (2016). Oil palm lumber drying method and system thereof (PI2016702162).

Choo, A C Y; Paridah, M T; Karimi, A; Bakar, E S; Abdan, K; Ibrahim, A and Loh, Y F (2011). Density and humidity gradients in veneers of oil palm stems. *Eur. J. Wood Prod.*, *69(3)*: 501-503.

Choo, A C Y; Paridah, M T; Karimi, A; Bakar, E S; Abdan, K; Ibrahim, A and Balkis, F A B (2013). Study on the longitudinal permeability of oil palm wood. *Ind. Eng. Chem. Res.*, *52(27)*: 9405-9410.

Eckelman, C A and Baker, J L (1976). Heat and air requirements in the kiln drying of wood. https://www.agriculture.purdue.edu/fnr/faculty/eckelman/documents/RB-933.pdf, accessed on 18 October 2020.

Garcia, R A; Cloutier, A and Riedl, B (2005). Dimension stability of MDF panel produced from fibers treated with maleated polypropylene wax. *Wood Sci. Technol.*, *39(8)*: 630-650.

Goh, C S; Tan, K T; Lee, K T and Bhatia, S (2010). Bio-ethanol from lignocellulose: Status, perspectives and challenges in Malaysia. *Bioresour. Technol.*, *101(13)*: 4834-4841.

Hamzah, N N; Bakar, E S; Zaidon, A and Lee, S H (2017). Assessment of oil palm wood quality improvement through integrated treatment process as function of sawing pattern and slab thickness. *J. Oil Palm Res., 29(3)*: 366-372.

Laemsak, N and Okuma, M (2000). Development of boards made from oil palm frond II. Properties of

binderless boards from steam-exploded fibres of oil palm frond. *J. Wood Sci.*, *46*: 322-336.

Lee, S H; Ashaari, Z; Lum, W C; H'ng, P S; Peng, T L; Chow, M J; Chai, E W and Chin, K L (2015). Properties of particleboard with oil palm trunk as core layer in comparison to three-layer rubberwood particleboard. *J. Oil Palm Res.*, *27(1)*: 67-74.

Lee, S H; Ashaari, Z; Ang, A F; Halip, J A; Lum, W C; Dahali, R and Halis, R (2018). Effects of two-step post heat-treatment in palm oil on the properties of oil palm trunk particleboard. *Ind. Crops Prod.*, *116*: 249-258.

Liew, K C; Jalaluddin, H; Paridah, M T; Zaman, M D K and Nor, M Y M (2000). Properties of oil palm frond-polypropylene composite. *Proc. of the Utilization of Oil Palm Tree-oil Palm Biomass: Opportunities and Challenges in Commercial Exploitation*. 9-11 May 2000. Selangor, Malaysia. p. 116-118.

Kong, S H; Loh, S K; Bachmann, R T; Rahim, S A and Salimon J (2014). Biochar from oil palm biomass: A review of its potential and challenges. *Renew. Sust. Energ. Rev.*, *39*: 729-739.

Lim, S C and Khoo, K C (1986). Characteristics of oil palm trunk and its potential utilization. *Malaysian For.*, *49*: 3-22.

MPOB (2020). Oil palm planted area 2013-2019. http://bepi.mpob.gov.my/images/area/2019/area_summary.pdf, accessed on 18 October 2020.

Mohammad Padzil, F N; Lee, S H; Ainun, Z M A; Lee, C H and Abdullah, L C (2020). Potential of oil palm empty fruit bunch resources in nanocellulose hydrogel production for versatile applications: A review. *Materials*, *13(5)*: 1245.

Nordin, K; Ariff Jamaludin, M; Ahmad, M; Samsi, H W; Hamid Salleh, A and Jalaludin, Z (2004). Minimizing the environmental burden of oil palm trunk residues through the development of laminated veneer lumber products. *Manag. Environ. Qual.*, *15(5)*: 484-490.

Onoja, E; Chandren, S; Abdul Razak, F I; Mahat, N A and Abdul Wahab, R (2018). Oil palm (*Elaeis guineensis*) biomass in Malaysia: The present and future prospect. *Waste Biomass Valor.*, *10(28)*: 2099-2117.

Pfeiffer, J R (1957). Air drying lumber with forced air circulation. https://ir.library.oregonstate.edu/downloads/12579t21x, accessed on 18 October 2020.

Ratnasingam, J and Ioras, F (2010). Static and fatigue strength of oil palm wood used in furniture. *J. Appl. Sci.*, *10(11)*: 986-990.

Tschernitz, J L and Simpson, W T (1979). Solar-heated, forced-air, lumber dryer for tropical latitudes. *Sol. Energy*, *22*: 563-566.

Xing, C; Zhang, S Y; Deng, J and Wang, S (2007). Investigation of the effect of bark fibre as core material and its resin content on three layer MDF performance by surface methodology. *Wood Sci. Technol.*, *41(7)*: 585-595.

Yano, H (2001). Potential strength for resin impregnated compressed wood. *J. Mater. Sci. Lett.*, *20(12)*: 1127-1129.

Yano, H; Hirose, A and Inaba, S (1997). High strength wood based material. *J. Mater. Sci. Lett.*, *16*: 1906-1909.

Yano, H; Mori, K; Collins, P J and Yazaki, Y (2000). Effects of element size and orientation in the production of high strength resin impregnated wood based materials. *Holzforschung*, *54*: 443-447.

Zawawi, M N A A; Muthusam, K; Majeed, A P P A; Musa, R M and Budiea, A M A (2020). Mechanical properties of oil palm waste lightweight aggregate concrete with fly ash as fine aggregate replacement. *J. Build. Eng.*, *27*: 100924.

Zhang, J; Li, D and Wang, Y (2020). Predicting uniaxial compressive strength of oil palm shell concrete using a hybrid artificial intelligence model. *J. Build. Eng.*, *30*: 101282.

Journal of Oil Palm Research Vol. 33 (3) September 2021 p. 493-513
DOI: https://doi.org/10.21894/jopr.2020.0089

QUALITY OF COMMERCIAL PALM-BASED COOKING OIL PACKED IN PLASTIC POUCH AND POLYETHYLENE TEREPHTHALATE (PET) BOTTLE

NORAZURA AILA MOHD HASSIM[1]*; NUR HAQIM ISMAIL[1]; SIVARUBY KANAGARATNAM[1]; WAN ROSNANI AWG ISA[1] and NOOR LIDA HABI MAT DIAN[1]

ABSTRACT

The study compared the quality of palm cooking oil sold in two types of packaging in Malaysia; plastic pouch (16 samples) and polyethylene terephthalate (PET) bottle (9 samples). The study was conducted because consumer perceived that the quality of palm cooking oil in plastic pouch is lower than in the PET bottle due to its lower price. Cooking oil in plastic pouch is subsidised by the Government of Malaysia and as such, it is sold at a cheaper price compared to bottled cooking oil. Therefore, comparison of the initial quality in terms of free fatty acid (FFA), fatty acid composition (FAC), triacylglycerol composition (TAG), total vitamin E, iodine value (IV), cloud point, smoke point, colour, polar compound, polymer compound and oxidative stability index (OSI) of the commercial palm cooking oils were conducted between the cooking oil in plastic pouch and PET bottle. The quality parameters of average FFA, FAC (oleic, linoleic, palmitic and stearic acids), IV and colour (red and yellow) of cooking oil in both packagings met the specifications or guidelines by either Malaysian Standard (MS) 682:2004, MS 816:2007 or Palm Oil Refiners' Association (PORAM) specifications/guidelines. However, quality parameters of TAG, total vitamin E, cloud point, smoke point, polar compound, polymer compound and OSI are not specified in any of the standards above. After conducting a 2-sample t-test to detect differences of cooking oil in both packagings, quality parameters of average FFA, FAC (oleic acid), total vitamin E, colour (red, yellow, neutral and blue), polar compound and polymer compound were comparable between cooking oil in plastic pouch and PET bottle. However, the FAC (palmitic acid, stearic acid and linoleic acid), TAG [UUU (unsaturated-unsaturated-unsaturated) and SUU (saturated-unsaturated-unsaturated)], IV and cloud point quality of cooking oil in PET bottle were better than in plastic pouch in which FAC (stearic acid and linoleic acid), TAG (UUU and SUU) and IV in PET bottle showed higher value while FAC (palmitic acid) and cloud point showed lower value than plastic pouch in this study. Notwithstanding this, the smoke point and OSI quality of commercial palm cooking oil in plastic pouch was better than in PET bottle, having higher values than PET bottle. TAG [SUS (saturated-unsaturated-saturated)] of commercial cooking oil in plastic pouch was also higher than in PET bottle but did not necessarily provide indication of good quality cooking oil.

Keywords: packed in PET bottle, packed in plastic pouch, palm cooking oil, palm olein, palm superolein.

Received: 9 July 2020**; Accepted:** 20 August 2020**; Published online:** 15 October 2020.

INTRODUCTION

There are 17 oils and fats produced and traded globally. Palm oil is regarded as one of the most important commodities, contributing to 57% of the global exportation of oils and fats in 2019 (MPOB, 2020). Palm oil and its fractions are vastly used in the food segment. Refined, bleached and deodourised (RBD) palm olein with iodine value (IV) of 56-59, the liquid fraction of palm oil from the first stage fractionation, has been widely used as cooking/frying oil especially in Malaysia due to its availability,

[1] Malaysian Palm Oil Board,
6 Persiaran Institusi, Bandar Baru Bangi,
43000 Kajang, Selangor, Malaysia.

* *Corresponding author e-mail: azuraaila@mpob.gov.my*

thermal stability and price competitiveness. Many studies have been conducted to look at the frying performance of palm olein during batch and continuous frying of food. Studies by Ahmad Tarmizi and Ismail (2008); Matthäus (2007); Ismail (2005); Sebedio *et al*. (1996) and Bracco *et al*. (1981) have shown that palm olein is a good and durable cooking oil. However, the number of studies conducted on frying performance of palm olein in batch frying had superseded continuous frying, possibly due to the costly operation of the latter. Palm olein is generally viewed as a heavy duty frying oil, which is commonly re-used in the snack food industry (Ahmad Tarmizi and Ismail, 2008; Nallusamy, 2006). Notwithstanding this, super olein with IV of 60-67, which is a liquid fraction of palm oil from the second stage fractionation produced by certain refineries, is also part of the cooking oil source.

Cooking oil functions as a medium of heat transfer to the food surface, with some of it being absorbed by the food, thus, ensuring its quality becomes very important. Despite that some of the oil is absorbed by the food (amount of absorption depends on the type of matrix and frying practices), household and industry are at great extend still practice cooking using oil as the process generates pleasing sensory properties of the food. As degradation (*i.e.* oxidation, hydrolysis, polymerisation, dehydration and cyclisation) occurs during the frying process, the initial quality of the oil has to be ensured before the cooking process. In this regards, Malaysian Standard (MS) 682:2004 (Department of Standards Malaysia, 2004) specifies requirements for cooking oil, covering blended and unblended cooking oil (refined and deodourised) which comprise free fatty acids (FFA), volatile matter and impurities, soap content, unsaponifiable matter and colour. Notwithstanding this MS 816:2007 (Department of Standards Malaysia, 2007) specifies the requirements for palm olein, covering parameters of apparent density, refractive index, saponification value, unsaponifiable matter, fatty acid composition (FAC), IV, slip melting point (SMP), total carotenoids, FFA, moisture and impurities, peroxide value and colour (Lovibond).

In Malaysia, there are two types of packaging for cooking oil, namely the plastic pouch/ packet and polyethylene terephthalate (PET) bottle. The price of cooking oil in plastic pouch/ packet packaging is subsidised and controlled by the Government of Malaysia and therefore, is cheaper than the price of PET bottle cooking oil. However, due to this scenario, consumers and consumer associations in Malaysia often regard cooking oil in pouch packaging as having lower quality compared to cooking oil in PET bottle. In view of this scenario and to correct the public misperception, several experiments have been conducted to analyse, confirm and compare the quality of cooking oil in both forms of packaging. Some crucial characteristics of palm-based cooking oil as mentioned in the Malaysian Standards, namely FFA, FAC, IV as well as colour and some additional crucial quality characteristics namely cloud point, smoke point, polar compound, polymer compound, oxidative stability index (OSI) and vitamin E (tocotrienols and tocopherols) in both plastic pouch and PET bottle were reported. Triacylglycerols (TAG) composition of the cooking oils was also analysed.

MATERIALS AND METHODS

Materials

The cooking oils (16 plastic pouches and nine 1 kg PET bottles) were purchased from Malaysian retail shops and hypermarkets. All chemicals used were analytical grade except for TAG analysis which used HPLC grade solvent.

Free Fatty Acid

The FFA value was determined according to the American Oil Chemists Society (AOCS) Official Method Ca 5a-40 (Firestone, 1998) using titration method. Oil sample (20 g) was dissolved in 50 ml isopropanol and 2 ml phenolphthalein indicator solution. 0.1 M sodium hydroxide is titrated to the mixture until first permanent colour of pink appeared. This colour must remain for at least 30 s. The FFA was calculated based on the percentage of palmitic acid.

Fatty Acid Composition

The FAC was determined using Gas Chromatography according to ISO 5508:1990 (1990) as fatty acid methyl ester (FAME) by dissolving 0.1 g samples with 1.8 ml of hexane before methylated it with sodium methoxide. The process followed with the addition of water. Mixing process using vortex mixer was performed intermittently between each step for 10 s. One µl FAME from sedimentation of the sodium glycerolate was injected into DuraBond DB-23 fused silica capillary column (60 m x 0.25 mm x 0.25 µm) (Agilent Technologies, Model 7890B) that was equipped with flame ionisation detector (FID). The detection temperature was set at 240°C while the oven temperature was set isothermally at 180°C. The flow rate of helium gas was at 0.8 ml min^{-1}. FAME standards were used for peak identification followed with the peak area normalisation method of the quantified area.

Triacylglycerols Composition

The TAG composition was determined using ultra high-performance liquid chromatography (U-HPLC) system (1290 Infinity LC System, Agilent Technologies, USA) and Agilent 1260 RI detector (Waters Corp., USA) according to AOCS Official Method Ce 5b-89 (Firestone, 1998). A Cortecs UPLC C18 column (2.1 x 150 mm length i.d; 1.6 µm particle size) (Waters Corp., Milford, Massachusetts, USA) maintained at 30°C was used to separate the TAG. The isocratic mobile phase used was a mixture of acetone-acetonitrile at 63.5:36.5 (v/v) ratio at a flow rate of 0.25 ml min^{-1}. Samples (0.1 g) was solubilised in 1 ml of acetone. Identification of individual peak was carried out by comparing the retention times of pure TAG standards and typical palm olein composition. Data was recorded as percent areas.

Vitamin E

Total vitamin E, tocotrienols and tocopherols were determined according to AOCS Official Method Ce 8-89 (Firestone, 1998) using high performance liquid chromatography (HPLC) (Gilson) fitted with a 250 x 4.6 mm column, packed with 5 µm of silica (Phenomenex, Torrance, USA). The sample was dissolved in *n*-hexane prior injecting into HPLC. Ratio of *n*-hexane and isopropanol at 99.6:0.04 (Merck, Germany) was used as mobile phase at a flow rate of 1 ml min^{-1}. Fluorescence detector was used to detect vitamin E at an excitation and emission wavelengths of 290 and 330 nm respectively. Comparison of the retention time of Standard Tocopherols and Tocotrienols was used to identify the tocols (Isomer Kits of ChromaDex, Santa Ana, USA).

Iodine Value (by calculation)

IV was calculated according to the FAC factors as described by Ham *et al.* (1998) using the formulation as below:

IV = (0.95*16:1) + (0.86*18:1) + (1.72*18:2) + (2.6*18:3)

Note: * is multiply; 16:1, 18:1, 18:2 and 18:3 is the value of each fatty acid.

Cloud Point

MPOB Test Method was used to determine the cloud point (MPOB, 2005). Oil sample of 60-75 g was filtered using Whatman No. 1 filter paper and heated for 5 min at 130°C for foreign matter and moisture removal. The sample (45 ml) was then put in a Beatson bottle, cooled (using water bath) and stirred until it reached 10°C. More vigorous stirring was applied below 10°C when near to the expected cloud point, to avoid supercooling and fat crystals solidification on the bottle surface (side and bottom). The sample was taken out from the water bath at certain intervals to check for the sample cloudiness. The test was repeated at 5°C (below recorded cloud point). Repeated test runs by a single operator should not vary by more than 0.6°C. The reading of the cloud point was taken once the thermometer immersed in the oil was not visible anymore.

Smoke Point

The smoke point was determined based on AOCS Official Method Cc 9a-48 (Firestone, 1998) using the Cleveland open-cup method. The oil sample was poured into the cup (usually brass) until the filling line and light beam was arranged at the centre of the cup. Thermometer is positioned at the centre of the cup and the cup was rapidly heated to 40°C-50°C. This is followed by regulating the heating at a rate of 5°C min^{-1}. The increased temperature will cause the oil to produce smoke. The temperature at which the sample produces smoke is recorded as the smoke point.

Colour

The colour of oil samples was measured using Lovibond Tintometer Model F (The Tintometer Ltd., Salisbury, United Kingdom) according to AOCS Official Method Cc 13e-92 (Firestone, 1998). Glass cells, 5 1/4-in. and 1-in. (13.3 and 2.5 cm) path lengths, were used for containing the test samples. Cooking oil samples were heated in an oven at 60 ± 2°C for 1 hr. The liquid oil was poured into a glass cell. The cell containing the sample was placed within the lighting cabinet. The lid of the lighting cabinet was closed and colour of the cooking oil sample was determined immediately using colour racks at a ratio of 10 yellow (Y) to 1 red (R) as the base line.

Polar Compound

Polar compounds were determined according to the Standard IUPAC Method 2.507 (IUPAC, 1987) using silica column chromatography gravimetrically. A 2.5 g oil sample was dissolved in 50 ml elution solvent having 87:13 v/v ratio of petroleum benzene and diethyl ether respectively. A 20 ml of the oil sample solution prepared above was introduced onto a 4.5-m glass column filled with a slurry of Silica Gel 60 (Merck, Darmstadt, Germany), sea sand and the elution solvent. Elution of non-polar fraction is carried out with 150 ml of the elution solvent within 60-70 min. The non-polar mixture was then collected in a flask. Removal of the solvent from the non-polar mixture was carried out

using rotary evaporator. Nitrogen was used to cool the residue at room temperature by flushing it in the flask. The determination of polar compounds was conducted by subtracting the non-polar compounds from the mass of the sample dissolved in the petroleum ether and diethyl ether mixture.

Polymer Compound

Polymer compounds were quantified according to Peled *et al.* (1975). The oil sample was added with 1% sulphuric acid (Systerm, Shah Alam, Malaysia) before refluxing it for 2.5 hr. The methanolic layer was separated from the semi-solid layer after cooling for 2.5 hr. The semi solid layer was then rinsed using methanol (Systerm, Shah Alam, Malaysia) and mixed with chloroform (LAB-SCAN, Dublin, Ireland) before being transferred to the conical flask. Chloroform was evaporated using a rotary evaporator and the remaining residue was dried at 130°C for 30 min. The dried residue was weighed after being cooled at room temperature.

Oxidative Stability Index

Induction period was determined using a 743 Rancimat (Metrohm, Herisau, Switzerland) according to AOCS Official Method Cd 12b-92 (Firestone, 1998). Sample was weighed about 0.3 g and put at the bottom of the reaction vessel and heated at 110°C with a gas flow of 20 litre hr^{-1}. The volatile products which were released during the oxidation process were collected in the flask containing 60 ml of distilled water. A chart of water conductivity *vs.* time was expressed from a multi-channel strip chart recorder and the induction period was affirmed by a micro-processor computed slope algorithm. The induction period is prescribed as the point of rapid transition as a result of oxidation, and expressed in hour (hr) (Aladedunye *et al.*, 2014).

Statistical Analysis

FFA, TAG composition, smoke point, colour, polar compound, polymer compound and OSI were carried out in duplicate while FAC, vitamin E, IV and cloud point were carried out in triplicate. Results were analysed with Minitab version 16.0 (Pennsylvania, USA) using one-way analyses of variance (ANOVA). Significant differences ($p \leq 0.05$) among all samples (total = 25) were analysed using the Tukey's Post-Hoc test. Results were also analysed using 2-sample t-test with similar Minitab version. Significant differences ($p \leq 0.05$) between two groups (*i.e.* plastic pouch and PET bottle) were analysed. Pearson correlation was used to assess linear correlation between two continuous variables and was used to obtain correlation between certain parameters only.

RESULTS AND DISCUSSION

Free Fatty Acid

One of the quality parameters of cooking oil is FFA. Low FFA is preferable as high FFA produces off-flavour which makes the oil less acceptable. FFA is mainly produced through hydrolysis of TAG. However, some FFA may come from decomposition of hydroperoxide of the cooking oil at elevated temperature together with the presence of air and moisture (Bensmira *et al.*, 2007). The FFA of commercial cooking oils in both plastic pouch and PET bottle is shown in *Table 1a.* Cooking oils in both plastic pouch and PET bottle have FFA values which ranged from 0.064%-0.208% and 0.077%-0.227%, respectively. This makes the overall range of cooking oil in both packaging to be between 0.064%-0.227% and was significantly different ($p<0.05$) based on ANOVA. However, there were cooking oils that were not significantly different from each other. Sample V (PET bottle) has the highest FFA followed by sample A (plastic pouch) and B (plastic pouch). Sample K (plastic pouch) has the lowest FFA value. Malaysia Standard for Palm Olein - MS 816:2007 (Department of Standards Malaysia, 2007) and Palm Oil Refiners Association of Malaysia (PORAM) has put a limit of 0.1% FFA for RBD palm olein. Malaysian Standard for Cooking Oils - MS 682:2004 (Department of Standards Malaysia, 2004) has also set a maximum limit of unblended cooking oil of 0.2% while for blended cooking oil is 1.0%. There was also recommendation by Gunstone (2008) that refined oils should have FFA value of less than 0.1%. This is due to refining process that FFA is removed from crude oils. Samples that met PORAM's and Gunstone (2008) criteria were samples H, J, K, M and N (plastic pouch) and sample S and Y (PET bottle). Higher FFA limits (0.2%) set by the Malaysian Standard for Cooking Oil – MS 682:2004 (Department of Standards Malaysia, 2004) for unblended cooking oil was the most fulfilled standard by the cooking oil in this study. It was fulfilled by samples C, D, E, F, G, I, L, O, P (plastic pouch) and samples Q, R, T, U and W (PET bottle). Samples V and X (PET bottle) which were blended cooking oils had fulfilled the Malaysian Standard for Cooking Oil – MS 682:2004 (Department of Standards Malaysia, 2004) for blended cooking oil having limit of 1.0% FFA. There were two samples (sample A and B in plastic pouch) that were unable to fulfill any standard or reference. Sometimes, the FFA value of commercial RBD palm olein may not fulfill any standards or references as the cooking oil has been on the shelf for a long time. An example of this was the cooking oil from the supermarket in Konya, Turkey used by Arslan *et al*. (2017) which recorded an FFA value of 0.77% (higher than Malaysian Standard and PORAM). Notwithstanding this, researches that used RBD

palm olein direct from refineries normally obtained FFA value of less than 0.1% (*i.e*. Roiaini *et al.*, 2015). A 2-sample t-test (*Table 1b*) showed that the average FFA of cooking oils in both plastic pouch and PET bottle was not significantly different (p>0.05) and therefore, was comparable.

TABLE 1A. FREE FATTY ACID (FFA) OF COMMERCIAL PALM-BASED COOKING OIL IN PLASTIC POUCH AND POLYETHYLENE TEREPHTHALATE (PET) BOTTLE PACKAGING IN MALAYSIA

Sample	Free fatty acid (%)
A (PP)	0.208 ± 0.004^{b}
B (PP)	0.205 ± 0.000^{b}
C (PP)	0.141 ± 0.000^{fg}
D (PP)	0.102 ± 0.000^{i}
E (PP)	0.131 ± 0.005^{g}
F (PP)	0.192 ± 0.000^{c}
G (PP)	0.179 ± 0.000^{d}
H (PP)	0.099 ± 0.005^{i}
I (PP)	0.115 ± 0.000^{h}
J (PP)	0.093 ± 0.005^{i}
K (PP)	0.064 ± 0.000^{k}
L (PP)	0.192 ± 0.000^{c}
M (PP)	0.093 ± 0.005^{i}
N (PP)	0.077 ± 0.000^{j}
O (PP)	0.166 ± 0.000^{e}
P (PP)	0.157 ± 0.004^{e}
Q (PB)	0.166 ± 0.000^{e}
R (PB)	0.141 ± 0.000^{fg}
S (PB)	0.077 ± 0.000^{j}
T (PB)	0.191 ± 0.000^{c}
U (PB)	0.187 ± 0.007^{cd}
V (PB)	0.227 ± 0.004^{a}
W (PB)	0.191 ± 0.000^{c}
X (PB)	0.144 ± 0.004^{f}
Y (PB)	0.077 ± 0.000^{j}

Note: Sample A-P - cooking oils in plastic pouch (PP).
Sample Q-Y - cooking oils in polyethylene terephthalate (PET) bottle (PB).
Means within each row bearing different superscript letters are significantly different (p<0.05).

TABLE 1B. 2-SAMPLE T-TEST OF FREE FATTY ACID (FFA) OF COMMERCIAL PALM-BASED COOKING OIL IN PLASTIC POUCH AND POLYETHYLENE TEREPHTHALATE (PET) BOTTLE PACKAGING IN MALAYSIA

Mean of FFA (%)		p-value
Plastic pouch	PET bottle	
0.138 ± 0.047	0.156 ± 0.051	0.238

Note: p-value<0.05 indicates that there is significant different between cooking oil in plastic pouch and PET bottle.

Fatty Acid Composition

Monitoring of FAC is usually conducted to confirm the authenticity of an oil or fat, as well as to know the stability and physicochemical properties of these products (Kostik *et al.*, 2013). In this survey, confirmation on palm cooking oil whether single or blended oil(s) and their fraction(s) can be determined using FAC. The FAC of all cooking oils (in plastic pouch and PET bottle) is shown in *Table 2a*. Oleic acid was the major FAC of cooking oil in both plastic pouch and PET bottle, having value of between 41.68%-45.52% and 42.28%-45.29%, respectively. This was followed by palmitic acid (between 34.79%-41.12% for plastic pouch and 35.64%-38.76% for PET bottle) and linoleic acid (between 10.66%-13.37% for plastic pouch and 12.00%-14.22% for PET bottle). FAC of all cooking oils (plastic pouch and PET bottle) was significantly different (p<0.05) based on ANOVA. However, there were cooking oils that were not significantly different from each other. These fatty acid trends were similar to the finding by Ahmad Tarmizi *et al.* (2014) on palm olein. Samples H (plastic pouch), L (plastic pouch), V (PET bottle) and O (plastic pouch) contained the highest level of oleic acid, palmitic acid, linoleic acid and stearic acid respectively. Samples O (plastic pouch), H (plastic pouch), M (plastic pouch) and F (plastic pouch) on the other hand, had the lowest level of oleic acid, palmitic acid, linoleic acid and stearic acid accordingly. Lauric, myristic, palmitoleic, linolenic and arachidic acid was present in the cooking oil but in very small quantity. FAC of cooking oil in both pouch and PET bottle should resemble the value of palm olein or palm superolein as both fractions are the common raw materials for cooking oil.

According to Malaysian Standard for Palm Olein - MS 816:2007 (Department of Standards Malaysia, 2007), RBD palm olein should have oleic acid value of 39.8%-43.9%, palmitic acid of 38.2%-42.9%, linoleic acid of 10.4%-12.7% and stearic acid of 3.7%-4.8% in which majority of the dominant FAC in the commercial cooking oil (plastic pouch and PET bottle) fall in this range. However, comparison to this standard indicated that samples H, J and P (plastic pouch) and Q, R, S, T, U, V, W and Y (PET bottle) have lower value of palmitic acid, samples C, D, H and P (plastic pouch) and R and W (PET bottle) have higher value of oleic, samples H (plastic pouch) and S, U, V and W (PET bottle) have higher range of linoleic acid and samples D, F, H and P (plastic pouch) have lower range of stearic acid. Notwithstanding this, based on 2-sample t-test, the average palmitic acid, stearic acid and linolenic acid of cooking oil in both packagings were significantly different (p<0.05) (*Table 2b*). However, the average of oleic acid was comparable for cooking oil in both packaging (p>0.05). Tabee *et al*. (2009) stated that

TABLE 2A. FATTY ACID COMPOSITION (FAC) OF COMMERCIAL PALM-BASED COOKING OIL IN PLASTIC POUCH AND POLYETHYLENE TEREPHTHALATE (PET) BOTTLE PACKAGING IN MALAYSIA

Sample	12:0	14:0	16:0	18:0	18:1	18:2	18:3	20:0	Oths	Mono	Poly	Sat
A (PP)	0.23 ± 0.01^{hi}	1.05 ± 0.04^{bcd}	39.92 ± 0.10^{bc}	4.09 ± 0.03^{bcde}	42.93 ± 0.19^{ghij}	10.77 ± 0.06^{k}	0.43 ± 0.47^{a}	0.26 ± 0.62^{cde}	0.11 ± 0.02^{abc}	43.15 ± 0.18^{hij}	11.20 ± 0.05^{jkl}	45.55 ± 0.14^{b}
B (PP)	0.31 ± 0.02^{ef}	0.96 ± 0.00^{defgh}	39.88 ± 0.13^{bc}	3.75 ± 0.06^{ghi}	43.67 ± 0.03^{defgh}	10.72 ± 0.13^{k}	0.25 ± 0.05^{cdef}	0.23 ± 0.00^{def}	0.00 ± 0.00^{c}	43.91 ± 0.05^{defgh}	10.97 ± 0.13^{kl}	45.13 ± 0.08^{bc}
C (PP)	0.19 ± 0.00^{k}	0.92 ± 0.00^{efgh}	39.67 ± 0.06^{cd}	3.72 ± 0.02^{ghi}	44.08 ± 0.00^{cdef}	10.81 ± 0.03^{jk}	0.15 ± 0.02^{g}	0.22 ± 0.01^{def}	0.00 ± 0.00^{c}	44.33 ± 0.02^{cdef}	10.95 ± 0.10^{kl}	44.72 ± 0.03^{c}
D (PP)	0.27 ± 0.00^{gh}	1.03 ± 0.00^{bcdef}	38.72 ± 0.07^{efg}	3.66 ± 0.01^{i}	44.31 ± 0.02^{bcde}	11.33 ± 0.03^{h}	0.21 ± 0.00^{defg}	0.22 ± 0.03^{def}	0.00 ± 0.00^{c}	44.56 ± 0.02^{bcde}	11.54 ± 0.03^{hij}	43.90 ± 0.03^{d}
E (PP)	0.19 ± 0.00^{ijk}	0.90 ± 0.01^{h}	40.06 ± 0.07^{bc}	$3.70 \pm 0.04h^{i}$	43.70 ± 0.06^{defgh}	10.75 ± 0.03^{k}	0.19 ± 0.00^{efg}	0.21 ± 0.00^{def}	0.00 ± 0.00^{c}	43.99 ± 0.08^{defgh}	10.94 ± 0.04^{l}	45.07 ± 0.05^{bc}
F (PP)	0.19 ± 0.00^{ijk}	0.91 ± 0.00^{gh}	40.07 ± 0.02^{bc}	3.63 ± 0.04^{i}	43.76 ± 0.02^{defg}	10.73 ± 0.02^{k}	0.19 ± 0.00^{fg}	0.21 ± 0.00^{def}	0.00 ± 0.00^{c}	44.07 ± 0.03^{defgh}	10.92 ± 0.01^{l}	45.01 ± 0.03^{bc}
G (PP)	0.24 ± 0.00^{hi}	0.91 ± 0.02^{fgh}	39.78 ± 0.20^{cd}	3.74 ± 0.05^{ghi}	43.83 ± 0.06^{defg}	10.71 ± 0.07^{k}	0.21 ± 0.00^{defg}	0.22 ± 0.00^{def}	0.00 ± 0.00^{c}	44.18 ± 0.07^{defg}	10.92 ± 0.06^{l}	44.90 ± 0.12^{bc}
H (PP)	0.51 ± 0.00^{b}	1.08 ± 0.01^{bcd}	34.79 ± 0.07^{l}	3.65 ± 0.00^{i}	45.52 ± 0.02^{a}	13.37 ± 0.05^{b}	0.30 ± 0.01^{bcd}	0.25 ± 0.00^{def}	0.00 ± 0.00^{c}	46.05 ± 0.03^{a}	13.67 ± 0.04^{b}	40.27 ± 0.08^{h}
I (PP)	0.27 ± 0.00^{gh}	1.00 ± 0.02^{cdefgh}	39.23 ± 0.05^{de}	4.02 ± 0.00^{cdef}	43.48 ± 0.05^{efghi}	11.01 ± 0.03^{hijk}	0.21 ± 0.02^{defg}	0.25 ± 0.00^{def}	0.00 ± 0.00^{c}	44.03 ± 0.06^{defgh}	11.23 ± 0.00^{jkl}	44.74 ± 0.07^{c}
J (PP)	0.31 ± 0.00^{ef}	1.00 ± 0.00^{cdefgh}	38.06 ± 0.08^{h}	4.05 ± 0.02^{cdef}	43.85 ± 0.02^{defg}	11.77 ± 0.07^{g}	0.15 ± 0.00^{g}	0.25 ± 0.00^{def}	0.00 ± 0.00^{c}	44.43 ± 0.05^{cdef}	11.92 ± 0.07^{ghi}	43.65 ± 0.08^{d}
K (PP)	0.23 ± 0.05^{ij}	1.06 ± 0.00^{bcd}	39.92 ± 0.00^{bc}	4.06 ± 0.00^{cdef}	42.92 ± 0.00^{ghij}	11.25 ± 0.00^{hi}	0.30 ± 0.00^{bcd}	0.00 ± 0.00^{g}	0.06 ± 0.05^{bc}	43.13 ± 0.00^{hij}	11.55 ± 0.00^{hij}	45.26 ± 0.05^{bc}
L (PP)	0.21 ± 0.00^{ijk}	1.09 ± 0.00^{bc}	41.12 ± 0.00^{a}	3.93 ± 0.00^{defg}	41.83 ± 0.00^{kl}	10.81 ± 0.00^{ijk}	0.26 ± 0.00^{cdef}	0.40 ± 0.02^{abc}	0.10 ± 0.00^{abc}	42.10 ± 0.00^{k}	11.10 ± 0.00^{jkl}	46.80 ± 0.00^{a}
M (PP)	0.35 ± 0.00^{d}	1.04 ± 0.03^{bcde}	39.61 ± 0.08^{cd}	4.15 ± 0.04^{bcd}	43.40 ± 0.09^{efghi}	10.66 ± 0.05^{k}	0.31 ± 0.03^{bcd}	0.14 ± 0.03^{efg}	0.13 ± 0.03^{abc}	43.61 ± 0.10^{efghi}	10.99 ± 0.01^{kl}	45.29 ± 0.09^{bc}
N (PP)	0.43 ± 0.00^{c}	1.05 ± 0.01^{bcd}	39.58 ± 0.31^{cd}	4.10 ± 0.14^{bcde}	43.07 ± 0.14^{ghij}	10.92 ± 0.23^{hijk}	0.34 ± 0.06^{abc}	0.12 ± 0.00^{fg}	0.16 ± 0.04^{ab}	43.28 ± 0.14^{ghij}	11.27 ± 0.29^{jkl}	45.29 ± 0.24^{bc}
O (PP)	0.14 ± 0.00^{l}	1.02 ± 0.00^{bcdefg}	40.39 ± 0.07^{b}	4.46 ± 0.00^{a}	41.68 ± 0.00^{l}	11.23 ± 0.00^{hij}	0.23 ± 0.00^{defg}	0.45 ± 0.00^{a}	0.16 ± 0.07^{ab}	41.92 ± 0.00^{k}	11.46 ± 0.00^{ijk}	46.46 ± 0.07^{a}
P (PP)	0.24 ± 0.00^{hi}	1.01 ± 0.02^{bcdefgh}	37.45 ± 0.65^{i}	3.66 ± 0.27^{i}	45.04 ± 1.18^{abc}	11.77 ± 0.02^{g}	0.28 ± 0.05^{bcdef}	0.30 ± 0.12^{bcd}	0.04 ± 0.07^{bc}	45.26 ± 1.18^{abc}	12.05 ± 0.07^{fgh}	42.66 ± 1.05^{ef}
Q (PB)	0.33 ± 0.00^{de}	0.99 ± 0.00^{cdefgh}	38.03 ± 0.02^{hi}	4.06 ± 0.00^{cdef}	42.73 ± 0.03^{hijk}	12.52 ± 0.06^{de}	0.23 ± 0.01^{defg}	0.26 ± 0.01^{def}	0.10 ± 0.00^{abc}	43.49 ± 0.00^{fghij}	12.75 ± 0.05^{cd}	43.66 ± 0.05^{d}
R (PB)	0.24 ± 0.00^{hi}	1.06 ± 0.02^{bcd}	36.60 ± 0.25^{j}	3.70 ± 0.06^{hi}	45.29 ± 0.63^{ab}	12.20 ± 0.50^{efg}	0.30 ± 0.08^{bcd}	0.35 ± 0.13^{abcd}	0.05 ± 0.08^{bc}	45.51 ± 0.59^{ab}	12.49 ± 0.58^{def}	41.95 ± 0.08^{fg}
S (PB)	0.28 ± 0.00^{fg}	1.12 ± 0.01^{ab}	37.67 ± 0.09^{hi}	3.90 ± 0.03^{efgh}	43.40 ± 0.02^{efghi}	12.95 ± 0.07^{bcd}	0.22 ± 0.02^{defg}	0.24 ± 0.04^{def}	0.00 ± 0.00^{c}	43.59 ± 0.02^{fghi}	13.18 ± 0.09^{bc}	43.20 ± 0.03^{de}
T (PB)	0.14 ± 0.01^{l}	0.97 ± 0.05^{cdefgh}	38.19 ± 0.03^{fgh}	4.01 ± 0.06^{cdef}	43.80 ± 0.09^{defg}	12.00 ± 0.02^{fg}	0.22 ± 0.01^{defg}	0.34 ± 0.02^{abcd}	0.10 ± 0.02^{abc}	44.04 ± 0.08^{defgh}	12.21 ± 0.03^{efg}	43.65 ± 0.04^{d}
U (PB)	0.12 ± 0.00^{l}	0.97 ± 0.00^{cdefgh}	38.14 ± 0.00^{gh}	4.31 ± 0.00^{ab}	42.28 ± 0.00^{jkl}	12.97 ± 0.00^{bc}	0.35 ± 0.00^{abc}	0.41 ± 0.00^{ab}	0.20 ± 0.00^{a}	42.54 ± 0.00^{jk}	13.32 ± 0.00^{b}	43.94 ± 0.00^{d}
V (PB)	0.49 ± 0.00^{b}	1.11 ± 0.00^{b}	35.65 ± 0.19^{k}	4.10 ± 0.04^{bcde}	43.24 ± 0.13^{fghij}	14.22 ± 0.19^{a}	0.37 ± 0.00^{ab}	0.44 ± 0.02^{ab}	0.09 ± 0.08^{abc}	43.54 ± 0.08^{fghi}	14.59 ± 0.19^{a}	41.79 ± 0.19^{g}
W (PB)	0.70 ± 0.00^{a}	1.24 ± 0.00^{a}	35.64 ± 0.00^{k}	3.83 ± 0.04^{fghi}	44.51 ± 0.00^{bcd}	12.93 ± 0.00^{cd}	0.41 ± 0.00^{a}	0.41 ± 0.00^{ab}	0.08 ± 0.04^{abc}	44.76 ± 0.00^{bcd}	13.33 ± 0.00^{b}	41.82 ± 0.04^{g}
X (PB)	$0.33 \pm 0.01d^{e}$	1.13 ± 0.16^{ab}	38.76 ± 0.40^{ef}	4.21 ± 0.12^{bc}	42.54 ± 0.50^{ijkl}	12.07 ± 0.09^{fg}	0.29 ± 0.03^{bcde}	0.34 ± 0.05^{abcd}	0.10 ± 0.10^{abc}	42.78 ± 0.46^{ijk}	12.36 ± 0.11^{defg}	44.76 ± 0.28^{c}
Y (PB)	$0.32 \pm 0.00d^{e}$	1.06 ± 0.04^{bcd}	38.12 ± 0.08^{h}	3.98 ± 0.05^{cdef}	43.32 ± 0.54^{fghi}	12.33 ± 0.28^{ef}	0.30 ± 0.07^{bcd}	0.34 ± 0.08^{abcd}	0.03 ± 0.06^{bc}	$43.52 \pm 0.52f^{ghi}$	12.63 ± 0.36^{de}	43.82 ± 0.11^{d}

Note: Sample A-P - cooking oils in plastic pouch (PP).
Sample Q-Y - cooking oils in polyethylene terephthalate (PET) bottle (PB).
Means within each row bearing different superscript letters are significantly different ($p<0.05$).
Oths - others; Mono - monounsaturated fatty acid; Poly - polyunsaturated fatty acid; Sat - total saturated fatty acid.

frying oil with high content of oleic acid (*i.e.* palm olein and sunflower oil) provides better health benefit. The linolenic acid in the palm cooking oil was well below 2% as higher linolenic acid imparts undesirable smell during frying and provide off-taste (bitter) to the fried product (Ahmad Tarmizi *et al*., 2014). According to Berger (2005), for industrial frying, linolenic acid value must be kept below 2%. The palm cooking oils contained a balanced saturated and unsaturated fatty acids that provide stability to the oil. This makes palm cooking oil good for deep frying, as it is not potent to thermal degradation that normally takes place in unsaturated fatty acid (Ahmad Tarmizi *et al*., 2013).

According to a 2-sample t-test, the average monounsaturated fatty acid of cooking oils in both plastic pouch and PET bottle was not significantly different ($p>0.05$) and thus, were comparable (*Table 2b*). However, both average polyunsaturated and total saturated fatty acid of cooking oils in both plastic pouch and PET bottle were significantly different ($p<0.05$). Notwithstanding this, comparison of average total unsaturated (poly and mono-unsaturated) and total saturated fatty acids of cooking oils in both plastic pouch and PET bottle using 2-sample t-test were significantly different ($p<0.05$). The finding showed that the average total unsaturated fatty acid in PET bottle cooking oil was higher (better) than those in plastic pouch. This result synchronised with the average saturated fatty acid findings when this fatty acid was lower (better) in PET bottle compared to those in the plastic pouch.

TABLE 2B. 2-SAMPLE T-TEST OF FATTY ACID COMPOSITION (FAC) GROUP OF COMMERCIAL PALM-BASED COOKING OIL IN PLASTIC POUCH AND POLYETHYLENE TEREPHTHALATE (PET) BOTTLE PACKAGING IN MALAYSIA

FAC group	Mean (%)		p-value
	Plastic pouch	PET bottle	
16:0 (Palmitic acid)	39.29 ± 1.47	37.40 ± 1.13	0.00
18:0 (Stearic acid)	3.85 ± 0.39	4.01 ± 0.18	0.04
18:1(Oleic acid)	43.59 ± 1.01	43.40 ± 1.02	0.44
18:2 (Linoleic acid)	11.17 ± 0.68	12.70 ± 0.70	0.00
Monounsaturated	43.89 ± 1.05	43.70 ± 0.97	0.42
Polyunsaturated	11.42 ± 0.69	13.01 ± 0.75	0.00
Total unsaturated	55.32 ± 1.54	56.71 ± 1.07	0.00
Saturated	44.64 ± 1.51	43.17 ± 1.04	0.00

Note: p-value<0.05 indicates that there is significant different between cooking oil in plastic pouch and PET bottle.

Triacylglycerols Composition

The TAG composition of palm-based commercial cooking oils in Malaysia is shown in *Tables 3a*, *3b* and *3c*. TAG was also conducted to check the authenticity of the oil. However, TAG of cooking and frying oils is the least conducted, as FAC analysis is normally sufficient. Based on ANOVA, all of the commercial palm cooking oils' TAG were significantly different ($p<0.05$) based on ANOVA. However, there were cooking oils that were not significantly different from each other. The cooking oils in plastic pouch and PET bottle contained diacylglycerols (DAG) of between 5.89%-7.45% and 5.92%-7.34%, respectively. This made TAG of cooking oils in both plastic bottle and PET to be between 92.55%-94.11% and 92.66%-94.08%, respectively. This is in line with the findings by Ahmad Tarmizi *et al*. (2015) reporting of about 93% TAG in his study. The amount of DAG contributes to higher level of polar compounds in palm cooking oil. POO, POP, PLO and PLP were the dominant TAG composition in these cooking oils. These TAG of cooking oil in plastic pouch were in the range of 26.18%-31.89%, 17.69%-28.66%, 10.94%-14.08% and 9.53%-10.45%, respectively while in PET bottle were in the range of 27.05%-30.88%, 21.01%-26.14%, 12.11%-13.48% and 10.10%-11.66%, respectively. This gave an overall range of between 26.18%-31.89%, 17.69%-28.66%, 10.94%-14.08%, 9.53%-11.66% of those TAG accordingly. This trend was similar to the palm olein TAG major composition in a study by Calliauw *et al.* (2007). In a study by Myat *et al.* (2009), it was found that the TAG composition of POO, POP, PLO and PLP of commercial palm olein from a supermarket in Kuala Lumpur was 31.69%, 26.89%, 14.43% and 10.14%, respectively. These TAG were in the range of the analysed commercial palm cooking oil in this study, except for PLO in which the TAG was not in the range. The TAG found in trace amounts were PPP, MLP, OLL and SOS. It was interesting to note that all palm cooking oils in PET bottle has 0% PPP while cooking oil in plastic pouch has PPP in the range of 0.00%-0.47%. UUU (unsaturated-unsaturated-unsaturated), SUU (saturated-unsaturated-unsaturated), SUS (saturated-unsaturated-saturated) and SSS (saturated-saturated-saturated) TAG of commercial palm cooking oils in plastic pouch in Malaysia ranged between 5.99%-8.35%, 42.68%-52.27%, 31.94%-44.77% and 0.00%-0.47%, respectively while the range for cooking oils in PET bottle were 6.43%-9.15%, 44.65%-50.10%, 34.53%-42.64% and 0.00, respectively. Based on ANOVA, UUU, SUU, SUS and SSS TAG of the commercial cooking oils in both plastic pouch and PET bottle were significantly different ($p<0.05$). However, there were cooking oils that were not significantly different from each other. In addition, the average UUU, SUU and SUS

TABLE 3A. TRIACYLGLYCEROL COMPOSITION (TAG) OF COMMERCIAL PALM COOKING OIL IN PLASTIC POUCH AND POLYETHYLENE TEREPHTHALATE (PET) BOTTLE PACKAGING IN MALAYSIA

Sample	DAG	POO	POP	PLO	PLP	POS	OOO
A (PP)	6.44 ± 0.04^{defgh}	26.81 ± 0.15^{hij}	27.68 ± 0.00^{cd}	11.18 ± 0.01^{jk}	9.86 ± 0.09^{lmn}	5.10 ± 0.05^{a}	4.28 ± 0.05^{hi}
B (PP)	6.11 ± 0.15^{jk}	27.15 ± 0.06^{gh}	27.30 ± 0.08f^{g}	11.28 ± 0.00^{hij}	9.96 ± 0.04^{jklm}	4.82 ± 0.05^{efg}	4.41 ± 0.03^{efgh}
C (PP)	6.26 ± 0.00^{hij}	27.14 ± 0.05^{gh}	27.19 ± 0.04^{g}	11.56 ± 0.01^{ghi}	9.66 ± 0.02^{no}	4.93 ± 0.05^{bcdef}	4.46 ± 0.00^{ef}
D (PP)	6.11 ± 0.02^{jk}	28.66 ± 0.02^{de}	24.83 ± 0.05^{j}	12.12 ± 0.03^{f}	10.16 ± 0.04^{ghijk}	4.59 ± 0.00^{h}	4.51 ± 0.00^{de}
E (PP)	6.50 ± 0.00^{de}	26.99 ± 0.13^{gh}	27.45 ± 0.11^{defg}	11.34 ± 0.04^{ghij}	9.90 ± 0.01^{klmn}	4.84 ± 0.03^{efg}	4.26 ± 0.08^{hi}
F (PP)	6.49 ± 0.02^{def}	26.95 ± 0.06^{ghi}	27.39 ± 0.06^{efg}	11.39 ± 0.14^{ghij}	9.90 ± 0.16^{klmn}	4.86 ± 0.08^{defg}	4.28 ± 0.04^{hi}
G (PP)	6.53 ± 0.00^{de}	27.07 ± 0.10^{gh}	27.24 ± 0.09^{fg}	11.36 ± 0.06^{ghij}	9.90 ± 0.04^{klmn}	4.87 ± 0.02^{cdefg}	4.34 ± 0.02^{fghi}
H (PP)	7.45 ± 0.01^{a}	31.89 ± 0.01^{a}	17.69 ± 0.03^{p}	14.08 ± 0.04^{a}	10.45 ± 0.01^{def}	3.00 ± 0.03^{n}	5.18 ± 0.00^{a}
I (PP)	6.31 ± 0.00^{fghi}	26.93 ± 0.04^{ghi}	27.85 ± 0.08^{c}	11.22 ± 0.05^{jk}	9.76 ± 0.06^{mno}	5.04 ± 0.02^{ab}	4.28 ± 0.04^{hi}
J (PP)	6.35 ± 0.02^{efghi}	26.90 ± 0.06^{ghi}	26.80 ± 0.00^{h}	11.60 ± 0.02^{g}	9.53 ± 0.02^{o}	5.00 ± 0.00^{abcd}	4.66 ± 0.02^{d}
K (PP)	6.56 ± 0.01^{d}	26.41 ± 0.05^{ijk}	27.51 ± 0.13^{def}	11.53 ± 0.04^{ghi}	10.24 ± 0.06^{fghi}	5.03 ± 0.00^{ab}	3.93 ± 0.10^{j}
L (PP)	6.36 ± 0.04^{efghi}	26.18 ± 0.00^{k}	28.25 ± 0.06^{b}	11.57 ± 0.09^{ghi}	10.30 ± 0.08^{efgh}	4.94 ± 0.04^{bcde}	3.86 ± 0.02^{jk}
M (PP)	6.41 ± 0.07^{defgh}	27.20 ± 0.11^{gh}	27.67 ± 0.04^{cd}	10.94 ± 0.02^{k}	9.69 ± 0.10^{mno}	4.87 ± 0.06^{cdefg}	4.45 ± 0.01^{efg}
N (PP)	5.89 ± 0.00^{l}	27.24 ± 0.07^{g}	27.63 ± 0.03^{cde}	11.27 ± 0.02^{ij}	9.97 ± 0.00^{ijklm}	4.85 ± 0.04^{efg}	4.35 ± 0.02^{fghi}
O (PP)	6.18 ± 0.02^{ij}	26.26 ± 0.08^{k}	28.66 ± 0.01^{a}	11.58 ± 0.06^{gh}	10.38 ± 0.11^{defg}	4.82 ± 0.03^{efg}	3.74 ± 0.01^{k}
P (PP)	6.39 ± 0.05^{defgh}	26.55 ± 0.11^{ijk}	27.61 ± 0.08^{cde}	11.46 ± 0.06^{ghij}	10.21 ± 0.04^{fghij}	5.00 ± 0.00^{abc}	3.98 ± 0.01^{j}
Q (PB)	5.96 ± 0.06^{kl}	27.05 ± 0.11^{gh}	26.14 ± 0.04^{i}	12.11 ± 0.15^{f}	10.65 ± 0.06^{cd}	4.76 ± 0.00^{g}	4.19 ± 0.03^{i}
R (PB)	6.27 ± 0.07^{ghij}	30.88 ± 0.00^{b}	21.38 ± 0.12^{m}	13.06 ± 0.02^{cd}	10.10 ± 0.12^{hijkl}	3.88 ± 0.02^{k}	5.01 ± 0.06^{b}
S (PB)	7.18 ± 0.01^{b}	29.02 ± 0.25^{d}	21.12 ± 0.00^{mn}	13.07 ± 0.04^{cd}	11.66 ± 0.12^{a}	3.93 ± 0.03^{k}	4.34 ± 0.02^{fghi}
T (PB)	6.46 ± 0.04^{defg}	28.39 ± 0.05^{ef}	24.53 ± 0.13^{k}	12.61 ± 0.01^{e}	10.38 ± 0.03^{defg}	4.36 ± 0.03^{j}	4.30 ± 0.00^{ghi}
U (PB)	6.43 ± 0.00^{defgh}	27.05 ± 0.00^{gh}	24.42 ± 0.50^{k}	12.94 ± 0.10^{d}	11.23 ± 0.04^{b}	4.51 ± 0.06^{hi}	3.89 ± 0.03^{jk}
V (PB)	7.17 ± 0.02^{b}	27.98 ± 0.01^{f}	21.01 ± 0.04^{n}	13.32 ± 0.10^{bc}	10.56 ± 0.04^{cde}	3.71 ± 0.01^{l}	4.83 ± 0.00^{c}
W (PB)	7.34 ± 0.06^{ab}	30.35 ± 0.06^{c}	19.84 ± 0.00^{o}	13.48 ± 0.16^{b}	10.42 ± 0.05^{defg}	3.37 ± 0.00^{m}	4.91 ± 0.06^{bc}
X (PB)	5.92 ± 0.07^{kl}	27.10 ± 0.22^{gh}	25.96 ± 0.04^{i}	12.11 ± 0.13^{f}	10.60 ± 0.07^{cd}	4.79 ± 0.05^{fg}	4.27 ± 0.02^{hi}
Y (PB)	6.77 ± 0.05^{c}	28.43 ± 0.14^{e}	23.50 ± 0.03^{l}	12.46 ± 0.10^{e}	10.82 ± 0.05^{c}	4.38 ± 0.01^{ij}	4.37 ± 0.04^{efgh}

Note: Sample A - P - cooking oils in plastic pouch (PP).
Sample Q - Y - cooking oils in polyethylene terephthalate (PET) bottle (PB).
Means within each row bearing different superscript letters are significantly different ($p<0.05$).
DAG - diacylglycerols; M - myristic; P - palmitic; S - stearic; O - oleic; L - linoleic.

TABLE 3B. TRIACYLGLYCEROL COMPOSITION (TAG) OF COMMERCIAL PALM COOKING OIL IN PLASTIC POUCH AND POLYETHYLENE TEREPHTHALATE (PET) BOTTLE PACKAGING IN MALAYSIA (continued)

Sample	SOO	PLL	OLO	SOS	OLL	MLP	PPP
A (PP)	2.56 ± 0.04^{cde}	2.46 ± 0.03^{h}	2.00 ± 0.02^{hijklmn}	0.59 ± 0.00^{bc}	0.49 ± 0.00^{defgh}	0.36 ± 0.00^{efghij}	0.23 ± 0.00^{e}
B (PP)	2.61 ± 0.00^{cde}	2.66 ± 0.06^{fgh}	2.01 ± 0.00^{hijkl}	0.61 ± 0.00^{abc}	0.49 ± 0.02^{efgh}	0.40 ± 0.02^{bcdefg}	0.24 ± 0.00d^{e}
C (PP)	2.62 ± 0.00^{cde}	2.53 ± 0.01^{gh}	2.03 ± 0.02^{hij}	0.64 ± 0.02^{ab}	0.47 ± 0.01^{efgh}	0.31 ± 0.00^{jk}	0.24 ± 0.00^{de}
D (PP)	2.65 ± 0.02^{cd}	2.72 ± 0.04^{efg}	2.06 ± 0.00^{ghi}	0.61 ± 0.04^{abc}	0.48 ± 0.00^{efgh}	0.39 ± 0.00^{cdefgh}	0.16 ± 0.02^{f}
E (PP)	2.57 ± 0.04^{cde}	2.52 ± 0.05^{gh}	1.98 ± 0.01^{ijklmn}	0.59 ± 0.00^{bcd}	0.46 ± 0.01^{fgh}	0.35 ± 0.00^{ghij}	0.29 ± 0.02^{c}
F (PP)	2.48 ± 0.02^{efg}	2.61 ± 0.08^{gh}	1.98 ± 0.04^{ijklmn}	0.59 ± 0.00^{bcd}	0.50 ± 0.00^{defgh}	0.35 ± 0.00^{ghij}	0.27 ± 0.01^{cd}
G (PP)	2.54 ± 0.01^{cdef}	2.51 ± 0.03^{gh}	2.01 ± 0.04^{hijklm}	0.60 ± 0.01^{bc}	0.47 ± 0.03^{efgh}	0.34 ± 0.01^{ghij}	0.26 ± 0.00^{cde}
H (PP)	3.00 ± 0.01^{a}	3.32 ± 0.04^{ab}	2.51 ± 0.00^{b}	0.38 ± 0.02^{f}	0.66 ± 0.02^{c}	0.43 ± 0.02^{abc}	0.00 ± 0.00^{g}
I (PP)	2.54 ± 0.01^{cdef}	2.46 ± 0.02^{h}	1.96 ± 0.00^{jklmn}	0.62 ± 0.00^{abc}	0.45 ± 0.01^{gh}	0.34 ± 0.00^{hij}	0.29 ± 0.00^{c}
J (PP)	2.62 ± 0.01^{cde}	2.47 ± 0.08^{h}	2.21 ± 0.03^{de}	0.60 ± 0.00^{bc}	0.82 ± 0.03^{b}	0.26 ± 0.02^{k}	0.22 ± 0.00^{e}
K (PP)	2.48 ± 0.08^{efg}	2.56 ± 0.07^{gh}	1.91 ± 0.01^{mn}	0.61 ± 0.02^{bc}	0.43 ± 0.02^{h}	0.36 ± 0.00^{fghij}	0.47 ± 0.03^{a}
L (PP)	2.37 ± 0.04^{g}	2.57 ± 0.03^{gh}	1.92 ± 0.01^{lmn}	0.61 ± 0.03^{abc}	0.45 ± 0.02^{gh}	0.33 ± 0.00^{ij}	0.33 ± 0.00^{b}
M (PP)	2.59 ± 0.08^{cde}	2.51 ± 0.06^{gh}	1.93 ± 0.02^{klmn}	0.60 ± 0.01^{bc}	0.49 ± 0.04^{efgh}	0.42 ± 0.04^{bcde}	0.26 ± 0.00^{cde}
N (PP)	2.52 ± 0.08^{def}	2.59 ± 0.00^{gh}	2.00 ± 0.02^{hijklmn}	0.60 ± 0.00^{bc}	0.52 ± 0.02^{defg}	0.39 ± 0.00^{cdefgh}	0.23 ± 0.01^{de}
O (PP)	2.40 ± 0.04^{fg}	2.61 ± 0.09^{gh}	1.81 ± 0.04^{o}	0.57 ± 0.03^{bcde}	0.44 ± 0.00^{gh}	0.34 ± 0.02^{hij}	0.24 ± 0.00^{de}
P (PP)	2.54 ± 0.01^{cdef}	2.56 ± 0.00^{gh}	1.90 ± 0.03^{no}	0.58 ± 0.00^{bcde}	0.48 ± 0.03^{efgh}	0.34 ± 0.00^{hij}	0.44 ± 0.00^{a}
Q (PB)	2.55 ± 0.04^{cde}	2.94 ± 0.04^{cde}	2.02 ± 0.06^{hijk}	0.70 ± 0.03^{a}	0.55 ± 0.00^{def}	0.40 ± 0.00^{bcdefg}	0.00 ± 0.00^{g}
R (PB)	2.87 ± 0.01^{ab}	2.86 ± 0.08^{def}	2.26 ± 0.00^{d}	0.53 ± 0.02^{cde}	0.51 ± 0.01^{defgh}	0.43 ± 0.00^{abc}	0.00 ± 0.00^{g}
S (PB)	2.83 ± 0.02^{b}	3.14 ± 0.04^{bc}	2.13 ± 0.00^{efg}	0.55 ± 0.03^{bcde}	0.58 ± 0.00^{cd}	0.48 ± 0.00^{a}	0.00 ± 0.00^{g}
T (PB)	2.67 ± 0.00^{c}	2.91 ± 0.06^{de}	2.00 ± 0.03^{hijklm}	0.56 ± 0.04^{bcde}	0.50 ± 0.05^{defgh}	0.37 ± 0.02^{defghi}	0.00 ± 0.00^{g}
U (PB)	2.59 ± 0.01^{cde}	3.36 ± 0.00^{ab}	2.00 ± 0.01^{hijklmn}	0.61 ± 0.01^{abc}	0.55 ± 0.01^{de}	0.45 ± 0.01^{ab}	0.00 ± 0.00^{g}
V (PB)	2.68 ± 0.02^{c}	3.52 ± 0.08^{a}	2.90 ± 0.02^{a}	0.49 ± 0.05^{e}	1.43 ± 0.03^{a}	0.42 ± 0.01^{bcd}	0.00 ± 0.00^{g}
W (PB)	2.88 ± 0.00^{ab}	3.39 ± 0.11^{a}	2.38 ± 0.01^{c}	0.50 ± 0.04^{de}	0.76 ± 0.00^{b}	0.41 ± 0.01^{bcdef}	0.00 ± 0.00^{g}
X (PB)	2.54 ± 0.03^{cdef}	2.94 ± 0.02^{cde}	2.17 ± 0.01^{def}	0.59 ± 0.02^{bcd}	0.66 ± 0.04^{c}	0.39 ± 0.00^{cdefgh}	0.00 ± 0.00^{g}
Y (PB)	2.65 ± 0.02^{cd}	2.97 ± 0.02^{cd}	2.08 ± .01^{fgh}	0.60 ± 0.01^{bc}	0.55 ± 0.00^{de}	0.45 ± 0.00^{ab}	0.00 ± 0.00^{g}

Note: Sample A - P - cooking oils in plastic pouch (PP).
Sample Q - Y - cooking oils in polyethylene terephthalate (PET) bottle (PB).
Means within each row bearing different superscript letters are significantly different ($p<0.05$).
M - myristic; P - palmitic; S - stearic; O - oleic; L - linoleic.

TABLE 3C. TRIACYLGLYCEROL COMPOSITION (TAG) GROUPING OF COMMERCIAL PALM-BASED COOKING OIL IN PLASTIC POUCH AND POLYETHYLENE TEREPHTHALATE (PET) BOTTLE PACKAGING IN MALAYSIA

Sample	UUU	SUU	SUS	SSS
A (PP)	6.76 ± 0.03^{ij}	43.00 ± 0.07^{no}	43.58 ± 0.15^{bc}	0.23 ± 0.01^{e}
B (PP)	6.91 ± 0.05^{efghi}	43.69 ± 0.01^{ij}	43.07 ± 0.18^{def}	0.24 ± 0.01^{de}
C (PP)	6.96 ± 0.01^{efgh}	43.84 ± 0.04^{i}	42.71 ± 0.04^{fg}	0.24 ± 0.01^{de}
D (PP)	7.04 ± 0.01^{ef}	46.14 ± 0.05^{g}	40.57 ± 0.04^{k}	0.16 ± 0.02^{f}
E (PP)	6.70 ± 0.08^{j}	43.40 ± 0.01^{jklm}	43.12 ± 0.12^{de}	0.29 ± 0.02^{c}
F (PP)	6.75 ± 0.01^{ij}	43.42 ± 0.02^{jkl}	43.08 ± 0.03^{def}	0.27 ± 0.01^{cd}
G (PP)	6.81 ± 0.08^{ghij}	43.48 ± 0.01^{jk}	42.94 ± 0.11^{efg}	0.25 ± 0.01^{cde}
H (PP)	8.35 ± 0.02^{b}	52.27 ± 0.08^{a}	31.94 ± 0.07^{p}	0.00 ± 0.00
I (PP)	6.68 ± 0.03^{j}	43.14 ± 0.01^{lmno}	43.60 ± 0.02^{bc}	0.29 ± 0.01^{c}
J (PP)	7.69 ± 0.04^{d}	43.59 ± 0.01^{ij}	42.17 ± 0.01^{i}	0.22 ± 0.00^{e}
K (PP)	6.27 ± 0.09^{kl}	42.97 ± 0.03^{nop}	43.74 ± 0.16^{b}	0.47 ± 0.03^{a}
L (PP)	6.22 ± 0.01^{l}	42.68 ± 0.09^{p}	44.42 ± 0.14^{a}	0.33 ± 0.00^{b}
M (PP)	6.86 ± 0.04^{fghij}	43.23 ± 0.16^{klmn}	43.24 ± 0.04^{cde}	0.26 ± 0.00^{cde}
N (PP)	6.86 ± 0.02^{fghij}	43.61 ± 0.03^{ij}	43.42 ± 0.04^{bcd}	0.23 ± 0.01^{de}
O (PP)	5.99 ± 0.05^{m}	42.84 ± 0.16^{op}	44.77 ± 0.08^{a}	0.24 ± 0.01^{de}
P (PP)	6.36 ± 0.04^{kl}	43.10 ± 0.06^{mno}	43.73 ± 0.02^{b}	0.44 ± 0.01^{a}
Q (PB)	6.76 ± 0.04^{ij}	44.65 ± 0.04^{h}	42.64 ± 0.01^{gh}	0.00 ± 0.00^{g}
R (PB)	7.76 ± 0.04^{d}	49.66 ± 0.11^{c}	36.30 ± 0.01^{n}	0.00 ± 0.00^{g}
S (PB)	7.04 ± 0.01^{ef}	48.05 ± 0.16^{d}	37.73 ± 0.18^{m}	0.00 ± 0.00^{g}
T (PB)	6.79 ± 0.08^{hij}	46.57 ± 0.03^{f}	40.19 ± 0.15^{k}	0.00 ± 0.00^{g}
U (PB)	6.43 ± 0.03^{k}	45.93 ± 0.08^{g}	41.22 ± 0.05^{j}	0.00 ± 0.00^{g}
V (PB)	9.15 ± 0.04^{a}	47.50 ± 0.02^{e}	39.19 ± 0.04^{n}	0.00 ± 0.00^{g}
W (PB)	8.04 ± 0.06^{c}	50.10 ± 0.01^{b}	34.53 ± 0.01^{o}	0.00 ± 0.00^{g}
X (PB)	7.09 ± 0.04^{e}	44.68 ± 0.14^{h}	42.31 ± 0.11^{hi}	0.00 ± 0.00^{g}
Y (PB)	7.00 ± 0.02^{efg}	46.50 ± 0.04^{f}	39.74 ± 0.01^{l}	0.00 ± 0.00^{g}

Note: Sample A-P - cooking oils in plastic pouch (PP).
Sample Q-Y - cooking oils in polyethylene terephthalate (PET) bottle (PB).
UUU - unsaturated-unsaturated-unsaturated.
SUU - saturated-unsaturated-unsaturated
SUS - saturated-unsaturated-saturated.
SSS - saturated-saturated-saturated.

TAG of the cooking oils in both plastic pouch and PET bottle were significantly different ($p<0.05$) too based on 2-sample t-test (*Table 3d*). Average UUU and SUU TAG of cooking oil in plastic bottle were higher (better) than those in plastic pouch. However, the average SUS TAG of cooking oil in PET bottle was lower (better) than those in plastic pouch. The 2-sample t-test for average SSS cannot be conducted as PET bottle has similar average SSS value.

TABLE 3D. 2-SAMPLE T-TEST OF TRIACYLGLYCEROL COMPOSITION (TAG) GROUP OF COMMERCIAL PALM-BASED COOKING OIL IN PLASTIC POUCH AND POLYETHYLENE TEREPHTHALATE (PET) BOTTLE PACKAGING IN MALAYSIA

TAG group	Mean (%)		p-value
	Plastic pouch	PET bottle	
UUU	6.82 ± 0.56	7.34 ± 0.82	0.03
SUU	44.02 ± 2.30	47.07 ± 1.89	0.00
SUS	52.50 ± 2.92	38.98 ± 2.83	0.00
SSS	-	-	-

Note: p-value<0.05 indicates that there is significant different between cooking oil in plastic pouch and PET bottle.
UUU - unsaturated-unsaturated-unsaturated.
SUU - saturated-unsaturated-unsaturated.
SUS - saturated-unsaturated-saturated.
SSS - saturated-saturated-saturated.

Vitamin E

Vitamin E consist of tocopherols and tocotrienols isomers that is fat soluble having potent anti-oxidative and other health-promoting properties (Sundram *et al*., 2003). Good dietary sources of vitamin E include vegetable oils and nuts, such as almonds, peanuts and hazelnuts.

Palm oil is rich in vitamin E (600-1000 ppm in crude palm oil). Palm oil's vitamin E is rich in tocotrienols (75%-80% of the total vitamin E) which seldom found in vegetable oil (Choo *et al*., 1996; Ng *et al*., 2004). The vitamin E provides oxidative stability to the oil (Sundram *et al*., 2003) as well as during heating and frying by decelerating oxidative degradation (Matthäus *et al.,* 2009). Many studies suggested that tocotrienols is a more potent antioxidant compared to tocopherols (Kamar *et al*., 1997). Many studies revealed that palm vitamin E demonstrates numerous health-benefits besides anti-oxidant. This includes cardioprotective, nephroprotective, neuroprotective, hepatoprotective, anti-cancer, anti-diabetic, cancer-suppression properties and bone metabolism positive effect (Siddiqui *et al*., 2010; 2013; Norazlina *et al*., 2010; Sen *et al*., 2010; Azlina *et al*., 2005; Mutalib *et al*., 2003; Nesaretnam *et al*., 1992; 1998; Goh *et al*., 1994; Serbinova and Packer, 1994; Ngah *et al*., 1991).

Total vitamin E, total tocotrienols and total tocopherols of cooking oils in the plastic pouch were in the range of 539.17-949.16 ppm, 443.58-640.21 ppm and 177.99-269.14 ppm, accordingly (*Table 4a*). The total vitamin E, total tocotrienols and total tocopherols of cooking oils in the PET bottle on the other hand were in the range of 498.02-856.00 ppm, 364.26-705.11 ppm and 133.76-235.65 ppm respectively. The overall range of total vitamin E, total tocotrienols and total tocopherols in commercial cooking oil (plastic pouch and PET bottle) were 498.02-949.16 ppm, 364.26-705.11 ppm and 133.76-269.14 ppm, respectively and were significantly different ($p<0.05$) based on ANOVA. However, there were cooking oils that were not significantly different from each other. Vitamin E in RBD palm olein was 561 ppm as reported by Nagendran *et al*. (2000). Sundram *et al*. (2001), on the other hand, disclosed that vitamin E in RBD palm olein was 824.3 ppm with 196.6 ppm of tocopherol and 627.7 ppm of tocotrienol. The level of tocotrienols decreases with refining when compared with crude palm oil. Sample E (plastic pouch) has the highest amount of total vitamin E and tocopherols while sample V (PET bottle) has the highest total tocotrienols. Sample Q (PET bottle) has the lowest amount of total vitamin E, tocotrienols and tocopherols. The total vitamin E of sample Q (498.02 ppm) is quite low if were to compare with the study by Sundram and Noor (2001). Apart from sample Q, other commercial cooking oils have considerable total vitamin E ranging from 539.17-949.19 ppm. Based on 2-sample t-test, $p<0.05$ was obtained for the average total tocopherols for cooking oils in both plastic pouch and PET bottle packagings which indicated that these packagings were significantly different with plastic pouch having higher (better) total tocopherols (*Table 4b*). However, average total

TABLE 4A. TOTAL TOCOLS COMPOSITION OF COMMERCIAL PALM-BASED COOKING OIL IN PLASTIC POUCH AND POLYETHYLENE TEREPHTHALATE (PET) BOTTLE PACKAGING IN MALAYSIA

Sample	Total tocopherols (ppm)	Total tocotrienols (ppm)	Total vitamin E (tocols) (ppm)
A (PP)	235.91 ± 4.07^{b}	640.21 ± 11.31^{b}	876.12 ± 15.38^{b}
B (PP)	230.49 ± 0.64^{bcd}	603.06 ± 1.13^{de}	833.55 ± 1.77^{cdef}
C (PP)	234.60 ± 4.20^{bc}	617.92 ± 11.19^{cde}	852.52 ± 15.39^{bcd}
D (PP)	231.29 ± 3.75^{bcd}	583.94 ± 10.65^{efg}	815.23 ± 14.39^{defg}
E (PP)	269.14 ± 6.55^{a}	608.01 ± 16.23^{a}	949.16 ± 22.78^{a}
F (PP)	226.41 ± 1.70^{bcde}	580.80 ± 3.58^{efg}	807.22 ± 5.28^{efg}
G (PP)	195.59 ± 2.81^{ij}	443.58 ± 6.56^{o}	539.17 ± 9.36^{m}
H (PP)	221.77 ± 5.59^{def}	540.99 ± 13.65^{hijkl}	762.77 ± 19.23^{hi}
I (PP)	213.20 ± 3.58^{fg}	569.95 ± 9.30^{fgh}	783.15 ± 12.87^{gh}
J (PP)	230.68 ± 3.97^{bcd}	556.93 ± 9.64^{ghijk}	787.61 ± 13.61^{gh}
K (PP)	200.04 ± 1.26^{hi}	533.98 ± 3.46^{jklm}	734.02 ± 4.47^{ij}
L (PP)	197.52 ± 5.97^{hi}	530.71 ± 2.63^{klm}	728.23 ± 7.95^{ijk}
M (PP)	228.83 ± 2.89^{bcd}	564.57 ± 8.73^{fghi}	793.41 ± 11.57^{fgh}
N (PP)	236.95 ± 1.77^{b}	582.25 ± 4.71^{efg}	819.20 ± 6.46^{cdefg}
O (PP)	177.99 ± 2.47^{kl}	509.80 ± 7.04^{mn}	687.79 ± 9.51^{kl}
P (PP)	208.97 ± 4.48^{gh}	520.74 ± 12.29^{lm}	729.71 ± 16.77^{ij}
Q (PB)	133.76 ± 1.51^{m}	364.26 ± 4.45^{p}	498.02 ± 5.95^{n}
R (PB)	216.83 ± 5.13^{efg}	639.18 ± 15.67^{bc}	856.00 ± 20.79^{bc}
S (PB)	198.32 ± 1.39^{hi}	560.97 ± 3.96^{ghij}	759.29 ± 5.27^{hij}
T (PB)	169.36 ± 3.22^{l}	484.77 ± 6.66^{n}	654.13 ± 9.88^{lm}
U (PB)	184.95 ± 1.74^{jk}	535.93 ± 5.44^{ijklm}	720.88 ± 7.13^{jk}
V (PB)	216.89 ± 1.72^{efg}	705.11 ± 7.47^{a}	922.00 ± 9.06^{a}
W (PB)	235.65 ± 5.68^{b}	585.91 ± 13.72^{efg}	821.56 ± 19.39^{cdefg}
X (PB)	233.72 ± 1.76^{bc}	610.02 ± 6.10^{cde}	843.74 ± 7.84^{bcde}
Y (PB)	233.40 ± 4.49^{cdef}	592.89 ± 13.74^{def}	816.29 ± 18.23^{cdefg}

Note: Sample A-P - cooking oils in plastic pouch (PP).
Sample Q-Y - cooking oils in polyethylene terephthalate (PET) bottle (PB).
Means within each row bearing different superscript letters are significantly different ($p<0.05$).

TABLE 4B. 2-SAMPLE T-TEST OF TOTAL TOCOLS COMPOSITION OF COMMERCIAL PALM-BASED COOKING OIL IN PLASTIC POUCH AND POLYETHYLENE TEREPHTHALATE (PET) BOTTLE PACKAGING IN MALAYSIA

Tocols	Mean (ppm)		p-value
	Plastic pouch	PET bottle	
Tocopherols	221.20 ± 21.50	201.40 ± 32.50	0.01
Tocotrienols	566.2 ± 55.10	564.30 ± 94.00	0.93
Vitamin E	787.40 ± 74.3	766.00 ± 123.00	0.41

Note: p-value<0.05 indicates that there is significant different between cooking oil in plastic pouch and PET bottle.

vitamin E (tocols) and total tocotrienols of cooking oils in both packaging were insignificantly different ($p>0.05$) and thus, were comparable.

Iodine Value

IV is a measure of degree of unsaturation of oils and fats. The higher the IV, the higher the unsaturated fatty acids content of the oils and fats (Yousefi *et al*., 2013) which resulted to higher incident of oxidation (Nawal *et al*., 2014) and frequency of oil discarded (Orthoefer and List, 2007). IV of cooking oils in both plastic pouch and PET bottle collected were ranged from 55.50%-63.44% and 58.33%-62.89%, respectively (*Table 5a*). Based on ANOVA, the IV of cooking oils in both packagings were significantly different ($p<0.05$) resulting to overall IV ranging from 55.50-63.44. However, there were cooking oils that were not significantly different from each other. The table also showed that most cooking oils in PET bottles have higher IV compared to cooking oils in pouches, except for sample H. Malaysian Standard for Palm Olein - MS 816:2007 (Department of Standards Malaysia, 2007) and PORAM has set a minimum standard of IV for RBD palm olein of 56. Alireza *et al*. (2010) reported that RBD palm olein bought in supermarket in Selangor, Malaysia has IV of 57.27 (packaging type was not mentioned) which was within PORAM specification. Two out of 25 cooking oils in plastic pouch had IV lower than the minimum requirement. However, their IVs were very close to 56 with IVs of 55.50 and 55.98. Notwithstanding this, sample H (plastic pouch) has the highest IV among all cooking oils in plastic pouches and PET bottles, with IV of 63.44. Samples V, W, R and S (PET bottle) had IV more than 60. An IV of more than 60 is considered as superolein, which is palm olein that has went through double fractionation. However, Malaysian Standard for Palm Olein - MS 816:2007 (Department of Standards Malaysia, 2007) indicates that the maximum observed range for palm olein is 59.1 in which IV of more than 59.1 maybe considered as superolein. By looking only at the average IV, the 2-sample t-test concluded that cooking oils in both plastic pouch and PET bottle was significantly different ($p<0.05$) (*Table 5b*). The commercial palm cooking oil in PET bottle has higher average IV (better) than in plastic pouch.

Cloud Point

The point when oil begins to become cloudy and no longer resist crystallisation is referred to as cloud point. As a common physical parameter, cloud point is always used to obtain rapid assessment of the oil's cold stability (Hasmadi *et al*., 2002). Cloud point is associated with unsaturation of oil. Lower cloud

TABLE 5A. IODINE VALUE (BY CALCULATION) OF COMMERCIAL PALM-BASED COOKING OIL IN PLASTIC POUCH AND POLYETHYLENE TEREPHTHALATE (PET) BOTTLE PACKAGING IN MALAYSIA

Sample	Calculated iodine (by calculation)
A (PP)	56.77 ± 0.5^{hi}
B (PP)	56.87 ± 0.18^{hi}
C (PP)	57.12 ± 0.02^{h}
D (PP)	58.38 ± 0.05^{g}
E (PP)	56.85 ± 0.01^{hi}
F (PP)	56.88 ± 0.02^{hi}
G (PP)	56.99 ± 0.15^{h}
H (PP)	63.44 ± 0.10^{h}
I (PP)	57.42 ± 0.05^{cde}
J (PP)	58.90 ± 0.12^{fg}
K (PP)	57.25 ± 0.00^{h}
L (PP)	55.50 ± 0.00^{j}
M (PP)	57.12 ± 0.70^{h}
N (PP)	56.92 ± 0.50^{n}
O (PP)	55.98 ± 0.00^{ij}
P (PP)	59.91 ± 0.85^{de}
Q (PB)	59.60 ± 0.06^{def}
R (PB)	60.91 ± 0.59^{bc}
S (PB)	60.48 ± 0.11^{cd}
T (PB)	59.99 ± 0.20^{efg}
U (PB)	59.83 ± 0.00^{de}
V (PB)	62.89 ± 0.27^{a}
W (PB)	61.81 ± 0.00^{b}
X (PB)	58.33 ± 0.20^{g}
Y (PB)	59.42 ± 0.23^{ef}

Note: Sample A - P - cooking oils in plastic pouch (PP).
Sample Q-Y - cooking oils in polyethylene terephthalate (PET) bottle (PB).
Means within each row bearing different superscript letters are significantly different ($p<0.05$).

TABLE 5B. 2-SAMPLE T-TEST OF IODINE VALUE (BY CALCULATION) OF COMMERCIAL PALM-BASED COOKING OIL IN PLASTIC POUCH AND POLYETHYLENE TEREPHTHALATE (PET) BOTTLE PACKAGING IN MALAYSIA

Mean of IV		p-value
Plastic pouch	PET bottle	
57.64 ± 1.85	60.26 ± 1.38	0.00

Note: p-value<0.05 indicates that there is significant different between cooking oil in plastic pouch and PET bottle.

point reveals that the oil is less saturated (Zaliha *et al*., 2003). The range of cloud point of cooking oils in both plastic pouch and PET bottle were between 4.00ºC-9.17ºC and 4.33ºC-8.00ºC, respectively (*Table 6a*). Therefore, based on ANOVA, cloud point of all cooking oils in Malaysia (plastic pouch and PET bottle) was significantly different ($p<0.05$) with overall range of between 4.00ºC-9.17ºC. According to Teoh *et al*. (2005), cloud point of palm olein (from refineries in Selangor, Malaysia) is about 11.5ºC while superolein is 5.0ºC. Palm olein has higher cloud point than soft oil (*i.e.* canola oil) as palm olein has higher content of saturated fatty acid which makes palm olein more stable for deep frying. It was also disclosed by Hasmadi *et al*. (2002) that cloud points of palm olein through RBD palm oil's fractionation at 15ºC, 18ºC and 21ºC, gave value of between 7.8ºC-8.9ºC. Notwithstanding this, a study by Chnadhapuram and Sunkireddy (2012) showed a cloud point of 13ºC for palm olein (from a study in Karnataka India). This showed that cloud point of the commercial cooking oils in Malaysia were below than that reported by Teoh *et al.* (2005) and Chnadhapuram and Sunkireddy (2012) and most of them were in the range reported by Hasmadi *et al*. (2002). Samples H and L (plastic pouch) have the lowest and highest cloud point accordingly. The 2-sample t-test provided $p<0.05$ (significantly different) of average cloud point for both cooking oil in plastic pouch and PET bottle (*Table 6b*). The test also showed that average cloud point in PET bottle was lower (better) than in plastic pouch. There was significant correlation of cloud point with FAC and TAG. Based on Pearson correlation, cloud point has negative correlation with FAC (monounsaturated and polyunsaturated) and TAG (UUU and SUU) while showing positive correlation with FAC (total saturated) and TAG (SUS and SSS).

TABLE 6A. 2-SAMPLE T-TEST OF CLOUD POINT OF COMMERCIAL PALM-BASED COOKING OIL IN PLASTIC POUCH AND POLYETHYLENE TEREPHTHALATE (PET) BOTTLE PACKAGING IN MALAYSIA

Sample	Cloud point (°C)
A (PP)	9.00 ± 0.00^{a}
B (PP)	8.00 ± 0.00^{b}
C (PP)	8.83 ± 0.29^{a}
D (PP)	6.00 ± 0.00^{d}
E (PP)	8.00 ± 0.00^{b}
F (PP)	8.00 ± 0.00^{b}
G (PP)	9.00 ± 0.00^{a}
H (PP)	4.00 ± 0.00^{g}
I (PP)	8.00 ± 0.00^{b}
J (PP)	8.00 ± 0.00^{b}
K (PP)	8.00 ± 0.00^{b}
L (PP)	9.17 ± 0.29^{a}
M (PP)	8.83 ± 0.29^{a}
N (PP)	7.67 ± 0.29^{b}
O (PP)	8.83 ± 0.29^{a}
P (PP)	8.67 ± 0.29^{a}
Q (PB)	6.67 ± 0.29^{c}
R (PB)	4.33 ± 0.29^{g}
S (PB)	5.00 ± 0.00^{ef}
T (PB)	8.00 ± 0.00^{b}
U (PB)	6.83 ± 0.29^{c}
V (PB)	5.00 ± 0.00^{ef}
W (PB)	4.50 ± 0.00^{fg}
X (PB)	6.67 ± 0.29^{c}
Y (PB)	5.33 ± 0.29^{e}

Note: Sample A-P - cooking oils in plastic pouch (PP).
Sample Q-Y - cooking oils in polyethylene terephthalate (PET) bottle (PB).
Means within each row bearing different superscript letters are significantly different ($p<0.05$).

TABLE 6B. 2-SAMPLE T-TEST OF CLOUD POINT OF COMMERCIAL PALM-BASED COOKING OIL IN PLASTIC POUCH AND POLYETHYLENE TEREPHTHALATE (PET) BOTTLE PACKAGING IN MALAYSIA

Mean of cloud point (°C)		p-value
Plastic pouch	PET bottle	
8.00 ± 1.30^{a}	5.81 ± 1.23^{b}	0.00

Note: p-value<0.05 indicates that there is significant different between cooking oil in plastic pouch and PET bottle.

Smoke Point

Smoke point occurs at the temperature when oil started to produce bluish smoke continuously, indicating fat breakdown to glycerol and FFA. Further breakdown of glycerol produces 2-propenal which is one of the major components for the bluish smoke (Katragadda *et al*., 2010). Matthäus, 2006 reported that the amount of FFA, DAG, monoacylglycerols (MAG) and volatile compounds which are the component having low molecular weight, influenced the amount of smoke produced. In this regards, better frying oil corresponds to higher smoke point and oils that have low thermal stability will have low smoke points.

Table 7a shows the smoke point of cooking oils in both plastic pouch and PET bottle. The smoke point of cooking oil in plastic pouch and PET bottle were in the range of 190.00ºC-218.00ºC and 184.50ºC-213.50ºC, respectively. Based on ANOVA, all cooking oils in plastic pouch and PET bottle were significantly different ($p<0.05$) with overall range of between 184.50ºC-218.00°C. However, there were

TABLE 7A. SMOKE POINT OF COMMERCIAL PALM-BASED COOKING OIL IN PLASTIC POUCH AND POLYETHYLENE TEREPHTHALATE (PET) BOTTLE PACKAGING IN MALAYSIA

Sample	Smoke point (°C)
A (PP)	190.00 ± 0.00^{gh}
B (PP)	214.50 ± 0.71^{abc}
C (PP)	200.00 ± 0.00^{cdefgh}
D (PP)	210.50 ± 0.71^{abcde}
E (PP)	208.00 ± 0.00^{abcdef}
F (PP)	202.00 ± 0.00^{bcdefg}
G (PP)	206.00 ± 0.00^{abcdef}
H (PP)	212.00 ± 0.00^{abcd}
I (PP)	216.00 ± 0.00^{ab}
J (PP)	218.00 ± 0.00^{a}
K (PP)	212.50 ± 19.09^{abcd}
L (PP)	200.50 ± 0.71^{bcdefg}
M (PP)	206.50 ± 0.71^{abcdef}
N (PP)	212.50 ± 0.71^{abcd}
O (PP)	207.00 ± 0.00^{abcdef}
P (PP)	$203.00 \pm 0.00^{abcdefg}$
Q (PB)	200.50 ± 0.71^{bcdefg}
R (PB)	197.00 ± 0.00^{defgh}
S (PB)	213.50 ± 0.71^{abc}
T (PB)	194.00 ± 0.00^{fgh}
U (PB)	190.00 ± 0.00^{gh}
V (PB)	184.50 ± 0.71^{h}
W (PB)	195.50 ± 0.71^{efgh}
X (PB)	194.00 ± 0.00^{fgh}
Y (PB)	$203.50 \pm 0.71^{abcdefg}$

Note: Sample A-P - cooking oils in plastic pouch (PP).
Sample Q-Y - cooking oils in polyethylene terephthalate (PET) bottle (PB).
Means within each row bearing different superscript letters are significantly different ($p<0.05$).

cooking oils that were not significantly different from each other. Two studies reported that RBD palm olein normally has smoke point of between 212°C-227°C (Ahmad Tarmizi *et al.*, 2016b; Ahmad Tarmizi and Ismail, 2014; 2008). Sample J (plastic pouch) has the highest smoke point followed by sample I (plastic pouch), sample B (plastic pouch) and sample S (PET bottle). Samples that have smoke point below 200°C were samples A (plastic pouch) and R, T, U, V, W and X (PET bottle). Ahmad Tarmizi and Ismail (2007) and Ismail (2001) reported that initial smoke point of any oil for frying should be higher than 215°C in which this is the recommendation from the food industry. Furthermore, Katragadda *et al*. (2010) suggested that smoke point of below 200°C is not suited for deep frying. Cooking oil in PET bottle has higher samples of smoke point value below 200°C and therefore, might be less superior than the cooking oil in pouch packaging. $p<0.05$ for average smoke point was observed for cooking oils in both plastic pouch and PET bottle through the 2-sample t-test (*Table 7b*). This showed that average cooking oils in both packagings were significantly different with cooking oil in plastic pouch, having higher (better) smoke point. Based on Pearson correlation, there were significant correlation between smoke point, SSS TAG and polyunsaturated FAC. Smoke point showed negative and positive correlation with SSS TAG and polyunsaturated FAC, respectively.

TABLE 7B. 2-SAMPLE T-TEST OF SMOKE POINT OF COMMERCIAL PALM-BASED COOKING OIL IN PLASTIC POUCH AND POLYETHYLENE TEREPHTHALATE (PET) BOTTLE PACKAGING IN MALAYSIA

Mean of smoke point (°C)		p-value
Plastic pouch	PET bottle	
207.44 ± 7.87^{a}	196.94 ± 8.07^{b}	0.00

Note: p-value<0.05 indicates that there is significant different between cooking oil in plastic pouch and PET bottle.

Colour

Colour is a common parameter to determine the oil quality. It has been broadly used as a guide of the quality of the cooking oil (Maskan, 2003). The oil darkening occurs due to the formations of the ketones, hydroperoxides, conjugated dienoic acids and hydroxides (Farhoosh *et al*., 2009). However, the darkening of the oil is not merely associated with the oxidative degradation. The colour of the palm-based oils is naturally darker than the other vegetable oils (Che Man and Tan, 1999). *Table 8a* shows that the colour range of cooking oil in plastic pouch were 2.05-3.20 Red, 10.20-31.00 Yellow, 0.00-0.20 Neutral and 0.01 Blue while for PET bottle were 2.10-4.00 Red, 10.00-40.00 Yellow and 0.00-0.15 Neutral. Based on ANOVA, the colour of all cooking oils (plastic pouch and PET bottle) was significantly different ($p<0.05$) with overall range of 2.05-4.00 Red, 10.00-40.00 Yellow, 0.00-0.20 Neutral and 0.01 Blue. However, there were cooking oils that were not significantly different from each other. The maximum colour of RBD palm olein set by the Malaysian Standard for Cooking Oil - MS 682:2004 (Department of Standards Malaysia, 2004) is 4.00 Red and 40.00 Yellow for unblended oil and 6.00 Red and 60.00 Yellow for blended oil. The Malaysian Standard for Palm Olein – MS 816:2007 (Department of Standard Malaysia, 2007) and PORAM on the other hand, has set maximum colour value of 3.00 Red. All of the cooking oils met the specification by Malaysian Standard of Cooking Oil - MS 682:2004 (Department of Standards Malaysia, 2004). Eleven

samples out of 25 cooking oil samples had red value beyond the limit set by Malaysian Standard for Palm Olein – MS 816:2007 (Department of Standards Malaysia, 2007) and PORAM in which five samples were in plastic pouch while six samples were in PET bottle. Ahmad Tarmizi *et al.* (2016b) also confirmed that the colour (red) values of palm oil, single- and double- fractionated palm olein and palm-based shortening were in the range of 2.10-3.10 Red. Sample V (PET bottle) had the highest red while sample I (plastic pouch) had the lowest red value. Karimah (2005) reported that the colour of standard palm olein was 2.60 Red compared to special quality palm olein which was 1.20 Red. Results in *Table 8a* shows that 13 out of 25 samples had red value below 3.00 Red. The highest and lowest yellow values were detected in PET bottle which were sample U (40.00 Yellow) and W (10.00 Yellow), respectively. Karimah (2005) claimed that the yellow value of special quality of palm olein is 12 Yellow. The difference in the colour of palm olein is affected from the refining process. Crude palm oil is refined to obtain desirable attributes such as neutral taste, light colour and stable from oxidation (Gibon *et al*., 2007; Sampaio *et al*., 2011). The refining process includes bleaching and deodorisation/ deacidification step which eliminates the colour of the crude palm oil (Silva *et al*., 2014). Rossi *et al*. (2001) added that the colour of the finished palm oil is totally depending on the temperature as compared to the treatment with adsorbent clays and synthetic silica. It can be concluded from the 2-sample t-test that the average colour (red, yellow, neutral and blue) of cooking oil in both plastic pouch and PET bottle were comparable (p>0.05) (*Table 8b*).

TABLE 8A. COLOUR OF COMMERCIAL PALM-BASED COOKING OIL IN PLASTIC POUCH AND POLYETHYLENE TEREPHTHALATE (PET) BOTTLE PACKAGING IN MALAYSIA

Sample	Red	Yellow	Neutral	Blue
A (PP)	3.20 ± 0.00^{bc}	20.10 ± 0.00^{bcd}	0.10 ± 0.00^{abc}	ND
B (PP)	2.25 ± 0.07^{gh}	10.20 ± 0.28^{d}	0.05 ± 0.07^{bc}	ND
C (PP)	3.10 ± 0.00^{bc}	20.00 ± 0.00^{bcd}	0.00 ± 0.00^{c}	ND
D (PP)	2.45 ± 0.07^{efgh}	12.00 ± 0.00^{d}	0.10 ± 0.00^{abc}	ND
E (PP)	3.10 ± 0.00^{bc}	31.00 ± 1.41^{ab}	0.20 ± 0.00^{a}	ND
F (PP)	2.85 ± 0.21^{cdef}	21.00 ± 1.41^{bcd}	0.00 ± 0.00^{c}	ND
G (PP)	3.00 ± 0.00^{bcd}	15.50 ± 6.36^{bcd}	0.00 ± 0.00^{c}	0.01 ± 0.00
H (PP)	2.25 ± 0.07^{gh}	30.50 ± 13.44^{abc}	0.15 ± 0.07^{ab}	ND
I (PP)	2.05 ± 0.07^{h}	20.50 ± 4.95^{bcd}	0.00 ± 0.00^{c}	ND
J (PP)	2.80 ± 0.42^{cdef}	30.50 ± 13.44^{abc}	0.10 ± 0.00^{abc}	ND
K (PP)	2.90 ± 0.00^{cde}	30.00 ± 0.00^{abc}	0.15 ± 0.07^{ab}	ND
L (PP)	2.40 ± 0.14^{fgh}	20.10 ± 0.00^{bcd}	0.00 ± 0.00^{c}	ND
M (PP)	3.15 ± 0.07^{bc}	30.00 ± 0.00^{abc}	0.10 ± 0.00^{abc}	ND
N (PP)	2.15 ± 0.07^{gh}	20.00 ± 0.00^{bcd}	0.10 ± 0.00^{abc}	ND
O (PP)	2.40 ± 0.14^{fgh}	13.50 ± 0.70^{cd}	0.00 ± 0.00^{c}	ND
P (PP)	$3.10 \pm 0.00b^{c}$	30.00 ± 0.00^{abc}	0.00 ± 0.00^{c}	ND
Q (PB)	3.10 ± 0.00^{bc}	26.50 ± 4.95^{abcd}	0.10 ± 0.00^{abc}	ND
R (PB)	3.40 ± 0.14^{b}	30.00 ± 0.00^{abc}	0.05 ± 0.07^{bc}	ND
S (PB)	2.10 ± 0.00^{h}	10.10 ± 0.00^{d}	0.10 ± 0.00^{abc}	ND
T (PB)	3.10 ± 0.00^{bc}	23.00 ± 1.41^{abcd}	0.10 ± 0.00^{abc}	ND
U (PB)	3.15 ± 0.07^{bc}	40.00 ± 0.00^{a}	0.10 ± 0.00^{abc}	ND
V (PB)	4.00 ± 0.00^{a}	20.60 ± 0.57^{bcd}	0.00 ± 0.00^{c}	ND
W (PB)	2.60 ± 0.14^{defg}	10.00 ± 0.00^{d}	0.00 ± 0.00^{c}	ND
X (PB)	3.00 ± 0.14^{bcd}	30.15 ± 0.21^{abc}	0.05 ± 0.07^{bc}	ND
Y (PB)	2.30 ± 0.00^{gh}	20.05 ± 0.07^{bcd}	0.15 ± 0.07^{ab}	ND

Note: Sample A-P - cooking oils in plastic pouch (PP).
Sample Q-Y - cooking oils in polyethylene terephthalate (PET) bottle (PB).
Means within each row bearing different superscript letters are significantly different (p<0.05).

TABLE 8B. 2-SAMPLE T-TEST OF COLOUR OF COMMERCIAL PALM-BASED COOKING OIL IN PLASTIC POUCH AND POLYETHYLENE TEREPHTHALATE (PET) BOTTLE PACKAGING IN MALAYSIA

Colour	Mean		p-value
	Plastic pouch	PET bottle	
Red	2.70 ± 0.41	2.97 ± 0.56	0.08
Yellow	22.18 ± 8.05	23.38 ± 9.48	0.66
Neutral	0.07 ± 0.07	0.07 ± 0.06	0.72

Note: p-value<0.05 indicates that there is significant different between cooking oil in plastic pouch and PET bottle.

Polar Compound

Deteriorative measurement of cooking oil is mostly conducted through polar compound analysis (Mohamed Sulieman *et al*., 2006) especially for in-used and discarded frying oil as it is non-volatile and thus, exhibit major reactions in the oil. Dobarganes *et al*. (2003) described that polar compound may consist of oxidised and polymerised TAG, DAG and FFA. Thus, it also includes hydroperoxides, aldehydes, acids, alcohols, ketones and epoxides (Melton *et al*., 1994). Slower accumulation of polar compound in heated oil without food compared to the addition of food was reported by Chen *et al.* (2013).

Polar compound of cooking oils in both plastic pouch and PET bottle were 6.02%-8.65% and 6.38%-8.43%, accordingly (*Table 9a*). Overall polar compound of the cooking oils in both packagings in Malaysia were found to be in the range of 6.02%-8.65% and they were significantly different (p<0.05) from one another based on ANOVA. However, there were cooking oils that were not significantly different from each other. Polar compound of fresh palm olein was reported to be 9.8% by Tabee *et*

TABLE 9A. POLAR COMPOUND OF COMMERCIAL PALM-BASED COOKING OIL IN PLASTIC POUCH AND POLYETHYLENE TEREPHTHALATE (PET) BOTTLE PACKAGING IN MALAYSIA

Sample	Polar compound (%)
A (PP)	6.98 ± 0.11^{defghij}
B (PP)	6.54 ± 0.06^{ghijk}
C (PP)	7.23 ± 0.15^{defgh}
D (PP)	7.62 ± 0.13^{bcde}
E (PP)	7.69 ± 0.07^{bcd}
F (PP)	6.15 ± 0.21^{jk}
G (PP)	7.22 ± 0.00^{defgh}
H (PP)	8.65 ± 0.21^{a}
I (PP)	7.43 ± 0.19^{cde}
J (PP)	7.52 ± 0.16^{cde}
K (PP)	6.92 ± 0.14^{defghij}
L (PP)	6.19 ± 0.32^{jk}
M (PP)	6.49 ± 0.04^{ghijk}
N (PP)	6.02 ± 0.06^{k}
O (PP)	6.27 ± 0.47^{ijk}
P (PP)	6.66 ± 0.18^{fghijk}
Q (PB)	6.38 ± 0.07^{hijk}
R (PB)	6.64 ± 0.18^{fghijk}
S (PB)	8.43 ± 0.38^{ab}
T (PB)	7.31 ± 0.45^{defg}
U (PB)	7.30 ± 0.18^{defg}
V (PB)	8.33 ± 0.06^{abc}
W (PB)	7.74 ± 0.01^{bcd}
X (PB)	7.09 ± 0.16^{defghi}
Y (PB)	6.78 ± 0.25^{efghijk}

Note: Sample A-P - cooking oils in plastic pouch (PP).
Sample Q-Y - cooking oils in polyethylene terephthalate (PET) bottle (PB).
Means within each row bearing different superscript letters are significantly different ($p<0.05$).

al. (2009). Tarmizi *et al*. (2016b) and Berger (2005), however, reported that fresh palm-based oil has polar compound of 6%-8% due to the existence of DAG. Liquid oil on the other hand, has lower polar compound of between 2%-3%. A survey by Sebastian *et al.* (2014) showed that fresh canola and hydrogenated vegetable oil used as frying oil in restaurant in Toronto have polar compound of 1%-3% only. Sample N (plastic pouch) has a lowest polar content of 6.02%, while sample H (plastic pouch) has the highest polar content of 8.65%. Three cooking oils namely sample H (plastic pouch), S (PET bottle) and V (PET bottle) have higher level of polar compounds of more than 8%. The 2-sample t-test confirmed that the average polar compound of cooking oils both in plastic pouch and PET bottle were comparable ($p>0.05$) (*Table 9b*).

TABLE 9B. 2-SAMPLE T-TEST OF POLAR COMPOUND OF COMMERCIAL PALM-BASED COOKING OIL IN PLASTIC POUCH AND POLYETHYLENE TEREPHTHALATE (PET) BOTTLE PACKAGING IN MALAYSIA

Mean of polar compound (%)		p-value
Plastic pouch	PET bottle	
6.971 ± 0.712	7.332 ± 0.718	0.096

Note: p-value<0.05 indicates that there is significant different between cooking oil in plastic pouch and PET bottle.

Polymer Compound

Polymerisation is one of the stages in the oxidation reaction (Nayak *et al*., 2016) that normally takes place at higher frying temperatures. Polymer compounds increased as the number of frying cycle and temperature increased (Choudhary and Grover, 2013). As the polymer compounds developed, further deterioration of the oil is accelerated, escalating the viscosity of the oil, decreasing the heat transfer, foaming during frying, darkening the colour of the oil and increasing the oil absorption into the food (Choe and Min, 2007) which imparts bitterness (Maskan, 2003). Serjouie *et al.* (2010) reported that the polymer content of fresh RBD palm olein was 0%. However, this value can escalate during frying, that makes many countries to set their own discard value for maximum level of polymer compound. The Netherlands, for example, sets 16% of polymer compound in used oil as their maximum limit (Berger, 2005). *Table 10a* shows that the polymer compound of cooking oils in both plastic pouch and PET bottle were in the range of 0.54%-0.83% and 0.58%-0.80%, respectively. The polymer compound of cooking oils in both packagings was significantly different ($p<0.05$) with overall range of 0.54%-0.83%. However, there were cooking oils that were not significantly different from each other. Notwithstanding this, their significance were very close to each other. The highest and the lowest level of polymer compounds were found in samples M (0.83%) and B (0.54%). Both samples were in the plastic pouch. In terms of average polymer compound, cooking oils in both plastic pouches and PET bottles were found to be comparable ($p>0.05$) (*Table 10b*).

Oxidative Stability

Oxidative stability is a crucial aspect in determining the quality of cooking oil, especially those used for deep-frying. In deep-frying study, oxidative stability determination involves immersing food in oil at high temperatures (165ºC-190°C). At this point, the frying oil undergoes degradation such as oxidation, hydrolysis and polymerisation (Naz *et al*., 2004). A good quality cooking oil should have higher resistant

TABLE 10A. POLYMER COMPOUND OF COMMERCIAL PALM-BASED COOKING OIL IN PLASTIC POUCH AND POLYETHYLENE TEREPHTHALATE (PET) BOTTLE PACKAGING IN MALAYSIA

Sample	Polymer compound (%)
A (PP)	0.59 ± 0.07^{bc}
B (PP)	0.54 ± 0.03^{c}
C (PP)	0.60 ± 0.06^{bc}
D (PP)	0.76 ± 0.03^{abc}
E (PP)	0.62 ± 0.09^{abc}
F (PP)	0.66 ± 0.03^{abc}
G (PP)	0.67 ± 0.04^{abc}
H (PP)	0.71 ± 0.09^{abc}
I (PP)	0.74 ± 0.08^{abc}
J (PP)	0.59 ± 0.03^{bc}
K (PP)	0.69 ± 0.06^{abc}
L (PP)	0.69 ± 0.08^{abc}
M (PP)	0.83 ± 0.04^{a}
N (PP)	0.60 ± 0.03^{bc}
O (PP)	0.73 ± 0.09^{abc}
P (PP)	0.69 ± 0.04^{abc}
Q (PB)	0.63 ± 0.04^{abc}
R (PB)	0.63 ± 0.64^{abc}
S (PB)	0.80 ± 0.01^{ab}
T (PB)	0.67 ± 0.04^{abc}
U (PB)	0.71 ± 0.04^{abc}
V (PB)	0.58 ± 0.04^{bc}
W (PB)	0.71 ± 0.07^{abc}
X (PB)	0.60 ± 0.02^{bc}
Y (PB)	0.71 ± 0.06^{abc}

Note: Sample A-P - cooking oils in plastic pouch (PP).
Sample Q-Y - cooking oils in polyethylene terephthalate (PET) bottle (PB).
Means bearing different superscript letters are significantly different ($p<0.05$).

TABLE 10B. 2-SAMPLE T-TEST OF POLYMER COMPOUND OF COMMERCIAL PALM-BASED COOKING OIL IN PLASTIC POUCH AND POLYETHYLENE TEREPHTHALATE (PET) BOTTLE PACKAGING IN MALAYSIA

Mean of polymer compound (%)		p-value
Plastic pouch	PET bottle	
0.667 ± 0.086	0.668 ± 0.0755	0.980

Note: p-value<0.05 indicates that there is significant different between cooking oil in plastic pouch and PET bottle.

towards oxidation in order to increase its shelf life. Oxidative deterioration of fat resulted in the development of a pungent and offensive off-flavour. *Table 11a* shows that the OSI of cooking oil in both plastic pouch and PET bottle ranged between 20.94-27.90 hr and 17.71-23.97 hr, respectively. The OSI of cooking oil in both packaging was significantly different ($p<0.05$) with overall range of 17.71-27.90 hr. However, there were cooking oils that were not significantly different from each other. Sample E (plastic pouch) had the highest OSI while sample S (PET bottle) had the lowest OSI. Ahmad Tarmizi *et al*. (2016a) reported that the OSI of palm olein is 28.1 hr while Womeni *et al*. (2016) stated that the OSI of palm olein is 20.1 hr. The 2-sample t-test showed that the average OSI of cooking oils in both plastic pouch and PET bottle was significantly different ($p<0.05$), with plastic pouch cooking oil has higher (better) OSI compared to PET bottle cooking oil

TABLE 11A. OXIDATIVE STABILITY OF COMMERCIAL PALM COOKING OIL IN POUCH AND POLYETHYLENE TEREPHTHALATE (PET) BOTTLE PACKAGING IN MALAYSIA

Sample	Oxidative stability (hr)
A (PP)	24.83 ± 0.69^{bcd}
B (PP)	22.94 ± 0.68^{defg}
C (PP)	20.94 ± 0.97^{gh}
D (PP)	21.86 ± 0.64^{efgh}
E (PP)	27.90 ± 0.35^{a}
F (PP)	27.30 ± 0.13^{a}
G (PP)	26.83 ± 0.63^{ab}
H (PP)	22.26 ± 0.33^{efgh}
I (PP)	27.78 ± 0.43^{a}
J (PP)	22.83 ± 0.09^{defg}
K (PP)	21.78 ± 0.83^{efgh}
L (PP)	27.65 ± 0.35^{a}
M (PP)	23.66 ± 0.50^{def}
N (PP)	25.88 ± 0.46^{abc}
O (PP)	26.75 ± 0.74^{ab}
P (PP)	27.72 ± 1.03^{a}
Q (PB)	20.44 ± 0.21^{h}
R (PB)	23.97 ± 0.03^{cde}
S (PB)	17.71 ± 0.88^{i}
T (PB)	22.97 ± 0.37^{defg}
U (PB)	21.47 ± 0.25^{fgh}
V (PB)	23.04 ± 0.45^{defg}
W (PB)	20.85 ± 0.06^{gh}
X (PB)	21.46 ± 0.33^{fgh}
Y (PB)	21.52 ± 0.05^{fgh}

Note: Sample A-P - cooking oils in plastic pouch (PP).
Sample Q-Y - cooking oils in polyethylene terephthalate (PET) bottle (PB).
Means within each row bearing different superscript letters are significantly different ($p<0.05$).

(*Table 11b*). Based on Pearson correlation, there was a negative significant correlation between OSI and polyunsaturated FAC.

TABLE 11B. 2-SAMPLE T-TEST OF OXIDATIVE STABILITY OF COMMERCIAL PALM-BASED COOKING OIL IN PLASTIC POUCH AND POLYETHYLENE TEREPHTHALATE (PET) BOTTLE PACKAGING IN MALAYSIA

Mean of oxidative stability (hr)		p-value
Plastic pouch	PET bottle	
24.93±2.55	21.49±1.79	0.00

Note: p-value<0.05 indicates that there is significant different between cooking oil in plastic pouch and PET bottle.

CONCLUSION

Most of the important quality characteristics (FFA, FAC (oleic acid), total vitamin E, colour (red, yellow, neutral and blue), polar compound and polymer compound of the commercial palm-based cooking oils sold in plastic pouches and PET bottles were statistically comparable. Therefore, consumers' perception of plastic pouch having lower quality was misleading. Notwithstanding this, from the authors perspective, better quality cooking oil was skewed towards PET bottle when other important quality characteristics of cooking oil namely FAC (palmitic acid, stearic acid and linolenic acid), TAG (UUU and SUU), IV and cloud point quality of commercial palm cooking oil in PET bottles were better than in pouches. Nevertheless, FAC and IV of plastic pouch cooking oil still met either the MS 682:2004, MS 816:2007 or Palm Oil Refiners' Association (PORAM) specification/guideline. In addition, the cloud point of cooking oils in plastic pouch was better than the cloud point cited in many earlier studies. TAG on the hand, does not specify in any Malaysian Standard or PORAM's specification/guideline.

ACKNOWLEDGEMENT

The authors thank the Director-General of MPOB for permission to publish this article. The authors also thank the skilled staff of Food Technology Group for their analytical assistance in ensuring the success of this study.

REFERENCES

Ahmad Tarmizi, A H and Ahmad, K (2015). Feasibility of continuous frying system to improve the quality indices of palm olein for the production of extruded product. *J. Oleo Sci., 65*: 1259-1266.

Ahmad Tarmizi, A H and Ismail, R (2007). Frying performance of standard of palm olein and special quality palm olein during continuous frying of potato chips. Proc. of the 2007 PIPOC International Palm Oil Congress. 26-30 August 2007. Kuala Lumpur Convention Centre, Malaysia.

Ahmad Tarmizi, A H and Ismail, R (2008). Comparison of the frying stability of standard palm olein and special quality palm olein. *J. Amer. Oil Chem. Soc., 85*: 245-251.

Ahmad Tarmizi, A H and Ismail, R (2014). Use of pilot plant scale continuous fryer to simulate industrial production of potato chips: Thermal properties of palm olein blends under continuous frying conditions. *Food Sci. Nutri., 2*: 28-38.

Ahmad Tarmizi, A H; Ahmad, K; Mat Sahri, M and Choo, Y M (2016a). Rancimat test for measuring the oxidative stability of cooking oils upon prolonged frying: Short communication. *J. Oil Palm Res., 28*: 531-535.

Ahmad Tarmizi, A H; Ismail, R and Kuntom, A (2016b). Effect of frying on the palm oil quality attributes – A review. *J. Oil Palm Res., 28*: 143-153.

Ahmad Tarmizi, A H; Niranjan, K and Gordon, M (2013). Physico-chemical changes occurring in oil when atmospheric frying is combined with post-frying vacuum application. *Food Chem., 136*: 902-908.

Aladedunye, F; Kersting, H J and Matthäus, B (2014). Phenolic extract from wild rose hip with seed: Composition, antioxidant capacity, and performance in canola oil. *Eur. J. Lipid Sci. Technol., 116*: 1025-1034.

Alireza, S; Tan, C P; Hamed, M and Che Man, Y (2010). Effect of frying process on fatty acid composition and iodine value of selected vegetable oils and their blends. *Int. Food Res. J., 17*: 295-302.

Arslan, N F; Şapçi, A N; Duru; F and Kara, H (2017). A study on monitoring of frying performance and oxidative stability of cottonseed and palm oil blends in comparison with original oil. *Int. J. Food Prop., 20*: 704-717.

Azlina, M F; Nafeeza, M I and Khalid, B A (2005). A comparison between tocopherol and tocotrienol effects on gastric parameters in rats exposed to stress. *Asia Pac. J. Clin. Nutr., 14*: 358-365.

Bensmira, M; Jiang, B; Nsabimana, C and Jian, T (2007). Effect of lavender and thyme incorporation in sunflower seed oil on its resistance to frying temperatures. *Food Res. Int., 40*: 341-346.

Berger, K G (2005). *The Use of Palm Oil in Frying*. Malaysian Palm Oil Council, Selangor, Malaysia.

Bracco, U; Dieffenbacher, A and Kolarovic, L (1981). Frying performance of palm oil liquid fractions. *J. Amer. Oil Chem. Soc., 58*: 6-12.

Calliauw, G; Gibon, V; Greyt, W D; Plees, L; Foubert, I and Dewettinck, K (2007). Phase composition during palm olein fractionation and its effect on soft PMF and superolein quality. *J. Amer. Oil Chem. Soc., 84*: 885-891.

Che Man, Y B and Tan, C P (1999). Effects of natural antioxidants on changes in refined, bleached and deodorized palm olein during deep-fat frying of potato chips. *J. Amer. Oil Chem. Soc., 76*: 331-339.

Chen, W-A; Chiu, C P; Cheng, W-C; Hsu, C-K and Kuo, M-I (2013). Total polar compounds and acid values of repeatedly used frying oils measured by standard and rapid method. *J. Food Drug Anal., 21*: 58-65.

Chnadhapuram, M and Sunkireddy, Y R (2012). Preparation of palm olein enriched with medium chain fatty acids by lipase acidolysis. *Food Chem., 132*: 216-221.

Choe, E and Min, D B (2007). Chemistry of deep-fat frying oils. *J. Food Sci., 72*: 77-86.

Choo, Y M; Yap, S C; Ooi, C K; Ma, A N; Goh, S H and Ong, A S H (1996). Recovered oil from palm-pressed fiber: A good source of natural carotenoids, vitamin E and sterols. *J. Amer. Oil Chem. Soc., 73*: 599-602.

Choudhary, M and Grover, K (2013). Effect of deep-fat frying on physicochemical properties of rice bran oil blends. *IOSR J. Nurs. Health Sci., 1*: 1-10.

Department of Standards Malaysia (2004). MS 682:2004-Cooking Oils-Specification (First Revision).

Department of Standards Malaysia (2007). MS 816:2007-Palm Olein-Specification (Second revision).

Dobarganes, M C; Velasco, J and Dieffenbacher, A (2003). Determination of polar compounds, polymerized and oxidized triacylglycerols and diacylglycerols in oils and fats: Results of collaborative studies and the standardized method. *Pure Appl. Chem., 72*: 1563-1575.

Farhoosh, R; Kenari, R E and Poorazrang, H (2009). Frying stability of canola oil blended with palm olein, olive and corn oils. *J. Amer. Oil Chem. Soc., 86*: 71-76.

Firestone, D (1998). *Official Methods and Recommended Practices of the AOCS, 5th edition*. American Oil Chemists' Society, Champaign, IL, USA.

Gibon, V; De Greyt, W and Kellens, M (2007). Palm oil refining. *Eur. J. Lipid Sci. Technol., 109*: 315-335.

Goh, S H; Hew, N F; Norhanom, A E and Yadar, M C (1994). Inhibition of tumour growth promotion by various palm oil tocotrienols. *Int. J. Cancer, 57*: 529-531.

Gunstone, F D (2008). Chapter 8. Oils and Fats in the Food Industry. First edition. Wiley-Blackwell, USA.

Ham, B; Shelton, R; Butler, B and Thionville, P (1998). Calculating the iodine value for marine oils from fatty acids profiles. *J. Amer. Oil Chem. Soc., 75*: 1445-1446.

Hasmadi, M; Nor Aini, S and Yusuf, M S A (2002). The effect of different types of stirrer and fractionation temperatures during fractionation on the yield, characteristics and quality of oleins. *J. Food Lipids, 9*: 295-307.

Ismail, R (2001). The performance of palm olein during the industrial production of fried food. Paper presented at the 92nd AOCS Annual Meeting and Expo, Minneapolis, USA.

Ismail, R (2005). Palm oil and palm olein frying applications. *Asia Pac. J. Clin. Nutr., 14*: 414-419.

ISO 5508:1990 (1990). Animal and vegetable fats and oils: Analysis of gas-liquid chromatography methyl ester of fatty acids. International Organization for Standardization, Switzerland.

IUPAC (1987). Standard Method 2.507: Determination of polar compounds in frying fats. *Standard Methods for the Analysis of Oils, Fats and Derivatives, 7th edition*. International Union of Pure and Applied Chemistry, Blackwell, Oxford, United Kingdom.

Kamar, J P; Sarma, H D; Devasageyam, T P A; Nesaretnam, K and Basiron, Y (1997). Tocotrienols from palm olein as effective inhibitors of protein oxidation and lipid peroxidation in rat liver microsomes. *Mol. Cell. Biochem., 170*: 131-137.

Karimah, A (2005). Performance of special quality and standard palm olein in batch frying of fish nuggets. *Palm Oil Developments, 43*: 10-15.

Katragadda, R H; Fullana, A; Sidhu, S and Carbonell-Barrachina, Á A (2010). Emissions of volatile aldehydes from heated cooking oil. *Food Chem., 120*: 59-65.

Kostik, V; Memeti, S and Bauer, B (2013). Fatty acid composition of edible oils and fats. *J. Hyg. Eng. Des.*, *4*: 112-116.

Maskan, M (2003). Change in colour and rheological behaviour of sunflower seed oil during frying and after adsorbent treatment of used oil. *Eur. Food Res. Technol., 218*: 20-25.

Matthäus, B (2006). Utilization of high-olein rapeseed for deep-fat frying of French fries compared to other commonly used edible oils. *Eur. J. Lipid Sci. Technol., 108*: 200-211.

Matthäus, B (2007). Use of palm oil for frying in comparison with other high stability oils. *Eur. J. Lipid Sci. Technol., 109*: 400-409.

Matthäus, B; Haase, N U and Unbehend, G (2009). Chemical and sensory characteristics of products fried in high-oleic, low-linolenic rapeseed oil. *J. Amer. Oil Chem. Soc., 86*: 799-808.

Melton, S L; Jafar, S; Sykes, D and Trigiano, M K (1994). Review of stability measurements for frying oils and fried food flavor. *J. Amer. Oil Chem. Soc., 71*: 1301-1308.

Mohamed Sulieman, A E; El-Makhzangi, A and Ramadan, M F (2006). Antiradical performance and physicochemical characteristics of vegetable oils upon frying French fries: A preliminary comparative study. *J. Food Lipids, 13*: 259-276.

MPOB (2005). Methods of test for palm oil and palm oil products. MPOB, Bangi.

MPOB (2020). Malaysian oil palm industry performance 2019 and prospects for 2020. Lead paper presented at the Palm Oil Economic Review & Outlook (R&O) Seminar 2020 - Maximising Palm Oil Opportunity and Sustainability Amidst Challenges. 16 January 2020. Sheraton Imperial Hotel, Kuala Lumpur. p. 3.

Mutalib, M S A; Khaza'ai, H and Wahle, K W J (2003). Palm tocotrienol rich fraction (TRF) is a more effective inhibitor of LDL oxidation and endothelial cell lipid peroxidation than α-tocopherol *in vitro*. *Food Res. Int., 36*: 405-413.

Myat, M W; Abdulkarim, S M; Ghazali, H M and Roselina, K (2009). Physicochemical and characteristics of palm olein and peanut oil blend. *J. Food Agric. Environ., 7*: 175-181.

Nagendran, B; Unnithan, U R; Choo, Y M and Sundram, K (2000). Characteristics of red palm oil, a carotene- and vitamin E-rich refined oil for food uses. *Food Nutr. Bull., 21*: 189-194.

Nallusamy, S (2006). The role of palm oil in the snack food industry. Presented at International Palm Oil Trade Fair and Seminar. 21-24 November 2006. Shangri-La Hotel, Kuala Lumpur, Malaysia.

Nawal, A-B; Shaista, A and Zubaida, A N B (2014). Characteristics and fatty acid composition of consumed cooking oil marketed locally in Riyadh city. *Int. J. Biosci., 4*: 227-238.

Nayak, P K; Dash, U; Rayaguru, K and Krishnan, K D (2016). Physico-chemical changes during repeated frying of cooked oil: A review. *J. Food Biochem., 40*: 371-390.

Naz, S; Sheikh, H; Siddiqi, R and Sayeed, S A (2004). Oxidative stability of olive, corn and soybean oil under different conditions. *Food Chem., 88*: 253-259.

Nesaretnam, K; Kor, H T; Ganeson, J; Chong, Y H; Sundram, K and Gapor, A (1992). The effect of vitamin E tocotrienols from palm oil on chemically-induced mammary carcinogenesis in female rats. *Nutr. Res., 12*: 63-75.

Nesaretnam, K; Stephen, R; Dils, R and Darbre, P (1998). Tocotrienols inhibit the growth of human breast cancer cells irrespective of estrogen receptor status. *Lipids, 33*: 461-569.

Ngah, W Z; Jarien, Z; San, M M; Marzuki, A; Top, G M; Shamaan, N A and Kadir, K A (1991). Effect of tocotrienols on hepatocarcinogenesis induced by 2-acetylaminofluorene in rats. *Am. J. Clin. Nutr., 53*: 1076S-1081S.

Ng, M H; Choo, Y M; Ma, A N; Chuah, C H and Hashim, M A (2004). Separation of vitamin E (tocopherol, tocotrienol and tocomonoenol) in palm oil. *Lipids, 39*: 1031-1035.

Norazlina, M; Hermizi, H; Faizah, O; Nazrun, A S; Norliza, M and Ima-Nirwana, S (2010). Vitamin E reversed nicotine-induced toxic effects on bone biochemical markers in male rats. *Arch. Med. Sci., 6*: 505-512.

Orthoefer, F T and List, G R (2007). Initial quality of frying oil. Deep Frying. AOCS Press. p. 33-48.

Peled, M; Gutfinger, T and Letan, A (1975). Effect of water and BHT on stability of cottonseed oil during frying. *J. Sci. Food Agric., 26*: 1655-1666.

Roiaini, M; Ardiannie, T and Norhayati, H (2015). Physicochemical properties of canola oil, olive oil and palm olein blends. *Int. Food Res. J., 22*: 1228-1238.

Rossi, M; Gianazza, M; Alamprese, C and Stanga, F (2001). The effect of bleaching and physical refining

on color and minor components of palm oil. *J. Amer. Oil Chem. Soc., 78*: 1051-1055.

Sampaio, K A; Ceriani, R; Silva, S M; Taham, T and Meirelles, A J A (2011). Steam deacidification of palm oil. *Food Bioprod. Process., 89*: 383-390.

Sebastian, A; Ghazani, S M and Marangoni, A G (2014). Quality and safety of frying oils used in restaurants. *Food Res. Int., 64*: 420-423.

Sebedio, J L; Dobarganes, C; Dobarganes, M C; Wester, I; Christie, W W; Dobson, G; Zwobada, F; Chardigmy, I M; Mariot, T H and Lahtinen, R (1996). Industrial production of crisps and prefried French fries using sunflower oils. *Grasas Aceitas, 47*: 5-13.

Sen, C K; Rink, C and Khanna, S (2010). Palm oil-derived natural vitamin E α-tocotrienol in brain health and disease. *J. Am. Coll. Nutr., 29*: 314S-323S.

Serbinova, A E and Packer, L (1994). Antioxidant properties of α-tocopherol and α-tocotrienol. *Method Enzymol., 234*: 354-366.

Serjouie, A; Tan, C P; Mirhosseini, H and Che Man, Y (2010). Effects of vegetable-based oil blends on physicochemical properties of oils during deep-fat frying. *Am. J. Food Technol., 5*: 310-323.

Siddiqui, S; Ahsan, H; Khan, M R and Siddiqui, W A (2013). Protective effects of tocotrienols against lipid-induced nephropathy in experimental type-2 diabetic rats by modulation in TGF-beta expression. *Toxicol. Appl. Pharmacol., 273*: 314-324.

Siddiqui, S; Khan, M R and Siddiqui, W A (2010). Comparative hypoglycemic and nephroprotective effects of tocotrienol rich fraction (TRF) from palm oil and rice bran oil against hyperglycemia induced nephropathy in type 1 diabetic rats. *Chem. Biol. Interact., 188*: 651-658.

Silva, S M; Sampaio, K A; Ceriani, R; Verhé, R; Stevens, C; Greyt, W D and Meirelles, A J A (2014). Effect of type of bleaching earth on the final color of refined palm oil. *LWT - Food Sci. Technol., 59*: 1258-1264.

Sundram, K and Nor, R M (2001). Analysis of tocotrienols in different sample matrixes by HPLC. *Methods in Molecular Biology* (Armstrong, A ed.). Vol. 186: Oxidative Stress Biomarkers and Antioxidant Protocols. Humana Press Inc., Totowa, New Jersey. p. 221-232.

Sundram, K; Sambanthamurthi, R and Tan, Y A (2003). Palm fruit chemistry and nutrition. *Asia Pac. J. Clin. Nutr., 12*: 355-362.

Tabee, E; Jägerstad, M and Dutta, P C (2009). Frying quality characteristics of French fries prepared in refined olive oil and palm olein. *J. Amer. Oil Chem. Soc., 86*: 885-893.

Teoh, C M; Nazaruddin, R; Ooi, T L; Mamot, S and Zalifah, K (2005). Strategies for decreasing the pour point and cloud point of palm oil products. *Eur. J. Lipid Sci. Technol., 107*: 505-512.

Womeni, H M; Djikeng, F T; Anjaneyulu, B; Karuna, M S L; Prasad, R B N and Linder, M (2016). Oxidative stabilization of RBD palm olein under forced storage conditions by old Cameroonian green tea leaves methanolic extract. *NFS Journal, 3*: 33-40.

Yousefi, M; Nateghi, L and Rezaee, K (2013). Investigation of physicochemical properties, fatty acids profile and sterol content in Malaysian coconut and palm oil. *Ann. Biol. Res., 4*: 214-219.

Zaliha, O; Chong, C L; Cheow, C S; Norizzah, A R and Kellens, M J (2003). Crystallization properties of palm oil by dry fractionation. *Food Chem., 86*: 245-250.

Journal of Oil Palm Research Vol. 33 (3) September 2021 p. 514-523
DOI: https://doi.org/10.21894/jopr.2020.0106

PREDICTION OF ACID, PEROXIDE AND TBA VALUES OF HEAT-TREATED PALM OIL USING A PARTIAL LEAST SQUARES–ORDINARY LEAST SQUARES MODEL BASED ON FOURIER TRANSFORM INFRARED SPECTROSCOPY

KUSNANDAR, F[1]*; LIOE, H N[1]; FARIDAH, D N[1]; ANGGRAENI, R[1] and PRICILIA[1]

ABSTRACT

Palm oil is widely used for frying food and is often used for repeated frying up to 40 hr or even longer. Frying causes a gradual quality decrease during heating due to fat oxidation or hydrolysis. The quality of fats and oils is commonly monitored by acid, peroxide and thiobarbituric acid values (AV, PV and TBAV, respectively). This study aimed to use a partial least squares–ordinary least squares (PLS-OLS) model obtained from Fourier transform infrared (FTIR) spectroscopy to predict AV, PV and TBAV values of heat-treated palm oil. Commercial palm oil was heated at 180°C for 72 hr. The multivariate mathematical models to predict AV, PV and TBAV were generated from the percentages of absorbance intensity of significant wavenumbers based on FTIR readings (721.4, 871.8, 968.3, 1033.9, 1095.6, 1377.2, 1462, 1751.4, 2731.2, 2839.2 and 3005.1 cm^{-1}). The PLS-OLS mathematical model satisfactorily predicted both AV and PV for palm oil samples heated up to 72 hr (R^2=0.962 and 0.857, respectively), whereas for TBAV, the time was 58 hr (R^2=0.845). This approach provides an alternative to monitoring palm oil quality during frying instead of the conventional methods in which the analytical procedures are time-consuming.

Keywords: fat oxidation, FTIR spectroscopy, heat stability, ordinary least square, palm oil.

Received: 15 December 2019; **Accepted:** 6 September 2020; **Published online:** 30 November 2020.

INTRODUCTION

The quality of oil gradually decreases due to fat oxidation and fat hydrolysis, which is proportional to frying time and/or frying cycles (Bhuiyan *et al*., 2016; Jaarin and Kamisah, 2012). Fat oxidation involves the reaction between the unsaturated carbon bonds of fatty acids and oxygen, resulting in the formation of unstable hydroperoxide as a primary product (Dana and Saguy, 2001; Gharby *et al*., 2014). Moreover, the hydroperoxide undergoes rapid degradation into stable aldehydes as secondary products, which are responsible for rancid odour (Frankel, 1987). Peroxide and thiobarbituric acid values (PV and TBAV, respectively) for indicating hydroperoxide and aldehyde formations, respectively, can describe the extension of oxidation. Additionally, the duration, method of frying, type of frying medium and characteristics of the fried product may influence the degree of rancidity (Bhuiyan *et al*., 2016).

Palm oil is commonly used as a heating medium for deep-fat frying in households, fast-food outlets, and restaurants with specific frying times of 12-40 hr and a temperature at least of 180°C (Bhuiyan *et al*., 2016; Faridah *et al*., 2015). Palm oil is susceptible to oxidation when it is used for frying under such conditions as it mainly consists of monounsaturated

[1] Department of Food Science and Technology, Bogor Agricultural University (IPB University), Dramaga Campus, Bogor 16680, Indonesia.

* *Corresponding author e-mail: fkusnandar@apps.ipb.ac.id*

fatty acids, such as oleic acid (C18:1) at 39.2% and polyunsaturated fatty acids, such as linoleic acid (C18:2) and linolenic acid (C18:3) at 10.5% (Mancini *et al.*, 2018). Additionally, hydrolysis, which is a splitting reaction of triglycerides into free fatty acids (FFA) and glycerol (Frankel, 1987), is also a cause of palm oil deterioration. The presence of short-chain FFA, expressed as acid value (AV), also contributes to the formation of rancid odour.

The monitoring of palm-based cooking oil during frying commonly focuses on the quantitative values of AV, PV and TBAV (Kalapathy and Proctor, 2000; Setiowaty and Che Man, 2003). However, the procedures involved (for example, sample preparation and titration) in determining these parameters are sometimes tedious. Therefore, an alternative method that may be substantial in cutting down the analytical times for measuring AV, PV and TBAV is needed and should be investigated.

Nowadays, Fourier transform infrared (FTIR) spectroscopy is widely used to analyse the quality of edible oils. The principle of FTIR is to measure the infrared spectrum of absorption over a range of wavenumbers. The identification of functional groups or bonds are possible by reading significant absorbance intensity at certain wavelengths. In this study, similar to the fingerprint method for identifying chemical substances, FTIR is considerably powerful, rapid, simple and relatively cost effective. Recent studies have shown that FTIR is capable of identifying the adulterated compounds in palm oil and reheated palm oil (Che Man *et al.*, 2014; Lim *et al.*, 2018; Faridah *et al.*, 2015), determining purity of olive oil and crude oil (Rohman and Che Man, 2010; Abdulkadir *et al.*, 2016) and authentify avocado oil (Rohman *et al.*, 2015). Moreover, Ang *et al.* (2019) and Wong *et al.* (2019) have reported the rapid quantification of processing contaminants [such as 3-mono-chloropropane-1,2-diol (MCPD) esters] in palm-based cooking oil using FTIR spectroscopy.

FTIR spectroscopy cannot be used to directly measure the intensity of oil deterioration. However, the results of FTIR analysis can correlate with the oil's quality parameters. For establishing this correlation, the partial least squares (PLS) in combination with an ordinary least squares (OLS) method may be used. PLS is a multivariate and covariance-based statistical method that compares the multiple response and explanatory variables (Höskuldsson, 1998) and thus, satisfactorily predicts 'y' from 'x' (Abdi, 2003). As a part of PLS, the OLS regression generates a mathematical model between the sample's data points and the predicted values (Farahani *et al.*, 2010). Therefore, the use of PLS-OLS is a powerful method for interpreting collinear data from FTIR measurements (Li, 2010). The use of the PLS-OLS regression model for the interpretation of FTIR measurements in palm oil during frying has been reported (Faridah *et al.*, 2015; Setiawaty and Che Man, 2003; Rohman and Che Man, 2010; Martín-Ramos *et al.*, 2018).

One of the reported advantages of PLS-OLS is the simplicity of the method when monitoring oil quality (Faridah *et al.*, 2015). On that note, it is a need to investigate such an alternative method that may be substantial in cutting down the analytical times for measuring AV, PV and TBAV exists. Hence, within this study, the use of a PLS-OLS mathematical model to correlate the FTIR measurements with AV, PV and TBAV of heated palm oil was demonstrated and verified.

MATERIALS AND METHODS

Materials

A commercial palm oil from a production batch was purchased from a local market in Bogor, Indonesia. The sample consisted of pure palm oil as mentioned on its label. The chemicals for analysis were potassium hydrogen phthalate (KHP) crystals, phenolphthalein in alcohol (1%), 96% technical alcohol, glacial acetic acid, 0.01 N $Na_2S_2O_3$ solution, 1% starch solution, saturated potassium iodide (KI) solution and thiobarbituric acid (TBA) reagent. All chemical reagents used were of analytical grade.

Sample Preparation and Analysis

Ten litres of cooking oil was heated using a controlled-temperature deep fat fryer (Getra model EF-88) at 180°C for up to 72 hr. The selected heating temperature and time were in accordance to Setiowaty and Che Man (2003). Samples were withdrawn every 2 hr, placed in dark glass bottles (with a capacity of 30-50 ml), and stored at a 3°C for further analyses. A non-heated sample was also prepared as a control. Samples were prepared in duplicate; hence, 74 samples were obtained.

AV Analysis

The determination of AV followed AOAC 940.28 (AOAC, 1984). The sample (2.5 g) was dissolved with 50 ml 96% alcohol in an Erlenmeyer flask. After a short period of heating on a hot plate, the sample was titrated using 0.01 M NaOH solution. The AV was calculated according to the Equation (1):

$$\text{AV (mg NaOH g}^{-1}\text{ sample)} = V_{NaOH} \times M_{NaOH} \times n_{NaOH} \quad (1)$$

in which V = volume (L), M = molarity (M) and n = mol. The molecular weight of NaOH is 40 g mol^{-1}.

PV Analysis

The PV analysis was determined according to a national standard method (SNI, 1998). Samples (0.25 g) were added to the mixture of 30 ml of glacial acetic acid solution and chloroform (3:2), 3 ml saturated potassium iodide, 30 ml of distilled water and 1 ml indicator (1% starch solution). After thoroughly agitating for 3 min, the sample was titrated with 0.01 N standard solution of sodium thiosulphate. PV was calculated with the Equation (2):

$$\text{PV (meq peroxide kg}^{-1}\text{ sample)} = (\text{Vs-Vb}) \times \text{N} \times 1000/\text{W} \quad (2)$$

in which Vs = volume of titration for sample (L), Vb = volume of titration for blank sample (L), N = normality of sodium thiosulphate solution (N = 0.01) and W = sample weight (g).

TBAV Analysis

The TBAV analysis followed the method of Tarladgis *et al.* (1962). Sample (10 g) was mixed with 2.5 ml of 4 M HCl to reach a pH of 1.5 and then diluted to a total volume of 100 ml with distilled water. The sample was then distilled to obtain 50 ml distillate. After stirring evenly, 5 ml of distilate was pipetted into a closed test tube and then 5 ml of TBA reagent (0.2883 g TBA 100 ml^{-1} of 90% glacial acetic acid) was added into the solution. After thorough mixing, the mixture was heated in a boiling water bath for 35 min until a red colour solution was obtained. The sample was immediately cooled, and the absorbance was monitored at 538 nm using a Genesys 10S UV-Vis spectrophotometer (Thermo Scientific, USA). The TBAV was calculated using the Equation (3):

$$\text{TBAV (mg malondialdehyde kg}^{-1}\text{ sample)} = (\text{Absorbance} \times 7.8 \times 10\ \text{g}^{-1}\text{ sample}). \quad (3)$$

FTIR Spectrum Analysis

The procedure for FTIR spectroscopy analysis referred to Faridah *et al.* (2015). FTIR spectroscopy (IR-Prestige 21 model, Shimadzu Corporation, Japan) identified major wavenumbers that indicates significant absorbance intensity. The potassium bromide (KBr) plate was previously cleaned, wiped with analytical grade n-hexane and then dried with lens tissue for each sample measurement. The oil sample was then dropped onto the KBr plate and covered with another KBr plate to form a sandwich plate. The absorbance was read in duplicate at wavenumbers of 400-4000 cm^{-1} at a resolution of 1.9. The wavenumbers with the significant reading of absorbance intensity were used to predict functional groups or bonds by referring to relevant published FTIR analysis. The relative percentage of an absorbance intensity (to the sum of all absorbance intensities of significant wavenumbers) was calculated for each significant wavenumber of FTIR reading. This value was used for multivariate analysis.

PLS-OLS Multivariate Analysis

The data of absorbance intensity selected from a significant wavenumber of an FTIR spectroscopy reading was previously converted to a percentage of absorbance intensity (%IA) according to the Equation (4) (Faridah *et al.*, 2015):

$$\%\ \text{IAx} = \frac{IAx}{IA\ total} \quad (4)$$

in which:
%IAx = percentage of absorbance intensity at sigificant wavenumbers
IAx = absorbance intensity at significant wavenumbers
IA total = total of absorbance intensity

The software of XLSTAT version 2013 (Microsoft Excel Series) was used to perform a PLS-OLS multivariate analysis. The multivariate mathematical models were generated to correlate the percentage of absorbance intensity (%IA) of selected wavenumbers at X axis with AV, PV, or TBAV at Y axis. The coefficient of determination (R^2) was used as the validity criteria for PLS-OLS mathematical model.

Verification

Verification was performed to ensure the validity of the generated mathematical models to predict AV, PV and TBAV. A cooking oil sample was heated at 180°C for 24 hr and analysed in terms of FTIR profile, AV, PV and TBAV were evaluated by applying the same methods described above. A paired t statistical analysis was performed to observe the degree of deviation between actual and predicted AV, PV or TBAV values.

RESULTS AND DISCUSSION

Spectrum Profile and Absorbance Intensity

Figure 1 depicts the absorbance intensity of palm oil samples for control and those heated at 180°C for up to 72 hr measured at wavenumbers of 400-4000 cm^{-1}. This wavenumber range was accessible with the use of KBr and has also been

used in previous studies (Faridah *et al.*, 2015; Vlachos *et al.*, 2006; Al-Degs *et al.*, 2011). The figure indicates a similar absorbance intensity profile between control samples and those heated at 180°C for 72 hr. A similar absorbance intensity profile was also shown at other heating times (data are not presented). The data indicate that the absorbance intensity from FTIR readings did not differ among tested samples.

Figure 1 shows 11 wavenumbers with significant absorbance intensities, for examples, 721.4, 871.8, 968.3, 1033.9, 1095.6, 1377.2, 1462, 1751.4, 2731.2, 2839.2 and 3005.1 cm^{-1}. Referring to the previous studies (Faridah *et al.*, 2015; Vlachos *et al.*, 2006; Al-Degs *et al.*, 2011), these wavenumbers indicate the presence of specific functional groups (*Table 1*). The wavenumber of 3005.1 cm^{-1} indicates the existence of alkene group (C=C) as described by Rohman and Che Man (2010) and Che Man and Setiowaty (1999b). This alkene group appears due to the presence of double bond of fatty acids in triglyceride molecules. Palm oil contains considerable amount of unsaturated fatty acids, such as oleic and linoleic acids (Edem, 2002; Mba *et al.*, 2015). The existence of triglycerides in palm oil can be confirmed by the existence of C=O group at wavenumbers of 1033.9 cm^{-1} (Rohman and Che Man, 2010) and 1095.6 cm^{-1}, C=O groups at 1751.4 cm^{-1} (Rohman and Che Man, 2010; Che Man and Setiowaty, 1999b) and the CH_2 and CH_3 groups at a wavenumber of 721.4 cm^{-1} (Che Man and Setiowaty, 1999a), 1377 cm^{-1} (Rohman and Che Man, 2010), and 1462 cm^{-1} (Che Man and Setiowaty, 1999b). These groups are the major groups of esterified fatty acids (Berger, 2010). The presence of ester bonds indicates that fatty acid chains are still linked to glycerol moeity leading to the existence of triglycerides. The wavenumber of 871.8 cm^{-1} indicates the existence of cis C=C group (Faridah *et al.*, 2015). This group might originate from the double bonds of fatty acids attached at the triglyceride chain. Significant absorbance was also detected at the wavenumber of 968 cm^{-1}, indicating the existence of a *trans* C=C group (Rohman and Che Man, 2010; Che Man and Setiowaty, 1999b). The presence of this group indicates that palm oil sample contained *trans* unsaturated fatty acid residues that might been formed during the heating process of palm oil (Song *et al.*, 2015; Bhardwaj *et al.*, 2016). The existence of aldehyde and ester groups as the result of secondary oxidation formation was indicated at a wavenumber of 2731.2 cm^{-1} (Guillen and Cabo, 1997), 2839.2 cm^{-1} (Al-Degs *et al.*, 2011), and 1751.4 cm^{-1} (Rohman and Che Man, 2010). The extensive heat treatment of palm oil caused the formation of unstable peroxide components that were rapidly converted to secondary components, such as aliphatic aldehyde, alcohol, ketone and other hydrocarbons (Wrolstad *et al.*, 2000).

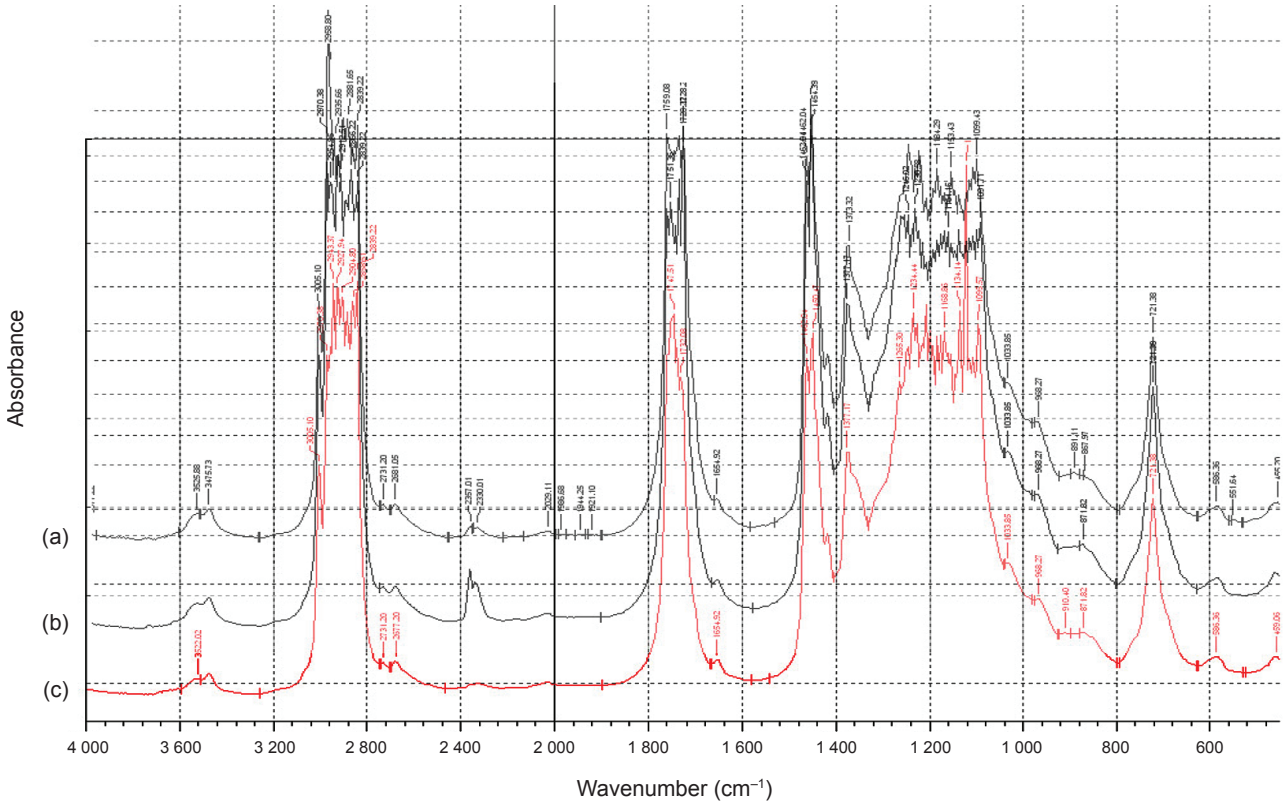


Figure 1. Fourier transform infrared (FTIR) absorbance intensities of (a) palm oil for control, (b) those heated at 180°C for 38 hr, and (c) 72 hr.

TABLE 1. PREDICTED FUNCTIONAL GROUPS OF PALM OILS BASED ON SIGINIFICANT FOURIER TRANSFORM INFRARED (FTIR) SPECTROSCOPY WAVENUMBERS

Wavenumber (cm^{-1})	Functional groups	References
721.4	$-CH_2-$	Che Man and Setiowaty (1999a)
871.8	Cis C=C	Faridah *et al.* (2015)
968.3	Trans C=C	Rohman and Che Man (2010); Che Man and Setiowaty (1999b)
1 033.9	C-O	Rohman and Che Man (2010)
1 095.6	C-O	Rohman and Che Man (2010)
1 377.2	$-CH_3$	Rohman and Che Man (2010)
1 462.0	$-CH_2-$ and $-CH_3$	Che Man and Setiowaty (1999b)
1 751.4	C=O	Che Man and Setiowaty (1999b)
2 731.2	-CHO	Guillen and Chabo (1997)
2 839.2	$-O-CH_3$	Al-Degs *et al.* (2011)
3 005.1	C=C	Rohman and Che Man (2010); Che Man and Setiowaty (1999b)

AV, PV and TBAV

The AV shows the concentration of FFA in fats and oils. A FFA is formed as a result of triglyceride breakage (Wrolstad *et al.,* 2000). *Figure 2a* shows the AV of cooking oil samples heated at 180°C for up to 72 hr. The AV increased linearly (R^2 = 0.964; $p<0.05$) corresponding to the increase in heating time. The increase of AV during heating of cooking oil was also reported in other studies (Farida and Siregar, 2006; Abdulkarim *et al*., 2007). The C=O groups shown at 1751.4 cm^{-1} of FTIR reading might originate from the carboxyl group of FFA measurable by the AV test.

Figure 2b shows the PV from cooking oil samples heated at 180°C for up to 72 hr. PV was unstable as heating time increased up to 44 hr before started to decrease at a prolonged heating up to 72 hr. Other studies have reported the same PV trends of heated cooking oils in which the PV increased during the first stage of frying (Abdulkarim *et al*., 2007; Chatzilazarou *et al.,* 2006; Faridah *et al*., 2015; Kaleem *et al.,* 2015; Tsaknis *et al*., 1998). The formation of unstable hydroperoxide at the initial stage of fat oxidation and then rapid degradation to form secondary oxidation products contributed to this PV profile.

The TBA reactive substance is commonly used as an indicator of lipid oxidation. The method uses the reaction of TBA and malondialdehyde in the glacial acetic acid medium. The higher concentration of malondialdehyde indicates the extent of fat oxidation. *Figure 2c* shows a significant increase in TBAV of palm oil samples with heating times for up to 44 min. The presence of unsaturated fatty acids in palm oil and the continuous heating process caused the formation of malondialdehyde, which contributed to the increase of TBAV. At a prolonged heating up to 72 hr, the TBAV tended to remain constant. The malondialdehyde probably changed gradually under an extended heating process to form more complex secondary oxidation products, such as higher molecular weight compounds that were not detectable when using TBA test (Shahidi *et al*., 2017).

PLS-OLS Models to Predict AV, PV and TBAV

Table 2 presents the linear regression models for correlating the percentage of absorbance intensity of significant wavenumbers of FTIR reading with the AV, PV and TBAV. All regression models were insignificant suggesting the FTIR reading at any wavenumbers cannot be directly correlated with the AV and TBAV results. For this reason, the PLS-OLS multivariate mathematical models were used to correlate the percentage of absorbance intensity with AV, PV and TBAV.

The PLS-OLS mathematical models in *Table 3* were useful for predicting the AV, PV and TBAV by inputting the percentage of absorbance intensity of each dominant wavenumber to the models. The fittest models were based on the significant degree of determination (R^2) that gave p-value (Pr>F) in the analysis of variance. The FTIR shows the 11 main wavenumbers, namely 721.4, 871.8, 968.3, 1033.9, 1095.6, 1377.2, 1462, 1751.4, 2731.2, 2839.2 and 3005.1 cm^{-1}, were provided by their significant absorbance intensities (*Table 2*). These wavenumbers represent the existence of functional groups of carbon double bonds (alkenes), esters and aldehydes. Alkene groups are found in many unsaturated fatty acids, while the ester group is negatively correlated with the amount of FFA. A higher number of ester groups indicates the higher fatty acids bound to glycerol. On the other hand, the fewer ester groups show that more hydrolysis reactions occur so that more FFA are produced. The higher amount of aldehyde group reflects the extent of fat oxidation.

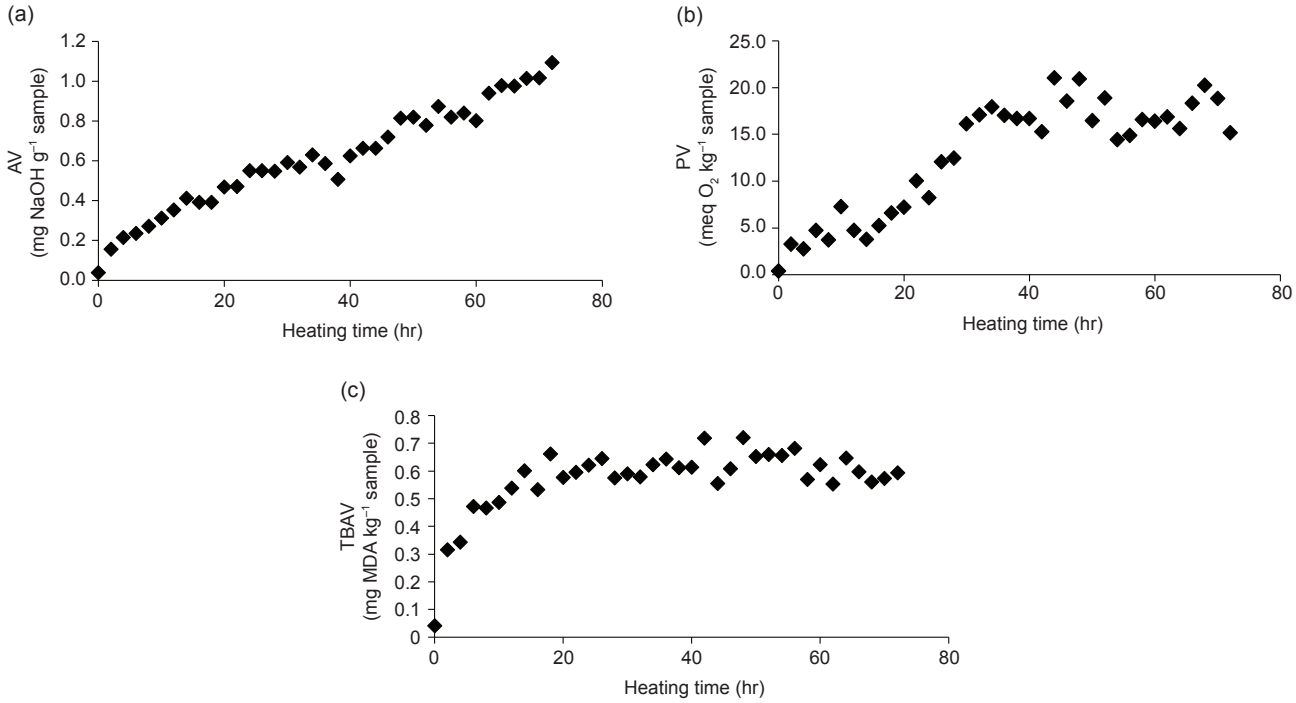


Figure 2. (a) Acid value (AV), (b) peroxide value (PV), and (c) thiobarbituric acid value (TBAV) of palm oil heated at 180°C for up to 72 hr.

TABLE 2. THE LINEAR REGRESSION MODELS FOR CORRELATING THE PERCENTAGE OF ABSORBANCE INTENSITY OF SIGNIFICANT WAVENUMBERS OF FTIR READING WITH THE AV, PV AND TBAV

Wavenumber (cm^{-1})	AV	R^2	PV	R^2	TBAV	R^2
721.4	-0.2277%IA + 2.8426	0.163	-0.0112%IA + 2.8463	0.206	-0.7735%IA + 3.1440	0.401
871.8	0.1170%IA + 2.6308	0.008	-0.0029%IA + 2.7398	0.003	-0.9612%IA + 3.2511	0.113
968.3	0.5134%IA + 2.3872	0.266	0.0138%IA + 2.5103	0.107	-0.0335%IA + 2.7218	0.000
1 033.9	-0.5085%IA + 3.0152	0.051	-0.0094%IA + 2.8863	0.021	-0.6368%IA + 3.0660	0.017
1 095.6	-0.0994%IA + 2.7638	0.001	-0.0210%IA + 2.9716	0.033	-1.2293%IA + 3.4040	0.046
1 377.2	0.0968%IA + 2.6452	0.025	0.0012%IA + 2.6874	0.003	-0.2007%IA + 2.8172	0.032
1 462.0	0.3464%IA + 2.4898	0.013	0.0147%IA + 2.5152	0.012	2.0290%IA + 1.5452	0.095
1 751.4	0.0543%IA + 2.6693	0.000	0.0074%IA + 2.8085	0.003	-0.6547%IA + 3.0762	0.011
2 731.2	1.3244%IA + 1.8888	0.151	0.0399%IA + 2.1922	0.072	-1.2223%IA + 3.4000	0.028
2 839.2	0.2357%IA + 2.5578	0.006	0.0148%IA + 2.5136	0.012	0.5361%IA + 2.3969	0.006
3 005.1	-0.1729%IA + 2.8089	0.004	-0.0388%IA + 3.1994	0.113	-2.1883%IA + 3.9511	0.147

Note: AV - acid values; PV - peroxide values; TBAV - thiobarbituric acid values; FTIR - Fourier transform infrared.

TABLE 3. PLS-OLS MATHEMATICAL MODELS OF PERCENTAGE OF ABSORBANCE INTENSITY (%IA) TO PREDICT THE AV, PV AND TBAV OF HEATED PALM OIL

Analysis	Multivariate equation models of FTIR measurement	R^2	P*
AV	$0.9880 - 0.8963x(\%IA_{721.28}) - 0.7138x(\%IA_{871.82}) + 1.8433x(\%IA_{968.27}) - 0.0123x(\%IA_{1033.9}) + 0.0346x(\%IA_{1095.6}) - 0.3841x(\%IA_{1377.2}) - 0.0103x(\%IA_{1462}) + 0.0118x(\%IA_{1751.4}) - 0.0478x(\%IA_{2731.2}) + 0.0051x(\%IA_{2839.2}) + 0.0319x(\%IA_{3005.1})$	0.962	< 0.0001
PV	$33.1672 - 16.1175x(\%IA_{721.28}) - 11.3624x\ (\%IA_{871.82}) + 29.2246x(\%IA_{968.27}) - 0.7629x(\%IA_{1033.9}) + 0.0570x(\%IA_{1095.6}) - 6.3644x(\%IA_{1377.2}) - 0.6087x(\%IA_{1462}) + 0.3081x(\%IA_{1751.4}) + 1.3272x(\%IA_{2731.2}) + 0.1276x(\%IA_{2839.2}) - 3.3650x(\%IA_{3005.1})$	0.857	< 0.0001
TBAV	$1.2264 - 0.8268x(\%IA_{721.28}) - 0.2581x(\%IA_{871.82}) + 0.9619x(\%IA_{968.27}) - 0.0246x(\%IA_{1033.9}) + 0.0090x(\%IA_{1095.6}) + 0.0336x(\%IA_{1377.2}) - 0.0128x(\%IA_{1462}) - 0.0284x(\%IA_{1751.4}) - 0.1266x(\%IA_{2731.2}) - 0.0031x(\%IA_{2839.2}) + 0.0480x(\%IA_{3005.1})$	0.845	< 0.0001

Note: *Significantly different at 5%; AV - acid values; PV - peroxide values; TBAV - thiobarbituric acid values; PLS-OLS - partial least squares-ordinary least squares.

A significant linear correlation (R^2 = 0.962; $p<0.05$) was shown between AV and the percentage of absorbance intensity of heated palm oil at 180°C for up to 72 hr (*Table 3*). This mathematical model was only valid for predicting AV under the experimental conditions applied in this study (10 litres of palm oil heated at 180°C for up to 72 hr). The plot of PLS-OLS (*Figure 3a*) shows adjacent values between the predicted and actual AV, suggesting a good prediction of the mathematical model. Similarly, the mathematical model fitted well (R^2 = 0.875; $p<0.05$) to predict PV at a heating time up to 72 hr (*Figure 3b*). A linear mathematical model for predicting TBAV was valid (R^2 = 0.845; $p<0.05$) for the heating process up to 58 hr that gave a TBAV of 0.58 mg malondialdehyde kg^{-1} sample. At prolonged heating times, the model was not accurate for predicting the TBAV (*Figure 3c*). This finding might result from the yield of volatiles or different polar molecules due to extended oxidation, which is difficult measure using the TBAV method (Aladedunye and Przybylski, 2014).

Table 4 shows the verification results of palm oil heated up to 180°C for 24 hr. The actual and predicted AV, PV and TBAV show insignificant deviation ($p>0.05$), indicating the differences in actual and calculated AV, PV and TBAV from the OLS models were not significant. Given this result, the mathematical models appear to be useful for predicting the degree of palm oil quality during frying by applying simple and rapid FTIR spectroscopy measurements.

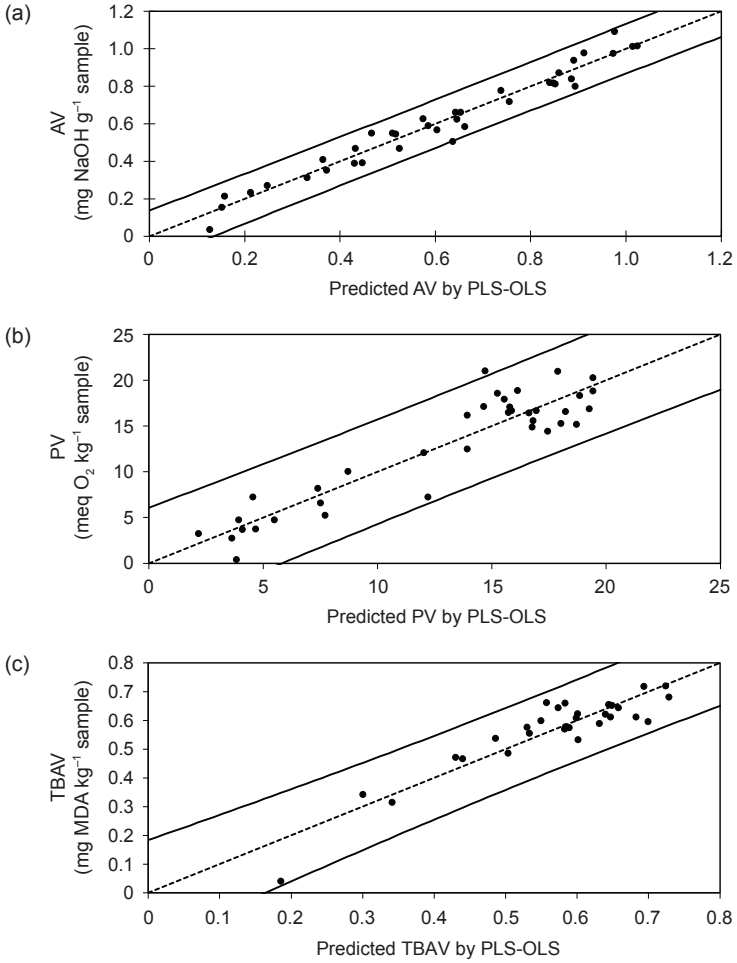


Figure 3. Plots of partial least squares-ordinary least squares (PLS-OLS) predicted values with actual values of palm oil heated at 180°C. (a) acid value (AV), (b) peroxide value (PV), (c) thiobarbituric acid value (TBAV). Dots show the plots between the predicted and actual values. Lines indicate the ideal curve if R^2=1.

TABLE 4.VERIFICATION OF COOKING OIL SAMPLE HEATED AT 180°C FOR 24 HR USING PAIR T TEST

Parameter	Actual value	Predicted value using PLS-OLS model	Sig. (2-tailed)*
Acid value (mg NaOH g^{-1} sample)	0.625	0.600	0.148
Peroxide value (meq O_2 kg^{-1} sample)	13.034	12.706	0.228
Thiobarbituric acid value (mg MDA kg^{-1} sample)	0.545	0.452	0.154

Note: *Not significantly different ($p>0.05$); PLS-OLS - partial least squares-ordinary least squares.

CONCLUSION

FTIR spectroscopy can be applied as an alternative to conventional methods of acid, peroxide and TBA value determinations for monitoring the quality changes of cooking oil during a long period of frying.

ACKNOWLEDGEMENT

The authors are very thankful to the Food Analysis Laboratory of Department of Food Science and Technology, Bogor Agricultural University (IPB University) Indonesia for the technical and financial supports of this research.

REFERENCES

Abdi, H (2003). Partial least squares (PLS) regression. *Encycl Soc. Sci. Res. Methods* (Lews-Beck, M; Bryman, A and Futing, T eds.). p. 792-795.

Abdulkadir, I; Uba, S; Salihu, A and Almustapham, M N (2016). A rapid method of crude oil analysis using FTIR spectroscopy. *Nig. J. Basic Appl. Sci., 24(1)*: 47-55.

Abdulkarim, S M; Long, K; Lai, O M; Muhammad, S K S and Ghazali, H (2007). Frying quality and stability of high-oleic *Moringa oleifera* seed oil in comparison with another vegetable oils. *Food Chem*., *105(4)*: 1382-1389.

Aladedunye, F and Przybylski, R (2014). Performance of palm olein and modified rapeseed, sunflower, soybean oils in intermittent deep-frying. *Eur. J. Lipid Sci. Technol*., *116(2)*: 144-152.

Al-Degs, Y S and Al-Ghouti, M S N (2011). Determination of frying quality of vegetable oils used for preparing falafel using infrared spectroscopy and multivariate calibration. *Food Anal. Methods*, *4(4)*: 540-549.

Ang, Y H; Yew, M Y; Abas W; Lai, M F; Wang, Y, Lai, O M and Tan, C P (2019). Rapid assessment of total MCPD esters in palm-based cooking oil using ATR-FTIR application and chemometric analysis. *Talanta, 198(5)*: 215-223. DOI: 10.1016/j.talanta.2019.01.111.

AOAC (1984). Official Methods of Analysis. Association of Official Analytical Chemistry. Washington DC, USA.

Bhardwaj, S; Passi, S; Misra, A; Pant, K; Anwar, K; Pandey, R and Kardam, V (2016). Effect of heating/reheating of fats/oils, as used by Asian Indians on *trans* fatty acid formation. *Food Chem*., *212*: 663-700. DOI: 10.1016/j.foodchem.2016.06.021.

Bhuiyan, M T H; Khan M; Rahman, A and Chowdhury, U C (2016). Effect of reheating on thermophysical properties of edible oil at high temperature. *Int. J. Adv. Res. Phys. Sci., 3(2)*: 30-34.

Chatzilazarou, A; Gortzi, O; Lalas, S; Zoidis, E and Tsaknis, J (2006). Physicochemical changes of olive oil and selected vegetable oils during frying. *J. Food Lipids*, *13(11)*: 27-35.

Che Man, Y B and Setiowaty, G (1999a). Application of fourier transform infrared spectroscopy to determine free fatty acid contents in palm olein. *Food Chem., 66(1)*: 109-114.

Che Man, Y B and Setiowaty, G (1999b). Multivariate calibration of fourier transform infrared spectra in determining iodine value of palm oil products. *Food Chem., 67(2)*: 193-198. DOI: 10.1016/S0308-8146(99)00102-8.

Che Man, Y B; Marina A M; Abdulrohman, H and Al-Kahtani, O N (2014). A fourier transform infrared spectroscopy method for analysis of palm oil adulterated with lard in pre-fried french fries. *Int. J. Food Prop., 17(2)*: 354-362.

Dana, D and Saguy, I (2001). Frying of nutritious food: Obstacles and feasibility. *Food Sci. Technol. Res., 7(4)*: 265-279. DOI: 10.3136/fstr.7.265.

Edem, D (2002). Palm oil: Biochemical, physiological, nutritional, hematological and toxicological aspects - A review. *Plant Foods Hum. Nutr., 57*: 319-341.

Farahani, H A; Rahiminezhad, A; Same, L and Immannezhad, K (2010). A comparison of partial least squares (PLS) and ordinary least squares (OLS) regressions in predicting of couples mental health based on their communicational patterns. *Procedia – Soc. Behav. Sci., 5*: 1459-1463.

Farida, Y and Siregar, I (2006). *Pengaruh pemanasan berulang terhadap sifat fisikokimia dan kandungan asam palmitat pada minyak goreng*. *J. Ilmu Kefarmasian Indonesia, 4(2)*: 83-91.

Faridah, D N; Lioe, H N; Palupi, N S and Kahfi, J (2015). Detection of FFA and PV values using FTIR for quality measurement in palm oil frying activitie. *J. Oil Palm Res*., *27(2)*: 156-167.

Frankel, E (1987). Secondary products of lipid oxidation. *Chem. Phys. Lipids, 44(2-4)*: 73-85.

Gharby, S; Hicham, H; Boulbaroud, S; Bouzoubaâ Z; El Madani, N; Chafchaouni, I and Charrouf, Z (2014). The stability of vegetable oils (sunflower, rapeseed and palm) sold on the Moroccan market at high temperature. *Int. J. Chem. Biochem. Sci., 5*: 47-54.

Guillen, M D and Cabo, N (1997). Infrared spectroscopy in the study of edible oils and fats. *J. Sci. Food Agric., 75*: 1-11.

H**ö**skuldsson, A (1998). PLS regression methods. *J. Chemometrics, 2(3)*: 211-228.

Jaarin, K and Kamisah, Y (2012). Repeatedly heated vegetable oils and lipid peroxidation. *Lipid Peroxidation* (Catala, A ed.). p. 211-228. DOI: 10.5772/46076.

Kalapathy, U and Proctor, A (2000). A new method for free fatty acid reduction in frying oil using silicate films produced from rice hull ash. *J. Amer. Oil Chem. Soc*., *77(6)*: 593-598.

Kaleem, S; Aziz, S; Iqtedar, M; Abdullah, R; Aftab, M; Rashid, F; Shakoori, F R and Naz, S (2015). Investigating changes and effect of peroxide values in cooking oils subject to light and heat. *Fuuast J. Biol., 5(2)*: 191-196.

Li, Y (2010). A comparison study of principle component regression, partial least squares regression, and ridge regression with application to FTIR data. Ph.D thesis, Uppsala University.

Lim, S Y; Mutalib, M S A; Khaza'ai, H and Chang, S (2018). Detection of fresh palm oil adulteration with recycled cooking oil using fatty acid composition and FTIR spectral analysis. *Int. J. Food Prop., 21(1)*: 2428-2451. DOI: 10.1080/10942912.2018.1522332.

Mancini, A; Imperlini, E; Nigro, E; Montagnese, C; Daniele, A; Orrù, S and Buono, P (2018). Biological and nutritional properties of palm oil and palmitic acid: Effects on health. *Molecules, 20(9)*: 17339-17361. DOI:10.3390/molecules200917339.

Martín-Ramos, P; Maria, T M R; Correa-Guimaraes, A; Carrión-Prieto, P; Hernández-Navarro, S and Martín-Gil, J (2018). Crude and refined oils from *Elaeis guineensis*: Facile characterization by FTIR and thermal analysis techniques. *Int. J. Food Prop., 20(53)*: S2739-2749. DOI: 10.1080/10942912.2017.1372470.

Mba, O I; Dumont, M J and Ngadi, M (2015). Palm oil: Processing, characterization and utilization in the food industry – A review. *Food Biosci., 10(1)*: 26-41. DOI: 10.1016/j.fbio.2015.01.003.

Rohman, A and Che Man, Y (2010). Fourier transform infrared (FTIR) spectroscopy for analysis of extra virgin olive oil adulterated with palm oil. *Food Res. Int., 43(3)*: 886-892.

Rohman, A; Wibowo, D; Sudjadi; Lukitaningsih, E and Rosman, A (2015). Use of fourier transform infrared spectroscopy in combination with partial least square for authentication of black seed oil. *Int. J. Food Prop., 18(4)*: 775-784.

Setiowaty, G and Che Man, Y (2003). A rapid Fourier transform infrared spectroscopic method for the determination of 2-TBARS in palm olein. *Food Chem., 81(1)*: 147-154. DOI: 10.1016/S0308-8146(02)00396-5.

Shahidi, F; Wang, J and Wanasundara, U (2017). Methods for measuring oxidative rancidity in fats and oils. *Food Lipids: Chemistry, Nutrition and Biotechnology* (Akoh, C C and Min, D eds.). Second edition. CRC Press. p. 519-542.

SNI (1998). Cooking Oil SNI 01-3555-1998. National Standardization Agency of Indonesia.

Song, J; Park, P; Jung, J; Lee, C; Gim, S Y; Ka, H J; Yi, B; Kim, M; Kim, C and Lee, J (2015). Analysis of *trans* fat in edible oils with cooking process. *Toxicol Res., 31(3)*: 307-312. DOI: 10.5487/TR.2015.31.3.307.

Tarladgis, B G; Pearson, A M and Dugan, L (1962). The chemistry of the 2-thiobarbituric acid test for the determination of oxidative rancidity in foods. *J. Amer. Oil Chem. Soc., 39(1)*: 34-39. DOI: 10.1007/BF02633347.

Tsaknis, J; Lalas, S; Gergis, V; Dourtoglou, V and Spiliotis, V (1998). Quality changes of *Moringa oleifera*, variety of blantyre seed oil during frying. *La Riv Ital Sostanze Grasse, 75(4)*: 181-190. DOI: 10.3989/gya.2002.v53.i2.305.

Vlachos, N; Skopelitis, Y; Psaroudaki, M; Konstantinidou, V; Chatzilazarou, A and Tegou, E (2006). Application of fourier transform infrared spectroscopy to edible oils. *Anal. Chim. Acta., 573-574*: 459-465.

Wong, Y H; Goh, K M; Abas, F; Maulidiani M; Nyam, K L; Nehdi, I A; Sbihi, H M; Gewik, M M and Tan, C P (2019). Rapid quantification

of 3-monochloropropane-1,2-diol in deep-fat frying using palm olein: Using ATR-FTIR and chemometrics. *LWT. 100*: 404-408. DOI: 10.1016/j.lwt.2018.10.088.

Wrolstad, R E; Acree, T E; Decker, E A; Penner, M H; Reid, D S; Schwartz, S J; Shoemaker, C F; Smith, D M and Sporns, P (2000). *Handbook of Food Analytical Chemistry.* John Wiley and Sons, Inc. New Jersey.

Journal of Oil Palm Research

MPOB

Journal of Oil Palm Research ISSN 1511-2780
An international refereed journal on oil palm
Impact Factor: 2.057 (2020)
CiteScore: 3.0 (2020)
SJR: 0.498 (2020)

MALAYSIA'S RESEARCH STAR AWARD & PENGIKTIRAFAN JURNAL CREME 2019

HOME | HISTORY | EDITORIAL BOARD | HOW TO PUBLISH | GUIDE TO AUTHORS | CONTACT US | UPCOMING ISSUE | USER SURVEY

Select Issue 2021 Vol 33 June

OIL PALM ECONOMIC PERFORMANCE IN MALAYSIA AND R&D PROGRESS IN 2020 – *Review Article*
DOI:https://doi.org/10.21894/jopr.2021.0026
Published online: 11 June 2021

Vol. 33 June 2021 p. 181-214
Author(s): GHULAM KADIR AHMAD PARVEEZ*; AZMIL HAIZAM AHMAD TARMIZI*; SHAMALA SUNDRAM*; SOH KHEANG LOH*; MEILINA ONG-ABDULLAH*; KOSHEELA DEVI POO PALAM*; KAMALRUDIN MOHAMED SALLEH*; SHEILYZA MOHD ISHAK* and ZAINAB IDRIS*

Show Abstract / Summary | View Full Article

POTENTIAL OF *Syncephalastrum racemosum* AND *Rhizopus arrhizus* ISOLATED FROM OIL PALM TRUNKS PRODUCE CHITOSANS THAT INHIBIT THE GROWTH OF *Ganoderma boninense*

and SABRINA, T*

OPEN ACCESS

CALL FOR PAPERS
Manuscript Submission
ARTICLE IN PRESS

2.057 Impact Factor (2020)

Scan this code

CiteScore
CiterScore Metrics
3.0 (2020)

SJR
Scientific Journal Rank
0.498 (2020)

Tel: +603-8925 6332
Fax: +603-89259446
Email : pub@mpob.gov.my

Contact Us
Malaysian Palm Oil Board (MPOB)
No. 6, Persiaran Institusi, Bandar Baru Bangi, 43000 Kajang, Selangor, Malaysia.

http://jopr.mpob.gov.my

http://mpob.gov.my | Malaysian Palm Oil Board | mpob_tweets | Malaysian Palm Oil Board

Journal of Oil Palm Research Vol. 33 (3) September 2021 p. 524-531
DOI: https://doi.org/10.21894/jopr.2020.0102

DEVELOPMENT OF PALM-BASED VANASPATI (VEGETABLE GHEE): EFFECTS OF CRYSTALLISATION PROCEDURES ON THE PRODUCT TEXTURE

RAFIDAH ABD HAMID[1]*; SIVARUBY KANAGARATNAM[1]; NORAZURA AILA MOHD HASSIM[1]; NUR HAQIM ISMAIL[1]; WAN ROSNANI AWG ISA[1] and NOOR LIDA HABI MAT DIAN[1]

ABSTRACT

Trans *free vanaspati (vegetable ghee) formulated using a blend of refined, bleached and deodourised (RBD) palm stearin with iodine value of 30 (POs IV30) and palm olein with iodine value of 58 (POo IV58) in 40:60 w/w ratio was produced. The effect of mixing procedure on the crystallisation of the blend was investigated. VC-1 treatment which involved mixing of POs IV30 at 24ºC into POo IV58 at 65ºC and mixing the blend to a complete melt at room temperature followed by tempering at 25ºC produced a granulated vanaspati with spherical or granular shape crystals. VC-2 treatment which involved the mixing of POs IV30 at 55ºC into POo IV58 at 24ºC and mixing the blend to a complete melt at room temperature followed by tempering at 25ºC produced small crystals which is suitable for the production of smooth textured vanaspati. Vanaspati produced using VC-3 treatment which involved the mixing of POs IV30 at 24ºC into POo IV58 at 65ºC but was not mixed to a complete melt, followed by tempering at 25ºC produced small crystals and loosely packed structure which led to the formation of a slightly grainy textured vanaspati. Thus, a consistent and homogenous grainy textured vanaspati could be produced under controlled conditions using treatment VC-1 and this will be able to resolve the problem of inconsistency of texture in 100% palm-based grainy vanaspati. Grainy vanaspati is preferred by consumers in India and Pakistan where the demand of vanaspati is very high.*

Keywords: crystallisation procedure, granular texture, palm olein, palm stearin, smooth texture, vanaspati, vegetable ghee.

Received: 29 June 2020**; Accepted:** 14 September 2020; **Published online:** 24 December 2020.

INTRODUCTION

Vanaspati, also known as vegetable ghee, is an all-purpose fat widely used in the Indo-Pakistan subcontinent and Middle Eastern countries. It is used for cooking purposes in different domestic and commercial places (Ahmad *et al.*, 2006). In India, the consumption of edible oils and vanaspati is comparatively high compared to other countries with a production of about 1.2 million tonnes annually (NPCS, 2020). Meanwhile, vanaspati has emerged as one of the most essential ingredients of human diet in Pakistan (Ahmad *et al.*, 2006) and Iran (Farmani *et al.*, 2007).

Originally, vanaspati was developed as an alternative to the traditional ghee made from butter fat. Vanaspati is required to have a coarse granular structure at ambient temperature, with crystal required to melt at 37°C-39°C (Nor Aini *et al.*, 1997). The texture preference of this product varies for different consumers. In India and Pakistan, graininess is a required criterion. Unlike the Indian counterparts who prefer their vanaspati to be grainy, yet dry and crumbly, Pakistani consumers prefer grainy crystals among liquid oil (Siew, 2011).

[1] Malaysian Palm Oil Board,
6 Persiaran Institusi, Bandar Baru Bangi,
43000 Kajang, Selangor, Malaysia.

* *Corresponding author e-mail: rafidah@mpob.gov.my*

Initially, fully or partially hydrogenated fats have been found to be the most suitable and widely used fats in the production of vanaspati. However, hydrogenated fats contain undesirable and health threatening *trans* fatty acids. Palm oil (PO) is the most promising material in terms of price, availability and functionality for vanaspati. PO which has similar physical characteristics such as melting points, melting profile and semi-solid consistency at ambient temperature to butter fat has been widely used in the making of vanaspati. Palm stearin (POs) which is the solid fraction of PO, can also be used for making vanaspati. Although naturally PO and POs do not develop the desired granular appearance, vanaspati of satisfactory granular consistency can be obtained by employing interesterification (IE) on the palm-based vanaspati oil blends (Kheiri and Oh, 1983; Nor Aini *et al.*, 1997; Siew, 2011). Furthermore, more PO fractions can be incorporated in vanaspati with IE process (Nor Aini and Noor Lida, 2005). Nor Aini *et al.* (1997; 1999) and Nor Aini and Noor Lida (2005) reported that *trans* free vanaspati having characteristics similar to those of hydrogenated vanaspati can be produced using blends of POs and liquid oils such as rapeseed, soyabean and sunflower oils, either by direct blending or by employing IE. When PO products are used in high amounts, it can facilitate separation of liquid and solid phases through slow cooling. Phase separation characteristic is associated with melting points of various triacylglycerols (TAG) present in PO. This property of PO can assist production of vanaspati which targets grainy crystals among liquid oil (Sivaruby and Noor Lida, 2007).

Besides blending formulations and ingredients, processing conditions also play a very important role because they have great capability to determine the properties of vanaspati. Processing conditions can affect the physical properties of the vanaspati including its appearance, texture, and crystallisation behaviour (Farmani and Gholitabar, 2015). In some countries, especially in India, Pakistan and Bangladesh, granularity is considered as an important criterion of quality and purity of vanaspati. To achieve granular texture, the oil/blend is cooled slowly in a cold room maintained at 15ºC with adequate cold air circulation (Kheiri, 1985). On slow cooling, β′ crystal would first form followed by the α-crystal surrounding the β′ crystal that acts as nuclei for crystallisation (Blaurock, 1999; Nor Aini *et al.*, 2010). Products with smooth texture are obtained by rapidly cooled the oil/blend on a scraped-surface heat exchanger (Kheiri, 1985; Noor Lida *et al.*, 2017). Hot oil that is rapidly cooled to a temperature below melting point would most probably crystallise in α form followed by the formation of β′ and β crystals (Blaurock, 1999; Nor Aini *et al.*, 2010). Besides various temperature conditions, emulsifier with different hydrophobic properties would also affect fat properties by accelerating or retarding crystallisation and polymorphic transformation (Garti, 2002; Miskandar *et al.*, 2002a; 2002b).

The dynamic slow crystallisation will promote crystal formation in spherical shape, while dynamic fast crystallisation, produces needle shaped small crystals (Martini *et al.*, 2002; Miskandar *et al.*, 2004). Slow agitation will produce crystal with denser crystal structure, while higher agitation rate results in the formation of many small crystals mainly transparent, with lower amount of solid in each crystal (Herrera and Hartel, 2000). Crystallisation without agitation will cause the crystals to be densely arranged and bigger in size (Martini *et al*., 2002).

Although palm-based oils are widely used in the making of vanaspati, information on the effects of manufacturing procedures on the physical characteristics of palm-based vanaspati are scarce. This article reports the effect of crystallisation procedure on the blend of POs with iodine value of 30 (POs IV30) and palm olein with iodine value of 58 (POo IV58) at 40:60 w/w ratio in a vessel type crystalliser on the texture of vanaspati made of the said blend.

MATERIALS AND METHODS

Materials

Refined, bleached and deodourised (RBD) POs IV30 and POo IV58 were obtained from a local refinery in Malaysia.

Fatty Acid Composition (FAC)

FAC was determined as fatty acid methyl esters (FAME) according to the procedures described in Noor Lida *et al.* (2019). FAME was prepared by dissolving 50 mg of a melted and homogenised fat blend in 950 µl hexane and 50 µl of 1 M sodium methoxide. The mixture was then mixed vigorously with a vortex mixer for 10 s or until it became cloudy before centrifugation at 2000 rpm for 2 min to separate the mixture into two distinct layers. The upper clear supernatant consisting of FAME was decanted. One µl of FAME was then injected and analysed using a Hewlett Packard HP 6890 Series (Palo Alto, USA) gas chromatography system equipped with a flame ionisation detector. Separation was performed using a Durabond DB-23 fused silica capillary column (60 m length x 0.25 mm *i.e*. x 0.25 µm film thickness) (Agilent, Santa Clara, USA). Injector and detector temperatures were set at 240°C, whereas the column temperature was isothermal at 185°C. The flow rate of the carrier gas helium was 0.8 ml min^{-1}. Peaks were identified by FAME standards and quantified using the peak area normalisation method.

Slip Melting Point (SMP)

SMP of a sample was determined according to the procedures described in MPOB Test Method p4.2:2004 (MPOB, 2004). A molten sample was placed in three capillary tubes (50-60 mm length x 1.1-1.3 mm i.d. x 1.4-1.5 e.d.) with openings at both ends, filling each to a length of 10 mm. The sample in the tube was then solidified by rolling the tube on an ice cube. The capillary tube was then placed in a test tube, and held in a water bath equilibrated at 10°C for 16 hr. The tube was then attached to a thermometer (graduated in divisions of 0.1°C-0.2°C) with a rubber band, before immersing both into a beaker containing 400 ml of cold distilled water with a temperature of 5°C-10°C below the expected SMP of the sample. The water bath was agitated with a magnetic stirrer and heat was applied continuously to increase the bath temperature at a rate of 0.5°C min^{-1}. The temperature at which the fat column rose due to hydrostatic pressure was recorded as SMP of the fat sample.

Solid Fat Content (SFC)

SFC of the oil blend was determined with a Bruker Minispec MQ20 Pulsed Nuclear Magnetic Resonance (p-NMR) analyser (Karlsruhe, Germany) according to the procedures described in MPOB Test Method p4.8:2004-Non-stabilised Serial procedures (MPOB, 2004). A molten sample was filled up to 3 cm height of a p-NMR tube, re-melted at 70°C for 30 min to erase any crystal memory, chilled at 0°C for 90 min and held at the respective measuring temperatures for 30 min prior to measurement of total solid fat (%) at each measuring temperature from 5°C-50°C at intervals of 5°C.

The isothermal SFC of vanaspati sample which had been tempered at 25°C for 24 hr and 48 hr was also determined with the Bruker Minispec MQ20 p-NMR analyser. The vanaspati was filled up to 3 cm height of a p-NMR tube and the SFC of the vanaspati was then measured at 25°C.

Microscopic

Microscopic examination for fat crystal morphology and distribution in the vanaspati was done by placing a small amount (about 1-10 mg) of vanaspati on a glass slide. A glass cover slip was placed on top of the sample and slightly pressed to ensure thin distribution of sample. The sample was immediately viewed under a polarised microscope (Olympus model BH-2, Olympus Corporation, Tokyo, Japan) at room temperature (around 25°C). The microscope was attached to a video camera (Leica Q500mc Qwin Vol 0.02; Leica Cambridge Ltd., Cambridge, United Kingdom) to capture the crystals images. The photomicrograph of the crystal was taken at 100X magnification.

Vanaspati Production

The vanaspati samples were produced using a blend of POs IV30 and POo IV58 at 40:60 w/w ratio. Blend of POs and POo was used in this study based on previous study by Rustaman *et al*. (2000) who had successfully produced vanaspati using blend of POs and POo. Minimising types of oils and fats used in a formulation is an effective cost saving option that is preferable in a commercial vanaspati production (Sivaruby and Noor Lida, 2007). Three different process conditions were evaluated as detailed in *Table 1*. Temperature of 65°C was chosen to destroy all memory of crystals in POo and 55°C was chosen to observe the effect of using temperature just around the melting point of POs to start nucleation. Temperature 24°C was chosen to represent ambient temperature. Crystallisation of the blend was carried out in a double jacketed 3000 ml vessel with a continuous stirring of 50 rpm speed. Cooling of the fat in the vessel to form vanaspati was carried out using a water bath at a selected controlled temperature. Treatment 1 (VC-1) involved the mixing of POs IV30 at 24°C into POo IV58 at 65°C and kept mixing the blend to a complete melt at room temperature prior to tempering. Treatment 2 (VC-2) involved the mixing POs IV30 at 55°C into POo IV58 at 24°C and continuously mixed to homogeneity at room temperature prior to tempering. Treatment 3 (VC-3) involved the mixing of POs IV30 at 24°C into POo IV58 at 65°C. In VC-3 treatment, the mixture was not mixed until complete melt, instead, the mixing was stopped once the mixture had formed a slurry. The vanaspati from VC-1, VC-2 and VC-3 treatment were then filled into a 300 ml round shaped plastic containers and tempered at 25°C for 24 hr and 48 hr.

TABLE 1. THE CRYSTALLISATION TREATMENTS OF PALM STEARIN WITH IODINE VALUE OF 30 (POs IV30) AND PALM OLEIN WITH IODINE VALUE OF 58 (POo IV58) BLEND AT 40:60 W/W RATIO IN THE MAKING OF VANASPATI

Treatment	Oil temperature		Mixing procedure
	POs IV30 (40%)	POo IV58 (60%)	
VC-1	24°C	65°C	50 rpm, complete mixing/melt, room temperature
VC-2	55°C	24°C	50 rpm, complete mixing/melt, room temperature
VC-3	24°C	65°C	50 rpm, incomplete mixing/melt, slurry form, room temperature

RESULTS AND DISCUSSION

Characteristics of the Vanaspati Oil Blend

The FAC and SFC profile of the blends of POs IV30 and POo IV58 at 40:60 w/w ratio, having SMP of 47°C and IV of 47.95 are shown in *Table 2* and *Figure 1*, respectively. The blend consisted of 53.36% saturated, 37.50% monounsaturated and 9.02% polyunsaturated fatty acids. The major fatty acids were palmitic and oleic acids with significant amount of linoleic and stearic acids. The SFC at the application and storage temperatures of 25°C-40°C ranged from 24% at 25°C to 12% at 40°C. Hence, this blend has the potential to remain solid at this temperature range, which is also the crucial temperature of storage that ranges from 25°C-40°C.

TABLE 2. FATTY ACID COMPOSITION (%) OF THE BLENDS OF PALM STEARIN WITH IODINE VALUE OF 30 (POs IV30) AND PALM OLEIN WITH IODINE VALUE OF 58 (POo IV58) AT 40:60 W/W RATIO

Fatty acids	Composition (%)
Lauric acid (C12:0)	0.21 ± 0.02
Myristic acid (C14:0)	1.10 ± 0.00
Palmitic acid (C16:0)	47.34 ± 0.02
Palmitoleic acid (C16:1)	0.17 ± 0.00
Stearic acid (C18:0)	4.39 ± 0.00
Oleic acid (C18:1 n9t)	0.00 ± 0.00
Oleic acid (C18:1 n9c)	37.33 ± 0.02
Oleic acid (C18:1 n9ci)	0.00 ± 0.00
Linoleic acid (C18:2n6t)	0.12 ± 0.00
Linoleic acid (C18:2n6c)	8.82 ± 0.00
Linolenic acid (C18:3)	0.20 ± 0.00
Arachidic acid (C20:0)	0.32 ± 0.01
Total saturated fatty acid	53.36 ± 0.02
Total monounsaturated fatty acid	37.50 ± 0.02
Total polyunsaturated fatty acid	9.02 ± 0.00

The SFC of the vanaspati produced using VC-1 treatment which was tempered at 25°C for 24 hr and 48 hr is shown in *Table 3*. The SFC of the vanaspati after 24 hr and 48 hr of tempering were 20.95% and 21.71%, respectively, showing that there was no drastic increase in SFC between 24-48 hr of tempering at 25°C. The SFC of the vanaspati VC-1 after 48 hr of tempering was lesser by 2.69% than the SFC of the oil blend at 25°C (24.4%, *Figure 1*). These results indicated that crystal growth was very effective during production of the palm-based vanaspati using the VC-1 treatment.

TABLE 3. SOLID FAT CONTENT (SFC) OF VANASPATI MADE OF PALM STEARIN WITH IODINE VALUE OF 30 (POs IV30) AND PALM OLEIN WITH IODINE VALUE OF 58 (POo IV58) AT 40:60 W/W RATIO AFTER TEMPERING AT 25°C FOR 24 HR AND 48 HR

Tempering time (hr)	SFC (%)		
	Vanaspati VC-1	Vanaspati VC-2	Vanaspati VC-3
24	20.95	18.93	10.40
48	21.71	19.21	11.36

When POs IV30 at 24°C was added into POo IV58 at 65°C, the low melting TAG (with SMP of less than 65°C) of the POs IV30 melted. However, some high melting TAG primarily tripalmitin (PPP) were not melted. As the fat was cooled to 24ºC, the high melting TAG became the centre of crystallisation creating big crystal agglomerates. The crystal morphology of vanaspati VC-1 at 24 hr and 48 hr is shown in *Figure 2*. Theoretically, when bulk oil is crystallised, the entire mass does not crystallise at the same time, but crystallisation begins at discrete sites when the temperature reaches a level that creates crystallisation nuclei (Lawler and Dimick, 2008; De Oliveira *et al*., 2015). The time for the whole bulk to crystallise depends on the rate of interaction between the crystallised fats and the neighbouring liquid

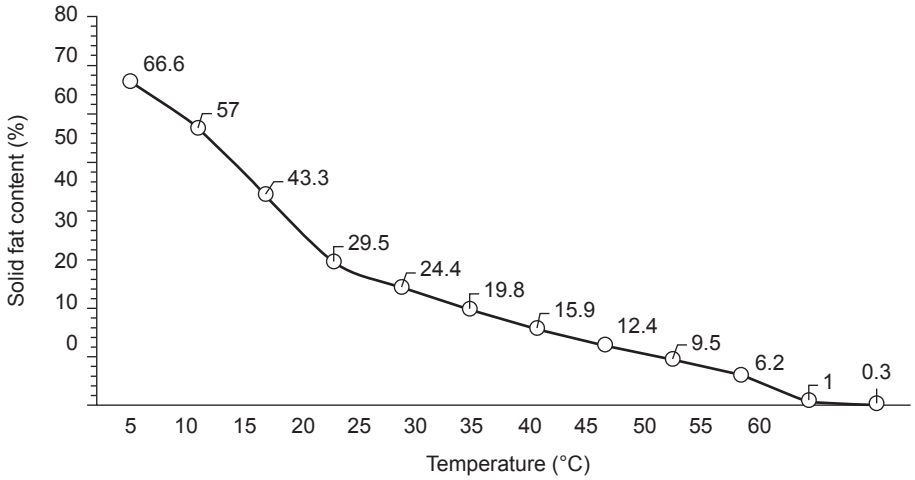


Figure 1. Solid fat content of the blend of palm stearin with iodine value of 30 (POs IV30) and palm olein with iodine value of 58 (POo IV58) at 40:60 w/w ratio.

phase (Normah *et al*., 2013). The crystallisation pattern is also influenced by the parameter setting of agitation. The VC-1 treatment was able to produce discrete crystal structures. The addition of POs IV30 at 24°C into POo IV58 at 65°C was able to induce slow nucleation with nuclei that were able to create discrete crystals. There was no major change observed in crystal morphology after 24 hr as discrete crystals in liquid oil was observed. *Figure 3* shows coarseness of the blend's texture after 48 hr of tempering. This observation complemented the morphology of the coarse crystals observed by the microscope (*Figure 2*). The coarse crystals morphology is normally observed in granular type vanaspati. Thus, VC-1 treatment on the blend of POs IV30 and POo IV58 at 40:60 w/w ratio is recommended for the production of granular type vanaspati.

The SFC of vanaspati produced using VC-2 treatment which was tempered at 25°C for 24 hr and 48 hr is shown in *Table 3*. The SFC of vanaspati after tempering for 24 hr and 48 hr were 18.93% and 19.21%, respectively, showing no drastic increase in the SFC between 24-48 hr of tempering. The SFC of vanaspati VC-2 after 48 hr of tempering was lesser by 5.19% than the SFC of the oil blend at 25°C (24.4%, *Figure 1*) and was 2.5% lesser than that of vanaspati VC-1 (21.71%). These observations denoted that less liquid was entrapped into the crystal matrix, hence, resulted in lower SFC than vanaspati VC-1 and the oil blend. The results also indicated that VC-2 treatment produced lesser crystal development as shown by the low SFC (18.93%) at 25°C, indicating that crystallisation could be less efficient as compared to VC-1 treatment.

Figure 4 shows the crystal morphology of vanaspati VC-2 after 24 hr and 48 hr of tempering at 25°C. The addition of POs IV30 with temperature of 55°C into POo IV58 of temperature 24°C induced fast nucleation. The fast nucleation was caused by rapid drop of temperature of POs IV30 from 55°C to 24°C. The instant inducement of nuclei produced large number of nucleus, which in turn produced small crystals during tempering at 25°C as shown in *Figure 4*. Discrete crystal structure such as observed in vanaspati VC-1 was not detected in vanaspati VC-2. There was no major change observed in crystal morphology between 24-48 hr of tempering. *Figure 5* shows the smooth texture of vanaspati VC-2 after 48 hr of tempering. The texture of vanaspati VC-2 complemented the crystals morphology by the microscope. Thus, VC-2 treatment on the blend of POs IV30 and POo IV58 at 40:60 w/w ratio produced small crystals which is suitable for the production of smooth textured vanaspati.

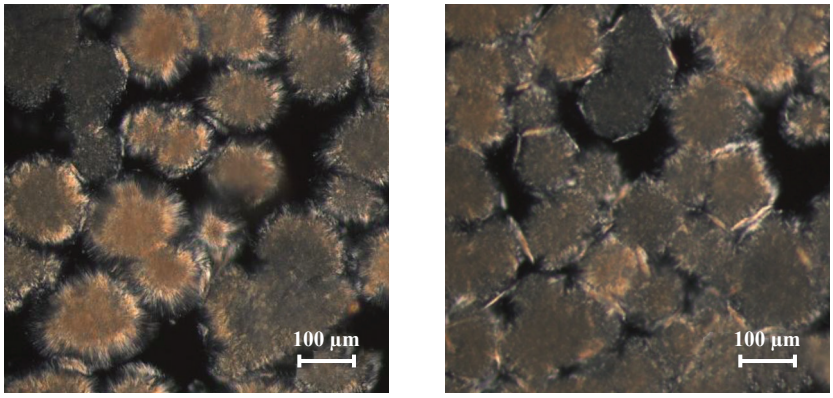


Figure 2. Crystal morphology of vanaspati VC-1 made of palm stearin with iodine value of 30 (POs IV30) and palm olein with iodine value of 58 (POo IV58) at 40:60 w/w ratio after (a) 24 hr, and (b) 48 hr of tempering at 25°C.

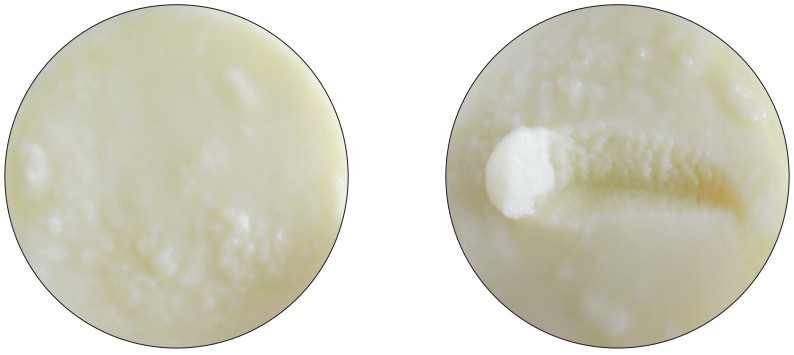


Figure 3. Physical appearance of vanaspati VC-1 made of palm stearin with iodine value of 30 (POs IV30) and palm olein with iodine value of 58 (POo IV58) at 40:60 w/w ratio after 48 hr of tempering at 25°C.

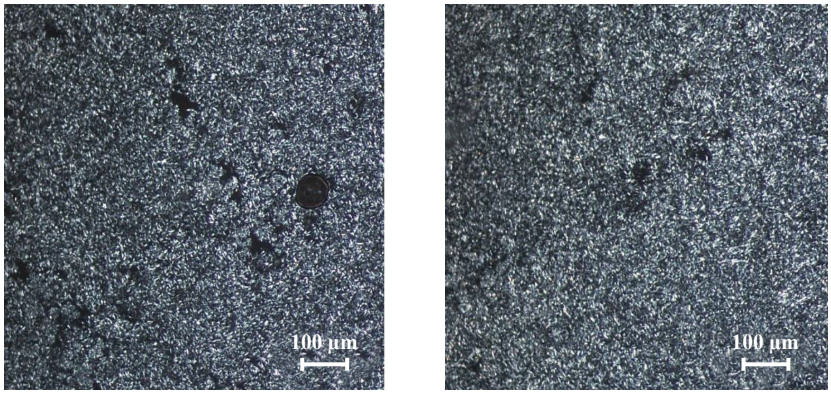


Figure 4. Crystal morphology of vanaspati VC-2 made of palm stearin with iodine value of 30 (POs IV30) and palm olein with iodine value of 58(POo IV58) at 40:60 w/w ratio after (a) 24 hr, and (b) 48 hr of tempering at 25°C.

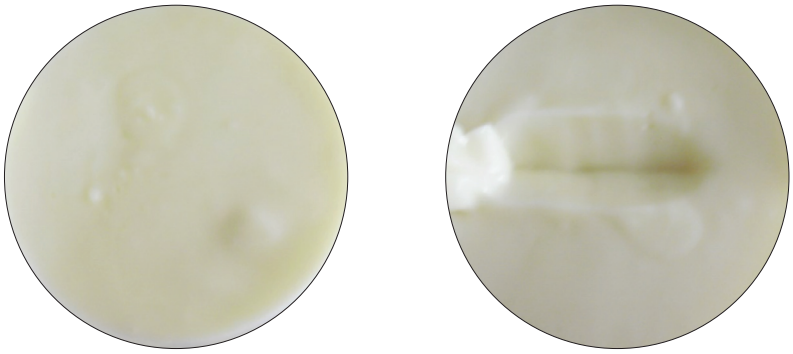


Figure 5. Physical appearance of vanaspati VC-2 made of palm stearin with iodine value of 30 (POs IV30) and palm olein with iodine value of 58 (POo IV58) at 40:60 w/w ratio after 48 hr of tempering at 25°C.

The SFC of vanaspati produced using VC-3 treatment after tempering at 25°C for 24 hr and 48 hr were 10.40% and 11.36%, respectively (*Table 3*), denoting only a slight increase in the SFC between 24-48 hr of tempering at 25°C. The SFC obtained after 48 hr of tempering was lesser by 13.04% than the SFC of the oil blend at 25°C (24.4%, *Figure 1*). The SFC of vanaspati VC-3 was also lesser than that of vanaspati VC-1 (10.35% less) and vanaspati VC-2 (7.85% less). These observations denoted that only approximately 50% of the oil blend crystalised and 50% remained in liquid state. In order for a crystal to entrap liquid oil in its structure, the crystal should form (starting from nucleation) and grow from a liquid state until it reaches stabilisation state. In VC-3 treatment, the POs IV30 which was already in crystallised form was not fully melted when it was mixed with the POo IV58 of 65°C. The mixture was not homogenised and was kept in slurry form prior to tempering at 25°C. Hence, the crystals were not able to entrap the liquid oil within the crystal matrix at 25°C, thus, resulted in lower SFC.

Figure 6 shows the crystal morphology of vanaspati VC-3 at 24 hr and 48 hr of tempering at 25°C. Although, the temperature treatment of VC-3 was similar to VC-1 treatment, VC-3 treatment did not produce big crystal agglomerations. In VC-3 treatment, the low melting TAG of the POs IV30 were not completely melted. The slurry mixture of POs IV30 and POo IV58 contained a huge amount of crystals (high and low melting TAG) that acted as nuclei, thus, crystallisation was not focussed to small number of sites but had taken place in a big number of crystallisation sites. The crystals experienced only limited growth. This situation resulted in formation of small crystals which were more in number and loosely packed as compared to the crystals formed in vanaspati produced using VC-1 treatment. The small crystals and loosely packed structure led to the formation of a slightly grainy texture. There was no major change observed in crystal morphology between 24-48 hr. Discrete crystal structure such as observed in vanaspati VC-1 was not detected in vanaspati VC-3. Based on the crystal morphology, vanaspati VC-3 had smaller crystals and denser than vanaspati VC-1, but its crystals were bigger and less dense than vanaspati VC-2. *Figure 7* shows the texture of the blend after 48 hr of tempering. This observation complemented the morphology of crystals observed by the microscope. Hence, VC-3 treatment is recommended for the production of vanaspati with slightly grainy texture.

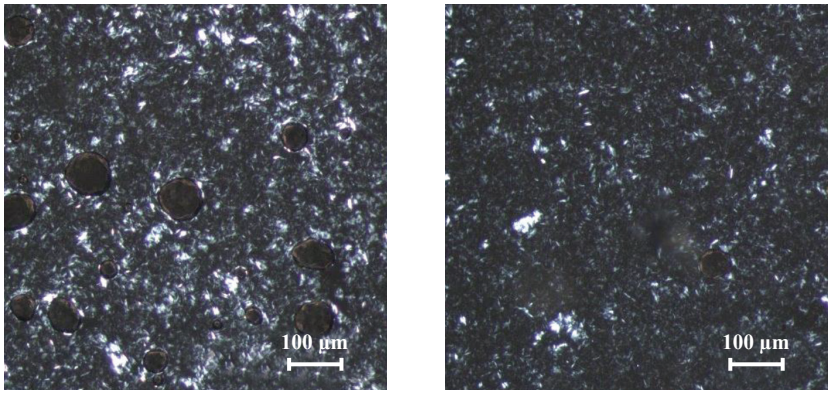


Figure 6. Crystal morphology of vanaspati VC-3 made of palm stearin with iodine value of 30 (POs IV30) and palm olein with iodine value of 58 (POo IV58) at 40:60 w/w ratio after (a) 24 hr and (b) 48 hr of tempering at 25°C.



Figure 7. Physical appearance of vanaspati VC-3 made of palm stearin with iodine value of 30 (POs IV30) and palm olein with iodine value of 58 (POo IV58) at 40:60 w/w ratio after 48 hr of tempering at 25°C.

CONCLUSION

VC-1 treatment which involved mixing of POs IV30 at 24°C into POo IV58 at 65°C and mixing the blend to a complete melt at room temperature followed by tempering at 25°C produced a granulated vanaspati with spherical or granular shape crystals. VC-2 treatment which involved the mixing of POs IV30 at 55°C into POo IV58 at 24°C and mixing the blend to a complete melt at room temperature followed by tempering at 25°C produced small crystals which is suitable for the production of smooth textured vanaspati. Vanaspati produced using VC-3 treatment which involved the mixing of POs IV30 at 24°C into POo IV58 at 65°C but was not mixed to complete melt, followed by tempering at 25°C produced small crystals and loosely packed structure which led to the formation of a slightly grainy textured vanaspati.

ACKNOWLEDGEMENT

The authors thank the Director-General of MPOB for permission to publish this article. The authors also thank Dr. Miskandar Mat Sahri for his expert advice and the staff of Food Technology Group for their skilful technical assistance in ensuring the success of this study.

REFERENCES

Ahmad, W; Mustafa, K and Ahmad, T (2006). Factors influencing customer's preference for purchase of vegetable ghee: A comparison of two 'ghee firms' in Punjab. *Pak. J. Agri. Sci., 43(1-2)*: 82-85.

Blaurock, A E (1999). Fundamental understanding of the crystallisation of oils and fats. *Physical Properties of Fats, Oils and Emulsifiers* (Widlak, N ed.). AOCS Press, Champaign, IL, USA. p. 1-30.

De Oliveira, G M; Ribeiro, A P B; dos Santos, A O; Cardoso, L P and Kieckbusch, T G (2015). Hard fats as additives in palm oil and its relationships to crystallization process and polymorphism. *LWT-Food Sci. Technol., 63(2)*: 1163-1170.

Farmani, J and Gholitabar, A (2015). Characterization of vanaspati fat produced in Iran. *J. Amer. Oil Chem. Soc., 92(5)*: 709-716.

Farmani, J; Hamedi, M; Safari, M and Madadlou, A (2007). *Trans*-free Iranian vanaspati through enzymatic and chemical transesterification of triple blends of fully hydrogenated soybean, rapeseed and sunflower oils. *Food Chem., 102(3)*: 827-833.

Garti, N (2002). Food emulsifiers: Structure-reactivity relationships, design and applications. *Physical Properties of Lipids*. CRC Press. p. 268-389.

Herrera, M L and Hartel, R W (2000). Effect of processing conditions on crystallization kinetics of a milk fat model system. *J. Amer. Oil Chem. Soc., 77(11)*: 1177-1188.

Kheiri, M S A (1985). Palm oil products in cooking fats. *J. Amer. Oil Chem. Soc., 62(2)*: 410-416.

Kheiri, M S A and Oh, F C (1983). Formulation of vegetable ghee/vanaspati. *Palm Oil Product Technology in the Eighties.* p. 449-468.

Lawler, P J and Dimick, P S (2008). Crystallization and polymorphism of fats. *Food Lipids.* Third edition (Casmir, C A and David, B M eds.). CRC Press, Florida, USA. p. 245-267.

Martini, S; Herrera, M L and Hartel, R W (2002). Effect of cooling rate on crystallization behavior of milk fat fraction/sunflower oil blends. *J. Amer. Oil Chem. Soc., 79(11)*: 1055-1062.

Miskandar, M S; Che Man, Y B; Yusoff, M S A and Abdul Rahman, R (2002a). Effect of emulsion temperature on the physical properties of palm oil-based margarine. *J. Amer. Oil Chem. Soc., 79(12)*: 1163-1168.

Miskandar, M S; Che Man, Y B; Abdul Rahman, R; Nor Aini; and Yusoff, M S A (2002b). Effect of scraped-surface tube cooler temperature on physical properties of palm oil margarine. *J. Amer. Oil Chem. Soc., 79(9)*: 931-936.

Miskandar, M S; Che Man, Y B; Abdul Rahman, R; Nor Aini and Yusoff, M (2004). Palm oil crystallization: Effects of cooling time and oil content. *J. Food Lipids, 11(3)*: 190-207.

MPOB (2004). A compendium of test on palm oil products, palm kernel products, fatty acids, food-related products and others. *MPOB Test Methods*. MPOB, Bangi.

Normah, I; Cheow, C S and Chong, C L (2013). Crystal habit during crystallization of palm oil: Effect of time and temperature. *Int. Food Research J., 20(1)*: 417-422.

Noor Lida, H M D; Lee, Y Y; Nik Aznizan, N I; Norazura Aila, M H; Saw, M H; Tan, C P and Lai, O M (2019). Low-temperature directed interesterification increases triunsaturated and trisaturated triacylglycerols of palm oil and affects its thermal, polymorphic and microstructural properties. *J. Oil Palm Res., 31(1)*: 95-109.

Noor Lida, H M D; Rafidah, A H; Sivaruby, K; Wan Rosnani, A I; Norazura Aila, M H; Nurhaqim, I; Zaliha, O and Miskandar, M S (2017). Palm oil and palm kernel oil: Versatile ingredients for food applications. *J. Oil Palm Res., 29(4)*: 487-511.

Nor Aini, I; Hanirah, H; Maimon, C H; Zawiah, S and Che Man, Y B (2010). Physico-chemical properties and quality of palm-based vegetable ghee. *Sains Malays., 39(5)*: 791-794.

Nor Aini, I and Noor Lida, H M D (2005). Interesterified palm products as alternatives to hydrogenation. *Asia Pac. J. Clin. Nutr., 14(4)*: 396-401.

Nor Aini, I; Che Maimon, C H; Hanirah, H; Zawiah, S and Che Man, Y B (1999). *Trans*-free vanaspati containing ternary blends of palm oil-palm stearin-palm olein and palm oil-palm stearin-palm kernel olein. *J. Amer. Oil Chem. Soc., 76(5)*: 643-648.

Nor Aini, I; Mohd Suria Affandi, Y and Mohd Arif, S (1997). Palm-based *trans* free vanaspati. *PORIM Information Series No. 66*. MPOB, Bangi.

NPCS (2020). Vanaspati ghee industry. NIR Project Consultancy Services (NPCS) Report on https://www.entrepreneurindia.co/blog-description/6836/vanaspati +ghee+industry, accessed on 25 March 2020.

Rustaman, A; Muchtadi, T R and Adawiyah, D R (2000). Vegetable ghee formulation with blending technique from palm olein and palm stearin fraction. *Prosiding Seminar Nasional Industri Pangan, Surabaya (Indonesia)*. 10-11 October 2000. Perhimpunan Ahli Teknologi Pangan Indonesia.

Siew, W L (2011). Palm oil. *Vegetable Oils in Food Technology: Composition, Properties and Uses* (Gunstone, F D ed.). John Wiley and Sons Ltd., West Sussex, United Kingdom. p. 25-54.

Sivaruby, K and Noor Lida, H M D (2007). Maximizing the use of palm stearin in vegetable ghee (Vanasapati). *Proc. of the PIPOC 2007 International Palm Oil Congress - Product Development and Nutrition Conference*. MPOB, Bangi.

Journal of Oil Palm Research Vol. 33 (3) September 2021 p. 532-541
DOI: https://doi.org/10.21894/jopr.2020.0100

IS PALM MID FRACTION A HEALTHIER CHOICE AS A COCOA BUTTER EQUIVALENT?

VOON, P T[1]*; TOH, S W H[2]; NG, T K W[3]; LEE, V K M[2]; YONG, X S[2]; NG, Y T[1] and NESARETNAM, K[4]

ABSTRACT

Palm mid fraction (PMF) is a fraction of palm oil rich in 1, 3-dipalmitoyl-2- oleoylglycerol (POP) triacylglycerol (TAG) that is obtained through re-fractionation of either palm olein or palm stearin. POP-, 1(3)-1, 3 distearoyl-2-oleoylglycerol (SOS)- and triolein (OOO)- type of fats have different melting characteristics that may affect postprandial lipid and glucose metabolism. We aimed to study the effects of palmitic, stearic or oleic acid situated at the sn-*1 and* sn-*3 positions of edible fats on postprandial lipemia, glucose and insulin responses. A randomised, double-blind crossover (3 x 3 arms) orthogonal Latin-square design was used. A total of 36 healthy adults received three different test muffins, each containing 53 g of test fat from palm mid fraction (PMF as POP-rich fat), shea stearin (SS as SOS-rich fat) or high-oleic sunflower oil (HOSF as OOO-rich fat) plus a low-fat milkshake in random order separated by two weeks. No significant differences (P>0.05) were observed between the three test meals for postprandial responses in plasma total cholesterol, Lp(a), glucose and insulin levels. However, plasma TAG levels were found significantly higher (P<0.05) in PMF- and HOSF- subjects compared with SS- subjects after 90 min. Plasma C-peptide levels were found lower (P<0.05) in the SS-subjects compared to the PMF- and HOSF- subjects. The results suggested that dietary fats containing palmitic (PMF) and oleic acid (HOSF) at the* sn-*1, 3 positions of the TAG backbone exert similar postprandial lipid and glucose responses compared with that of a stearic acid-rich* sn-*1,3 dietary fat (SS). In the food industry, there is demand for edible fats with different forms of TAG which can serve as a cocoa butter equivalent (CBE)* i.e. *as an important alternative for chocolates and other confectionary products.*

Keywords: fatty acids, glucose, insulin, postprandial lipemia, *sn*-1, *sn*-3.

Received: 15 July 2020**; Accepted:** 15 September 2020; **Published online:** 12 November 2020.

INTRODUCTION

The effects of edible fats on cholesterolemia have been well-documented (Hu *et al*., 2001). Different types of saturated fatty acids (SFA) pose different effects on blood lipid. In fact, equations arising from human feeding trials have been formulated to predict blood cholesterol/lipid levels brought about by changes in dietary fat (Hegsted *et al*., 1965; Mensink *et al*., 2003).

Much of our knowledge on the impact of dietary fats on cardiovascular heart diseases is based on measurements of plasma lipid and lipoprotein profile in the fasting state, with the lowest low density lipoprotein cholesterol (LDL-c), LDL-c/high density lipoprotein cholesterol (HDL-c) and triacylglycerol (TAG) being considered ideal. Lopez-Miranda and Marin (2010) highlighted the importance of dietary and physiological impacts on postprandial lipid metabolism. In this connection,

[1] Malaysian Palm Oil Board,
6 Persiaran Institusi, Bandar Baru Bangi,
43000 Kajang, Selangor, Malaysia.

[2] International Medical University (IMU),
Bukit Jalil, 57000 Kuala Lumpur, Malaysia.

[3] Department of Allied Health Sciences,
Faculty of Science, Universiti Tunku Abdul Rahman,
Jalan Universiti, Bandar Barat, 31900 Kampar,
Perak, Malaysia.

[4] Jalan Kelab Golf,
40100 Shah Alam, Selangor, Malaysia.

* *Corresponding author e-mail: vptee@mpob.gov.my*

postprandial hypertriglyceridemia is reported to increase the risk of type 2 diabetes mellitus, obesity, atherosclerosis, cardiovascular heart disease and stroke (Ortega *et al*., 2012).

The effects of stereospecific positioning of fatty acids in TAG molecules of dietary fats have been studied. Previous studies reported that palm oil has 41% palmitic acid (C16:0) with the majority of the fatty acid located at the *sn*-1 and *sn*-3 positions, but with only 3%-5% of its C16:0 at the *sn*-2 position (Karupaiah and Sundram, 2007; Kritchevsky, 2000). Chemical interesterification of palm oil is able to increase the amount of C16:0 at the *sn*-2 position to 13.6% which results in a significant increase in atherogenicity of the interesterified fat (Karupaiah and Sundram, 2007; Kritchevsky, 2000).

In animal models, Storlien *et al*. (1991; 1993) found that diets high in saturated, monounsaturated (ω-9) and polyunsaturated (ω-6) fatty acids induced severe insulin resistance, whereas long-chain omega (ω-3) fatty acids normalised the insulin action. However, published studies on the effects of different dietary fats on postprandial lipemia and insulin response in humans have not been consistent. Tholstrup *et al*. (2001) reported that the intake of long-chained saturated acids (palmitic acid and stearic acid) by 16 healthy men resulted in a relatively lower lipemic response than did intake of the unsaturated fatty acids. In a randomised, crossover study with 10 healthy men, Teng *et al*. (2011) found that palm olein (POP-rich fat) and olive oil (OOO-rich fat) caused a higher increase in postprandial lipemia than lard (SPO-rich fat). In contrast, Zampelas *et al.* postprandial study (Zampelas *et al*., 1994) and Galgani *et al.* (2008) extensive review reported that the positional distribution of fatty acids on dietary TAG or dietary fat quality does not influence postprandial lipemia nor insulin response.

The positional distribution of fatty acids in the TAG molecule varies greatly among fats and oils of different origins. In the food industry, there is a demand for edible fats with different forms of TAG which can serve as a CBE *i.e.* as an important alternative for chocolates and other confectionary products. Palm oil, illipe and shea are listed in the European Chocolate Directive 2000/36EEC as CBE (EU Commission, 2000). Besides, vegetable oils such as PMF, olive oil, mango fats, kokum and teaseed oil have also been used to prepare CBE. PMF is a fraction of palm oil rich in POP TAG that is obtained through re-fractionation of either palm olein or palm stearin. Therefore, it is important to find out if a CBE such as PMF has similar effects as SS on postprandial lipoprotein metabolism, glycemia and insulinemic response. This forms the research question as well as the justification for the present study reported.

SUBJECTS AND METHODS

Subjects

Thirty-six healthy adults (18 males and 18 females, aged between 25 to 50 years) were recruited to participate in this study. All volunteers underwent a health screening which included: a) an abbreviated medical/physical examination [blood pressure, weight, height, body mass index (BMI)], b) serum lipid profiling, c) plasma glucose determination, d) liver function tests [serum glutamic-oxaloacetic transaminase (SGOT) and serum glutamic-pyruvic transaminase (SGPT)] and e) kidney function test (serum creatinine). The inclusion criteria for this study were BMI 18.5-25.0 kg m^{-2}, systolic pressure <140 mmHg, diastolic pressure <90 mmHg, fasting total cholesterol (TC) <6.2 mM $litre^{-1}$ (<240 mg dL^{-1}), fasting TAG <1.70 mmol $litre^{-1}$ (<150 mg dL^{-1}), fasting glucose 4.0-7.0 mmol $litre^{-1}$. Exclusion criteria for this study were individuals on cholesterol or blood glucose medication, substance abuse (*e.g*. alcohol, cigarette smoking), going overseas during period of study, having blood clotting problem and pregnant or lactating for women.

This study was approved by the IMU Joint-Committee of Research and the Ethics Committee, International Medical University, Kuala Lumpur, Malaysia and this trial was registered at clinicaltrials.gov.my as *NCT01428960*.

Study Design

A randomised, double-blind crossover (3 x 3 arms) orthogonal Latin-square design was used. Blood collections were conducted according to the study protocol at every 30 min interval. Each subject received three experimental test meals in a random order, two weeks apart, over a six-week period. Subjects were randomly allocated to one of following six treatment sequences: ABC, BCA, CAB, ACB, CBA, or BAC, with PMF as A, SS as B and HOSF as C. Each set of test meal contained a muffin and a glass milkshake. The test meal provided 875.6 kcal, 16 g protein, 83 g carbohydrate and 53 g test fat.

Sample Size Calculation

Sample size was calculated based on 90% power at $P<0.017$ for cross-over within group comparison to detect a 0.5-SD unit change in the area under the curve (AUC) for plasma TAG concentrations, that provided a sample size of 36 subjects after allowing for 10% dropout. Secondary outcomes were changes in TC, Lp(a), glucose, insulin and C-peptide. The characteristics of the study participants are shown in *Table 1*.

Test Fats

The three test fats were PMF (iodine value = 34.9) and SS (iodine value = 34.1) which were obtained from Wilmar PGEO Edible Oils Sdn. Bhd. while HOSF was obtained from Intercontinental Specialty Fats Sdn. Bhd., Selangor, Malaysia. PMF contained a similar proportion of SFA (62.7% *vs*. 62.6%) and oleic acid (33.7% *vs*. 33.0%) when compared to SS but contained more palmitic acid (57.1% *vs*. 1.8%) and less stearic acid (5.0% *vs*. 60.8%). PMF and SS were blended with a small amount of sunflower oil (Mazola, Switzerland) so that linoleic acid (C18:2,w-6) was standardised across the diets at 7% kcal. The fatty acid composition of the test fats is shown in *Table 2*. The test fats were incorporated into muffins, labelled with a code, and stored frozen until being consumed.

The TAG composition of the test fats is illustrated in *Table 3*. PMF consists mainly of the TAG species 1, 3-dipalmitoyl-2- oleoylglycerol (POP) (67.6%), while the majority of the TAG species in SS is 1(3)- 1, 3 distearoyl-2-oleoylglycerol (SOS) (74.2%) with oleic acid in the *sn*-2 positions. The main TAG species of HOSF is triolein (OOO) (66.5%).

The three test fats consist of approximately equal oleic acid (C18:1) at the *sn*-2 position [(PMF = 72%, SS = 80%, HOSF = 88%)]. Differential scanning calorimetry showed that PMF shows a single sharp melting peak at approximately 31.3°C, whereas SS shows a higher melting point at approximately 38.0°C. HOSF shows a melting point at approximately 0.14°C.

Postprandial Protocol

Subjects were asked to avoid consuming foods high in fat as well as not to participate in strenous exercise the day preceding each test meal and to fast overnight beginning at 2200 hr. A low-fat meal (500-700 kcal containing, 10 g fat) was provided to the subjects as their evening meal. The subjects were requested to consume the low-fat meal before 2200 hr and fast overnight.

On the morning of the postprandial test, participants attended the Nutrition Group Clinic between 0800 hr and 1000 hr when a 22G" Vasofix® Brannule (Cat No. 426 8091B, B. Braun, Germany) was inserted into the antecubital vein of the forearm and held in place with a Connecta (Cat No. 394601, Becton – Dickinson, Sweden). Blood was collected by syringe and dispensed into appropriate uncapped blood collection containers. Samples for TAG, TC, Lp(a), insulin and C-peptide analysis were collected using serum vacutainer tubes. The samples collected were allowed to clot at room temperature before centrifugation. Samples for plasma glucose was collected using fluoride containing tube. The serum and plasma were aliquoted accordingly and stored in -80°C freezer prior to analyses.

The subjects were given 10 min to consume a set of test meal. Venous blood samples were collected every 30 min for 4 hr after the test meal. Blood collection was performed by registered staff nurse supervised by medical officer or family physician using antiseptic technique. Drinking water was provided to the subjects over 4 hr. At the end of 4 hr, the subjects were provided with an *ad-libitum* lunch.

TABLE 1. BASELINE CHARACTERISTICS OF THE STUDY PARTICIPANTS

Variable	Participants		
	Women (n=18)	Men (n=18)	All (n=36)
Age (yr)	23.0 ± 1.1	23.0 ± 1.9	23.3 ± 1.5
Weight (kg)	52.0 ± 5.6	63.1 ± 7.6	57.5 ± 8.7
Height (cm)	160.0 ± 4.2	172.0 ± 5.7	166.0 ± 8.0
BMI (kg m^{-2})	20.3 ± 1.6	21.3 ± 2.0	20.8 ± 1.8
Systolic blood pressure (mmHg)	111.0 ± 6.1	122.0 ± 10.0	116.0 ± 9.9
Diastolic blood pressure (mmHg)	73.0 ± 5.0	75.0 ± 7.6	74.0 ± 6.4
Total cholesterol (mmol $litre^{-1}$)	4.9 ± 0.7	4.4 ± 0.8	4.7 ± 0.8
HDL-c (mmol $litre^{-1}$)	1.7 ± 0.3	1.4 ± 0.3	1.5 ± 0.3
LDL-c (mmol $litre^{-1}$)	2.9 ± 0.6	2.7 ± 0.7	2.8 ± 0.6
TAG (mmol $litre^{-1}$)	0.7 ± 0.3	0.7 ± 0.4	0.7 ± 0.3
Fasting glucose (mmol $litre^{-1}$)	4.6 ± 0.6	4.7 ± 0.3	4.6 ± 0.3

Note: All values are mean ± SD.
BMI - body mass index; HDL-c - high-density lipoprotein cholesterol; LDL-c - low-density lipoprotein cholesterol; TAG - triacylglycerol; PMF - palm mid fraction; SS - shea stearin; HOSF - high-oleic sunflower oil.

TABLE 2. FATTY ACID COMPOSITIONS OF THE TEST FATS

Fatty acids	Mol %		
	PMF	SS	HOSF
C14:0	0.61	ND	ND
C16:0	52.85	2.40	4.44
C18:0	4.87	57.20	2.41
C18:1	33.73	32.29	85.58
C18:2	7.93	7.63	7.56
Others	0.01	0.48	0.01
SFA	58.33	59.60	6.85
MUFA	33.73	32.29	85.58
PUFA	7.93	7.63	7.56

Note: ND - not detected; SFA - saturated fatty acids; MUFA - monounsaturated fatty acids; PUFA - polyunsaturated fatty acids; PMF - palm mid fraction; SS - shea stearin; HOSF - high-oleic sunflower oil.

TABLE 3. TAG COMPOSITION OF THE TEST FATS

TAG	Mol %		
	PMF	SS	HOSF
PLL	0.1	ND	ND
MLP	0.2	ND	ND
OLO	0.2	ND	6.3
PLO	1	ND	1.1
PLP	8.7	ND	0.2
OOO	0.9	0.3	66.5
POO	3.1	0.6	9
POP	67.6	1	0.5
PPP	2.5	3.2	ND
SOO	0.3	7.1	5.9
POS	13.3	7.4	0.4
PPS	0.4	0.2	ND
SOS	1.5	74.2	ND
Others	ND	5.9	10.1
Slip melting point (°C)	31.1	37.9	<1.0

Note: ND - not detected; TAG - triacylglycerol; L - linoleic acid (18:2n–6); M - myristic acid (14:0); O - oleic acid (18:1n–9); P - palmitic acid (16:0); S - stearic acid (18:0); PMF - palm mid fraction; SS - shea stearin; HOSF - high-oleic sunflower oil.

Analytical Methods

Serum TAG, TC, Lp(a) and plasma glucose were analysed using enzymatic colourimetric assays with a Hitachi 902 autoanalyser (Roche Diagnostics GmbH). The fatty acid composition of test fats was measured using gas-liquid chromatography on an SP-2560 column (100 m x 0.23 mm x 0.2 mm; Agilent Technologies) with a flame ionisation detector on an autosystem (Perkin Elmer). The carrier gas (helium) pressure and injector temperature were set to 40 psi and 250°C, respectively. The oven temperature was set isothermal at 240°C for 42 min. Hydrogen and compressed air were used for ignition. A fatty acid methyl esters mixture (Sigma-Aldrich, Australia) was used as the external standard.

TAG composition of the test fats was determined by reversed-phase High Performance Liquid Chromatography (HPLC) system. The method of analysis was modified from the AOCS Official Method Ce 5c-93, slip-melting point was determined according to MPOB Test Method (MPOB, 2004).

Meanwhile, both C-peptide and insulin samples were analysed using (Elecsys module) immunoassay analysers. Although the 'Homeostatic Model Assessment' (HOMA= fasting insulin concentration × fasting glucose concentration /22.5) (Matthews *et al.*, 1985) and the quantitative insulin sensitivity check index [QUICKI= the inverse of the sum of the logarithms of the fasting insulin and fasting glucose, *i.e.* [1 / (log (fasting insulin) + log (fasting glucose)] (Katz *et al.*, 2000) are normally used for fasting blood samples, these indices of insulin resistance were calculated for the 4 hr time-point following the three test meals, which may be considered as the early fasting phase in the study.

Statistical Analyses

Repeated measure analysis of variance (ANOVA) with *Bonferroni post hoc* analysis was conducted using GraphPad Prism version 5 (GraphPad Software, La Jolla, CA 9203, USA) and PASW Statistics 18 to assess the significant difference between diets. The normal distribution of data was assessed using Shapiro-Wilk's normality test and logarithmic transformations were used when necessary. Data are expressed as mean with 95% CI.

RESULTS

Table 4 and *Figure 1* show the postprandial changes in serum TAG and following the three test meals. The meal × time interaction (P=0.000) for the change in postprandial TAG indicated differences between test meals; plasma TAG increased more rapidly following PMF and HOSF compared with that of a SS test meal.

There were significant differences in serum TAG levels between the test diets at 120 min and 180 min. Postprandial changes in TAG between the HOSF and SS showed a significant meal × time interaction (P=0.0041) at 120 min; the difference was 0.24 (95% CI, 0.064, 0.41). Meanwhile, comparison of PMF and HOSF with the SS meal showed a significant meal × time interaction (P=0.0075) at 180 min in which the differences between HOSF and PMF with the SS meal in the change of TAG were 0.26 (95% CI, 0.052, 0.47) and -0.21 (95% CI, -0.42, -0.00076) respectively.

The differences between HOSF and PMF with the SS meal in the change of TAG at 150 min were 0.25 (95% CI, 0.12, 0.37) and -0.22 (95% CI, -0.35, -0.094) respectively, at 180 min 0.23 (95% CI, 0.096, 0.36) and -0.17 (95% CI, -0.30, -0.040) and at 210 min 0.22 (95% CI, 0.084, 0.36) and -0.20 (95% CI, -0.34, -0.060). Moreover, the release of C-peptide following PMF test meals was significantly different (P=0.0028) from SS at 240 min time-point *i.e.* -0.29 (95% CI, -0.48, -0.090).

TAG responses did not differ significantly between the three types of test meal given at 60 min and 240 min. Moreover, there were no significant differences (P>0.05) between meals and times in TC (*Table 5*), Lp(a) (*Table 6*), glucose and insulin.

Figure 2 illustrates the postprandial changes in serum C-peptide following the test meals. The meal x time interaction (P=0.000) for the change in postprandial C-peptide indicated differences between test meals. The total amount of C-peptide released by pancreatic β-cells following PMF and HOSF test meals were higher as compared to the SS test meal. Comparison of the postprandial changes between the HOSF and SS showed a significant difference at 120 min (P<0.048); the difference was 0.15 (95% CI, 0.0021, 0.31). Meanwhile, comparison of PMF and HOSF with the SS meal showed a significant meal × time interaction difference at 150 min (P<0.0001), at 180 min (P=0.0002) and at 210 min (P=0.003).

TABLE 4. POSTPRANDIAL CHANGES IN TAG FOLLOWING THE THREE TEST MEALS

Time (min)	Changes in TAG of test meals (mmol litre^{-1})		
	HOSF	SS	PMF
0	0.77 (0.66, 0.89)	0.86 (0.75, 0.97)	0.82 (0.69, 0.94)
60	0.83 (0.69, 0.95)	0.83 (0.72, 0.94)	0.84 (0.70, 0.97)
120	1.19 (0.99, 1.38)^{a}	0.95 (0.81, 1.1)^{b}	1.12 (0.95, 1.28)^{a}
180	1.47 (1.22, 1.68)^{a}	1.2 (1.01, 1.39)^{b}	1.41 (1.19, 1.62)^{a}
240	1.46 (1.21, 1.68)	1.37 (1.16, 1.56)	1.49 (1.26, 1.69)

Note: Values are geometric means; 95% CIs in parentheses; (n = 36; 18 men, 18 women) for all treatments. Values were log-transformed, analysed by repeated-measures analysis of variance (ANOVA) and showed a diet × time interaction (P=0.000); the meal × gender, time × gender and meal × gender × time interaction were not significant. Different superscript letters in the same row indicate that values showed statistically significant differences (P<0.05, Bonferroni multiple comparison test) between corresponding columns.
TAG - triacylglycerol; PMF - palm mid fraction; SS - shea stearin; HOSF - high-oleic sunflower oil.

TABLE 5. POSTPRANDIAL CHANGES IN TC FOLLOWING THE THREE TEST MEAL

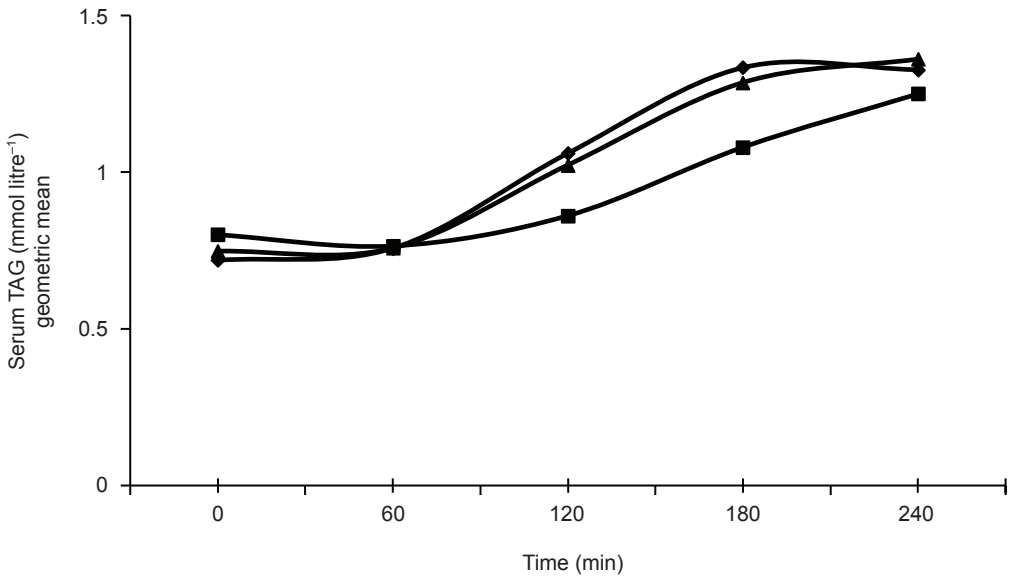
Time (min)	Changes in TC of test meals (mmol litre^{-1})		
	HOSF	SS	HOSF
0	5.00 (4.72, 5.28)	4.90 (4.64, 5.17)	4.97 (4.73, 5.21)
60	4.88 (4.59, 5.17)	4.69 (4.42, 4.95)	4.72 (4.50, 4.94)
120	4.86 (4.58, 5.14)	4.75 (4.46, 5.04)	4.74 (4.53, 4.96)
180	4.85 (4.58, 5.12)	4.74 (4.47, 5.00)	4.74 (4.52, 4.96)
240	4.92 (4.65, 5.19)	4.77 (4.52, 5.03)	4.79 (4.58, 5.01)

Note: Values are means; 95% CIs in parentheses; (n = 36; 18 men, 18 women) for all treatments. Values were analysed by repeated-measures analysis of variance (ANOVA) and diet x time, the meal x gender, time x gender and meal x gender x time interaction were not significant (P>0.05).
TC - total cholesterol; PMF - palm mid fraction; SS - shea stearin; HOSF - high-oleic sunflower oil.

TABLE 6. POSTPRANDIAL CHANGES IN LP(A) FOLLOWING THE THREE TEST MEALS

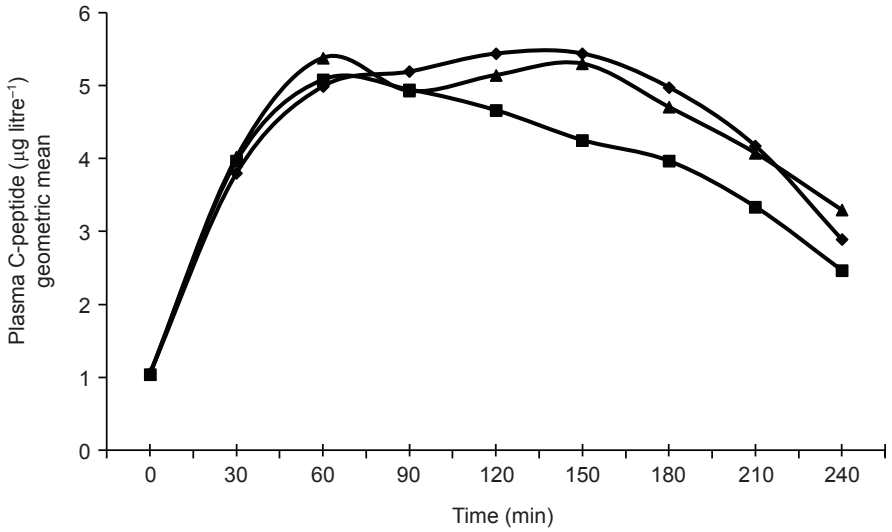
Time (min)	Changes in Lp(a) of test meals (mg dL^{-1})		
	HOSF	SS	HOSF
0	31.05 (25.46, 37.87)	29.99 (24.15, 37.25)	28.15 (22.67, 34.96)
60	29.95 (24.35, 36.83)	28.56 (23.01, 35.47)	29.23 (23.76, 35.96)
120	33.69 (27.78, 40.86)	31.71 (25.61, 39.27)	33.41 (27.50, 40.60)
180	36.44 (30.28, 43.84)	35.24 (28.67, 43.32)	36.56 (30.10, 44.42)
240	37.65 (31.56, 44.91)	38.70 (31.65, 47.32)	38.15 (31.56, 46.11)

Note: Values are geometric means; 95% CIs in parentheses; (n = 36; 18 men, 18 women) for all treatments. Values were log-transformed, analysed by repeated-measures analysis of variance (ANOVA) and diet x time, the meal x gender, time x gender and meal x gender x time interaction were not significant (P>0.05).
Lp(a) - lipoprotein(a); PMF - palm mid fraction; SS - shea stearin; HOSF - high-oleic sunflower oil.



Note: PMF - palm mid fraction; SS - shea stearin; HOSF - high-oleic sunflower oil; TAG - triacylglycerol.

Figure 1. Postprandial concentrations of serum TAG geometric mean (n = 36; 18 men, 18 women) following three test meals containing 53 g test fat from HOSF (♦), SS (■), and PMF (▲). Deviations from postprandial values were analysed by repeated measures analysis of variance (ANOVA); meal × time interaction P=0.000. Comparisons between meals were adjusted by using a Bonferroni multiple-comparison test.



Note: PMF - palm mid fraction; SS - shea stearin; HOSF - high-oleic sunflower oil.

Figure 2. Postprandial concentrations of plasma C-peptide geometric mean (n = 36; 18 men, 18 women) following three test meals containing 53 g test fat from HOSF (♦), SS (■), and PMF (▲). Deviations from postprandial values were analysed by repeated measures analysis of variance (ANOVA); meal × time interaction P=0.000. Comparisons between meals were adjusted by using a Bonferroni multiple-comparison test.

DISCUSSION

PMF and SS are widely used as CBE due to their desirable mouth-feel effects arising from their respective melting point of 31.3°C and 38.0°C (Lipp and Anklam, 1998). PMF displays a steep melting profile, with a narrow melting interval around 35.0°C which makes it an important component of confectionary fats, being the source of palmitic acid-rich TAG in the formulation of CBE (Salas *et al.*, 2009).

To date, there are lack of human studies comparing both PMF and SS as test fats in diets. However, there are several reports of SS being used in postprandial test meals (Berry and Sanders, 2005; Sanders and Berry, 2005). In the present study, the amounts of oleic acid at *sn*-2 position in all the three types of TAG molecules of PMF, SS and HOSF were approximately equal, linoleic acid content was standardised across diets, and the major difference between the test fats are the fatty acid type in the *sn*-1 and *sn*-3 positions, namely palmitic acid in the case of PMF (POP), oleic acid for HOSF (OOO) and stearic acid in the case of SS (SOS). In this study, the PMF and HOSF test fats exerted a similar postprandial TAG profile, which not only suggests that palmitic acid and oleic acid have comparable postprandial triglyceridemic effects but also the two types of fatty acids were similarly absorbed. The SS- (SOS) meal however, resulted in a lower postprandial TAG response compared to HOSF- (OOO) and PMF- (POP) meal.

The lower postprandial level of lipemia following SS in the present study is in agreement with results reported by Sanders and Berry (2005) that non-randomised SS resulted in decreased lipemia as compared to a test meal containing 50 g HOSF. Sanders *et al.* (2000) suggested that the lower postprandial lipemic effect of a stearic acid-rich SS meal was due to a slower absorption rate and led to the formation of smaller lipoprotein particles compared to an oleic acid-rich HOSF meal with a faster absorption rate and larger chylomicrons formation. However, the mechanism involved warrant further investigations. Evidently, differences in the physical characteristics of fats and stereospecific structure of TAG molecules influence the metabolism of lipids and the level of postprandial lipemia. In this connection, Berry *et al.* (2007) proposed that SS contains a higher proportion of solid fat at 37°C compared with HOSF and PMF and this may cause SS to be emulsified less readily and is less absorbed due to its higher melting point, resulting in a slower increase in serum TAG levels. This would suggest that SS might be cleared from the circulation faster than HOSF and PMF and resulted in a more prolonged postprandial lipemia which explains our results obtained.

Meanwhile, there were no significant differences in postprandial serum TC and Lp(a) levels after ingestion of the three test meals. Our present findings for TC levels are in accordance to the results obtained by Forsythe *et al.* (2007) who reported that that a *sn*-1 + *sn*-3 palmitic acid-rich fat such as palm oil is non-cholesterolemic. In contrast, Tholstrup and Samman (2004) reported that postprandial Lp(a) is affected differently by specific individual dietary fatty acids in healthy young men, while Sanders *et al.* (2000) found that shorter-chain fatty acids will clear Lp(a) at a faster rate after a post-meal study with high and normal fat loads.

TABLE 7. PLASMA GLUCOSE, INSULIN, HOMA AND QUICKI VALUES FOLLOWING THE THREE TEST MEALS AT 240 MIN

Plasma index	HOSF	SS	PMF
HOMA	4.43 (2.90, 5.97)	4.68 (2.91, 6.44)	7.27 (4.85, 9.69)
QUICKI	0.34 (0.32, 0.36)	0.34 (0.32, 0.35)	0.32 (0.30, 0.34)
Glucose	5.15 (4.93, 5.37)	5.27 (4.98, 5.57)	5.54 (5.25, 5.84)
Insulin	18.71 (12.34, 25.07)	18.96 (12.03, 25.90)	28.54 (19.07, 38.00)

Note: Values are means; 95% CIs in parentheses (n = 36; 18 men, 18 women) for all treatments. Values were log-transformed, analysed by repeated-measures analysis of variance (ANOVA); HOMA, diet × time interaction (P>0.05); QUICKI, diet × time interaction (P>0.05).
HOMA - Homeostatic Model Assessment; QUICKI - Quantitative Insulin Sensitivity Check Index; PMF - palm mid fraction; SS - shea stearin; HOSF - high-oleic sunflower oil.

C-peptide and insulin are initially synthesised in the same polypeptide. The C-peptide component is later cleaved off leaving the A- and B-chains which form insulin. C-peptide concentrations specifically reflect β-cell function because C-peptide is secreted in equimolar amounts with insulin and is not removed in the first pass through the liver (Hills and Brunskill, 2009; Kim *et al.*, 2012). Moreover, C-peptide is a more stable biomarker of insulin secretion than is the direct measurement of plasma insulin because C-peptide has a substantially longer half-life than insulin (Nimptsch *et al.*, 2011). In the present postprandial study, C-peptide responses peaked in the three test-fat groups about 60 min after the test meals were consumed and its serum concentrations decreased significantly (P<0.05) to around 2.8 μg litre^{-1} towards the end of the 4 hr study. There were significant differences in C-peptide responses among the three groups. Overall, postprandial C-peptide concentrations were lower (P<0.05) after a SS-meal compared to the HOSF and PMF-meals. This suggests that C-peptide concentrations following the SS-meal were cleared faster as compared to the HOSF- and PMF-meals.

Postprandial glucose and insulin concentrations did not differ following the meals high in palmitic acid- (POP) and rich in stearic acid- (SOS) compared to HOSF which was rich in oleic acid- (OOO). The comparable postprandial insulin concentration across the three test-fat groups also strengthens our suggestion that C-peptide concentrations were cleared at a faster rate in the SS-meal group. Our results are consistent with the findings of Lopez *et al.* (2011) which showed no significant difference in postprandial glucose response in subjects who consumed monounsaturated and saturated fats. In agreement with the previous study of Teng *et al.* (2011), a single high fat load may not affect the changes in glucose and insulin levels, as the meal x time interaction was not significant indicating that the peak insulin concentration was reached at the same time across meals, which was at 30 min. Our results suggest that POP-, SOS- and OOO- type of fats did not affect postprandial glucose and insulin responses. The HOMA and QUICKI (*Table 7*) indices at the 4 hr time-point (early fasting phase) were also comparable across the three test-fat groups.

CONCLUSION

The preponderance of either palmitic (16:0), stearic (18:0) or oleic acid (18:1) of the three test fats with different physical characteristics used in the present acute study did not induce any significant differences in postprandial Lp(a), glucose or insulin concentrations. Our findings, however, demonstrated that PMF (POP) and HOSF (OOO) fats induced higher TAG and C-peptide postprandial concentrations compared with the SS (SOS) fat.

ACKNOWLEDGEMENT

We thank all the participants in the study, the medical team which played a key role in blood sample collection and Wilmar PGEO Edible Oils Sdn. Bhd. and Intercontinental Specialty Fats Sdn. Bhd. for providing the test fats used. We also thank the Director-General of MPOB for permission to publish the data.

REFERENCES

Berry, S E and Sanders, T A (2005). Influence of triacylglycerol structure of stearic acid-rich fats on postprandial lipaemia. *Proc. Nutr. Soc., 64(2)*: 205-212.

Berry, S E; Miller, G J and Sanders, T A (2007). The solid fat content of stearic acid-rich fats determines their postprandial effects. *Am. J. Clin. Nutr., 85(6)*: 1486-1494.

EU Commission (2000). Directive 2000/36/EC of the European Parliament and of the Council of 23 June 2000 relating to cocoa and chocolate products intended for human consumption. *Official J. European Communities EG 197*: 19.

Forsythe, C E; French, M A; Goh, Y K and Clandinin, M T (2007). Cholesterolaemic influence of palmitic acid in the *sn*-1, 3 v. the *sn*-2 position with high or low dietary linoleic acid in healthy young men. *Br. J. Nutr., 98(2)*: 337-344.

Galgani, J E; Uauy, R D; Aguirre, C A and Diaz, E O (2008). Effect of the dietary fat quality on insulin sensitivity. *Br. J. Nutr., 100(3)*: 471-479.

Hegsted, D M; McGandy, R B; Myers, M L and Stare, F J (1965). Quantitative effects of dietary fat on serum cholesterol in man. *Am. J. Clin. Nutr., 17(5)*: 281-295.

Hills, C E and Brunskill, N J (2009). Cellular and physiological effects of C-peptide. *Clin. Sci. (Lond), 116(7)*: 565-574.

Hu, F B; Manson, J E and Willett, W C (2001). Types of dietary fat and risk of coronary heart disease: A critical review. *J. Am. Coll. Nutr., 20(1)*: 5-19.

Karupaiah, T and Sundram, K (2007). Effects of stereospecific positioning of fatty acids in triacylglycerol structures in native and randomized fats: A review of their nutritional implications. *Nut. Metab., 4*: 16.

Katz, A; Nambi, S S; Mather, K; Baron, A D; Follmann, D A; Sullivan, G and Quon, M J (2000). Quantitative insulin sensitivity check index: A simple, accurate method for assessing insulin sensitivity in humans. *J. Clin. Endocrinol. Metab., 85(7)*: 2402-2410.

Kim, B Y; Jung, C H; Mok, J O; Kang, S K and Kim, C H (2012). Association between serum C-peptide levels and chronic microvascular complications in Korean type 2 diabetic patients. *Acta Diabetol., 49(1)*: 9-15.

Kritchevsky, D (2000). Overview: Dietary fat and atherosclerosis. *Asia Pac. J. Clin. Nutr., 9(2)*: 141-145.

Lipp, M and Anklam, E (1998). Review of cocoa butter and alternative fats for use in chocolate - Part A. Compositional data. *Food Chem., 62(1)*: 73-97.

Lopez-Miranda, J and Marin, C (2010). Dietary, physiological, and genetic impacts on postprandial lipid metabolism. *Fat detection: taste, texture, and post ingestive effects.* CRC Press/Taylor and Francis.

Lopez, S; Bermudez, B; Ortega, A; Varela, L M; Pacheco, Y M; Villar, J; Abia, R and Muriana, F J (2011). Effects of meals rich in either monounsaturated or saturated fat on lipid concentrations and on insulin secretion and action in subjects with high fasting triglyceride concentrations. *Am. J. Clin. Nutr., 93(3)*: 494-499.

Matthews, D R; Hosker, J P; Rudenski, A S; Naylor, B A; Treacher, D F and Turner, R C (1985). Homeostasis model assessment: Insulin resistance and beta-cell function from fasting plasma glucose and insulin concentrations in man. *Diabetologia, 28(7)*: 412-419.

Mensink, R P; Zock, P L; Kester, A D and Katan, M B (2003). Effects of dietary fatty acids and carbohydrates on the ratio of serum total to HDL cholesterol and on serum lipids and apolipoproteins: A meta-analysis of 60 controlled trials. *Am. J. Clin. Nutr., 77(5)*: 1146-1155.

MPOB (2004). *MPOB Test Method* (Aini, K; Siew, W L; Tan, Y A; Nor Aini, I; Tang, T S and Nurul, A I eds.). MPOB, Bangi.

Nimptsch, K; Brand-Miller, J C; Franz, M; Sampson, L; Willett, W C and Giovannucci, E (2011). Dietary insulin index and insulin load in relation to biomarkers of glycemic control, plasma lipids, and inflammation markers. *Am. J. Clin. Nutr., 94(1)*: 182-190.

Ortega, A; Varela, L M; Bermudez, B; Lopez, S; Abia, R and Muriana, F J (2012). Dietary fatty acids linking postprandial metabolic response and chronic diseases. *Food Funct., 3(1)*: 22-27.

Salas, J J; Bootello, M A; Martinez-Force, E and Garces, R (2009). Tropical vegetable fats and butters: Properties and new alternatives. *OCL, 16(4)*: 254-258.

Sanders, T A and Berry, S E (2005). Influence of stearic acid on postprandial lipemia and hemostatic function. *Lipids, 40(12)*: 1221-1227.

Sanders, T A; De Grassi, T; Miller, G J and Morrissey, J H (2000). Influence of fatty acid chain length and cis/trans isomerization on postprandial lipemia and factor VII in healthy subjects (postprandial lipids and factor VII). *Atherosclerosis, 149(2)*: 413-420.

Storlien, L H; Jenkins, A B; Chisholm, D J; Pascoe, W S; Khouri, S and Kraegen, E W (1991). Influence of dietary fat composition on development of insulin resistance in rats. Relationship to muscle

triglyceride and omega-3 fatty acids in muscle phospholipid. *Diabetes, 40(2)*: 280-289.

Storlien, L H; Pan, D A; Kriketos, A D and Baur, L A (1993). High fat diet-induced insulin resistance. Lessons and implications from animal studies. *Ann. N Y Acad. Sci., 683*: 82-90.

Teng, K T; Nagapan, G; Cheng, H M and Nesaretnam, K (2011). Palm olein and olive oil cause a higher increase in postprandial lipemia compared with lard but had no effect on plasma glucose, insulin and adipocytokines. *Lipids, 46(4)*: 381-388.

Tholstrup, T and Samman, S (2004). Postprandial lipoprotein(a) is affected differently by specific individual dietary fatty acids in healthy young men. *J. Nutr., 134(10)*: 2550-2555.

Tholstrup, T; Sandstrom, B; Bysted, A and Holmer, G (2001). Effect of 6 dietary fatty acids on the postprandial lipid profile, plasma fatty acids, lipoprotein lipase and cholesterol ester transfer activities in healthy young men. *Am. J. Clin. Nutr., 73(2)*: 198-208.

Zampelas, A; Williams, C M; Morgan, L M; Wright, J and Quinlan, P T (1994). The effect of triacylglycerol fatty acid positional distribution on postprandial plasma metabolite and hormone responses in normal adult men. *Br. J. Nutr., 71(3)*: 401-410.

Journal of Oil Palm Research Vol. 33 (3) September 2021 p. 542-554
DOI: https://doi.org/10.21894/jopr.2020.0110

RHEOLOGICAL PROPERTIES OF PALM-BASED CARBOXYMETHYL CELLULOSE SOLUTIONS

NOR ZULIANA YUSOF[1]*; ZAFARIZAL ALDRIN AZIZUL HASAN[1]; NUR ELIYANTI ALI OTHMAN[1] and YUSRABBIL AMIYATI YUSOF[1]

ABSTRACT

Palm empty fruit bunches have been value added into carboxymethyl cellulose (CMC). However, its potential as rheological modifiers in cosmetic and personal care has yet to be explored. Therefore, the aim of this study was to investigate the rheological performance of the CMC solutions (1%, 2%, 3% and 4%) against two commercially available CMC (cotton-based and wood-based CMC). Our study revealed that all the CMC solutions studied gave flow behaviour index of less than 1, which indicated the pseudoplastic or shear-thinning properties. Among the three CMC studied, 2% and 3% CMC from palm empty fruit bunches (PEFB-CMC) and cotton-based CMC exhibited viscoelastic solid properties where the storage modulus (G') was larger than loss modulus (G") on amplitude sweep test. On the other hand, all the wood-based CMC did not exhibit any viscoelastic solid properties. In addition, the 2% palm-based CMC exhibited higher gel strength as compared to 2% cotton-based CMC solution, while the wood-based CMC exhibited fluid-structure through frequency sweep test. The palm-based CMC exhibited potential application as rheological modifier in consumer products particularly for the development of cosmetic and personal care products.

Keywords: palm-based carboxymethyl cellulose, shear-thinning properties, viscoelastic solid.

Received: 29 June 2020; **Accepted:** 3 October 2020; **Published online:** 9 December 2020.

INTRODUCTION

The conventional sources of cellulose include cotton linters and wood pulp. However, there are continuous global efforts to search for cellulose biomass from other sources as an alternative feedstock to expensive cotton linters and wood pulp, which nowadays are discouraged due to environmental regulations (Varshney and Naithani, 2011). Nonetheless, cellulose can also be extracted and is readily available in large quantities from non-wood alternatives. One such viable source is oil palm empty fruit bunch (OPEFB) fibre, a by-product of the oil palm industry (Wan Rosli *et al*., 2011). OPEFB is considered the cheapest natural fibre with good properties and exist abundantly in Malaysia (Padzil *et al*., 2020). Oil palm fibre comprises of 40%-50% cellulose, 20%-30% hemicellulose and 15%-20% lignin (Rosnah *et al*., 2002; Ariffin *et al*., 2008). Several studies on cellulose extraction from OPEFB with the yield of 64% (Nazir *et al*., 2013), 58.5% (Ching and Ng, 2014), 43.22% (Sisak *et al*., 2015), 37% (Rosnah *et al*., 2012) and 34.1% (Astimar *et al*., 2002) were reported.

Cellulose is not water-soluble, it should be modified to enable it to be applied as a thickener, a gelling agent or a stabilising agent (Hutomo *et al*., 2012). In order to make water-soluble cellulose, cellulose is derivatised through the etherification process to produce carboxymethyl cellulose (CMC), hydroxyethyl cellulose, hydroxypropyl cellulose, methylcellulose and hydroxypropyl methylcellulose (Rowe *et al*., 2013). CMC is the most important water-soluble cellulose derivative with many applications in the food, pharmaceutical, cosmetics, detergent, textile, paper, and many other industries. It is a white to off-white, non-toxic, odourless and biodegradable powder. CMC is used to enhance the viscosity, to control the rheology of a solution, to avoid separation of water

[1] Malaysian Palm Oil Board,
6 Persiaran Institusi, Bandar Baru Bangi,
43000 Kajang, Selangor, Malaysia.

* *Corresponding author e-mail: zuliana@mpob.gov.my*

from a suspension, and to improve the surface of barrier properties (Stigsson *et al*., 2001).

CMC is one of the thickeners used in various products such as creams, lotions and toothpaste formulation (Benchbane and Bekkour, 2008). Furthermore, due to its polymeric structure that acts as a film-forming agent, it has also been used to improve moisturising effects (Benchabane and Bekkour, 2008). The rheological properties of CMC depend on the concentration of polymer and the degree of substitution, which varies from 0.5-1.2 (Barba *et al*., 2002). Rheological properties such as flow behaviour are important and it can be correlated with the spreadability and flow of cosmetic products from the bottle (Niraula *et al*., 2004). CMC is regarded as polyelectrolyte, and once it is dissolved in water, the molecule is separated into sodium cations and anionic polymer. CMC dispersions exhibited thixotropic and viscoelastic behaviour at high CMC concentrations (Ghannam and Esmail, 1997).

The palm-based CMC from OPEFB has been reported to potentially contribute towards the development of an oil palm-based specialty chemical industry (Rosnah *et al*., 2004; Eliza *et al*., 2015; Parid *et al*., 2018). A study conducted by Amin *et al*. (2007) suggested that CMC from OPEFB can be used as a film-coating agent for pharmaceutical industry.

So far, very little attention has been paid to the role of palm-based CMC in various applications, especially in Malaysia. Therefore, palm-based CMC has huge potential in the development of sustainable cosmetic and personal care. This article described the rheological properties of palm-based CMC solutions.

MATERIALS AND METHODS

Materials

Palm-based CMC (PH 2000) is a yellowish-white powder obtained from Waris Nove Sdn. Bhd., Pahang, Malaysia. Two commercial CMC from other sources; cotton and wood were also used in this study for comparison. The two commercial CMC were cotton-based CMC sodium salt, C5013 (Sigma-Aldrich, Missouri, USA) and wood-based CMC, Walocel™ CRT 2000 PA (The Dow Chemical Company, USA).

Scanning Electron Microscope Measurement and Degree of Substitution Determination by Energy Dispersive X-ray Analysis

The morphology of palm-based CMC was examined by Hitachi S-3400N Scanning Electron Microscope (SEM) (Hitachi, USA) equipped with Energy Dispersive X-ray (EDX) (Bruker XFlash 6I10) analysis. The test parameters used were as follows; Chamber pressure: 10 Pa; High voltage: 20.00 kV; Tilt: 0.00; Take-off: 35.00; Amplification time: 102.4; Resolution: 133.44. The powdered samples were analysed without coating and carbon cement adhesive. The degree of substitution was calculated using EDX data and the following Equation (1) (Singh and Kathri, 2012):

$$\text{Degree of substitution} = \frac{162 \times \% \text{ Sodium}}{2300 - (80 \times \% \text{ Sodium})} \quad (1)$$

where 162 is the molecular weight of the anhydrous glucose unit, 80 is the net increment in the anhydrous glucose unit for every substituted sodium carboxymethyl group, and 23 is the molecular weight of Na.

Characterisation of CMC by Infrared Spectroscopy

The Fourier transform infrared spectroscopy (FTIR) spectra were recorded using Perkin Elmer FTIR Spectrum 100 equipped with Universal ATR Attachment, recording the spectra over a wavenumber range of 650-4000 cm^{-1}. The average value of eight scans with 4 cm^{-1} resolution was collected for each sample.

Preparation of CMC Solutions

Palm-based, cotton-based and wood-based CMC solutions were prepared at 1%, 2%, 3% and 4% (w/v) solution in ultrapure water (ELGA PURELAB Flex 3, High Wycombe, United Kingdom) by dissolving the CMC powder in ultrapure water with gentle magnetic stirring for 30 min at ambient temperature.

Viscosity Measurement

Viscosity measurement of CMC solutions was carried out using DV-III Ultra Rheometer (Brookfield Eng. Lab. Inc., Middleborough, USA). The measurements were performed at room temperature, speed 30 rpm and more than 10% torque. The viscosity of solutions was measured at Day 1, after Day 7 and Day 30 of storage at room temperature.

Rheological Measurement

The rheological measurements were performed using a stress-controlled rheometer (Anton Paar MCR300, Anton Paar GmbH, Graz, Austria). The geometry used was a cone plate with a diameter of 50 mm and a gap height of 1.000 mm. Rheological measurements were carried out at ambient temperature with a fresh sample each time. Samples were placed on the rheometer plate and equilibrated for 5 min before measurements.

Rotational test. The flow properties of CMC solutions were measured in continuous flow conditions, with a controlled shear rate test, by recording viscosity values at increasing shear rate (0–100 s^{-1}).

Oscillation test. Amplitude sweep studies were examined in a log strain ramp from 0.1%-1000% at an angular frequency of 10 $rads^{-1}$. Amplitude sweep is designed to measure the viscoelastic properties of samples without the disruption of the internal structures. A sinusoidal stress as a function of the angular frequency (ω) and the stress amplitude was applied to the samples. Frequency (small deformation) measurements were performed within the linear viscoelastic region by varying frequency from 0.1-100 $rads^{-1}$.

RESULTS AND DISCUSSION

We have carried out the EDX analysis of SEM of palm-based CMC, cotton-based CMC and wood-based CMC. The SEM images with 100 µm magnification, along with the EDX analysis, are shown in *Figure 1*. The results are tabulated in *Table 1*. Palm-based and cotton-based CMC showed a similar morphology structure; long-shaped with relatively smooth surface (*Figures 1a* and *1b*). However, the surface morphology of wood-based CMC is different where the particles are compactly gathered together (*Figure 1c*).

The degree of substitution (DS) is an important CMC parameter, which could influence its performance, such as its solubility in water. The theoretical maximum of the DS value for CMC is 3.0, but the DS value of commercially available CMC grades is generally in the range of 0.4-1.5 (Heinze and Koschella, 2005). *Table 1* listed the calculated DS value based on the wt % sodium (Na) from EDX analysis. Cotton-based CMC recorded the highest wt %Na (13.08) and gives calculated DS value of 1.69, followed by palm-based CMC with wt %Na (9.88) and calculated DS value of 1.06. While, wood-based CMC recorded wt %Na (8.94) and gives calculated DS value of 0.91. The calculated DS value was compared to the DS value given from the certificate of analysis (CoA) of each CMC (*Table 1*), provided by the CMC's supplier which usually determined according to ASTM D1439 test method. The method evolves the conversion of the CMC to free acid then again forming CMC by adding excess alkali and finally titrating the excess alkali with standard hydrochloric acid. Then, the DS value was determined by the used volume of the standard alkali (ASTM, 1995). Calculated DS values for palm-based and wood-based CMC are close to values reported by CoA. However, cotton-based CMC recorded a higher calculated DS value as compared to CoA (*Table 1*). According to Singh and Khatri (2012), the EDX analysis has a limitation to predict the exact DS value if the sample is not pure. Free sodium chloride (NaCI) in the sample would be reflected in the wt %Na value and so in the DS value. According to Borsa and Racz (1995), CMC has good water solubility above DS value of 0.6. Palm-based, cotton-based and wood-based CMC have DS value above than 0.6 and it was observed that all CMC soluble in water and gives clear solution.

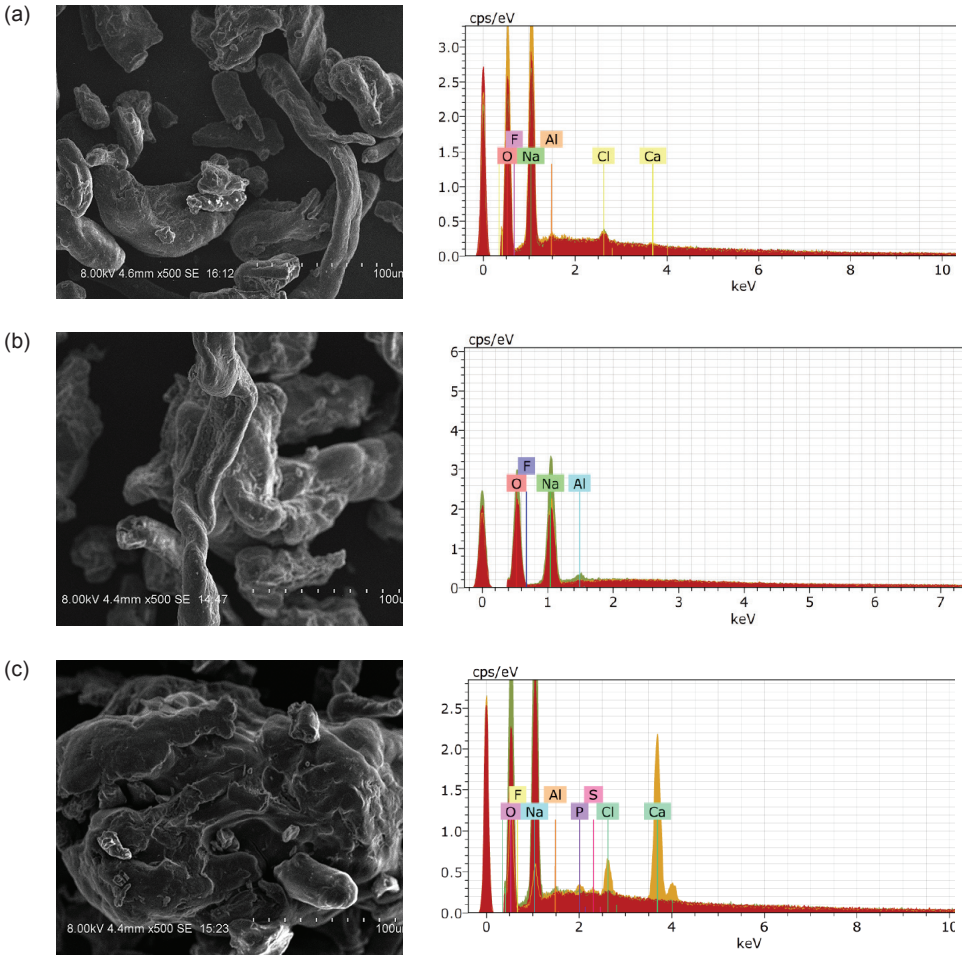
Figure 2 depicts the FTIR spectra of palm-based, cotton-based and wood-based CMC. The spectra pattern was similar to the spectra of CMC from OPEFB as reported by Eliza *et al.* (2015) and spectra of CMC as prepared by Ramli *et al.* (2015). In this study, it was clearly shown that all CMC have a broad band located within the region of 3600-3200 cm^{-1}, attributable to an -OH stretching vibration consistent with the polyhydroxylated saccharide backbone. The band at 2921.69 cm^{-1} is attributed to CH stretching vibration (3000 cm^{-1}). All CMC recorded a weak absorption band at 2887-2933 cm^{-1} consistent with the C-H stretching within each glucose unit. The strong absorption band observed at 1585.88, 1586.61 and 1589.90 cm^{-1} are due to presence of carboxyl group -C(O)O, while the peaks at 1412 and 1415 cm^{-1} are relevant to CH_2-stretching. The ether groups (-O-) stretching was observed at peak 1000-1200 cm^{-1} (Eliza *et al.*, 2015; Ramli *et al.*, 2015).

A non-Newtonian fluid is a fluid whose flow properties differ in many ways from those of

TABLE 1. DEGREE OF SUBSTITUTION OF PALM-BASED, COTTON-BASED AND WOOD-BASED CMC BY EDX ANALYSIS AS COMPARED TO CoA

CMC	EDX analysis (wt. %Na)	Calculated DS	DS value from CoA
Palm-based	9.88 ± 1.73	1.06	>0.70
Cotton-based	13.08 ± 2.97	1.69	0.89
Wood-based	8.94 ± 4.29	0.91	0.82-0.95

Note: DS - degree of substitution; CoA - certificate of analysis; CMC - carboxymethyl cellulose; EDX - energy dispersive X-ray.



Note: CMC - carboxymethyl cellulose.

Figure 1. Scanning electron microscope (SEM) images with Energy Dispersive X-ray (EDX) of sample (a) palm-based CMC, (b) cotton-based CMC, and (c) wood-based CMC.

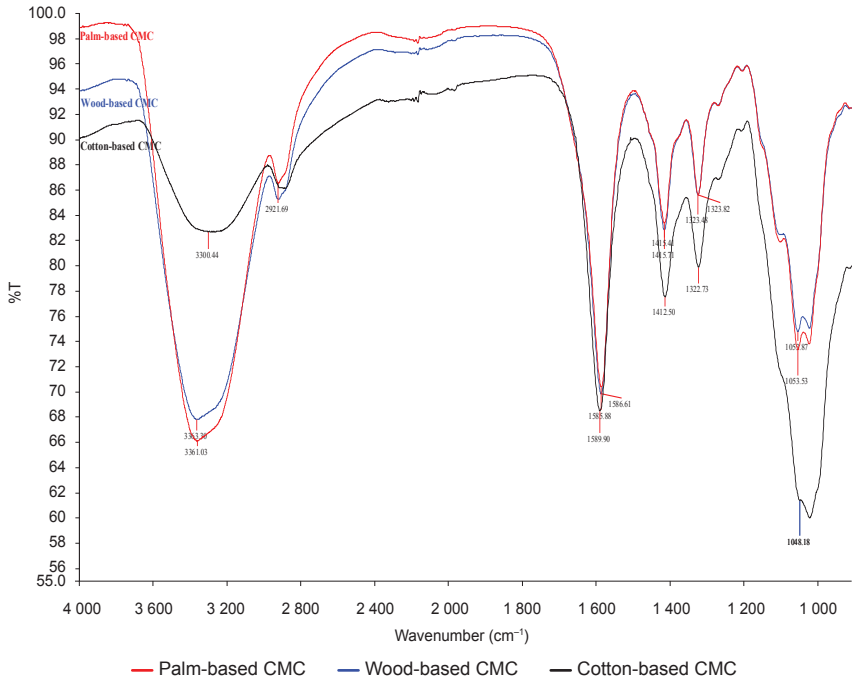


Figure 2. Infrared spectra of palm-based, cotton-based and wood-based carboxymethyl cellulose (CMC).

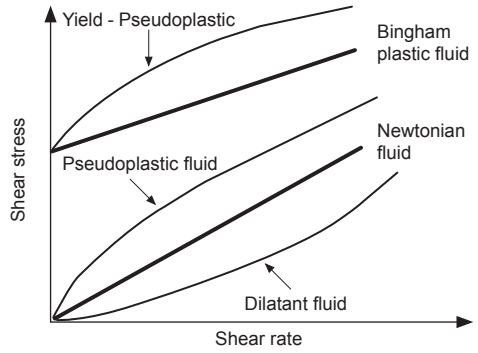
Newtonian fluids. In practice, many fluid materials exhibit non-Newtonian fluid behaviour such as salt solutions, toothpaste, starch suspensions, paint, shampoo *etc*. *Figure 3* shows the flow curves of different types of time-independent non-Newtonian fluid (Nguyen and Nguyen, 2012). The rheology of a non-Newtonian fluid is often described by the power law equation as in Equation (2).

$$\tau = K\gamma^n \quad (2)$$

where τ is the shear stress, K is the flow consistency index, γ is the shear rate and n is the flow behaviour index. The larger the deviation of n from 1, the more non-Newtonian is the behaviour of the fluid. For a Newtonian fluid, n is equal to 1, for a dilatant or shear-thickening fluid, n is greater than 1 and for pseudoplastic or shear-thinning fluid, n is less than 1. The smaller the value of n, the greater is the degree of shear-thinning (Holdsworth, 1971). *Table 2* summarises the value of n and description of the flow behaviour of palm-based, cotton-based and wood-based CMC solutions.

The values of flow behaviour index (*n)* for palm-based CMC, cotton-based CMC, and wood-based CMC solutions were all less than 1, indicating the pseudoplastic or shear-thinning properties. Upon increasing the concentration, the value of n decreased, revealing more-obvious pseudoplastic or shear-thinning behaviour. The degree of shear-thinning properties of palm-based CMC and cotton-based CMC solutions were comparable and greater as compared to wood-based CMC solution at 1%, 2%, 3% and 4% (w/v) in water, respectively as listed in *Table 3*. *Figure 4* shows the flow curves of palm-based CMC, cotton-based CMC and wood-based CMC solutions, at different concentrations plotted of viscosity (mPa.s) and shear stress (Pa) over shear rate (s^{-1}). At higher concentration (4%) and shear rate 1 s^{-1}, cotton-based CMC solution recorded a highest viscosity (270 000 mPa.s) (*Figure 4a*), followed by palm-based CMC (212 000 mPa.s) (*Figure 4b*) and wood-based CMC (10 600 mPa.s) (*Figure 4c*). According to Newton's Law, shear stress is viscosity times shear rate. Therefore, the viscosity is shear stress divided by shear rate. This explained why wood-based CMC solutions have lower shear stress (Pa) (*Figure 4c*) value as compared to palm-based and cotton-based CMC solutions (*Figures 4a* and *b*). The flow curves in *Figure 4* clearly show that all CMC solutions exhibited pseudoplastic or shear-thinning behaviour with reference to *Figure 3*.

The results of amplitude sweeps are presented as a diagram with strain or shear stress plotted on the x-axis, and storage modulus (G') and loss modulus (G") plotted on the y-axis; both axes on



Source: Nguyen and Nguyen (2012).

Figure 3. Types of time-independent non-Newtonian fluid.

TABLE 2. VALUE OF *n* AND DESCRIPTION OF FLOW BEHAVIOUR OF CMC SOLUTIONS

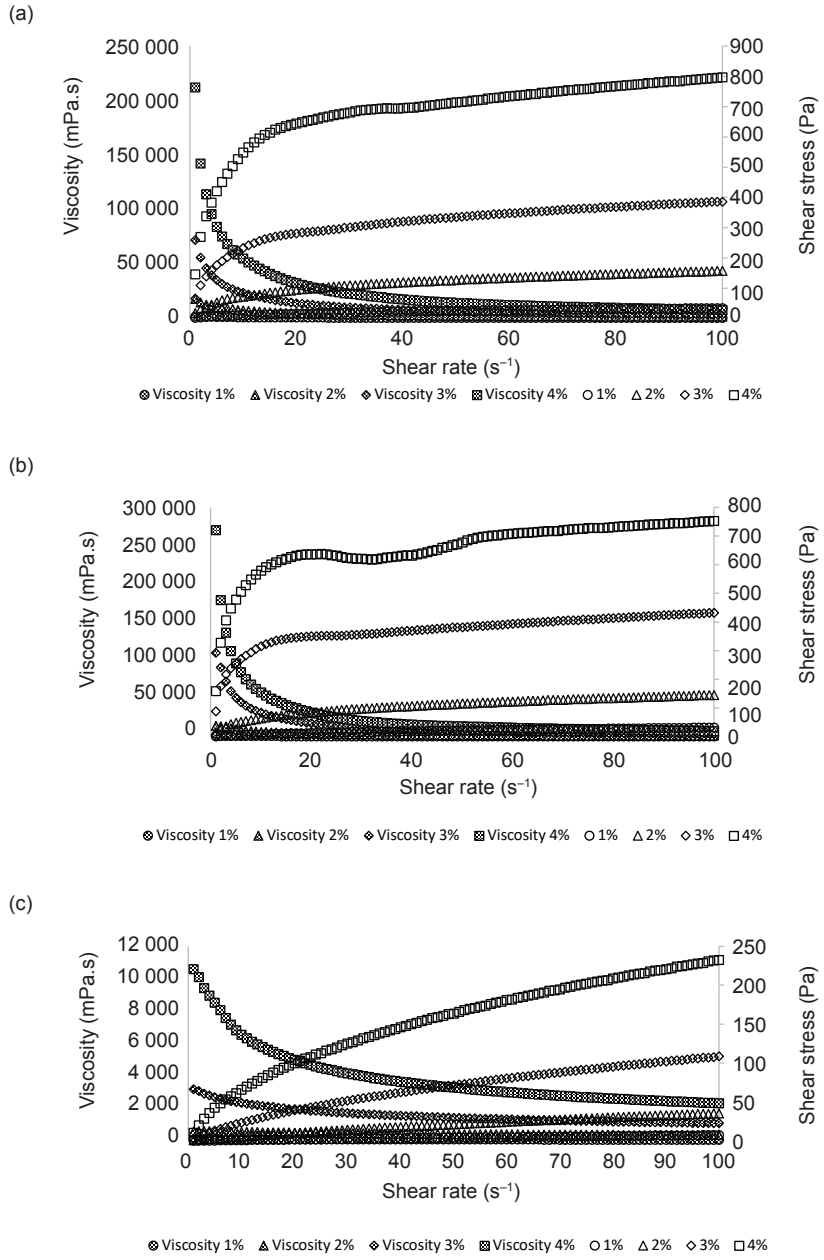
CMC	% solution in water (w/v)	Flow behaviour index (*n*)	Flow consistency index (*K*)
Palm-based	1	0.50	3.52
	2	0.34	33.28
	3	0.24	131.19
	4	0.19	344.57
Cotton-based	1	0.57	2.42
	2	0.35	28.76
	3	0.17	202.03
	4	0.15	378.87
Wood-based	1	0.90	0.12
	2	0.77	1.04
	3	0.64	5.77
	4	0.54	19.96

Note: CMC - carboxymethyl cellulose.

TABLE 3. POSITION OF G' AND G" AND FLOW POINT VALUES (crossover G'=G") OF CMC SOLUTIONS

CMC solutions	G' and G"	Flow point (Pa)
Palm-based		
1%	G" > G'	No crossover
2%	G' > G"	39.6
3%	G' > G"	241.0
4%	G' > G"	514.0
Cotton-based		
1%	G" > G'	No crossover
2%	G" > G'	No crossover
3%	G' > G"	247.0
4%	G' > G"	691.0
Wood-based		
1%	G" > G'	No crossover
2%	G" > G'	No crossover
3%	G" > G'	No crossover
4%	G" > G'	No crossover

Note: G' - storage modulus; G" – loss modulus; CMC - carboxymethyl cellulose.



Note: CMC - carboxymethyl cellulose.

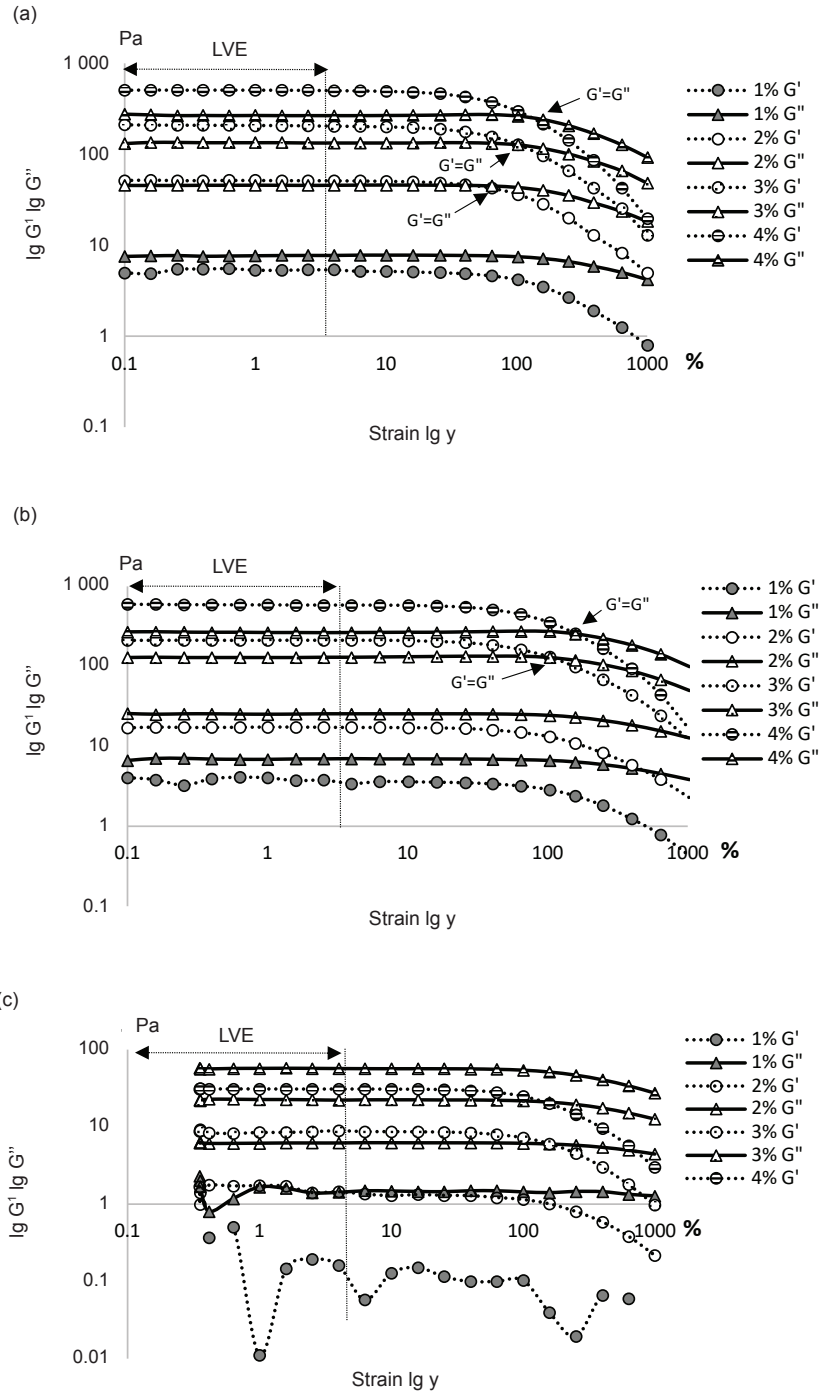
Figure 4. Flow behaviour curves of (a) palm-based CMC solutions, (b) cotton-based CMC solutions, and (c) wood-based CMC solutions at varying concentrations: 1%, 2%, 3% and 4%.

a logarithmic scale as depicted in *Figure 5*. The limit of the linear viscoelastic (LVE) region is first determined. The LVE region indicates the range in which the test can be carried out without destroying the structure of the sample. The LVE region will give an information on the structure and firmness of the sample. The longer the LVE, the more firm or structured the test sample, while the shorter the LVE, the less firm it appears (Ho and Dodou, 2007). The LVE region analysed by the software is 5% strain and the region was depicted on the left side of the diagram in *Figure 5*.

Figure 5a shows the amplitude sweeps of palm-based CMC solutions at varying concentrations: 1%, 2%, 3% and 4%. The results showed that palm-based CMC at 1% solution exhibited viscoelastic liquid properties where the loss modulus (G″) is larger than the storage modulus (G′) in the LVE region, thus, making the sample fluid. At 2% palm-based CMC solutions, first, it can be seen that at small strains, G′ is close and little bit higher than G″ in the LVE region, implying that the polymer fluids are more solid like or viscoelastic solid. As the strain increase, G′ falls faster than G″ and crossover of G′=G″ or flow point occurred at strain 39.6 Pa. When the CMC concentration increased, viscoelastic properties become stronger where the distance between G′ and G″ is more obvious and larger (G′>G″) for 3% and

4% palm-based CMC solutions. The flow point was also increased to 241.0 Pa and 514.0 Pa, respectively. The amplitude sweeps results for cotton-based CMC solutions at 1%, 2%, 3% and 4% are depicted in *Figure 5b*. Cotton-based CMC solutions showed viscoelastic liquid properties at 1% and 2% solutions where the G" is larger than G' in the LVE region (*Figure 5b*). However, at 3% and 4%, it behaved as a viscoelastic solid material (G'>G") with flow points that occurred at 247.0 Pa and 691.0 Pa, respectively. Wood-based CMC at 1%, 2%, 3% and 4% solutions showed viscoelastic liquid properties over the entire range of strain where G">G' in the LVE region (*Figure 5c).*

The LVE region determined in the amplitude sweeps test helps to further characterise the CMC solutions structure using a frequency sweep at a strain below the critical strain. In a frequency sweep,

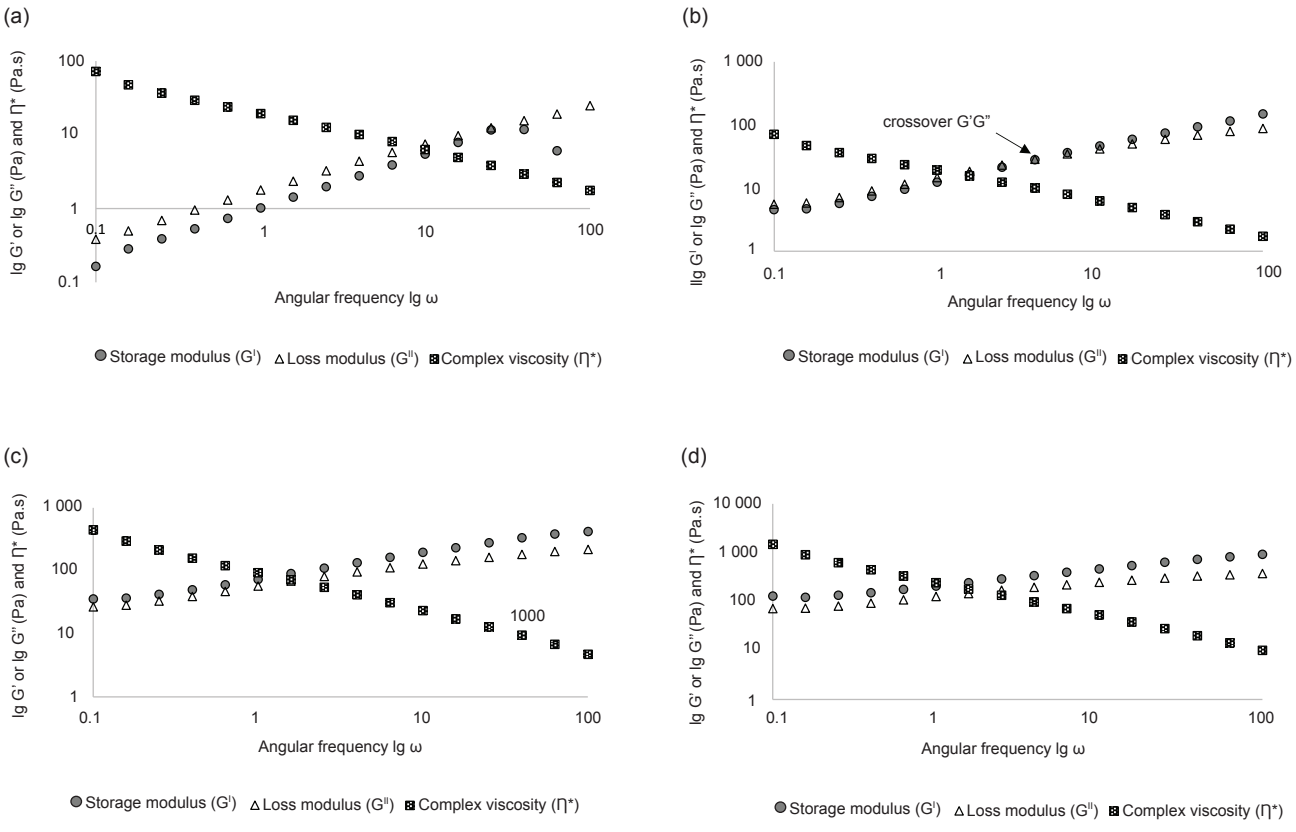


Note: CMC - carboxymethyl cellulose; LVE - linear viscoelastic; G - storage modulus; G" - loss modulus.

Figure 5. Amplitude sweeps of (a) palm-based CMC solutions, (b) cotton-based CMC solutions, and (c) wood-based CMC solutions at varying concentrations: 1%, 2%, 3% and 4%.

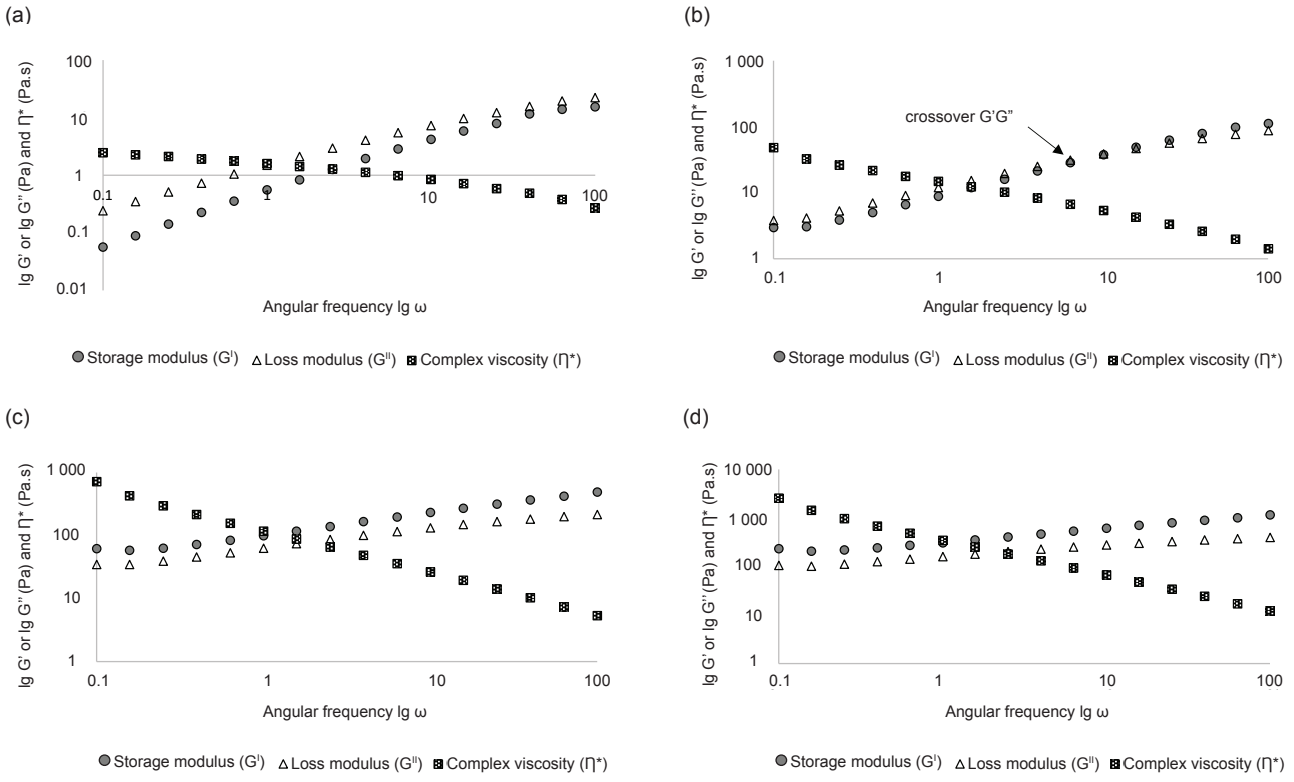
measurements are made over a range of oscillation frequencies at a constant oscillation amplitude. Since frequency is inverse of time, low frequencies allow the samples time to relax and respond, and thus, the flow properties dominate, and as the frequency increases, the sample behaves more and more in elastic fashion; hence, the G′ increases with the increase in the frequency (Menard, 2008). The change in G′ (a function of frequency) increases with the viscoelasticity of the materials studied and in case of gels, the weaker the gel strength, the greater is the dependence of G′ on frequency (Osada and Khokhlov, 2001).

The frequency sweep performed within the linear viscoelastic (strain=5%) in the range of 0.1-100 rads^{-1} for palm-based CMC at 1%, 2%, 3% and 4% are shown in *Figure 6*. The results showed that a 1% palm-based CMC solution exhibited fluid-structure within the frequency regime where G″ is higher than G′ (*Figure 6a*). While 2% palm-based CMC solution exhibited fluid-structure at low frequencies and behaved more elastic at the crossover frequency (G′=G″) of 3.98 rads^{-1}. At 3% and 4%, the solutions exhibited a stable gel-like or elastic solid structure with no crossover between G′ and G″ within the frequency regime (*Figures 6c* and *6d*). The frequency sweep result for cotton-based CMC at 1% exhibited fluid-structure properties where G″ is higher than G′ (*Figure 7a*). At 2%, fluid-structure or liquid-like properties were observed at low frequencies and the transition solid-like or elastic behaviour occurred at the crossover frequency (G′=G″) of 10.0 rads^{-1} (*Figure 7b*). The transition from liquid-like to solid-like for 2% cotton-based CMC solution occurred at a higher angular frequency (10.0 rads^{-1}) as compared to 2% palm-based CMC (3.98 rads^{-1}). This explained that palm-based CMC has higher gel strength as compared to cotton-based CMC at 2% concentration and it is consistent with the result of amplitude sweep where palm-based CMC at 2% showed a viscoelastic solid properties while cotton-based CMC at 2% showed viscoelastic liquid properties (*Figure 5*). At 3% and 4%, the solutions exhibited a stable gel-like or elastic solid structure with no crossover between G′ and G″ within the frequency regime (*Figures 7c-d*). Wood-based CMC at 1%, 2%, 3% and 4% solutions showed fluid structure within the frequency regime where G″ is higher than G′ (*Figure 8*).



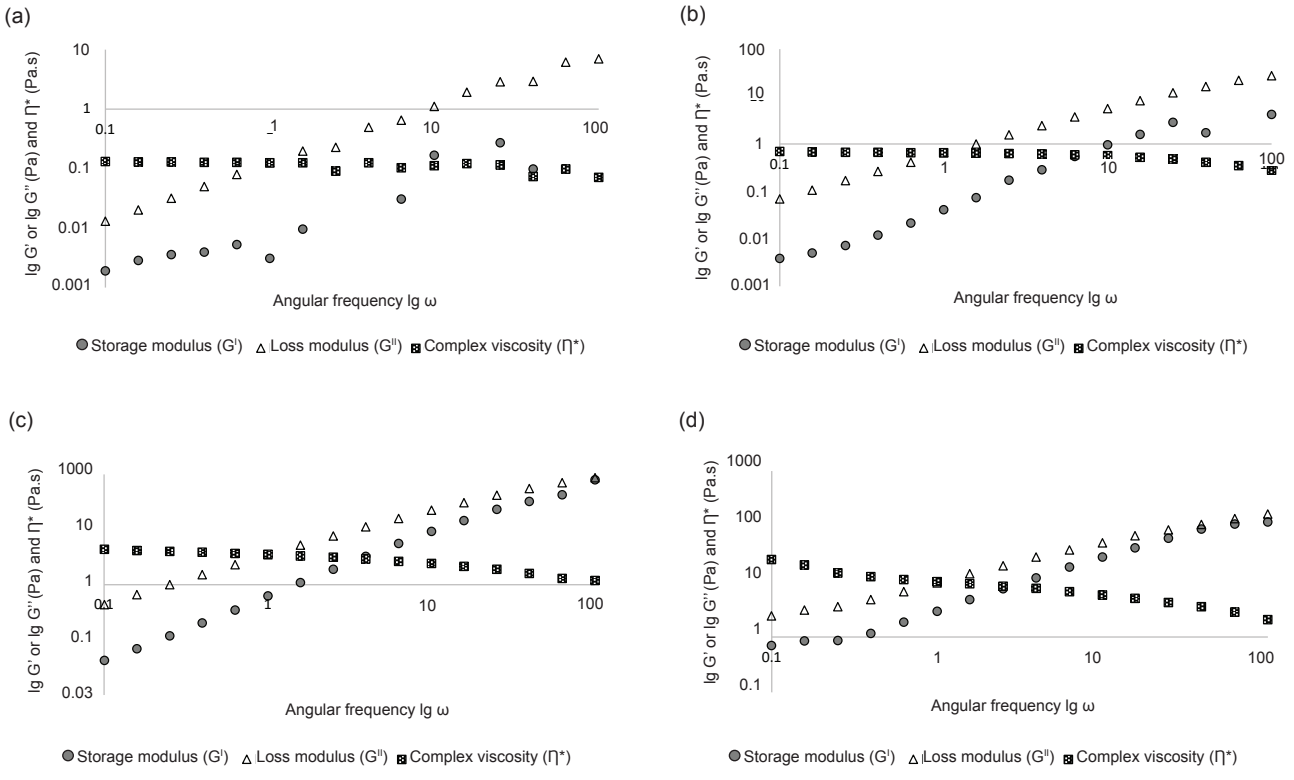
Note: CMC - carboxymethyl cellulose.

Figure 6. Angular frequency sweeps of palm-based CMC solutions at varying concentrations of (a) 1%, (b) 2%, (c) 3%, and (d) 4%.



Note: CMC - carboxymethyl cellulose.

Figure 7. Angular frequency sweeps of cotton-based CMC solutions at varying concentrations of (a) 1%, (b) 2%, (c) 3%, and (d) 4%.

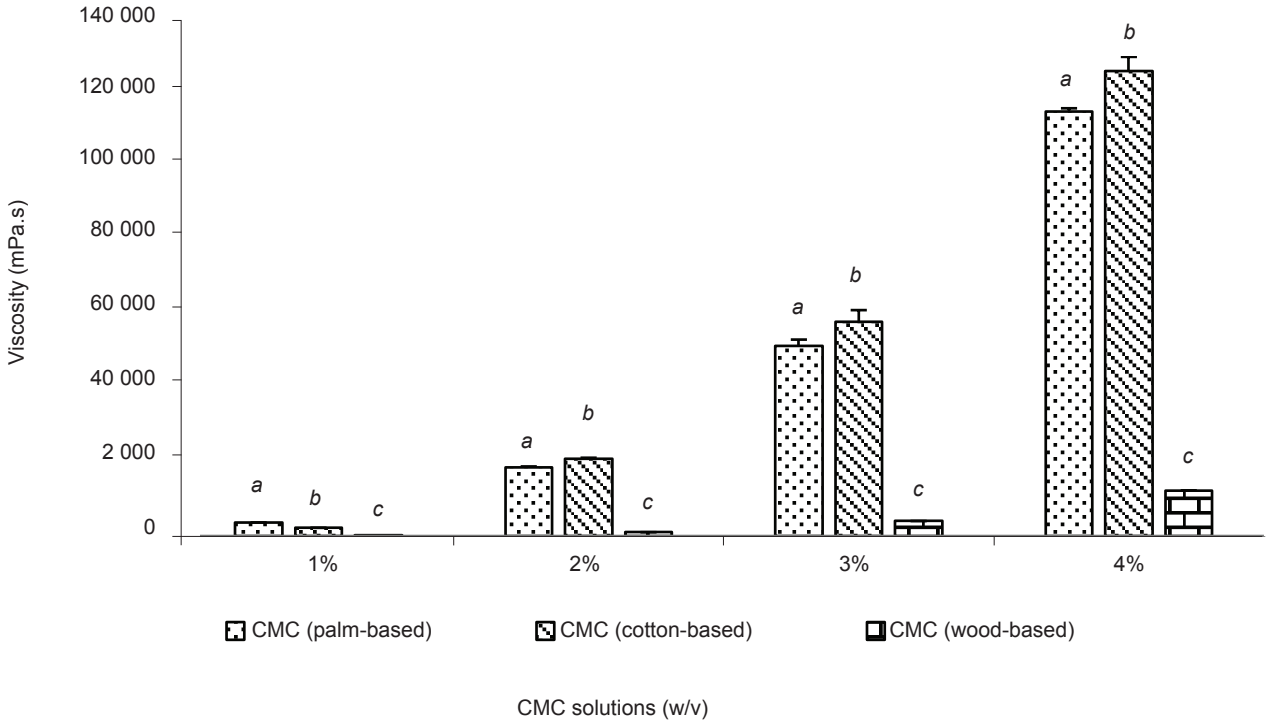


Note: CMC - carboxymethyl cellulose.

Figure 8. Angular frequency sweeps of wood-based CMC solutions at varying concentrations of (a) 1%, (b) 2%, (c) 3%, and (d) 4%.

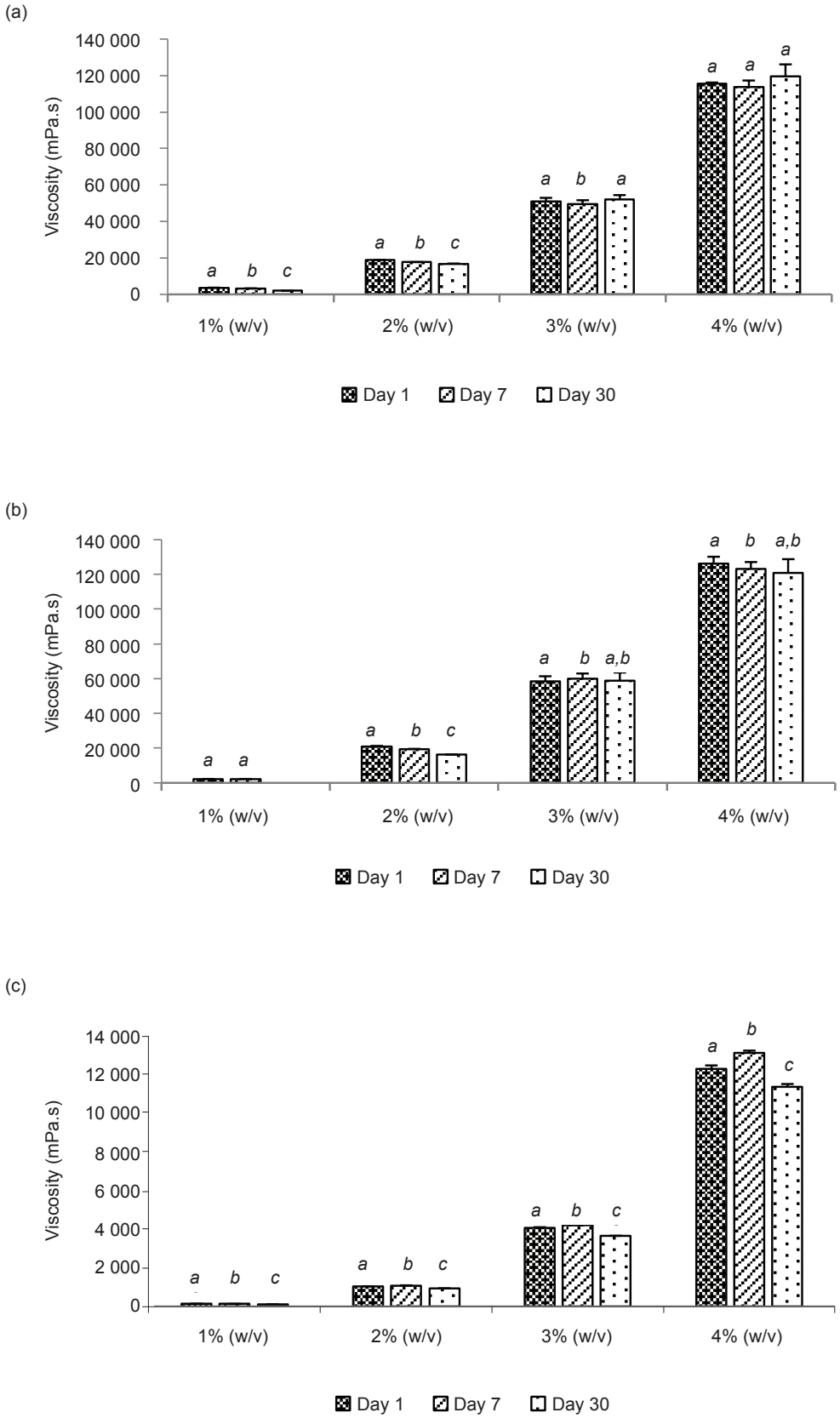
The viscosity of CMC solutions can also be measured through Brookfield DV-III Ultra Rheometer. The measurement was conducted at room temperature and speed of 30 rpm, with more than 10% torque. The result shows that at 1% solution, palm-based CMC recorded the highest viscosity (3563 ± 122 mPa.s) as compared to cotton-based CMC (2210 ± 35 mPa.s) and wood-based CMC (140 ± 0 mPa.s). However, at varying concentrations, cotton-based CMC solutions recorded the highest viscosity as compared to palm-based and wood-based CMCs; 2% solution (21 033 ± 232 mPa.s), 3% solution (58 266 ± 3104 mPa.s) and 4% solution (126 311 ± 3855 mPa.s) as shown in *Figure 9*. These results may be due to a higher DS value of cotton-based CMC (DS=1.69), followed by palm-based CMC and wood-based CMC that explained why the flow point of cotton-based CMC solution was higher than palm-based CMC solutions at 3% and 4%. The viscosities recorded were significantly different with $p<0.05$.

The viscosity was further measured after Day 7 and Day 30 of storage at room temperature as depicted in *Figure 10*. The viscosity of wood-based CMC solutions was significantly different ($p<0.05$) at all concentrations throughout the storage. Wood-based CMC solutions are liquid-like and recorded the lowest viscosity as compared to palm-based and cotton-based CMC solutions. Therefore, the changes in viscosity over time are more affected. Meanwhile, the viscosity of palm-based CMC solutions was significantly different ($p<0.05$) at 1% and 2% throughout the measurement at Day 1, Day 7 and Day 30 of storage. Cotton-based CMC solution at 1% recorded insignificant difference ($p>0.05$) in viscosity measurement at Day 1 and Day 7 of storage. However, the viscosity measurement could not be performed after Day 30 of storage due to the instability of the test sample. Cotton-based CMC solution at 2% recorded a significant difference ($p<0.05$) in viscosity throughout the 30 days of storage. At 3%, both palm-based and cotton-based CMC solutions recorded insignificant difference ($p>0.05$) in viscosity measurement after 30 days of storage. At higher concentration of 4%, palm-based CMC solutions could be considered stable where the viscosity was not significantly different ($p>0.05$) at Day 1, after Day 7 and Day 30 of storage (*Figure 10a*) as compared to cotton-based (*Figure 10b*) and wood-based (*Figure 10c*) CMC solutions.



Note: CMC - carboxymethyl cellulose.

Figure 9. Viscosity of palm-based, cotton-based and wood-based CMC at varying concentrations (1%, 2%, 3% and 4%), measurement at room temperature, speed 30 rpm and more than 10% torque; values with different superscript letters within the same concentration are statistically different ($p<0.05$).



Note: CMC - carboxymethyl cellulose.

Figure 10. Viscosity of (a) palm-based, (b) cotton-based and (c) wood-based CMC at varying concentrations (1%, 2%, 3% and 4%) at Day 1, after Day 7 and Day 30 of storage at room temperature; values with different superscript letters within the same concentration are statistically different ($p<0.05$).

CONCLUSION

The values of flow behaviour for all CMC solutions were less than 1, indicating the pseudoplastic or shear thinning properties. At a minimum of 2%, palm-based CMC solution exhibited viscoelastic solid properties where transition from liquid-like to solid-like occurred at lower frequency. While, cotton-based CMC exhibited viscoelastic solid properties at 3% solution and transition from liquid-like to solid-like occurred at higher frequency. At 2% solution, palm-based CMC provide better gel strength compared to cotton-based CMC. Wood-based CMC exhibited viscoelastic fluid properties with no gelling behaviour at all concentrations. Palm-based CMC may potentially replace CMC from other sources as rheological modifier for the development of sustainable cosmetic and personal care products.

ACKNOWLEDGEMENT

The authors wish to thank the Director-General of MPOB for permission to publish this article. The authors would also like to thank the Safety and Efficacy Assessment Group (Rosmah Umam), Consumer Product Development Unit of Advanced Oleochemical Technology Division and Biomass Technology Unit of Engineering and Processing Division, MPOB for their technical assistance.

REFERENCES

Amin, M C I; Soom, R M; Ahmad, I and Lian, H H (2007). Carboxymethyl cellulose from palm oil empty fruit bunch-their properties and use as a film coating agent. *Jurnal Sains Kesihatan Malaysia, 4(2)*: 53-62.

Ariffin, H; Hassan, M; Kalsom, M U; Abdullah, N and Shirai, Y (2008). Effect of physical, chemical and thermal pre-treatments on the enzymatic hydrolysis of oil palm empty fruit bunch. *J. Trop. Agric. Food. Sci., 36(2)*: 259-268.

ASTM (1995). Designation: D 1439-97. Standard test methods for sodium carboxymethylcellulose. Annual Book of ASTM Standards. American Society of Testing and Materials (ASTM).

Astimar, A A; Husin, M and Anis, M (2002). Preparation of cellulose from oil palm empty fruit bunches via ethanol digestion: Effect of acid and alkali catalysts. *J. Oil Palm Res., 14(1)*: 9-14.

Barba, C; Montane, D; Farriol, X; Desbrieres, J and Rinaudo, M (2002). Synthesis and characterization of carboxymethylcelluloses from non-wood pulps II: Rheological behaviour of CMC in aqueous solution. *Cellulose, 9(3)*: 327-335.

Benchabane, A and Bekkour, K (2008). Rheological properties of carboxymethyl cellulose (CMC) solutions. *Colloid Polym. Sci., 286*: 1173-1180.

Borsa, J and Racz, I (1995). Carboxymethyl cellulose of fibrous character, a survey. *Cellul. Chem. Technol., 29*: 657-663.

Ching, Y C and Ng, T S (2014). Effect of preparation conditions on cellulose from oil palm empty fruit bunch fibre. *BioRes., 9(4)*: 6373-6385.

Eliza, M Y; Shahruddin, M and Wan Rosli, W D (2015). Carboxymethyl cellulose (CMC) from oil palm empty fruit bunch (OPEFB) in the new solvent dimethyl sulfoxide (DMSO)/tetrabutylammonium fluoride (TBAF). *J. Phys.: Conf. Ser., 622*: 012026.

Ghannam, M T and Esmail, M N (1997). Rheological properties of carboxymethyl cellulose. *J. Appl. Polym. Sci., 64(2)*: 289-301.

Heinze, T and Koschella, A (2005). Carboxymethyl ethers of cellulose and starch: A review. *Macromol. Symp., 223(1)*: 13-40.

Ho, K Y and Dodou, K (2007). Rheological studies on pressure-sensitive silicone adhesives and drug-in-adhesive layers as a means to characterise adhesive performance. *Int. J. Pharm., 333(1-2)*: 24-33.

Holdsworth, S D (1971). Applicability of rheological models to the interpretation of flow and processing behaviour of fluid food products. *J. Texture Stud., 2(4)*: 393-418.

Hutomo, G S; Marseno, D W; Anggrahini, S and Supriyanto, (2012). Synthesis and characterization of sodium carboxymethylcellulose from pod husk of cacao (*Theobroma cacao* L.). *Aust. J. Fr. Stud., 6(6)*: 180-185.

Menard, K P (2008). *Dynamic Mechanical Analysis: A Practical Introduction*. CRC Press, Boca Raton. 240 pp.

Nazir, M S; Wahjoedi, B A; Yussof, A W and Abdullah, M A (2013). Eco-friendly extraction and characterization of cellulose from oil palm empty fruit bunches. *BioRes., 8(2)*: 2161-2172.

Nguyen, Q H and Nguyen, N D (2012). Incompressible non-newtonian fluid flows. *Continuum Mechanics - Progress in Fundamentals and Engineering Applications*. (Yong Gan eds.). IntechOpen, London. p. 1-27.

Niraula, B; King, T C and Misran, M (2004). Evaluation of rheology property of dodecyl maltoside, sucrose dodecanoate, Brij 35p and SDS stabilized o/w emulsion: Effect of head group structure on rheology property and emulsion stability. *Colloids Surf. A Physicochem. Eng. Asp., 251(1-3)*: 59-74.

Osada, Y and Khokhlov, A (2001). *Polymer Gels and Networks*. Taylor and Francis, Boca Raton. 400 pp.

Padzil, F N M; Lee, S H; Ainun, Z M A; Lee, C H and Abdullah, L C (2020). Potential of oil palm empty fruit bunch resources in nanocellulose hydrogel production for versatile application: A review. *Materials (Basel), 13(5)*: 1245.

Parid, D M; Abd Rahman, N A; Baharuddin, A S; Mohammed, M A P; Mat Johari, A and Abdul Razak, S Z (2018). Synthesis and characterization of carboxymethyl cellulose from oil palm empty fruit bunch stalk fibres. *BioResources, 13(1)*: 535-554.

Ramli, S; Mohd Ja'afar, S; Abdul Sisak, M A; Zainuddin, N and Abdul Rahman, I (2015). Formulation and physical characterization of microemulsions based carboxymethyl cellulose as vitamin C carrier. *Malays. J. Anal. Sci., 19(1)*: 275-283.

Rosnah, M S; Astimar, A A; Wan Hasamudin, W H and Gapor, M T (2012). Conversion of lignocellulose from oil palm biomass into water-soluble cellulose ether. *J. Oil Palm Res., 24*: 1412-1420.

Rosnah, M S; Abd Gapor, M T and Wan Hasamudin, W H (2004). Production of carboxymethylcellulose (CMC) from oil palm empty fruit bunch. *MPOB Information Series No. 228*.

Rosnah, M S; Ku Halim, K H and Wan Hasamudin, W H (2002). The potential of oil palm lignocellulosic fibres for the cellulose derivatives production. *Proc. of the Research and Consultancy Seminar*. Faculty of Mechanical Engineering, UiTM Shah Alam, Malaysia. p. 140-145.

Rowe, R C; Sheskey, P J and Quinn, M E (2013). *Handbooks of Pharmaceutical Excipients*. Seventh edition. Pharmaceutical Press, London. 1033 pp.

Singh, R K and Khatri, O P (2012). A scanning electron microscope based new method for determining degree of substitution of sodium carboxymethyl cellulose. *J. Microsc., 246(1)*: 43-52.

Sisak, M A A; Daik, R and Ramli, S (2015). Characterization of cellulose extracted from oil palm empty fruit bunch. *AIP Conf. Proc. 1678: 050016*. DOI: 10.1063/1.4931295.

Stigsson, V; Kloow, G and Germgard, U (2001). An historic overview of carboxymethyl cellulose (CMC) production on an industrial scale. *Pap.Asia, 17(10)*: 16-21.

Varshney, V K and Naithani, S (2011). Chapter 2: Chemical functionalization of cellulose derived from nonconventional sources. *Cellulose Fibres: Bio- and Nano-Polymer Composites: Green Chemistry and Technology* (Kalia, S; Kaith, B S and Kaur, I eds.). Springer-Verlag, Berlin. p. 43-60.

Wan Rosli, W D; Rohaizu, R and Ghazali, A (2011). Synthesis and characterization of cellulose phosphate from oil palm empty fruit bunches microcrystalline cellulose. *Carbohydr. Polym., 84(1)*: 262-267.

SHORT COMMUNICATION

Journal of Oil Palm Research Vol. 33 (3) September 2021 p. 555-564
DOI: https://doi.org/10.21894/jopr.2020.0103

PRINCIPAL COMPONENT ANALYSIS (PCA) EVALUATION OF LIQUID CHROMATOGRAPHY-MASS SPECTROMETRY (LC-MS) DATASETS OF *Ganoderma boninense* INTRACELLULAR METABOLITES

ZAIN NURAZAH[1]*; ABRIZAH OTHMAN[1] and UMI SALAMAH RAMLI[1]

ABSTRACT

Liquid chromatography-mass spectrometry (LC-MS) has become a powerful analytical technique for studying broad coverage of chemical datasets describing complex biological systems and events. In order to interpret the underlying information in such datasets, multivariate analysis method such as principal component analysis (PCA) is crucial for multiple sample comparisons and multivariate data reduction. PCA has been used for evaluation of large-scale datasets derived from LC-MS analysis of fungal metabolites for many applications. Therefore, in this study, we describe on PCA as a descriptive tool to cope with large LC-MS datasets of intracellular metabolites of oil palm basal stem rot (BSR) fungal pathogen, Ganoderma boninense *from* in vitro *liquid culture system. The results revealed a classification and grouping of* G. boninense *intracellular metabolites according to time trend, where the primary metabolites,* i.e. *glucose, gluconic acid, mannitol and malic acid were found differentially expressed in* G. boninense. *The presented findings suggest that the PCA model provides a general approach for handling, analysis and interpretation of large LC-MS datasets to reveal time-dependent changes of intracellular metabolites that may indicate* G. boninense *developmental process* in vitro.

Keywords: *Ganoderma,* liquid chromatography-mass spectrometry, multivariate analysis, PCA.

Received: 2 June 2020**; Accepted:** 14 September 2020**; Published online:** 20 November 2020.

INTRODUCTION

A range of technical approaches have been used for the analysis of metabolites in biological samples including liquid chromatography-mass spectrometry (LC-MS). The technological advancement of LC-MS has been extensively reviewed elsewhere (Hayden *et al.*, 2019; Yuan *et al.*, 2019; Robison *et al.*, 2018) and increasingly become leading-edge instrumental developments due to its high sensitivity for the detection of metabolic signatures in the analysis of pathogen (Chen *et al.*, 2019; Tugizimana *et al.*, 2019). LC-MS analysis generates information-rich multivariate datasets comprising of samples and variables that provide insight into the relationship of metabolites and changes in the status of complex biological systems and events. To interpret the underlying information within the complex LC-MS datasets towards reliable conclusions, it is of great importance that a practical and organised statistical modelling tool is applied.

The multivariate statistical analysis and data mining approaches for pattern discovery have facilitated information retrieval from the vast amount of biological data (Ivosev *et al.*, 2008; Jonsson *et al.*, 2005; Holmes and Antti, 2002). Principal component

[1] Malaysian Palm Oil Board,
6 Persiaran Institusi, Bandar Baru Bangi,
43000 Kajang, Selangor, Malaysia.

* *Corresponding author e-mail: nurazah@mpob.gov.my*

analysis (PCA) is a popular dimension reduction method to reduce high-dimensional data into a low-dimensional subspace component (DesRochers *et al.*, 2020; Gotthardt *et al.*, 2019; de Falco *et al.*, 2019; Diana and Tommasi, 2002). The information needs to be interrogated in a way that enables scientists to make a prediction and increases the interpretability of the large datasets, at the same time, minimising the loss of important information. Furthermore, PCA provides knowledge on the nature of the variables and assigns a large number of variables to a smaller number of groups that can be more readily visualised and understood (Ivosev *et al.*, 2008).

Ganoderma boninense is a well-recognised basidiomycete fungal pathogen associated with oil palm basal stem rot disease (Chong *et al.*, 2017) that causes significant economic losses by reducing the yield of fresh fruit bunches. The ability to generate and mine large-scale datasets of biological molecules, *i.e.* proteins, metabolites combined with recent advances in high-throughput instrumentation analysis and data mining tools may have a profound effect on the systems-level understanding of the pathogenicity of *G. boninense* (Othman *et al.*, 2019). Multivariate statistical analysis and data mining such as PCA has been used to evaluate large-scale datasets derived from LC-MS analysis of fungal metabolites for many applications, *i.e.* differentiation of virulent and avirulent species, assessment of metabolic behaviour in different culture environments and evaluation of metabolic difference in spores and mycelia (DesRochers *et al.*, 2020; Siless *et al.*, 2018; Son *et al.*, 2018; Liu *et al.*, 2015). Harnessing the complexity of the metabolomics data derived from the various analytical platforms remains as major challenges in metabolomics. To the best of our knowledge, up to now, there are no studies reported on the statistical evaluation and data mining of large-scale datasets from the *G. boninense* pathogen.

In that perspective, our study aimed to focus on multivariate statistical evaluation using PCA to cope with the large-scale LC-MS datasets from the *G. boninense* intracellular metabolites. This approach is important for a robust and reliable comparison of *G. boninense* intracellular metabolites measured over time using statistical strategy applied to the complex LC-MS datasets.

MATERIALS AND METHODS

Chemicals and Reagents

Acetonitrile, methanol and acetic acid of high performance liquid chromatography (HPLC) grade were purchased from Merck, Germany. Difco™ potato dextrose agar (PDA) and Difco™ malt extract broth (MEB) were purchased from Becton, Dickinson and Company (BD), USA. Ammonium phosphate monobasic [$(NH_4)H_2PO_4$], ammonium phosphate dibasic [$(NH_4)_2HPO_4$], potassium phosphate monobasic (KH_2PO_4), magnesium sulphate heptahydrate $MgSO_4.(7H_2O)$, iron (III) sulphate heptahydrate ($FeSO_4.7H_2O$), zinc sulphate heptahydrate ($ZnSO_4.7H_2O$), sodium molybdate dihydrate ($NaMoO_4.2H_2O$), copper (II) sulphate pentahydrate ($CuSO_4.5H_2O$), manganese (II) chloride tetrahydrate ($MnCl_2.4H_2O$), 2-N-morpholinoethanesulphonic acid (MES) and glucose (≥99.5%) were purchased from Sigma-Aldrich, USA. Water was purified by a Milli-Q system (Millipore, USA).

Fungal Material Preparation and Liquid Culture Condition

Ganoderma boninense isolate PER71 was obtained from the Plant Pathology and Biosecurity Unit, Malaysian Palm Oil Board, Bangi, Selangor, Malaysia. *G. boninense* liquid culture protocol was previously described by Rees (2006). *G. boninense* was grown on Difco™ PDA (Becton, Dickinson and Company, USA) plate and incubated at 27 ± 1°C for eight days. A plug of 9.5 mm of *G. boninense* was harvested from eight days old culture on PDA plate. Biological replicates for each *G. boninense* were grown by inoculating one plug from each six individual PDA plates into 50 ml of MEB (Becton, Dickinson and Company, USA) in 175 cm^3 Nunclon™ cell culture flask (ThermoFisher Scientific, USA). A total of six mycelial plugs were grown in the cell culture flask at 27 ± 1°C for six days. After six days, the *G. boninense* mycelial plugs were then collected on sterile filter paper, washed three times with sterile distilled water and inoculated into the 50 ml of growth medium supplemented with carbon and nitrogen sources in 175 cm^3 Nunclon™ cell culture flask (ThermoFisher Scientific, USA). The growth medium consisted of: 0.9 g $(NH_4)H_2PO_4$; 2.0 g $(NH_4)_2HPO_4$; 1.0 g KH_2PO_4; 0.5 g $MgSO_4.(7H_2O)$; 1 ml of 100x trace elements (1.11 g $FeSO_4.7H_2O$, 5.75 g $ZnSO_4.7H_2O$, 0.09 g $NaMoO_4.2H_2O$, 0.1 g $CuSO_4.5H_2O$ and 0.21 g $MnCl_2.4H_2O$ in 200 ml distilled water); 3.9 g 2-N-morpholinoethanesulphonic acid (MES) pH 5.5; 5.0 g glucose in 1 litre distilled water. The culture was grown at 27 ± 1°C. The *G. boninense* intracellular metabolites were sampled over time, on Days 2, 4, 6 and 8 for analysis.

Metabolite Extraction

The *G. boninense* mycelia containing intracellular metabolites were freeze-dried for two days using a FreeZone® Freeze Drier System (Labconco, USA). About 0.1 g of the powdered

mycelia was dissolved in 5 ml of methanol (Merck, Germany), vortexed for 1 min and sonicated for 15 min. The mixture was then centrifuged at 89 x g for 15 min at 25°C. The supernatant was collected and the pellet was re-extracted with 5 ml of methanol, vortexed for 1 min, sonicated for 15 min and then centrifuged at 89 x g for 15 min at 25°C. The supernatant was collected and pooled with the previous supernatant and dried under a nitrogen stream. The extract was dissolved in 3 ml of methanol (Merck, Germany) and filtered through a 0.2 µm cellulose acetate Minisart syringe filter (Merck, Germany). The filtered extracts were stored at -20°C before analysis. An aliquot of 10 µl was subjected to LC-MS analysis.

Liquid Chromatography-Mass Spectrometry (LC-MS)

Ganoderma boninense intracellular metabolites were separated using the Ultimate 3000 HPLC (Thermo Scientific, USA), where the separation was achieved on a Reversed-Phase Acclaim™ Polar Advantage II (C18 4.6 × 250 mm length, 5 µm particle size) (Thermo Scientific, USA). With a gradient elution program at a flow rate of 1.0 ml min^{-1} and an injection volume of 5 µl, the chromatographic separation was performed at 37°C. The mobile phase A was an aqueous solution containing 0.1% (v/v) acetic acid (Merck, Germany) and mobile phase B was acetonitrile (Merck, Germany) containing 0.1% (v/v) acetic acid (Merck, Germany). The gradient program was started at 5% of B and increased linearly to 60% of B for 22 min. To minimise the carry-over between injections, the column was washed for 5 min and equilibrated for 2 min. Blank water injection was applied in-between the sample injection. All samples and replicates were injected simultaneously as one batch in random order to distinguish between technical and biological variations.

For the MS analysis, the HPLC system was coupled to a MicrOTOF-Q™ quadrupole-time-of-flight (QTOF) mass spectrometer (Bruker Daltonik, Germany) with an electrospray ionisation (ESI) interface operating in negative ion mode and controlled by the HyStar Application version 3.2 software (Bruker Daltonik, Germany). The column effluent was set at 1.0 ml min^{-1}. A split ratio of 1:4 was used, so the flow arriving at the detector was 250 µl min^{-1}. Nitrogen was used as nebulising gas at 4.1 bar and 9.0 litre min^{-1} flow rate. The temperature and voltage of the capillary were set at 200°C and + 3.5 kV, respectively. The full MS scan covered the mass range of 50-1000 *m/z*. Tandem mass spectrometry (MS/MS) parameters were set to improve mass fragmentation, with collision energy varying from 15-35 eV.

LC-MS Data Evaluation and Principal Component Analysis (PCA)

LC-MS data evaluation was performed with DataAnalysis version 4.2 for chromatogram analysis and ProfileAnalysis version 2.1 (Bruker Daltonik, Germany) for PCA. Compounds in the raw LC-MS data were extracted using MS algorithm version 3.0, sensitivity 99%, absolute intensity of 1000 and minimum peak valley of 10% under Find Compounds – Chromatogram module in DataAnalysis version 4.2, for comprehensive detection of all compounds in LC-MS run. PCA was performed based on bucket tables of the MS data. The data was integrated from 2.0-22 min and 50.5-999.5 *m/z* in time- and *m/z*-buckets using time alignment parameters and spectral background subtraction in the advanced bucketing approach. The multivariate statistics, PCA, was performed where data were Pareto scaled. The LC-MS data were then normalised to the sum of bucket values for an analysis, which considered the total intensity in analysis and suitable for unknown samples. A full cross and test set validations were applied to validate the PCA model. In ProfileAnalysis version 2.1 (Bruker Daltonik, Germany), the SmartFormula module was used to process the accurate mass data of molecular ions. The list of possible elemental formulas that use CHNO algorithm such as minimum/maximum elemental range, electron configuration, ring-plus double bond equivalents and comparison of the theoretical with measured isotope patterns was provided in the module. Compounds identified were categorised based on MSI (Metabolomics Standard Initiative) (Sumner *et al.*, 2007).

RESULTS AND DISCUSSION

One of the challenges in LC-MS metabolomics studies is data analysis and metabolite annotation, *i.e.* identifying biological molecules from mass spectral data. The highly sensitive LC-MS platform allows the simultaneous detection of multiple analytes combined with data processing workflow using ProfileAnalysis analysis including peak picking, filtering, normalising and statistic analysing (Mamat *et al.*, 2018; Veeramohan *et al.*, 2018; Mazlan *et al.*, 2018; Tahir *et al.*, 2016). In this study, the number of peaks detected from *G. boninense* intracellular metabolites were increased over time, until Day 6 and decreased at Day 8 (*Figure 1*). The metabolites measured over time were further analysed using PCA.

Validation of *Ganoderma boninense* Intracellular Metabolite PCA Model

PCA was used as a processing tool to enable robust interpretation of large-scale data from the

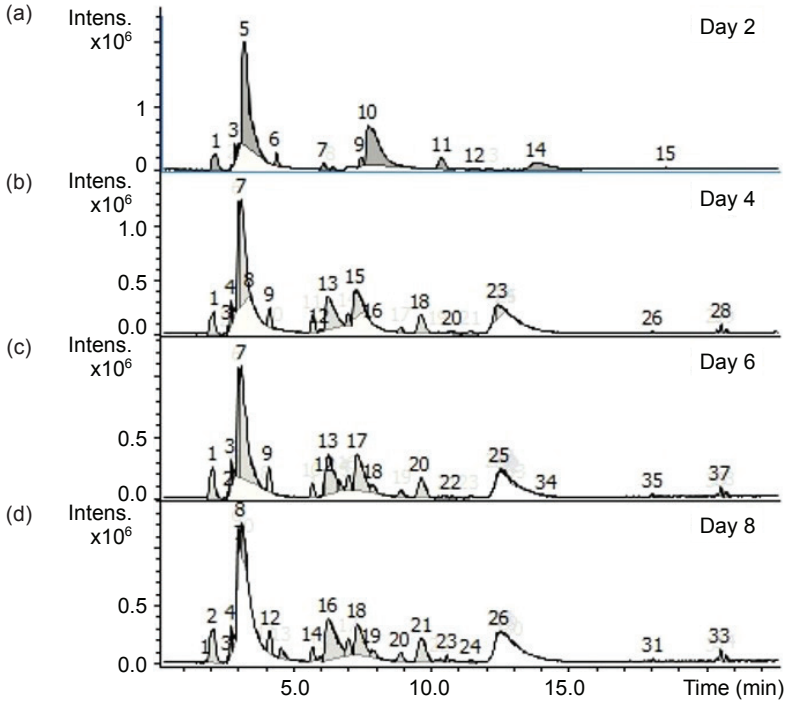


Figure 1. The liquid chromatography-mass spectrometry (LC-MS) base peak chromatograms (BPC) of Ganoderma boninense *extracellular metabolites at each time point of Day 2 (a), 4 (b), 6 (c) and 8 (d). The highest number of 37 peaks were detected at Day 6, followed by Day 8 with 33 peaks, Day 4 with 28 peaks and Day 2 with 15 peaks.*

G. boninense intracellular metabolites. Moreover, validation methods are crucial for the evaluation of model performance and prediction ability (Diana and Tommasi, 2002). The rule of cross validation (CV) technique is to test the significance and to correct the confidence limits and was applied to the PCA model for the *G. boninense* intracellular metabolites. As shown in *Figure 2*, full CV was applied to compare the predicted values with the actual ones. The influence plot of a PCA model for the *G. boninense* intracellular metabolites showed similar results before (a) and after (b) validation, where, no outlying behaviour outside the quadrant. This indicated the significance of the model at 95% confidence interval.

Besides, a test set validation of a PCA model was also applied to check the stability of the current model. Test set validation is suitable for large datasets (>50) (Kos *et al.*, 2003). *Figure 3* shows the influence plot of the original *G. boninense* intracellular metabolites PCA model (*Figure 3a*) and the new model after validation (*Figure 3b*). The new model described the test set analyses well, where the basic appearance of the scores plot did not change. This indicated the initial set of analyses all together resulted in a good and valid model.

Ganoderma boninense Intracellular Metabolite PCA Model

Large multivariate datasets generated from the LC-MS analysis of *G. boninense* intracellular metabolites require pattern recognition techniques that filter the important information from different time points and detect compounds that contribute to the groupings according to time trend. In this study, therefore, we employed an unsupervised method such as PCA to summarise the multidimensional data as well as to capture most of the variance in the datasets. PCA is a mathematical projection technique designed to extract many variables, displays and ranks the variance in a reduced data matrix (Jolliffe and Cadima, 2016). Furthermore, PCA extracts relevant statistics on the distribution of samples and group characteristics (Lazar *et al.*, 2015).

PCA is one of the most important and powerful methods in chemometrics (Bro and Smilde, 2014). Besides, it can also identify the effects of technical variation in the analysis of metabolic profiles, which is crucial for data quality evaluation in metabolomics studies (Gika *et al.*, 2014; Yin *et al.*, 2013). Following the pre-processing LC-MS data of the *G. boninense* intracellular metabolites, PCA allowed a descriptive evaluation of the samples distribution in order to assess the data quality and to identify natural groupings, patterns and outliers as explained and described in other reports (Tugizimana *et al.*, 2019). The samples presented in the PCA scores plot in *Figure 4a* showed close clustering between data points for each time interval. This indicated a good quality, stability, reliability and reproducibility of the analyses. The scores plot displays the relationship between

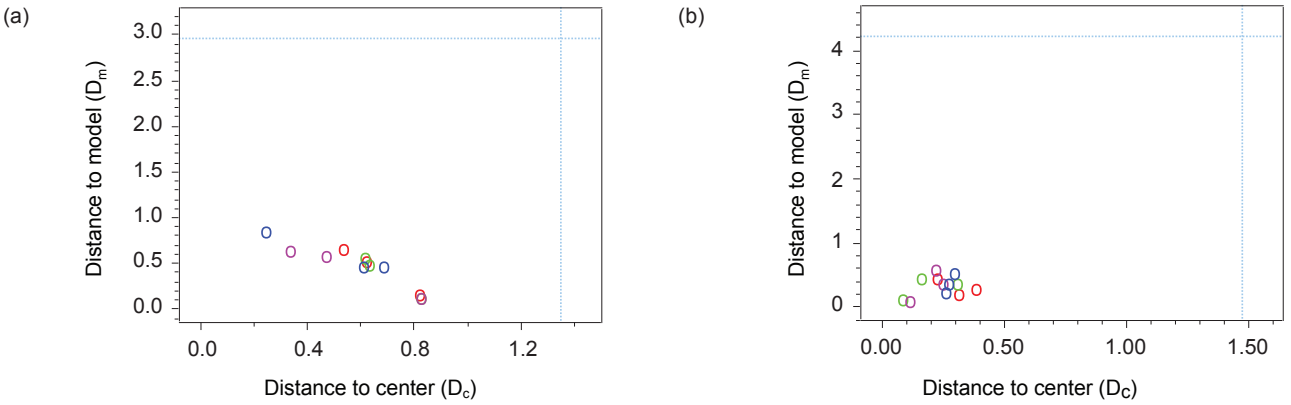


Figure 2. Full cross validation of Ganoderma boninense *intracellular metabolite principal component analysis (PCA) model. Influence plots (a) before and (b) after validation show no outlying behaviour outside the quadrant and indicated the significance of the model at 95% confidence interval.*

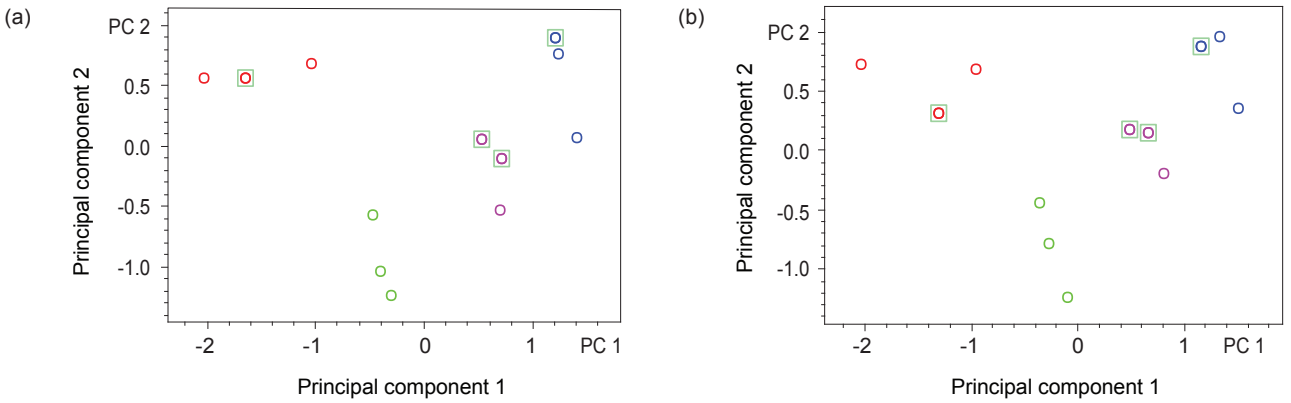


Figure 3. Test validation of Ganoderma boninense *intracellular metabolite principal component analysis (PCA) model. The scores plot shows (a) the selection of four test set analyses before (b) and after test set validation. The new PCA model (b) described the test set analyses well, where the basic appearance of the scores plot did not change and resulted in a good and valid model.*

G. boninense intracellular metabolites harvested at the different time intervals of Days 2, 4, 6 and 8.

Furthermore, in PCA, a linear transformation of the metabolic features in specific directions is called principal components, where they are taken seriously in explaining the most variation of the first component, followed by the second component, *etc.* (Jolliffe and Cadima, 2016; Alonso *et al.*, 2015). In this study, as shown in the scores plot, PC1 and PC2 explained 87.6% of the total variance present in the dataset. The first principal component summarises the global dataset since it captures most of the dataset variability in feature/metabolite patterns based on their similarity (Alonso *et al.*, 2015). In our results, PCA models revealed distinct time trend groupings in the *G. boninense* intracellular metabolites. Here, clear sample groupings indicate dynamic changes occurring in *G. boninense* developmental process *in vitro*, and observed as time-dependent stages, related by the time trend which was revealed by PC analyses (*Figure 4b*). PCA, as a standard model to deal with high-dimensional and complex metabolomics data, proved to uncover time-trends in a dataset (Tugizimana *et al.*, 2019). The PCA loadings plot (*Figure 4b*) represents 375 buckets (time and *m/z*) included in the PCA model. In this model, the four buckets that are far away from the central cloud are responsible for the variance within the dataset; (1) rT 3.6 min, *m/z* 179.0560, (2) rT 4.5 min, *m/z* 195.0514, (3) rT 2.9 min, *m/z* 181.0719 and (4) rT 6.6 min, *m/z* 133.0144.

Ganoderma boninense Intracellular Metabolite Signatures

From the PCA loadings plot analysis, four metabolites that were located far away from the central cloud, which were responsible for the variance within the dataset were selected and identified as differentially expressed metabolites. Metabolites were assigned as (1) glucose (*m/z* 179.0560), (2) gluconic acid (*m/z* 195.0514), (3) mannitol (*m/z* 181.0719) and (4) malic acid (*m/z* 133.0144) based on SmartFormula (Bruker Daltonik, Germany), comparison against KEGG database and tandem MS (MS/MS) (*Table 1*). MS/MS spectra and

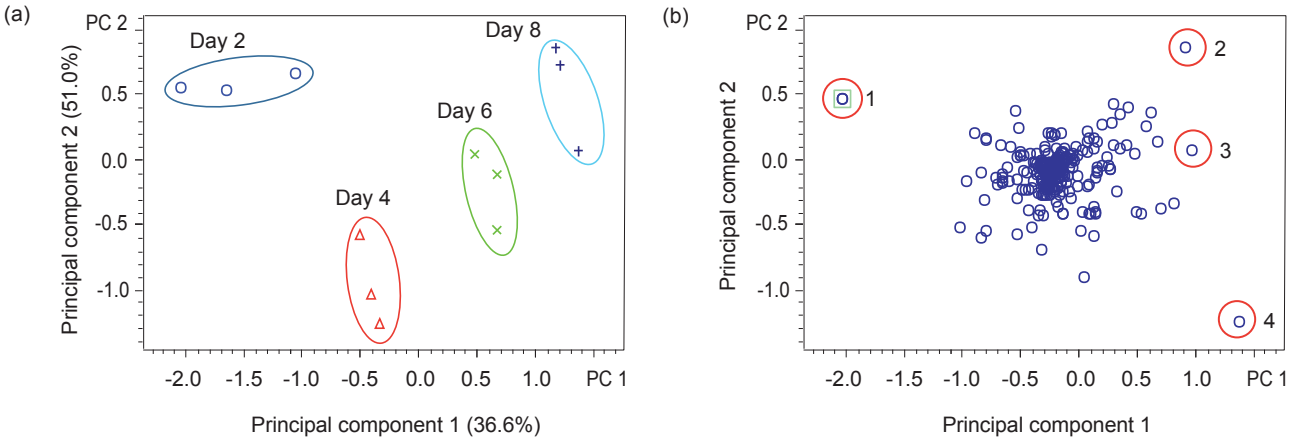


Figure 4. Principal component analysis (PCA) of the Ganoderma boninense *intracellular metabolite LC-MS data. Scores plot (a) and loadings plot (b) of negative mode data (Pareto-scaled) from intracellular samples. Each data point in the PCA scores plot represents an analysis included in the PCA model. A 2-component model, explaining 87.6% of the total variation in the Pareto-scaled data at 95% confidence level, from each time point at Days 2, 4, 6 and 8. A clear time-related trend is observed.*

chemical structures of all identified metabolites were presented on *Figures 5-8*. According to the PCA loadings plot, glucose showed relatively high abundance at Day 2 while gluconic acid, mannitol and malic acid showed relatively high abundance at Days 4, 6 and 8, respectively. Bucket statistics plot in the ProfileAnalysis enables a quick visual comparison of the differentially expressed metabolites according to time trend (*Figure 9*).

The differentially expressed intracellular metabolites in *G. boninense*, which were classified as primary metabolites, *i.e.* sugar and organic acid, play significant and essential roles in the growth, reproduction and development of the fungus. These metabolites are associated with the rapid initial growth phase and show maximum production at the end of the phase (Andersen, 2014; Wisecaver *et al.*, 2014; Sanchez and Demain, 2008). Mannitol, for example, is the most abundant soluble carbohydrates and plays a key role as carbon storage/ carbohydrate reserve within the mycelium of fungi (Patel and Williamson, 2016; Wiemken, 2007; Lewis and Smith, 1967). However, mannitol has recently been hypothesised to have a major role in fungal pathogenicity (Patel and Williamson, 2016).

CONCLUSION

Ganoderma boninense is an economically important pathogen in oil palm where a holistic and detailed understanding of the pathogen biology may

TABLE 1. PROPOSED DIFFERENTIALLY EXPRESSED INTRACELLULAR METABOLITES OF *Ganoderma boninense* AT DAYS 2, 4, 6 AND 8

No.	rT (min)	Metabolite	KEGG ID	MSI	Molecular formula	Monoisotopic mass (g mol^{-1})	*m/z* measured	*m/z* theoretical	Error (ppm)	MS^2 fragments
1.	3.6	Glucose	C00031	1	$C_6H_{12}O_6$	180.06	179.0560	179.0561	0.7	161.0433, 131.0372, 119.0374, 101.0252
2.	4.5	Gluconic acid	C00257	2	$C_6H_{12}O_7$	196.06	195.0514	195.0510	-2.0	177.0398, 159.0282, 129.0180
3.	2.9	Mannitol	C00392	2	$C_6H_{14}O_6$	182.08	181.0719	181.0718	-0.6	161.0465, 119.0334, 113.0217, 101.0222
4.	6.6	Malic acid	C00711	2	$C_4H_6O_5$	134.02	133.0144	133.0142	-1.4	115.0017, 89.0189

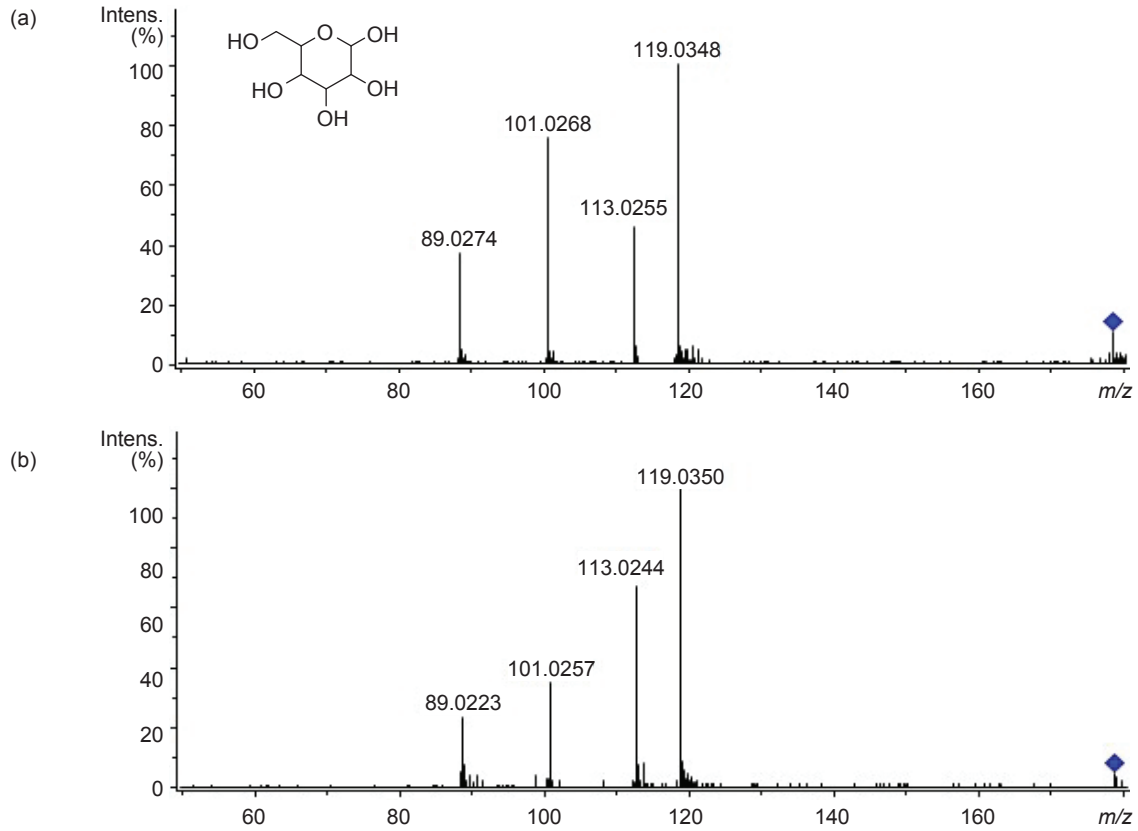


Figure 5. Negative ion mode mass spectrometry/mass spectrometry (MS/MS) spectra of glucose (m/z *179.0560,* $C_6H_{12}O_6$) *at a collision energy of 20 eV. Similar MS/MS spectra of (a) glucose in* Ganoderma boninense *mycelia sample and (b) glucose reference standard.*

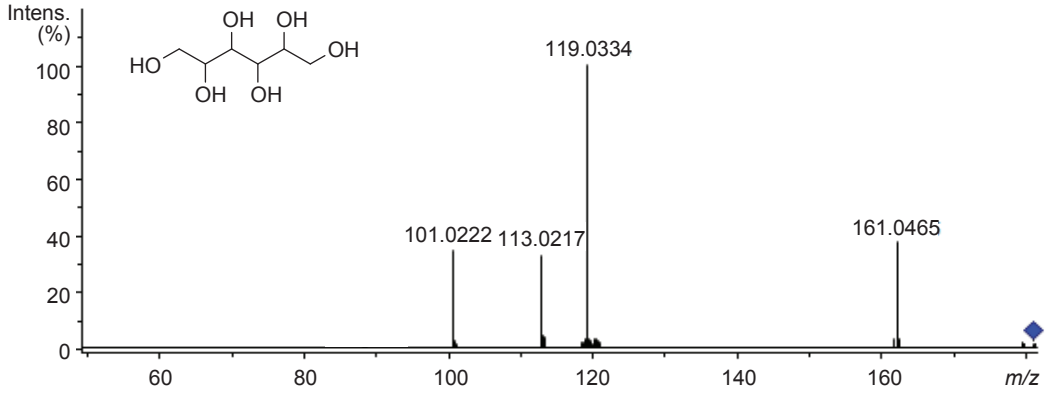


Figure 6. Negative ion mode mass spectrometry/mass spectrometry (MS/MS) spectrum of mannitol (m/z *181.0719,* $C_6H_{14}O_6$) *at a collision energy of 35 eV.*

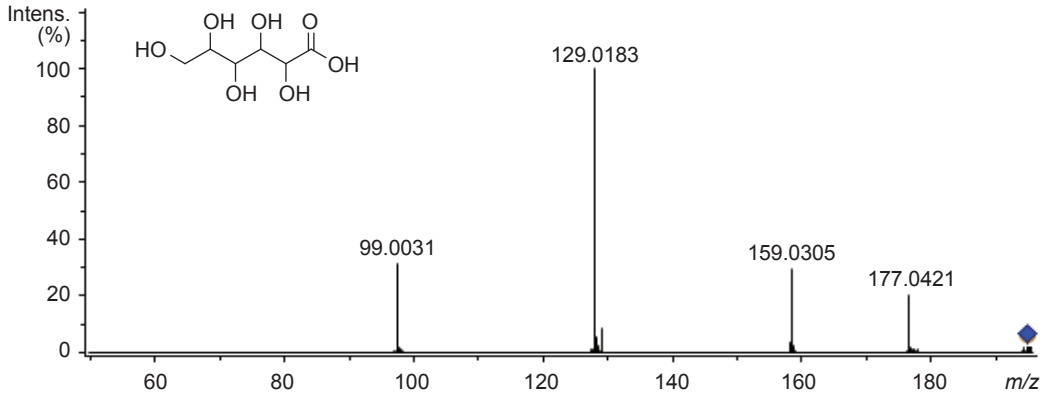


Figure 7. Negative ion mode mass spectrometry/mass spectrometry (MS/MS) spectra of gluconic acid (m/z *195.0514,* $C_6H_{12}O_7$) *at a collision energy of 15 eV.*

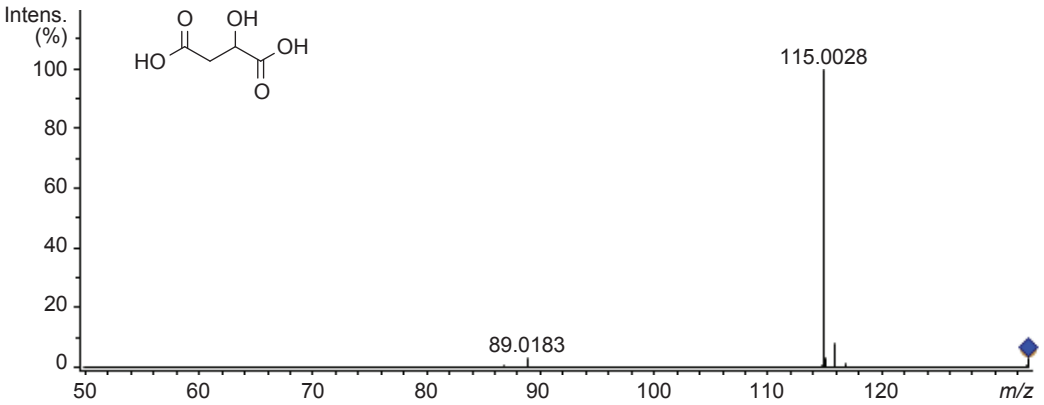


Figure 8. Negative ion mode mass spectrometry/mass spectrometry (MS/MS) spectra of malic acid (m/z *133.0144,* $C_4H_6O_5$) *at a collision energy of 15 eV.*

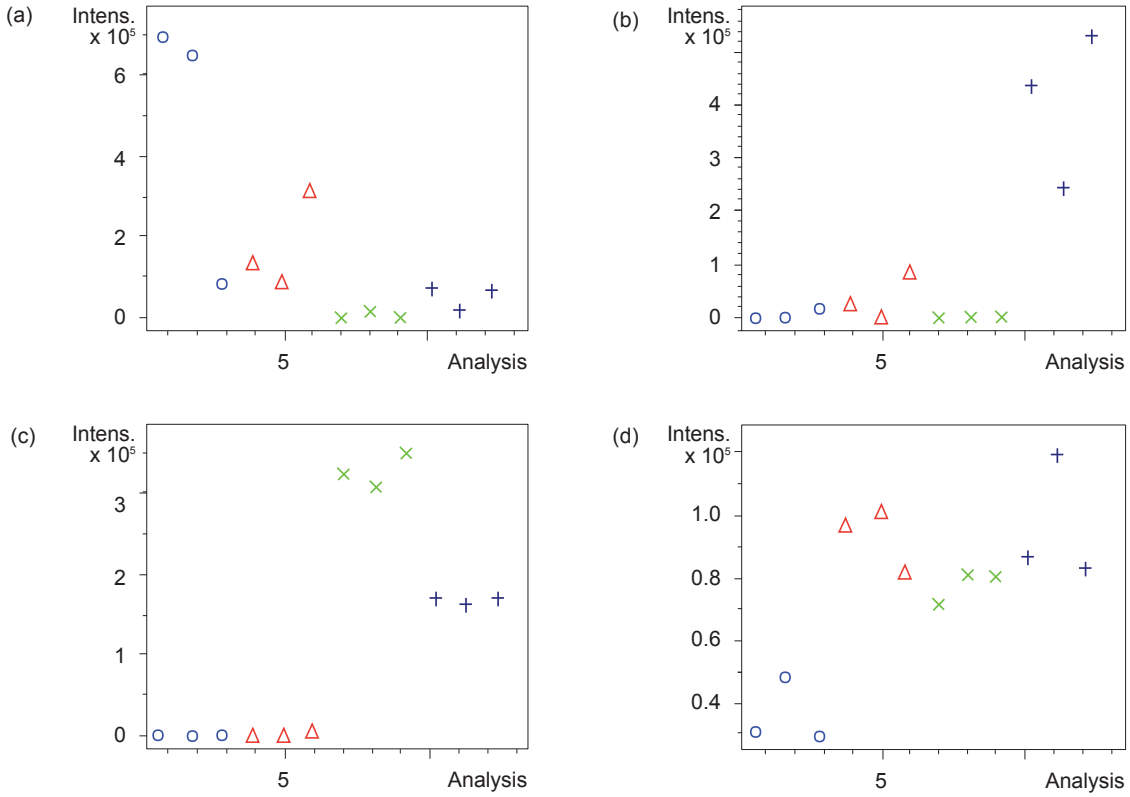


Figure 9. Bucket statistic plot of four differential metabolites observed in the loadings plot of principal component analysis (PCA) (● for Day 2, Δ for Day 4, × for Day 6 and + for Day 8). (a) Glucose ($C_6H_{12}O_6$, m/z *179.0560), (b) gluconic acid* ($C_6H_{12}O_7$, m/z *195.0514), (c) mannitol* ($C_6H_{14}O_6$, m/z *181.0719) and (d) malic acid* ($C_4H_6O_5$, m/z *133.0144).*

significantly improve targeted disease control and management strategies. The present study provides a necessary step for uncovering molecular events during the developmental process of *G. boninense* using LC-MS and multivariate statistical data analysis, particularly PCA. Albeit the interpretation of the large and complex LC-MS datasets of fungal metabolites is frequently challenging, our studies have demonstrated that PCA provides a robust and reliable comparison of temporal intracellular metabolite changes of *G. boninense*. This may indicate the dynamic changes occurring in *G. boninense* developmental process, *in vitro*. Furthermore, this information is of key importance that can complement the available transcriptomics and proteomics data of *G. boninense*, towards further understanding the *G. boninense* pathogenicity.

ACKNOWLEDGEMENT

The authors would like to thank the Director-General of MPOB for permission to publish this

article. We would also like to thank the members of the Proteomics and Metabolomics Unit, Advanced Biotechnology and Breeding Centre (ABBC), MPOB for their technical support and invaluable contribution. We acknowledge the support and assistance of Jayanthi Nagappan, Bioinformatics Unit, ABBC.

REFERENCES

Alonso, A; Marsal, S and Julia, A (2015). Analytical methods in untargeted metabolomics: State of the art in 2015. *Front. Bioeng. Biotechnol., 3*: 23-23.

Andersen, M R (2014). Elucidation of primary metabolic pathways in *Aspergillus* species: Orphaned research in characterizing orphan genes. *Brief Funct. Genomics, 13*: 451-455.

Bro, R and Smilde, A K (2014). Principal component analysis. *Anal. Methods, 6*: 2812-2831.

Chen, F; Ma, R and Chen, X L (2019). Advances of metabolomics in fungal pathogen–plant interactions. *Metabolites, 9(8)*: 169.

Chong, K P; Dayou, J and Alexander, A (2017). Pathogenic nature of *Ganoderma boninense* and basal stem rot disease. *Detection and Control of* Ganoderma boninense *in Oil Palm Crop*. Springer. p. 5-12.

De Falco, B; Manzo, D; Incerti, G; Garonna, A P; Ercolano, M and Lanzotti, V (2019). Metabolomics approach based on NMR spectroscopy and multivariate data analysis to explore the interaction between the leafminer *Tuta absoluta* and tomato (*Solanum lycopersicum*). *Phytochem. Anal., 30*: 556-563.

DesRochers, N; Walsh, J P; Renaud, J B; Seifert, K A; Yeung, K K-C and Sumarah, M W (2020). Metabolomic profiling of fungal pathogens responsible for root rot in American ginseng. *Metabolites, 10*: 35.

Diana, G and Tommasi, C (2002). Cross-validation methods in principal component analysis: A comparison. *Stat. Methods Appl., 11*: 71-82.

Gika, H G; Theodoridis, G A; Plumb, R S and Wilson, I D (2014). Current practice of liquid chromatography–mass spectrometry in metabolomics and metabonomics. *J. Pharm. Biomed. Anal., 87*: 12-25.

Gotthardt, M; Kanawati, B; Schmidt, F; Asam, S; Hammerl, R; Frank, O; Hofmann, T; Schmitt-Kopplin, P and Rychlik, M (2019). Comprehensive analysis of the *Alternaria mycobolome* using mass spectrometry based metabolomics. *Mol. Nutr. Food Res., 64(3)*: 1900558.

Hayden, H L; Rochfort, S J; Ezernieks, V; Savin, K W and Mele, P M (2019). Metabolomics approaches for the discrimination of disease suppressive soils for *Rhizoctonia solani* AG8 in cereal crops using 1H NMR and LC-MS. *Sci. Total. Environ., 651(1)*: 1627-1638.

Holmes, E and Antti, H (2002). Chemometric contributions to the evolution of metabonomics: Mathematical solutions to characterising and interpreting complex biological NMR spectra. *Analyst, 127*: 1549-1557.

Ivosev, G; Burton, L and Bonner, R (2008). Dimensionality reduction and visualization in principal component analysis. *Anal. Chem., 80*: 4933-4944.

Jolliffe, I T and Cadima, J (2016). Principal component analysis: A review and recent developments. *Phil. Trans. R. Soc. A., 374*: 20150202.

Jonsson, P; Bruce, S J; Moritz, T; Trygg, J; Sjöström, M; Plumb, R; Granger, J; Maibaum, E; Nicholson, J K; Holmes, E and Antti, H (2005). Extraction, interpretation and validation of information for comparing samples in metabolic LC/MS data sets. *Analyst, 130*: 701-707.

Kos, G; Lohninger, H and Krska, R (2003). Validation of chemometric models for the determination of deoxynivalenol on maize by mid-infrared spectroscopy. *Mycotoxin Res., 19*: 149-153.

Lazar, A G; Romanciuc, F; Socaciu, M A and Socaciu, C (2015). Bioinformatics tools for metabolomic data processing and analysis using untargeted liquid chromatography coupled with mass spectrometry. *Bull. Univ. Agric. Sci., 72*: 103-115.

Lewis, D and Smith, D (1967). Sugar alcohols (polyols) in fungi and green plants. I. Distribution, physiology and metabolism. *New Phytol., 66*: 143-184.

Liu, H; Zhao, X; Guo, M; Liu, H and Zheng, Z (2015). Growth and metabolism of *Beauveria bassiana* spores and mycelia. *BMC Microbiol., 15*: 267 pp.

Mamat, S F; Azizan, K A; Baharum, S N; Noor, N M and Aizat, W M (2018). ESI-LC-MS based-metabolomics data of mangosteen (*Garcinia mangostana* Linn.) fruit pericarp, aril and seed at different ripening stages. *Data Brief, 17*: 1074-1077.

Mazlan, O; Aizat, W M; Aziz Zuddin, N S; Baharum, S N and Noor, N M (2018). LC-MS data

for metabolomics analysis of *Garcinia mangostana* L. seed germination. *Data Brief, 21*: 2221-2223.

Othman, A; Abd Rasid, O; Nagappan, J; Leslie Low, E T; Fook Hwa, L; Nurazah, Z; Syahanim, S; Dzulkafli, S B; Rozali, N L; Bohari, B; Angel, L P L; Tahir, N I; Idris, A S; Marjuni, M; Sundram, S; Mohd Din, A; Ramli, U S and Mohamad Arif, A M (2019). Molecular characterisation of oil palm responses to *Ganoderma* infection. International Seminar on Breeding for *Ganoderma* Tolerance in Oil Palm. Kuala Lumpur Convention Centre, Kuala Lumpur. p. 137-146.

Patel, T K and Williamson, J D (2016). Mannitol in plants, fungi, and plant-fungal interactions. *Trends Plant Sci., 21*: 486-497.

Rees, R W (2006). Ganoderma *stem rot of oil palm* (Elaeis guineensis)*: Mode of infection, epidemiology and biological control*. Ph.D thesis, University of Bath, United Kingdom.

Robison, F M; Turner, M F; Jahn, C E; Schwartz, H F; Prenni, J E; Brick, M A and Heuberger, A L (2018). Common bean varieties demonstrate differential physiological and metabolic responses to the pathogenic fungus *Sclerotinia sclerotiorum*. *Plant Cell Environ., 41*: 2141-2154.

Sanchez, S and Demain, A L (2008). Metabolic regulation and overproduction of primary metabolites. *Microb. Biotechnol., 1*: 283-319.

Siless, G E; Gallardo, G L; Rodriguez, M A; Rincon, Y A; Godeas, A M and Cabrera, G M (2018). Metabolites from the dark septate endophyte *Drechslera* sp. evaluation by LC/MS and principal component analysis of culture extracts with histone deacetylase inhibitors. *Chem. Biodivers., 15*: e1800133.

Son, S Y; Lee, S; Singh, D; Lee, N-R; Lee, D-Y and Lee, C H (2018). Comprehensive secondary metabolite profiling toward delineating the solid and submerged-state fermentation of *Aspergillus oryzae* KCCM 12698. *Front. Microbiol., 9*: 1076.

Sumner, L W; Amberg, A; Barrett, D; Beale, M H; Beger, R; Daykin, C A; Fan, T W; Fiehn, O; Goodacre, R; Griffin, J L; Hankemeier, T; Hardy, N; Harnly, J; Higashi, R; Kopka, J; Lane, A N; Lindon, J C; Marriott, P; Nicholls, A W; Reily, M D; Thaden, J J and Viant, M R (2007). Proposed minimum reporting standards for chemical analysis Chemical Analysis Working Group (CAWG) Metabolomics Standards Initiative (MSI). *Metabolomics, 3(3)*: 211-221.

Tahir, N I; Shaari, K; Abas, F; Ishak, Z and Tarmizi, A (2016). Metabolome analysis of oil palm clone P325 of different planting trials. *J. Oil Palm Res., 28*: 431-441.

Tugizimana, F; Djami-Tchatchou, A T; Fahrmann, J F; Steenkamp, P A; Piater, L A and Dubery, I A (2019). Time-resolved decoding of metabolic signatures of *in vitro* growth of the hemibiotrophic pathogen *Colletotrichum sublineolum*. *Sci. Rep., 9*: 3290.

Veeramohan, R; Azizan, K A; Aizat, W M; Goh, H-H; Mansor, S M; Yusof, N S M; Baharum, S N and Ng, C L (2018). Metabolomics data of *Mitragyna speciosa* leaf using LC-ESI-TOF-MS. *Data Brief, 18*: 1212-1216.

Wiemken, V (2007). Trehalose synthesis in ectomycorrhizas-a driving force of carbon gain for fungi? *New Phytol., 174*: 228-230.

Wisecaver, J H; Slot, J C and Rokas, A (2014). The evolution of fungal metabolic pathways. *PLoS Genet., 10*: e1004816.

Yin, P; Peter, A; Franken, H; Zhao, X; Neukamm, S S; Rosenbaum, L; Lucio, M; Zell, A; Haring, H U; Xu, G and Lehmann, R (2013). Preanalytical aspects and sample quality assessment in metabolomics studies of human blood. *Clin. Chem., 59*: 833-845.

Yuan, S; Yan, J; Wang, M; Ding, X; Zhang, Y; Li, W; Cao, J and Jiang, W (2019). Transcriptomic and metabolic profiling reveals 'Green Ring' and 'Red Ring' on jujube fruit upon postharvest *Alternaria alternata* infection. *Plant Cell Physiol., 60*: 844-861.

JOURNAL OF OIL PALM RESEARCH
GUIDE FOR AUTHORS

Type of Articles

1. **Regular Article**
   Full-length original empirical investigations, consisting of introduction, materials and methods, results and discussion, conclusion. Original work must provide references and an explanation on research findings that contain new and significant findings. Conclusion should be brief and focus on the research output, should not be in point form. These manuscript should not exceed 6000 words of text (including tables, figures and references) and generally not more than a total of 10 figures and tables. After peer-review, the manuscript word count limit can be extended to a maximum of 8000 words to better address the reviewers' and editors' comments. Any additional figures or tables can be included in the supplementary data. Please note that manuscript submitted to JOPR will be sent back to authors because of poor figure resolution or exceeding the number of figures permitted.

2. **Short Communication**
   Significant new information to readers of the Journal in a short but complete form. Preferably not exceeding 3000 words (including tables, figures and references), and is intended for rapid publication. They are not intended for publishing preliminary results or to be a reduced version of regular article.

3. **Review Article**
   Critical evaluation of materials about current research that have already been published by organising, integrating, and evaluating previously published materials. Re-analyses as meta-analysis and systemic reviews are encouraged. Review articles provide systemic overview, evaluation and interpretation of research in a given field. They should not exceed 12 000 words (excluding references only) and should contain no more than a total of 20 figures and tables. Any additional figures or tables can be included in the supplementary data. Please note that manuscript submitted to JOPR will be sent back to authors because of poor figure resolution or exceeding the number of figures permitted. The same information should not be repeated in a figure and a table.

Language
Please write your text in good English (only British English is accepted). We do not accept American English or a mixture of these.

JOPR's Template
JOPR's template, which is a standard format that facilitates the manuscript writing and copyediting process. This template is created to provide a detail and clear house style of JOPR. The template is drafted according to JOPR's house style, but in standard word version format. When writing a manuscript, authors need to format their manuscript to fit into the journal's house style. To make this easier, Word templates are available for many of other established journals, ready for them to download and apply to their research article format. It is crucial for author to write a research article while considering formatting. Each journal has its own guidelines for formatting; hence, the template defines how an article will look when it is published online or in print.

JOPR's Aims and Scope
This is established to provide a detail and clear aims and scope for author reference. Authors should declare in the cover letter how the research fits the aims and scope of JOPR.

JOPR's House Style
A detail listing of JOPR's house style for authors and a checklist to facilitate the copyediting process and standardise the copyediting process. The JOPR's house style remains the same and is drafted into a detail version for author's reference.

Manuscript Submission
- Manuscripts should be submitted via: **https://mc04.manuscriptcentral.com/jopres**
- JOPR does not permit dual submission, publication and/or any archive platform (preprint) in violation of journal ethical practices.

For more details and to download the JOPR's House Style and Template, kindly surf **http://jopr.mpob.gov.my/guide-t/**

Journal of Oil Palm Research ISSN 1511-2780
An international refereed journal on oil palm
Impact Factor: 2.057 (2020)
CiteScore: 3.0 (2020)
SJR: 0.498 (2020)



Contents of the Coming Issue
Journal of Oil Palm Research
Vol. 33 (4) December 2021*

- Breeding *Virescens* Oil Palm
  Vengeta Rao and Chang, K C

- Genetic Transformation of Oil Palm-based on Selection with Hygromycin
  Bahariah, B; Rasid, O A; Rahmah, A R S; Ghulam Kadir Ahmad Parveez and Masani, M Y A

- Effect of Operating Temperature on Physiochemical Properties of Empty Fruit Bunch Cellulose-derived Biochar
  Stasha Eleanor Rosland Abel; Soh Kheang Loh; Noorshamsiana Abdul Wahab; Ondrej Masek; Musa Idris Tanimu and Robert Thomas Bachmann

- The Effect of Microwave Treatment and Delayed Harvesting on Oil Palm Fruitlets (*Elaeis guineensis*) Oil Quality
  Nu'man Abdul Hadi; Ng Mei Han; Rusnani Abd Majid and Che Rahmat Che Mat

- Characteristics of Retail Refrigerated and Non-Refrigerated Margarines/ Fat Spreads Sold in Malaysia
  Sivaruby Kanagaratnam; Teng Kim Tiu; Nur Haqim Ismail; Norazura Aila Mohd Hassim; Wan Rosnani Awg Isa and Noor Lida Habi Mat Dian

- Red Palm Oil in Laying Ducks Diets: Effects on Productive Performance, Egg Quality, Concentrations of Yolk Carotenoids
  Yifei Lu; Shunan Dong; Haiteng Zhou; Ligang Yang; Zhaodan Wang; Da Pan; Xian Yang; Hui Xia; Guiju Sun and Shaokang Wang

- Is There a Sustainable Future for Wildlife in Oil Palm Plantations in Malaysia?
  Jayasilan Mohd-Azlan and Lisa Lok

Note: * Subject to change.